An Electrochemical study of the Metal-Chalcogenide Glasses: Fundamentals and Applications in Ion Selective Electrodes.

by

M. C. Kennedy

Thesis presented for the degree of Doctor of Philosophy of the University of Edinburgh in the Faculty of Science.

1985

This thesis has been written by myself as a record of my own work. All other sources of information have been duly acknowledged.

Martin C Kennedy

October 1985

CONTENTS

CONTENTS(cont.)

ABSTRACT

The construction and possible applications of Cu^{2+} sensing Ion Selective Electrodes (ISEs) based on the chalcogenide glasses $Cu_x(As_2Se_3)_{100-x}$ and $Cu_y(As_2Se_{1.5}Te_{1.5})_{100-y}$ ($20<x<56$, $20<y<25$) are described. The electrodes show responses to Copper[ii] ion that are close to Nernstian behaviour for a two electron reaction. This type of behaviour is found for all the compositions studied as well as for electrodes that were not constructed from a single phase -homogeneous- glass. Slopes for the electrode potential vs. log(concentration) plots are lways less than the Nernstian value of 29.1 mV/decade. The largest difference being 7mV/decade.

The only interferents found are Ag^+, Hg^{2+} and Cl^-, the electrodes continue to respond to differences in Copper ion concentration in the presence of Hg and Cl. For Ag concentrations in excess of 10^{-4}M all Cu ion sensitivity disappears however.

Cyclic Voltammograms of Redox couples have been recorded at the glass electrodes, these are compared with Voltammograms recorded at a Platinum electrode. Certain processes found at the metallic electrode were not observed at the glass electrodes, this is interpreted by assuming that electron transfer only occurs from/to ions with energy levels that coincide with those in the glass. A crude band diagram has been constructed and is compared with those derived from bulk electrical properties.

The electrode potentials of glassy $Cu_{20}(As_2Se_3)_{80}$ electrodes shift to more positive potentials when illuminated. This behaviour is never observed with tellurium containing glasses or those that contain some crystalline phases. The magnitude of the effect decreases with increasing Cu ion concentration in solution.

Chronopotentiograms have been recorded at several of the electrodes in Cu containing solutions.

The theory of solid state ISEs based on electronic conductors is discussed, it is pointed out that if the electron is treated as an ion with a well defined chemical potential existing theories of ionically conducting ISEs are easily adapted.

CHAPTER 1

Introduction: Ion Selective Electrodes (ISEs)

According to Light[1] an Ion Selective Electrode (ISE) can be defined as a "measuring electrode with a relatively high degree of specificity for a single ion or a class of ions". Devices conforming to this definition, with varying degrees of specificity, have been discovered for between 20 and 30 different types of ion at the time of writing. A list of ions that can be determined by ion selective electrodes is given in chapter 3. For most known devices, when the ion selective electrode is included in an electrochemical cell with a reference electrode, i.e. one with a potential that is assumed to be fixed, the overall cell potential (E) is related to the ion concentration by a Nernstian type relationship.

$$E = E^{O} + \frac{RT}{zF} \log_e \frac{a_i}{a^{O}_1} \qquad 1.1.1$$

where a_i is the activity of the ion of interest and E^{O} is the cell potential when a_i equals a reference concentration a^{O}_i. By definition the Ion Selective Electrode's potential depends mainly and preferably entirely, on the activity and hence concentration of one ion. Consequently, sample preparation is simpler and this, together with their direct electrical output, makes them very suitable for continuous monitoring of industrial processes or bio-medical and environmental systems such as rivers.

Unfortunately, ISEs suffer from some drawbacks. Firstly, ISEs are only available for certain ions and even then, in some cases, they are interferred with by ions other than the one they were designed to detect. Secondly, they only determine ions in polar solvents, notably water, whereas many industrial processes work in non-polar solvents or the gas phase. Both these problems can be overcome if a reaction of the species of interest can be found that produces a determinable ion in quantitative yield, the ion can then be analysed with an ISE. Using these "in-direct" methods sensors for the acid gases (CO_2, SO_2 & NO_x), ammonia and certain bio-molecules have been constructed.

Apart from the fundamental problems outlined above, ISEs have some important practical limitations as well. Most commercial ISEs are of the membrane type (figure 3.1) in which the ion selective material is formed as a hollow bulb. The bulb is filled with a reference solution of fixed concentration (a_0 in equation 1.1.1) and the potential difference across the bulb wall is then directly related to the unknown concentration a_i. Such devices are complex, delicate and expensive to produce. If the reference solution could be replaced by a direct electrical contact smaller, stronger and cheaper solid-state devices could be manufactured. Most ion selective materials are ionic conductors and this has some important consequences when trying to build a solid state device. The main problem with the solid state device is that the electrical contact to the ionic conductor is a so called blocking contact i.e. ions that carry the charge in the ion selective material can not pass beyond the junction with the electronically conducting contact. They will thus tend to pile up, altering the stoichiometry of the ionic conductor and possibly reacting with the back contact. If these are slow processes the solid state ISE will respond slowly to changes in ion concentration and the potential may drift with time; both un-desirable characteristics. How bad these problems are in practice has never been systematically studied, but they could be avoided altogether if electronically conducting ion selective materials were available.

It should be noted that there is nothing unusual in the concept of electronically conducting ion selective materials. In chapter 3 it is pointed out that the electron can usefully be considered as a chemical species like any other ion. Moreover, most chemistry courses introduce the concept of chemical cells using the examples of metals immersed in a solution of their own ions. Such electrodes are in no sense selective but illustrate how an electronic conductor can be used to determine ion concentrations. For an ISE, an electronic conductor is required that exchanges electrons with only one type of ion. Such materials were discovered by Jasinski[2,3] and co-workers in the 1970's. Electrodes selective to Fe^{3+} based on the semiconducting glasses Fe_x Sb Ge Se ($x = 0.2$) were discovered in 1974 and these were followed by Cu^{2+} sensitive $Cu_x(As_2\ S_3)_{100-x}$ ($5<x<30$) glasses in 1976. The latter have been studied at Edinburgh and the complementary selenides and selenide/tellurides have also been investigated. Unfortunately, very little work has been done to discover the underlying response mechanisms in these glasses. A good understanding of the mechanism might allow better compositions to be formulated and also might lead to the discovery of materials capable of sensing other ions.

CHAPTER 2

FUNDAMENTAL ELECTROCHEMISTRY

2.1 Chemical Cells

Chemical cells are of great fundamental and practical importance. In general a cell consists of two electronically conducting electrodes in contact with an ionically conducting electrolyte. The electrolyte may be common to both electrodes or there may be two separate electrolytes, connected by a solid or viscous ionic conductor, known as the salt bridge, which prevents the mixing of the electrolytes. The electrode and its surrounding electrolyte together comprise a half-cell. In general the electrode is solid, often a metal, but this is not necessary and mercury is an example of a liquid electrode. Furthermore the electrolyte is often a solution of a salt in a liquid solvent, but solid ionic conductors are becoming increasingly common in cells designed both for fundamental studies and for practical applications. In liquid electrolytes the salt dissolves to give ions which exchange electrons with the electrode together with ions of opposite charge, known as the counter-ions, which generally do not participate in the electrode reaction but serve to keep the electrolyte electrically neutral. For solid electrolytes there is normally only one type of mobile ion and the charge carried by these is neutralized by fixed charge centres of the opposite type.

Figure 2.1 illustrates a typical cell using metal electrodes and liquid electrolytes. The open circuit potential difference measured by a potentiometer or, more usually, a high impedance voltmeter is known as the equilibrium cell potential. The cell potential consists of the sum of potential differences across each interface of the cell and thus

$$E_{eqm} = (\phi_C^I - \phi_M) + (\phi_M - \phi_{M^{n+}}) + \Delta\phi_{LJ} + (\phi_{N^{n+}} - \phi_N) + (\phi_N - \phi_C^{II})$$

where ϕ_i is the electrostatic potential in medium i, ϕ_C^I and ϕ_C^{II}

2.1 GALVANIC CELL

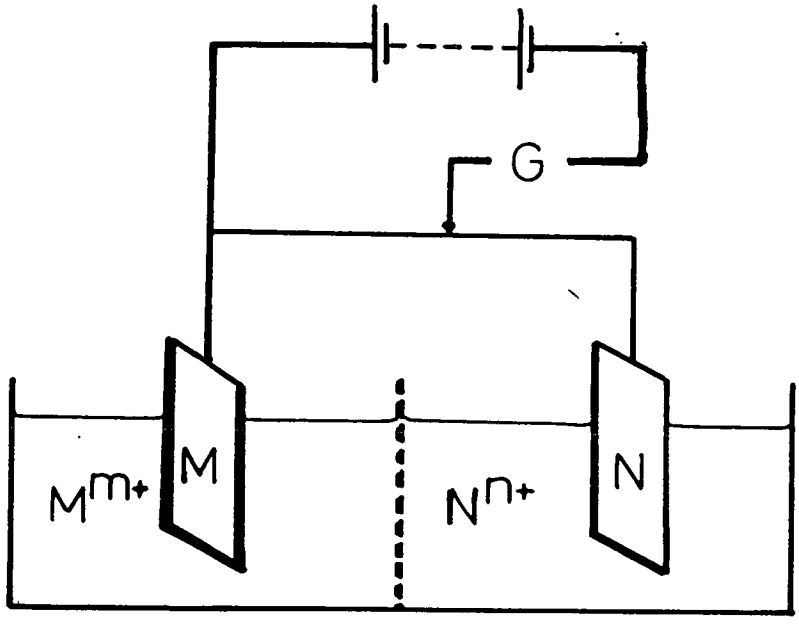

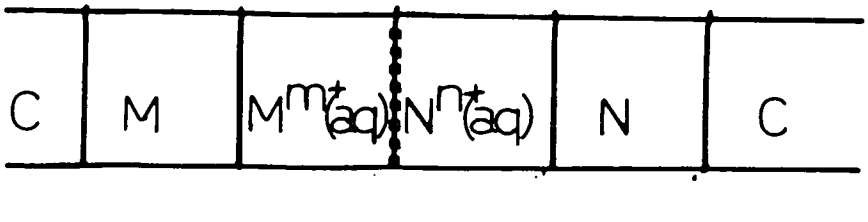

'C' is a conductor connecting the electrod to the potentiometer

are the electrostatic potentials in the contacts to M and N respectively and $\Delta\phi_{LJ}$ is the liquid junction potential that appears across the salt bridge.

The liquid junction potential and the two metal-metal junction potentials can usually be ignored so that

$$E_{eqm} = (\phi_M - \phi_{M^{m+}}) + (\phi_N - \phi_{N^{n+}})$$

The equilibrium potential thus depends on the potential differences between the electrodes and the electrolytes i.e. the two half-cell potentials. The potential difference at the electrode-electrolyte interface at equilibrium can be found from the electrochemical potentials ($\tilde{\mu}$) of the reactants and products. For the reaction

$$M^{z+}\ (\text{electrolyte}) + ze^-(\text{electrode}) \leftrightharpoons M(\text{electrode})$$

the condition for equilibrium is

$$\tilde{\mu}_{M^{z+}} + z\tilde{\mu}_{e^-} = \tilde{\mu}_M \qquad 2.1.1$$

The electrochemical potential for a charged species is given by

$$\tilde{\mu}_i = \mu_i + zF\phi \qquad 2.1.2$$

where μ is the chemical potential, F is the Faraday constant. Therefore

$$(\mu_{M^{z+}} + zF\phi_{SOLN}) - (z\mu_{e^-} + zF\phi_{ELECTRODE}) = \tilde{\mu}_M \qquad 2.1.3$$

$$\phi_{SOLN} - \phi_{ELECTRODE} = \frac{1}{zF}(\tilde{\mu}_M + z\mu_{e^-} - \mu_{M^{z+}}) \qquad 2.1.4$$

Although eqn. 2.1.4 has been derived for a solution-electrode interface it is applicable to any half-cell. It is not possible to measure $(\phi_{SOLN} - \phi_{ELEC})$ as this necessitates making an electrical contact to the solution, thereby creating a second half-cell. Normally electrical contact is made indirectly to the test solution by the electrode of a second half-cell (via a salt bridge) which is selected for its stability and reproducibility. This second half-cell has a well-defined potential and is known as the reference electrode. The reference electrode thus fixes the value of ϕ_{SOLN} and the potential difference measured between the reference electrode and the test half-cell gives $(\phi_{SOLN} - \phi_{ELECTRODE})$ relative to $(\phi_{SOLN} - \phi_{REFERENCE})$. Note that strictly the reference electrode is a reference half-cell, but the term 'electrode' has become common usage.

It is found that cell potentials depend on temperature and the concentration of ions in the electrolytes. They may also depend on other factors such as the presence of impurties or illumination. The dependence on temperature and concentration is a result of the definition of the chemical potential as

$$\mu_{M^{z+}}(T, C_{M^{2+}}) = \mu^{0}_{M^{2+}}(T) + RT \log_e \gamma_{M^{z+}}(T, C_{M^{z+}})\, C_{M^{z+}} \qquad 2.1.5$$

where $\mu^{0}_{M^{z+}}$ is the standard chemical potential, T is the absolute temperature, $C_{M\,z+}$ is the concentration of M^{z+} and $\gamma_{M^{z+}}$ is the activity coefficient. Substitution of 2.1.5 into 2.1.4 allows the variation of cell potential with concentration of the electrolyte to be found. The result is the Nernst equation, i.e:

$$E(T, C_{M\,z+}) = E^{\circ}(T) + \frac{RT}{zF} \log_e \gamma_{M z+} C_{M\,z+} \qquad 2.1.6a$$

$$E^{\circ}(T) + \frac{RT}{zF} \log_e a_{M\,z+} \qquad 2.1.6b$$

where a_i is the activity of species i. For a perfect solution the activity is equal to the concentration[10], for real solutions this is generally not true. The difference is due to the interactions between solvent and solute molecules. For the case of salts dissolving in a polar solvent the interactions include electrostatic forces between, and solvation of, individual ions.

2.2 Electrode Kinetics

An electrode reaction is one in which electrons are exchanged between species in the electrolyte and the electrode itself. Two basic cases can be identified:

(i) Both the reduced and oxidised forms of the couple remain in the electrolyte, in which case the electrode acts simply as a source or a sink for electrons

(ii) Either the reduced or the oxidised form is intimately associated with the electrode surface.

An example of the latter is the case of a metal in a solution of its own ions.

At equilibrium, the forward and reverse electron exchanges occur at equal rates. This is the situation that would prevail under open circuit conditions with the potentiometer removed. If the potentiometer used to measure the equilibrium cell potential in Fig 2.1 is adjusted to another value ($E_{applied}$), a current will flow until the values of of $C_M{}^{m+}$ and $C_N{}^{n+}$ have adjusted to the values predicted by the Nernst equation, with the new value of $E_{applied}$. For the cell in Fig 2.1 this is[10,32]

$$\frac{C_{M^{m+}}}{C_{N^{n+}}} = \frac{Y_{N^{n+}}}{Y_{M^{m+}}} \exp \frac{zF}{RT}(E_{applied} - E^{\circ}) \qquad 2.2.1$$

Experiments involving the passage of a current through chemical cells are of great importance for determining mechanisms of electrode reactions and are generally referred to as voltammetric techniques. Voltammetry is one form of a general method of obtaining information on reaction kinetics and mechanisms by causing a change in conditions and following the relaxation of the system to its new equilibrium position. Electrochemical systems are particularly susceptible to changes in applied potential, and a convenient property to measure is the resulting current. The nature of the perturbation defines the technique and the most commonly used perturbations are:

(i) A potential step, with current being measured as a function of

time - Chrono amperometry.
(ii) A potential ramp, with current being measured as a function of potential and hence time - D.C. sweep voltammetry.
(iii) A sawtooth change in potential with current being followed as a function of potential - cyclic voltammetry.
(iv) A sinusoidal change in potential (possibly superimposed on a ramp) with the current amplitude and phase being determined as functions of frequency and /or D.C. potential - A.C. voltammetry.

In addition to the controlled potential experiments, the complementary controlled current experiments, in which potential is the measured property, are also employed.

When a cell is not at equilibrium and a current is flowing there are two possible directions of current flow; for each electrode these are referred to as anodic or cathodic currents depending on whether there is a net transfer of electrons to or from the electrode, respectively. Similarly the associated electron transfer reactions are termed anodic when electrons are being transferred to the electrode and cathodic when they are being transferred from the electrode.

In general the rate of electron transfer and hence current depends on the usual rate-determining factors such as temperature, concentration of ions in solution and the density of electrons at the surface. Thus, in general

$$J_{CAT} = k_{CAT}\, e\, n_s\, C_{ox} \exp(-U_{CAT} / RT) \qquad 2.2.2$$

and

$$J_{AN} = k_{AN}\, e\, p_s\, C_{Red} \exp(-U_{AN} / RT) \qquad 2.2.3$$

where J_i is the current density, U_i is the activation energy, k_i is the rate constant, e is the charge on the electron, n_s is the surface density of electrons and p_s is the surface density of unoccupied states. The subscripts AN and CAT refer to anodic and cathodic reactions, respectively, and C_{ox} and C_{Red} are the surface concentrations of the oxidised species (ox) and the reduced species (Red) in the redox reaction

$$Ox + ze \rightleftharpoons Red$$

For metals, n_s and p_s vary very little with potential and can be incorp-

orated into the rate constants. For semiconductor electrodes this is not permissible.

The activation energies U_{CAT} and U_{AN} are potential-dependent, so that the electron transfer rates are also potential-dependent. If E is the applied potential then it can be shown by considering potential profiles for the above redox reaction that [1,2]

$$U_{CAT} = \alpha zFE \qquad 2.2.4a$$

$$U_{AN} = (1-\alpha)zFE \qquad 2.2.4b$$

where α is the transfer coefficient.
For an electrode reaction[3] the current is given by

$$I = zFA\ (J_{CAT} + J_{AN}) \qquad 2.2.5$$

where A is the surface area of the electrode. Equation 2.2.5 can be expanded using 2.2.4, 2.2.2 and 2.2.3 to give

$$I = zFA\left(k_{CAT} n_s \exp \frac{-\alpha zFE}{RT} C_{ox} - k_{AN} p_s \exp \frac{(1-\alpha)zFE}{RT} C_{Red}\right) \qquad 2.2.6$$

At equilibrium I=0, so that

$$\frac{C_{ox}}{C_{Red}} \frac{k_{CAT} n_s}{k_{AN} p_s} = \exp \frac{zF}{RT} E_{eqm} \qquad 2.2.7$$

This equation can be arranged to give one form of the Nernst equation:

$$E_{eqm} = \frac{RT}{zF} \log_e \frac{k_{CAT} n_s}{k_{AN} p_s} + \frac{RT}{zF} \log_e \frac{C_{ox}}{C_{Red}} \qquad 2.2.8$$

For metallic electrodes, n_s and n_p are independent of E so that equations 2.2.2 and 2.2.3 can be rewritten using 2.2.4a to give

$$J_{CAT} = k'_{CAT} C_{ox} \exp (-\alpha zFE / RT) \qquad 2.2.9a$$

Hence,

$$\log_{10} I_{CAT} = \log_{10} zAFk'_{CAT} C_{ox} - \frac{1}{2.3} \frac{\alpha zFE}{RT} \qquad 2.2.9b$$

2.2 CURRENT-VOLTAGE RELATIONSHIPS FOR AN ELECTRODE

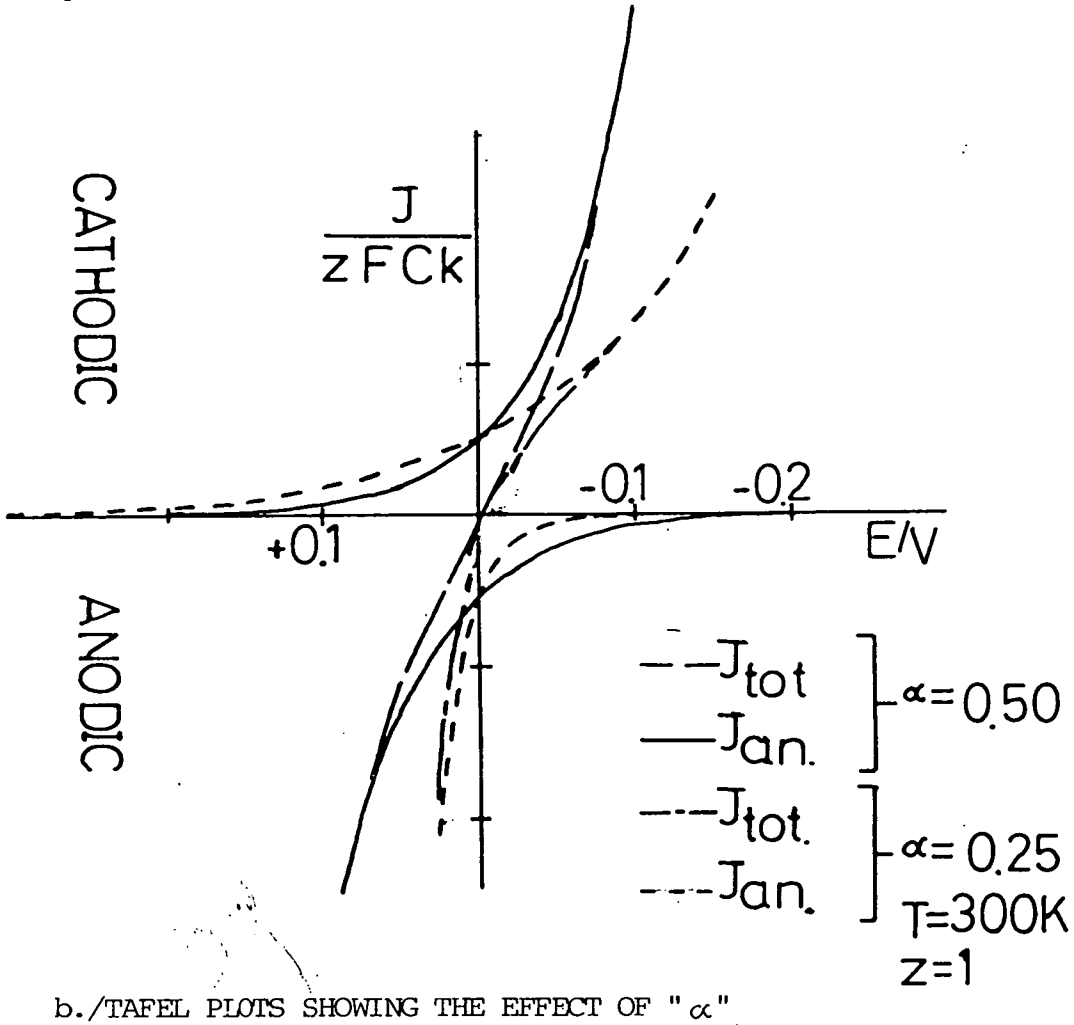

b./TAFEL PLOTS SHOWING THE EFFECT OF "α"

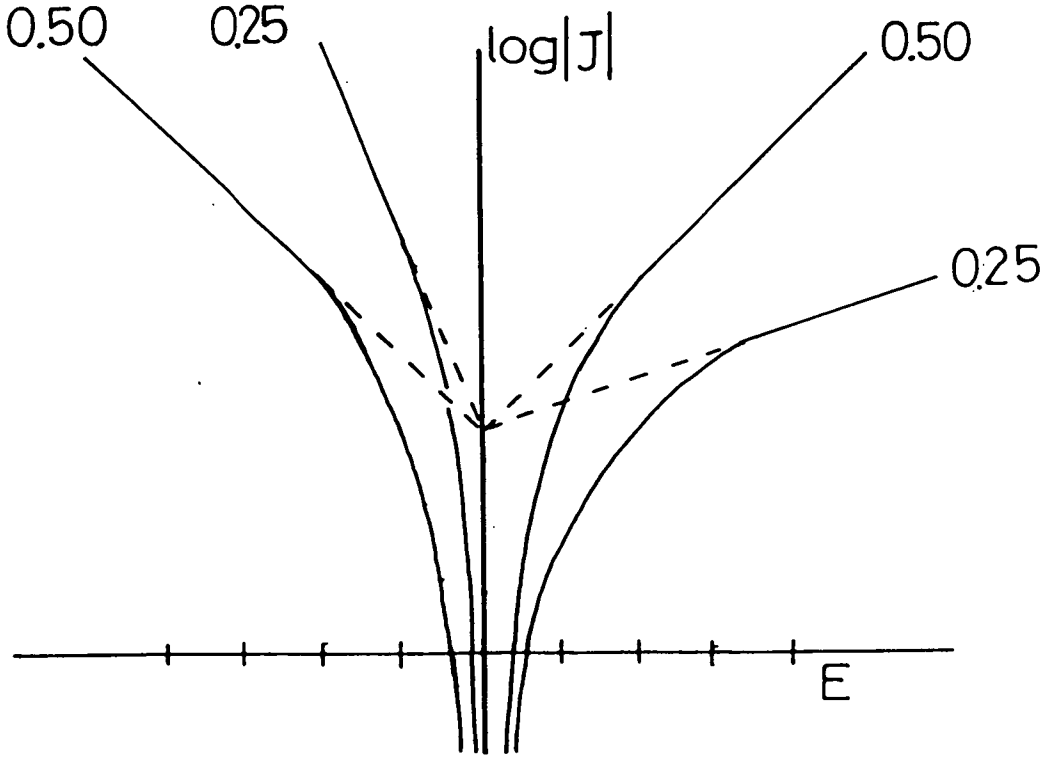

Similarly,

$$J_{AN} = k'_{AN}\, C_{Red} \exp\ (1-\alpha)zFE\ /\ RT \qquad 2.2.10a$$

$$\log_{10} I_{AN} = \log_{10} zAFk'_{AN} C_{Red} + \frac{1}{2.3}(1-\alpha)\frac{zFE}{RT} \qquad 2.2.10b$$

Equations 2.2.9b and 2.2.10b are known as Tafel equations and allow α and z to be determined from measurements of I as a function of E. At extreme values of E the current will be predominantly anodic or cathodic and a plot of log I versus E will approach linearity, allowing α and z to be obtained from the slope, and k'_{AN} and k'_{CAT} to be found from the intercept on the $\log_{10} J$ axis (Fig 2.2).

The analysis above applies principally to case (1), i.e. where both Red and Ox are soluble. It could easily be adapted, however, to a surface process in which case either C_{ox} or C_{Red} must be replaced by a surface concentration or activity. For the case of a dissolving metal or the discharge of ions onto a surface composed of the parent metal this is not difficult, since the surface concentration or activity is constant. However, for dissolution of a compound electrode, or deposition onto a second phase, this is no longer the case and k' may vary with surface concentration. Other complications arise for consecutive reactions, where there is no well-defined rate-determining step, and for competing reactions[3].

2.3 Junction Potentials

As a general rule there is a difference in potential associated with any boundary between chemically-distinct phases. The potential difference between an electrode and a contacting electrolyte was considered in section 1. However, in a cell there will usually be other potential differences that are associated with the presence of the salt bridge and also of the contacts between the external circuit and the electrodes. The latter junctions will either be of the metal-metal type exploited in thermocouples or, if the electrode is a semi-conductor, of the Schottky type[4]. The potential difference can be found by an identical procedure used to establish equation 2.1.4, i.e. by equating the electrochemical potential of the electrons (μ_e) in the two phases.

$$\phi_I - \phi_{II} = \frac{1}{F}(\mu_e^{II} - \mu_e^{I}) \qquad 2.3.1$$

For metal-metal junctions, the junction potential is usually of the order of a few millivolts and can usually be ignored. For a semiconductor-metal junction, the junction potential may be sufficiently high to produce a rectifying contact which will effect the I-V characteristics of the entire cell.

In the cell of Fig 2.1 there will be a potential difference across the salt bridge, the purpose of which is to prevent mixing of the M^{m+} and N^{n+} solutions whilst at the same time allowing a current to flow. The salt bridge takes various forms from a simple porous partition, to an ionically conducting gel that bridges two separate containers. At the junction between two ionic conductors containing different mobile ions, an electric potential gradient appears because of the different diffusion rates of the ions that are present. The simple porous partition is an example of such a junction, whilst the gel bridge gives rise to two such junctions. If no current flows through the junction then

$$\sum_i J_i = 0 \qquad J_i \text{ is current density of species i.}$$

$$\sum_i z_i F j_i = 0 \qquad 2.3.2$$

where j_i is the mass flux of species i and is given by the Nernst Planck

Equation

$$j_i = -U_i RT \frac{da_i}{dx} - z_i F U_i a_i \frac{d\phi}{dx} \qquad 2.3.3$$

$$U_i = \frac{D_i}{RT} \qquad 2.2.4$$

where D_i is the diffusion coefficient. Substitution of 2.3.3 into 2.3.2 yields

$$\frac{d\phi}{dx} = \frac{-RT}{F} \frac{\Sigma_i z_i U_i \frac{da_i}{dx}}{\Sigma_j z_j^2 U_j a_j} = \frac{-RT}{F} \frac{\Sigma_i z_i U_i a_i \frac{d \log_e a_i}{dx}}{\Sigma_j z_j^2 U_j a_j} \qquad 2.3.5$$

If the substitution

$$t_i = \frac{z_i^2 U_i a_i}{\Sigma_j z_j^2 U_j a_j} \qquad 2.3.6$$

is made, 2.3.5 simplifies to

$$\frac{d\phi}{dx} = \frac{-RT}{F} \sum_i \frac{t_i}{z_i} \frac{d \log_e a_i}{dx} \qquad 2.3.7$$

The quantity t_i is known as the transport number and represents the fraction of the current carried by the species i.

The junction potential is then given by

$$\Delta\phi_L = \phi_{x_2} - \phi_{x_1} = \frac{-RT}{F} \int_{x_1}^{x_2} \Sigma \frac{t_i}{z_i} d \log_e a_i \qquad 2.3.8$$

This potential is often referred to as a liquid junction potential since it was for this case that equation 2.3.8 was originally developed. To preserve generality however, it will be referred to as a diffusion potential. Various solutions to equation 2.3.8 have been proposed. General solutions that make no assumptions on the distribution of ions within the junction were proposed by Planck[5] and much later by Schlogl[6]. Planck's solution is not convenient to use as it results in an implicit equation. A frequently-used expression for $\Delta\phi_L$ involves the Henderson[7] approximation in which it is assumed that concentrations vary linearly

across the junction, i.e.

$$C_i(x) = C_i(0) + [C_i(L) - C_i(0)] \frac{x}{L} \qquad 2.3.9$$

where L is the width of the junction. Equation 2.3.9 can be substituted into 2.3.8 to give the Henderson formula

$$\Delta\phi_L = -\frac{RT}{F} \frac{\sum_i z_i U_i [C_i(L) - C_i(0)]}{\sum_i z_i^2 U_i [C_i(L) - C_i(0)]} \log_e \frac{\sum_i z_i^2 U_i C_i(L)}{\sum_i z_i^2 U_i C_i(0)} \qquad 2.3.10$$

The Henderson formula applies only to a time invariant junction but if this limitation is accepted it predicts values to within 1-2 mV of the accepted values[8]. This accuracy together with its convenience makes it the most widely used expression for $\Delta\phi_L$. In addition to solutions of an entirely general form for 2.3.8, there are also solutions for the particularly simple situation of a single electrolyte at different concentrations on either side of the junction.

In addition to the case where the junction potential results from the different diffusion rates of the ions, there is also the possibility that the passage of one or more ions through the junction is stopped completely; the potential resulting from this situation is known as a Donnan potential[9] $\Delta\phi_D$. Two basic cases for Donnan equilibria can be distinguished:

(i) Common Diffusible Ion.

(ii) Common Non-diffusible Ion.

The simplest example of (i) occurs where a salt BX is on one side of the junction while BY is on the other, and B and X can diffuse through the junction but Y cannot. If the two sides of the junction are designated by I and II, then for electroneutrality -

$$C_B^I = C_X^I \qquad 2.3.11$$

and $$C_B^{II} = C_X^{II} + C_Y^{II} \qquad 2.3.12$$

For equilibrium

$$C_B^I C_X^I = C_B^{II} C_X^{II} \qquad 2.3.13$$

from which

$$(C_X^I)^2 = C_B^{II} C_X^{II} \qquad 2.3.14$$

Equation 2.3.12 shows that

$$C_B^{II} > C_X^{II} \qquad \text{and therefore}$$

$$C_X^I > C_X^{II}$$

The non-uniform distribution of X and B will give rise to a potential difference of the form:

$$\Delta\phi_D = \frac{RT}{F} \log_e \frac{C_M^I}{C_M^{II}} = \frac{RT}{F} \log_e \frac{C_X^{II}}{C_X^I} \qquad 2.3.15$$

The case of a common non-diffusible ion and more complicated examples involving more than two salts are dealt with in a precisely analagous manner[9].

2.4 Membrane Potentials and Ion Selective Electrodes.

It has long been known that a potential difference often develops between two solutions of differing composition that are separated by an ionically conducting membrane. The origin of this potential is related to the Donnan equilibrium and all membranes that exhibit this property are permeable only to certain ions. Everett[10] has described a simple derivation of membrane potentials assuming them to be a limiting form of the liquid junction potential. The equation derived by Everett is valid only for a single salt; the cell potential, including the effect due to the liquid junction, is given by

$$E = (1-t)\frac{2RT}{zF}\left[\log_e \frac{C_2}{C_1} + \frac{1}{2}\log_e \frac{\gamma_M^{II}\,\gamma_X^{II}}{\gamma_M^{I}\,\gamma_X^{I}}\right] \qquad 2.4.1$$

where t is the transport number for either M or X (since only two ions are present, one value of t is sufficient to describe the entire process). If t=0 for one of the ions, then 2.4.1 reduces to

$$E_M = \frac{2RT}{zF}\left[\log_e \frac{C_2}{C_1} + \frac{1}{2}\log_e \frac{\gamma_M^{II}\,\gamma_X^{II}}{\gamma_M^{I}\,\gamma_X^{I}}\right] \qquad 2.4.2$$

The membrane potential can be measured by placing a suitable reference electrode in the solution on either side of the membrane. This configuration is derived directly from that shown in Fig 2.1 and if the potentials of the metal-metal ion half cells can be independently measured then the potential across the salt bridge can be found from the overall cell potential.

Although Everett's analysis highlights the importance of membranes that are permeable only to certain ions, the fact that it is restricted to the case of a single salt means that it cannot explain the important property that certain membranes develop a potential which depends only on the concentration of one type of ion and which is unaffected by the presence and relative amounts of other ions. Such membranes form the

basis of Ion Selective Electrodes (ISEs). As with the term 'Reference Electrode' the name 'Ion Selective Electrode' is a misnomer, particularly when applied to the membrane type described here; they are in fact complete cells.

The complete membrane potential is given by

$$\Delta\phi_M = \Delta\phi_D(x=L) + \phi(L) - \phi(0) + \Delta\phi_D(x=0) \qquad 2.4.3$$

where the $\Delta\phi_D$'s are the Donnan potentials at either side of the membrane and $(\phi(L) - \phi(0))$ is the diffusion potential across the membrane. The diffusion potential can be calculated from equation 2.3.8 providing all the mobile ions in the membrane have been identified. In general only certain ions will be mobile in the membrane (often only one type) and these may be different from the species in the solution. The high selectivity of the membrane derives from the fact that the concentrations of the mobile species are fixed at the boundaries of the membrane by a highly selective ion exchange reaction occuring at the surface.

$$J^+(sol) + K^+(mem) \rightleftharpoons J^+(mem) + K^+(sol)$$

characterised by an equilibrium constant

$$K_{JK} = \frac{C_J(mem)\ a_K(sol)}{C_K(mem)\ a_J(sol)} \qquad 2.4.4$$

$$= \exp\frac{1}{RT}\left(\tilde{\mu}_J(sol) + \tilde{\mu}_K(mem) - \tilde{\mu}_J(mem) - \tilde{\mu}_K(sol)\right) \qquad 2.4.5$$

At equilibrium

$$\tilde{\mu}_J(sol) = \tilde{\mu}_J(mem) \qquad 2.4.6$$

hence

$$\phi(\text{sol}) - \phi(\text{mem}) = \frac{1}{F}(\mu_J(\text{mem}) - \mu_J(\text{sol})) \qquad 2.4.7$$

$$= \frac{1}{F}(\mu_K(\text{mem}) - \mu_K(\text{sol}))$$

By expanding 2.4.7

$$\phi_{SOL} - \phi_{MEM} = \frac{1}{F}[\mu_J^\circ(\text{mem}) - \mu_J^\circ(\text{sol})] + \frac{RT}{F}\log_e \frac{a_J(\text{sol})}{C_J(\text{mem})}$$

$$= \frac{1}{F}[\mu_K^\circ(\text{mem}) - \mu_K^\circ(\text{sol})] + \frac{RT}{F}\log_e \frac{a_K(\text{sol})}{C_K(\text{mem})} \qquad 2.4.8$$

Equation 2.4.8 gives an expression for the Donnan potentials in 2.4.3. The diffusion potential ($\phi(L) - \phi(0)$) is found from equation 2.3.8. If it is assumed that the only species that are mobile in the membrane are J and K and that the Henderson formula (2.3.10) can be used, then this takes the simple form:

$$\phi(L) - \phi(0) = \frac{RT}{F}\log_e\left[\frac{\frac{U_J}{U_K}C_J(0) + C_K(0)}{\frac{U_J}{U_K}C_J(L) + C_K(L)}\right] \qquad 2.4.9$$

Substituting 2.4.8 and 2.4.9 into 2.4.3 gives

$$\Delta\phi_M = \frac{RT}{F}\log_e \frac{C_J(L)\, a_J(\text{sol } 0)}{C_J(0)\, a_J(\text{sol } L)} - \frac{RT}{F}\log_e\left[\frac{\frac{U_J}{U_K}C_J(L) + C_K(L)}{\frac{U_J}{U_K}C_J(0) + C_K(0)}\right] \qquad 2.4.10$$

Using 2.4.4, the concentrations and activities can be written in terms of the ion exchange equilibrium constant K_{JK} to give

$$\Delta\phi_M = \frac{RT}{F} \log_e \left[\frac{a_K(\text{sol O}) + K_{KJ}\frac{U_J}{U_K}\, a_J(\text{sol O})}{a_K(\text{sol L}) + K_{KJ}\frac{U_J}{U_K}\, a_J(\text{sol L})} \right] \qquad 2.4.11$$

The terms $K_{KJ}U_J/U_K$ are known as the potentiometric selectivity coefficients K^{POT}_{KJ}. Equation 2.4.11 is often referred to as the Nikolsky equation . A more general form of 2.4.11 has been obtained by Conti and Eisenmann[11].

$$\Delta\phi_M = \frac{RT}{z_1F} \log_e \frac{a_1(\text{sol I}) + \sum_{i=1}^{n} K^{POT}_{1i}\, a_i(\text{sol I})^{z_1/z_i}}{a_1(\text{sol II}) + \sum_{i=1}^{n} K^{POT}_{1i}\, a_i(\text{sol II})^{z_1/z_i}} \qquad 2.4.12$$

It should be noted that the symmetry of the membrane configuration results in the particularly simple form of equations 2.4.11 and 2.4.12. If this symmetry is removed by replacing one of the solution membrane boundaries with a metal-membrane interface then equation 2.4.3 becomes

$$\Delta\phi = \Delta\phi_D(L) + \phi(L) - \phi(0) + \Delta\phi_I(0) \qquad 2.4.13$$

where the thickness of the membrane is L, the metal membrane junction is at x = 0 and the junction potential at this point is $\Delta\phi_I$.

It is also worth considering the possibility of using a purely electronic or a mixed conductor as the ion selective membrane. Since the electron can be considered as a charged chemical species, it can be treated in the same way as an ion. Thus, equations 2.4.11 and 2.4.12 apply and the ion exchange process becomes a redox reaction.

$$\text{Red (sol)} \leftrightharpoons \text{Ox} + e^-(\text{mem})$$

Obviously, Ox may either be associated with the surface or may be a species in solution. In ISE applications, electronic conductors are

useful only if the electron concentrations at the membrane boundary are affected by only one species. In other words, the Redox process must be highly specific, in the same way that the ion exchange process occuring at the surface of an ionic conductor must be highly specific. In fact the relation between an ionically conducting membrane and a double cell with the two cells connected by a metallic (electronic) conductor has been considered by Everett[10]. Generalized forms of these cells may be represented as

$$M|\ M^{z+} \vdots\vdots\ M^{Z+}|M$$
$$M|\ M^{z+}|M - M\ |M^{z+}|M$$

Consideration of equation 2.4.11 or the more general 2.4.12 shows that a selective sensor i.e. one that is only affected by the varying concentration of one type of ion, is obtained when either the potentiometric selectivity coefficient is much greater or much less than unity. In the former case, a membrane selective to J is obtained and in the latter case, a K selective membrane results.

$$K_{KJ}^{POT} = K_{KJ}\frac{U_J}{U_K} \qquad 2.4.14$$

A high value of K_{KJ}^{POT} requires one or more of the following criteria to be satisfied.

(1) K_{KJ} is large, so that the ion exchange equilibrium

$$J^+(sol) + K^+(mem) \rightleftharpoons J^+(mem) + K^+(mem)$$

is well to the right.

(2) U_J is large, so that J^+ is a highly mobile species.

(3) U_K is small, so that K^+ is a relatively immobile species.

Finally, it should be noted that J and K need not be chemically distinct species; some membranes, notably Ag_2S and LaF_3 have the same mobile ion as the species they sense.

2.5 Solid State Ion Selective Electrodes Using Ionic Conductors

In the present work, the term 'solid-state', as applied to ion-selective electrodes (ISEs), implies that the membrane surface which is not exposed to the test solution is in direct contact with a solid conductor, usually an electronic conductor. Thus, the so-called filling solution of the conventional membrane electrode is eliminated and the implication of the term solid-state in this context is that the electrode could, if necessary, be fabricated by the techniques used in solid state electronic technology, to be discussed later. There may be an intermediate layer of a mixed electronic/ionic conductor between the membrane material and the purely electronic back contact. The term 'solid-state' is also often applied to conventional ISEs in which the membrane is made from a crystalline compound (e.g. LaF_3 for F^- determination). This is a rather inappropriate use of the phrase however as the principles and technology of this type of device are basically the same as that of any other conventional membrane electrode.

Although membrane materials are known which are selective to a wide range of anions and cations the membrane configuration of conventional ISEs does have several practical disadvantages. The need for a filling solution and internal reference makes the device inherently bulky and it is often delicate and expensive to manufacture. These undesirable characteristics are undoubtedly responsible for the relatively restricted application of ISEs to problems of on-line monitoring and control. The development of a range of solid-state ISEs would avoid these problems and would also offer the possibility of integrating ISEs with data-processing circuitry, this is discussed in section 3.7.

In a solid-state device, the contact must play the same role as the filling solution and internal reference electrode in a membrane ISE; that is to establish a stable reproducible potential at the back contact of the sensing material. Fig 2.3c compares the potential distributions in the cells corresponding to a membrane ISE and a solid state ISE, in which stable potentials have been established.

2.3 POTENTIAL AND CHARGE DISTRIBUTIONS IN A SOLID STATE IONIC CONDUCTOR.

(Calculated by the method proposed in section 2.5)

a./ POTENTIAL DISTRIBUTION

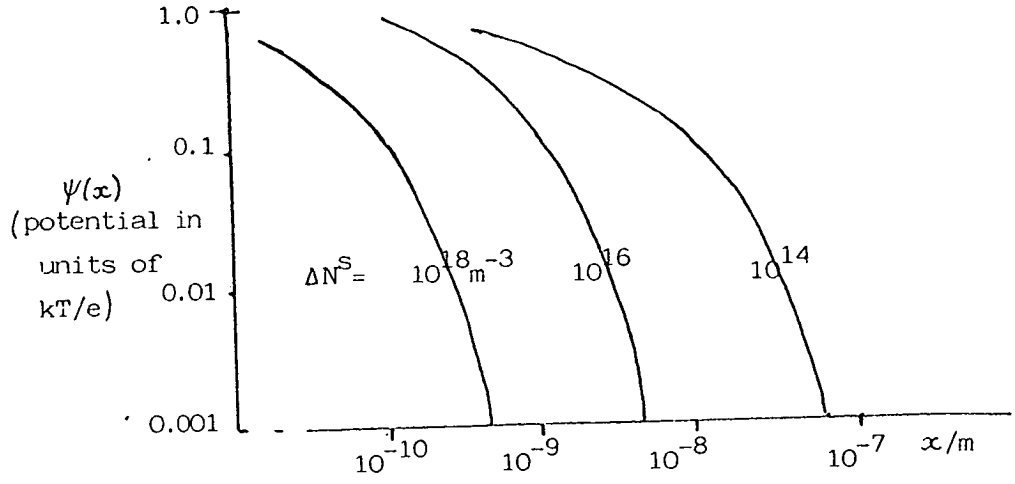

b./ DISTRIBUTION OF MOBILE ION CONCENTRATION

(note: the charge density at x is directly proportional to ΔN(x) -the excess number of mobile charge carriers)

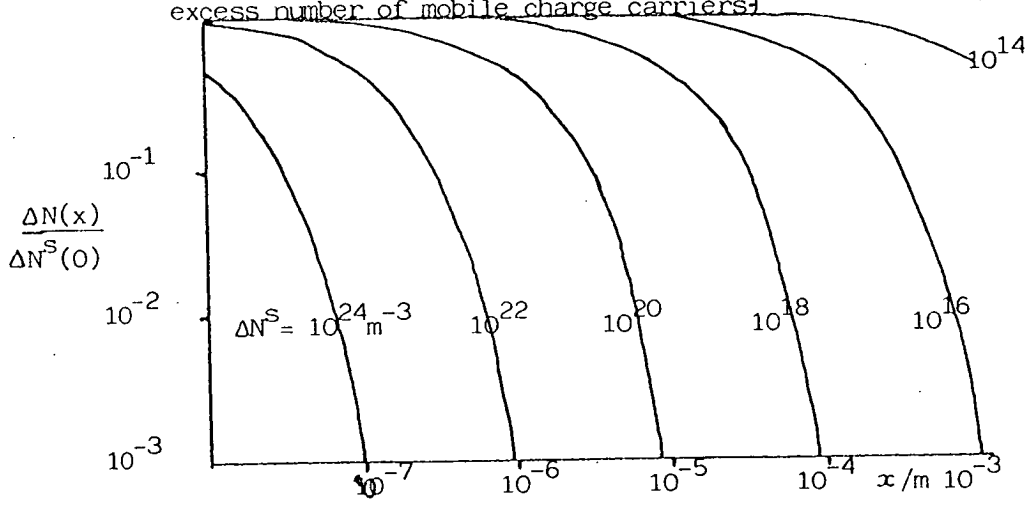

c./ POTENTIAL DISTRIBUTIONS THROUGH COMPLETE CHEMICAL CELLS USED AS ISEs.

i/membrane configuration

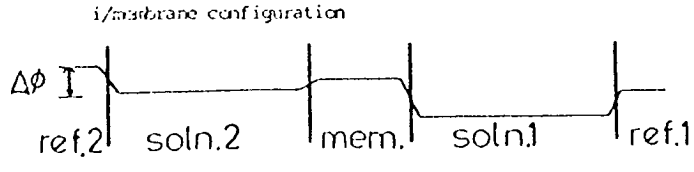

ii/solid state configuration

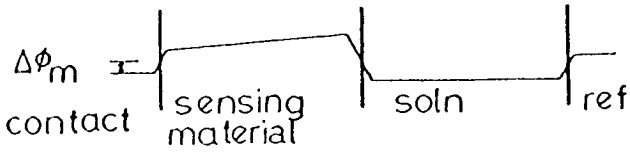

The main conceptual difficulty with the solid state configuration is that the symmetrical arrangement of the membrane, that leads to an expression for $\Delta\phi_M$ of the form

$$\Delta\phi_M = \Delta\phi_D(1) + \phi(L) - \phi(0) + \Delta\phi_D(2) \qquad 2.5.1$$

is lost. It is proposed that for the asymmetrical solid state structure $\Delta\phi_M$ should be given by

$$\Delta\phi_M = \Delta\phi_D(1) + \phi(L) - \phi(0) + \Delta\phi_I \qquad 2.5.2$$

in which $\Delta\phi_I$ is the potential difference across the sensing material-back contact interface. In section 4 it was shown that equation 2.5.1 leads to a compact expression for $\Delta\phi_M(a_J, a_K)$; this will no longer be the case for the solid state structure.

Four basic forms of the solid state structure can be envisaged. Using the following representation these are:

	solution	ionic conductor	electronic conductor
A	M^{z+}	M^{z+}	M
B	M^{z+}	M^{z+}	C
C	M^{z+}	N^{n+}	N
D	M^{z+}	N^{n+}	C

where M^{z+}, N^{n+} are the mobile ions in the sensing materials and M, N, C are the contacting materials. In general each configuration must be dealt with separately. This complication does not arise for the case of a membrane ISE because the filling solution will always contain the ion of interest at a well defined concentration (or activity). In solid-state electrodes it is not always possible to contact the sensing material with the same metal as the mobile ions, and configurations B and D must be invoked.

Configurations A and B have been considered by Koebel[12] for the special case of an Ag^+ electrode based on Ag_2S (this will be discussed in section 3.5). If M^{Z+} is solely responsible for electrical conduction in the sensing material (i.e. $t_{MZ+} = 1$), then at equilibrium the diffusion rates expressed by the U_i terms in the membrane potential, can be ignored. Furthermore if the distribution of M^{Z+} in the sensing material is only affected by the concentration in aqueous solution then for the surface of the sensor it is possible to write the condition

$$\tilde{\mu}_{M^{Z+}}^{SOL} = \tilde{\mu}_{M^{Z+}}^{SM} \qquad 2.5.3$$

from which

$$\phi_M - \phi_{SOL} = \frac{1}{zF}\left(\mu_{M^{Z+}}^{O,SOL} - \mu_{M^{Z+}}^{O,SM} - RT \log_e \frac{a_{M^{Z+}}^{SM}}{a_{M^{Z+}}^{SOL}} \right) \qquad 2.5.4$$

Subscripts SM and SOL refer to the sensing material and the solution respectively. If the sensing material is a perfect conductor, no electrostatic field can exist within it and thus no potential difference can occur across it (the effect of finite resistance of the membrane is considered later para. 5.5). The distribution of M^{Z+} ions will be uniform except at the surface. At the back contact in A the potential difference has the same origin as the potential difference between a metal and a solution of its ions.

$$\Delta\phi = \Delta\phi_O + \frac{RT}{zF} \log_e \frac{a_{M^{Z+}}}{a_{M^{Z+}}^{O}} \qquad 2.5.5$$

If the distribution of M^{Z+} ions is uniform then the overall potential difference between the solution and the back contact is given by the algebraic sum of equation 2.5.4 and equation 2.5.5. It should be noted that in equation 2.5.4 the activity of M^{Z+} in the sensing material is the same as in equation 2.5.5, even if there is an excess or deficit of M^{Z+} at the surface. This is because the overall potential drop at the solution interface is given by the sum of the potential

differences between the solution and the surface, and the surface and the bulk.

$$\phi_M - \phi_{SOL} = (\phi_M - \phi_M^{SURFACE}) + (\phi_M^{SURFACE} - \phi_{SOL}) \qquad 2.5.6$$

$$= \frac{RT}{zF} \log_e \frac{a_{M^{z+}}^{SM}}{a_{M^{z+}}^{SM,S}} + RT \log_e \frac{a_{M^{z+}}^{SM,S}}{a_{M^{z+}}^{SOL}}$$

$$= \frac{RT}{zF} \log_e \frac{a_{M^{z+}}^{SM}}{a_{M^{z+}}^{SOL}} \qquad 2.5.7$$

where $a_{M^{z+}}^{SM,S}$ is the surface activity of M^{z+}.

2.5.5 Thus far it has been assumed that the ionic conductor is perfect, thus giving rise to a uniform distribution of M^{z+}. In practice the membrane materials used in ISEs rarely have conductivities greater than $10^{-3}\,\Omega^{-1}cm^{-1}$ and lanthanum fluoride has a conductivity of about $10^{-7}\,\Omega^{-1}cm^{-1}$. An implicit expression for the M^{z+} distribution and potential distribution within an imperfect conductor can be derived in the following way. If the conductor is assumed to balance the charge due to the mobile M^{z+} ions, by fixed mono-valent anionic sites X^-, then the charge density $\psi(x)$ at a point x is given by

$$\rho(x) = e(zN_{M^{z+}}(x) - N_{X^-}) \qquad 2.5.8$$

where $N_{M^{z+}}(x)$ is the particle density of M^{z+} ions at x, e is the charge on the electron and N_{X^-} is the (constant) concentration of X^- sites. If the potential is $\psi(x)$, application of Poisson's equation gives

$$\frac{d^2\psi(x)}{dx^2} = -\frac{e}{\epsilon}(zN_{M^{z+}}(x) - N_{X^-}) \qquad 2.5.9$$

The electrostatic potential of an ion at potential $\psi(x)$ is

$$U = \frac{ze\psi(x)}{kT} \qquad \ldots 2.5.10$$

which leads to

$$\frac{d^2\psi}{dx^2} = \frac{-e}{\epsilon}\left[zN^{s}_{M^{z+}} \exp\left(\pm \frac{ze\psi(x)}{kT}\right) - N_{x^-}\right] \qquad \ldots 2.5.11$$

where $N^{s}_{M^{z+}}$ is the concentration of M^{z+} at the surface of the sensing material. If $N^{s}_{M^{z+}}$ is re-written as

$$N^{s}_{M^{z+}} = N^{o}_{M^{z+}} \pm \Delta N^{s}_{M^{z+}} \qquad \ldots 2.5.12$$

where $N^{o}_{M^{z+}}$ is the concentration of M^{z+} in the neutral bulk material and $\Delta N^{s}_{M^{z+}}$ is the surface excess (or deficit) of M^{z+} then equation 2.5.11 can be re-written

$$\frac{d^2\psi}{dx^2} = \frac{-e}{\epsilon}\left[z\Delta N^{s}_{M^{z+}} \exp\left(\pm \frac{ze\psi(x)}{kT}\right)\right] \qquad \ldots 2.5.13$$

since $zN^{o}_{M^{z+}} = N_{X^-}$

If $\psi << \frac{kT}{ze}$, equation 2.5.13 can be approximated by the first two terms of a Taylor expansion to give

$$\frac{d^2\psi}{dx^2} = \frac{-e}{\epsilon_o \epsilon_r}\left[z\Delta N^{s}_{M^{z+}} \pm \frac{ze\,(x)\Delta N^{s}_{M^{z+}}}{kT}\right] \qquad \ldots 2.5.14$$

for which the complete solution is

$$\psi(x) = \frac{kT}{e} + A \exp(Kx) + B \exp(-Kx) \qquad \ldots 2.5.15$$

where $K = \left(\frac{ze^2\Delta N^{s}_{M^{z+}}}{\epsilon_o \epsilon_r kT}\right)^{\frac{1}{2}}$ $\qquad \ldots 2.5.16$

and A and B are defined by the boundary conditions of the problem.

The charge distribution is found by substituting equation 2.5.15 back into the Poisson equation to give

$$\frac{\rho(x)}{\epsilon_0\epsilon_r} = \frac{(ze^2\Delta N^s_{Mz+})B \exp(-Kx)}{kT\epsilon_0\epsilon_r} \qquad ...2.5.17$$

The distance required for $\rho(x)$ to fall to e^{-1} of its value at the surface is K. The constant B can be found from the boundary condition

$$\frac{\rho(0)}{\epsilon_0\epsilon_r} = \frac{ze\Delta N^s_{Mz+}}{\epsilon_0\epsilon_r} \qquad ...2.5.18$$

from which $B = \frac{kT}{e}$

Thus

$$\rho(x) = ze\Delta N^s_{Mz+} \exp(-Kx) \qquad ...2.5.19$$

$$K = \frac{(1.86\times10^{-15}\ z\Delta N^s_{Mz+})^{\frac{1}{2}}}{T\epsilon_0\epsilon_r} \qquad ...2.5.20$$

For a temperature of 300K and a dielectric constant of 10^2, equation 2.5.20 gives

$$K = \frac{2\times10^{-10}\ z^{\frac{1}{2}}\ (\Delta N^s_{Mz+})^{\frac{1}{2}}}{\epsilon_0} \qquad ...2.5.21$$

Plots of $\rho(x)$ and $\psi(x)$ as a function of x are shown in fig. 2.3. If the Taylor approximation cannot be used the problem becomes considerably more difficult[13,14].

5.6. It is clear from fig. 2.3 that for most ionic conductors, if the thickness is in excess of 1μm the excess charge decays to zero at the back contact, in which case $\Delta\phi_I$ is unaffected by the activity of M^{z+} in the

solution and the back-contact presents a stable reference, once equilibrium is established. If the back-contact is of the same material as the mobile ion the equilibria will be of the form

$$M(C) \leftrightharpoons M^{z+}(SM) + ze^{-}$$

where C is the contact and SM the sensing material. Then

$$\tilde{\mu}_{M^{z+}} + ze\tilde{\mu}_{e^-} = \mu^{o}_{M} \qquad \ldots 2.5.22$$

and

$$\Delta\phi_I = \phi(SM) - \phi(C)$$

$$= \mu^{o}_{M} - z\mu_{e^-} - \mu^{o}_{M^{z+}} + RT \log_e \left[\frac{\gamma_{M^{z+}}(N_{M^{z+}} + \Delta N_{M^{z+}})}{N^{o}_{M^{z+}}}\right] \qquad \ldots 2.5.23$$

If $\Delta N_{M^{z+}}(x)$ decays to zero at the contact, $\Delta\phi_I$ is constant, otherwise $\Delta N_{M^{z+}}(x)$ depends on $N^{s}_{M^{z+}}$ and $\Delta\phi_I$ will vary. The consequence of a varying $\Delta\phi_I$ is that an additional solution concentration dependent term is introduced into the expression for $\Delta\phi_M$ which will thus no longer be related to concentration in a Nernstian way. Depending on whether $\Delta\phi_I$ increases or decreases with increasing solution activity a sub or super nernstian response can occur; this is illustrated in fig. 2.4. Since diffusion and reaction rates in the solid state are likely to be slow, $\Delta\phi_I$ may drift for an unacceptable length of time whilst an equilibrium distribution is established.

5.7. In many cases the type A structure is not practical because the metal M is prone to rapid oxidation. In that case a second metal, that does not react with the sensing material, can be used and $\Delta\phi_I$ is the result of a redox reaction. Electrons are exchanged between the contact and a couple comprising the ions M^{z+} and a reduced form of M.

$$M^{z+}(m) + (z-x)e^{-}(c) \leftrightharpoons M^{x+}(m)$$

24 a. Super-Nernstian

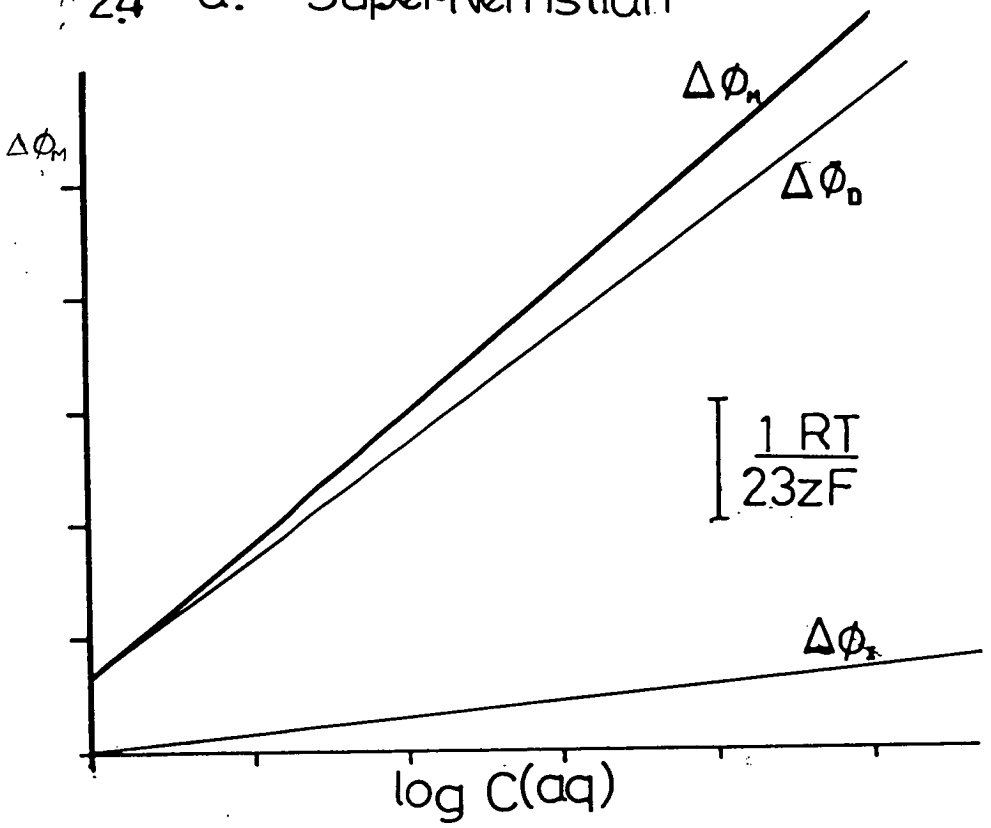

b/. Sub-Nernstian

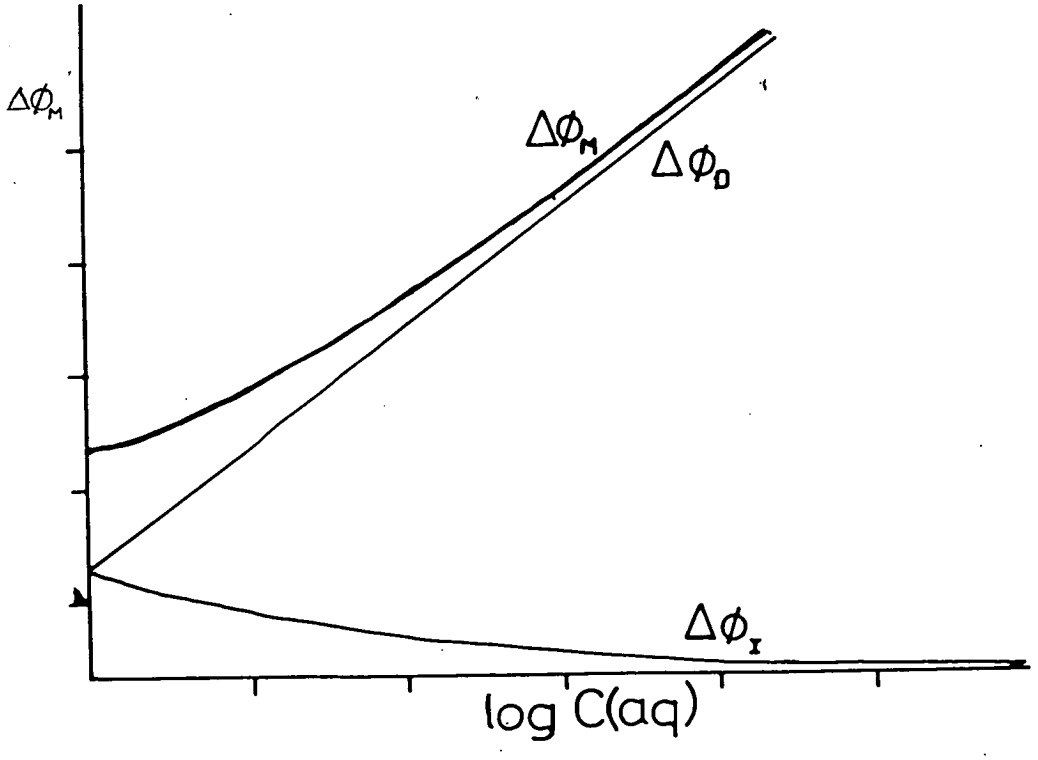

x may be zero. The problem here is that all redox couples, including those due to impurities, can exchange electrons and thus affect $\Delta\phi_I$. However, providing the impurity levels are constant their contribution should also be constant and $\Delta\phi_I$ is fixed.

5.8. So far the sensing material has been assumed to conduct electricity by the movement of only one type of ion. If more than one type of mobile charge carrier is present, then their relative numbers and diffusion rates must be taken into account. A method of doing this is proposed below

Poisson's equation is written

$$\frac{\partial^2\Psi}{\partial x^2} = -\frac{1}{\epsilon}\sum_i z_i N_{i0} e \exp\left(\frac{-z_i e\Psi}{kT}\right) \qquad \ldots 2.5.24$$

where i refers to any mobile charge carrier. The time dependence of the concentrations (N_i) is given by a form of the Nernst Planck equation[15].

$$\frac{\partial N_i}{\partial t} = U_i RT \frac{\partial^2 N_i}{\partial x^2} + F\frac{\partial}{\partial x}\left(N_i \frac{\partial\Psi}{\partial x}\right) \qquad \ldots 2.5.25$$

Under open circuit conditions, no current flows so that

$$\sum_i \frac{\partial N_i}{\partial t} = 0 \qquad \ldots 2.5.26$$

$$\Rightarrow \quad \sum_i \left(U_i RT \frac{\partial^2 N_i}{\partial x^2} + F\frac{\partial}{\partial x}\left(N_i \frac{\partial\Psi}{\partial x}\right)\right) = 0$$

Poisson's equation can be integrated once, if both sides are multiplied by $\frac{d\Psi}{dx}$

$$2\frac{d\Psi}{dx}\frac{d^2\Psi}{dx^2} = -\frac{2}{\epsilon}\sum_i z_i e N_{i0}\left[\exp(-z_i e/kT) - 1\right] \qquad \ldots 2.5.27$$

which leads to

$$\frac{d\psi}{dx} = \left(\frac{2kT}{\epsilon}\right)^{\frac{1}{2}} \left(\sum_i z_i e N_{i0} \exp(-z_i e\psi/kT) - 1\right)^{\frac{1}{2}} \quad \ldots 2.5.27$$

Equation 2.5.27 can be substituted into equation 2.5.26 to give an implicit formula for $N_i(x)$ and $\psi(x)$

$$RT\sum_i U_i \frac{\partial^2 N_i(x)}{\partial x^2} + F\sum_i \frac{\partial}{\partial x}\left(N_i \left(\frac{2kT}{\epsilon}\right)^{\frac{1}{2}} \left(\sum_i z_i e N_{i0} \exp\left(-\frac{ze\psi}{kT}\right) - 1\right)^{\frac{1}{2}}\right) = 0 \quad \ldots 2.5.28$$

Equation 2.5.28 can only be solved numerically and even then would require the development of suitable algorithms. In certain cases ψ may be assumed to be of the exponential form calculated in equation 2.5.16 (this corresponds to $\psi << kT/e$) in which case the ionic distributions could be calculated providing the diffusion coefficients are known. Effects similar to those described in section 2.4 for interfering ions are to be expected.

The electron represents an important special case of the presence of a second charge carrier, this is because

1. Most ionic conductors exhibit some electronic conductivity,
2. The chemical potential of the electron is usually strongly dependent on the exact composition of the substance.

Koebel, Ibl and Frei[16] investigated the dependence of electronic conductivity on composition in $Ag_{2+\delta}S$ and found the electronic conductivity varied from $1.35 \times 10^{-3}\Omega^{-1}cm^{-1}$ in Ag_2S equilibrated with Ag to $0.01 \times 10^{-3}\Omega^{-1}cm^{-1}$ in Ag_2S equilibrated with S. Wagner and Wagner[17] made similar investigation on Cu_2S. These results suggest that the chemical potential varies with composition and this variation must be taken into account when discussing the electron distribution. Interference to the electrode potential can be expected from redox couples which will affect the electron chemical potential in the sensing material. This is confirmed by the observation of Kolthoff and Sanders[18] that redox couples in solution do not affect the membrane potentials of AgCl membranes, but do affect the electrode potentials of solid state Ag|AgCl systems.

It should also be noted that in general the chemical potentials of all the ions will depend on composition. In all the arguments above it is tacitly assumed that the chemical potentials will not vary significantly over the composition ranges that occur.

At the back contact the electrons contribute to $\Delta\phi_I$ by

$$\Delta\phi_I = \frac{1}{F}(\mu_e^{SM} - \mu_e^c) \qquad \ldots 2.5.24$$

Thus if μ_e^{SM} is affected by a redox couple in solution, interference will result. Moreover if μ_e^{SM} is affected by the value of $\Delta N_{Mz+}^{SM}(x)$ at the back contact this can contribute another concentration dependent term to $\Delta\phi_I$.

5.9. Discussion of configurations C and D follows the same form as for A and B except that $\Delta N_{Mz+}^{SM,S}$ is then controlled by an exchange reaction. It should be noted that whilst attention has been restricted to cationic conductors, the arguments can be extended to anionic conductors for which only configuration analagous to B and D are possible.

5.10. All terms contributing to $\Delta\phi_M$, for any solid state ISE, will be temperature dependent. Since the temperature dependence of each term will differ, complex overall temperature dependences are to be expected[19].

2.6. Solid State Sensors Using Electronic Conductors

In section 2.4 it was noted that it should be possible to extend the analysis of the membrane potential to include electronic conductors, in which case the ion exchange reaction at the surface is replaced by a redox reaction. Koltoff and Saunders[18] compared membrane electrodes using AgCl discs with electrodes in which two Ag contacted AgCl discs were connected back-to-back. The pure AgCl disc electrode was found to be unaffected by redox couples, whereas the potential of the AgCl|Ag|AgCl structure was interfered with. Any metal electrode in a solution of its own ions is a sensor (it is also an electrode as defined in section 1 while the devices discussed in sections 4 and 5 are not). However it will not be ion selective since the half-cell potential will be affected by, -

(a) metal ions (N^{n+}) sufficiently concentrated to lead to the reaction

$$mN^{n+}(aq) + nM \leftrightharpoons nM^{m+} + nN$$

at the surface,
and by,
(b) redox couples exchanging electrons with the surface.

It should be noted that both of these affects will interfere with the response of materials that are usually considered as ionic conductors but show some electronic conductivity. In order to employ electronic conductors in either the membrane or the solid-state configuration, they must only exchange electrons with one couple or species in solution. That is to say, electron levels in the sensing material must only overlap the vacant energy levels of one species in solution. Conversely the filled energy levels of only one species in solution can overlap the vacant levels in the sensing material. Metals have a high density of filled and unfilled states at the surface and can thus readily exchange electrons with most species in solution. The only materials that can satisfy the criteria required for an ion selective electrode are semiconductors. Semiconductors are electronic conductors and if a semiconductor is in contact with an electrolyte the term Ion-Selective Electrode is an acceptable description. Semi-conducting glasses of the type

$Cu_x(As_2X_3)_{100-x}$ [20] ($5 < x < 30$, X-chalcogenide element) are known to be selective to Cu^{2+} and $Fe_x(Se_{60}Ge_{28}Sb_{12})$ [21] has been shown to be selective to Fe^{3+}. It is significant that the electronic sensing materials that have been discovered have been for transition elements which exhibit variable valency, this is a necessary property for electron exchange. Although any metal has at least two oxidation states including zero, the formation of the zero-valent state leads effectively to a metal surface which will result in interference in the ways described above.

Electronically conducting binary sulphides have been considered by Sato[22] who took the special cases of the cells

$$C\,|M\,|M^{Z+}(xm) \;\vdots\vdots\; M^{Z+}(xm),\ X^{Z-}(trace)\,|\,MX_{1+\gamma}\,|M'|C' \qquad \ldots A$$

and

$$C\,|X(Pt)\,|X^{Z-}(ym) \;\vdots\vdots\; X^{Z-}(ym),\ M^{Z+}(trace)\ MX_{1+\gamma}\,|M'|C' \qquad \ldots B$$

where γ is a small variation in stoichiometry. If the half-cells on the left are replaced by a conventional reference electrode (e.g. Ag|AgCl) then a 'chemical sensor' configuration is obtained. Sato pointed out that if $MX_{1+\gamma}$ is a purely electronic conductor then the passage of a current must necessarily alter the surface composition. Considering cell A, if C' is made negative electrons will pass from C' into M' and from M' into $MX_{1+\gamma}$. At the same time M^{Z+} ions will pass across the salt-bridge into the solution in contact with the sensor. At the interface between the $MX_{1+\gamma}$ and the solution the ions will be discharged leading to stoichiometry $M_{1+\delta}X_{1+\gamma}$. Consideration of the free energy versus composition diagram of the MX system leads to the following result:

$$\Delta G = \mu_M^c - \mu_M^o = RT\log_e(a_M)_{MX_{1+\gamma}} \qquad \ldots 2.6.1$$

where ΔG is the free energy change of the reaction

$$MX_{1+\gamma} + \delta M \leftrightharpoons M_{1+\delta}X_{1+\gamma} \qquad \ldots 2.6.2$$

as δ tends to zero. μ_M^c is the chemical potential of M in $MX_{1+\gamma}$, and μ_M^o is the chemical potential of pure M.

The cell potential of A is then given by

$$E = -\frac{\Delta G}{zF} \qquad \ldots 2.6.3$$

$$= -\frac{RT}{zF}\log_e(a_M)_{MX_{1+\gamma}} \qquad \ldots 2.6.4$$

For the case of a general reference electrode 2.6.4 becomes

$$E = E^{REF,O}_{M/M^{z+}} + \frac{RT}{zF}\log_e(a_{M^{z+}})_{SOL} - \frac{RT}{zF}\log_e(a_M)_{MX_{1+\gamma}} \qquad \ldots 2.6.5$$

where $E^{REF,O}_{M/M^{z+}}$ is the standard potential of the M/M^{z+} half-cell relative to the chosen reference electrode. Equation 2.6.5 simplifies to

$$E = E^{REF,O}_{M/M^{z+}} + \frac{RT}{zF}\log_e\frac{(a_{M^{z+}})_{SOL}}{(a_M)_{MX_{1+\gamma}}} \qquad \ldots 2.6.6$$

It is important to note that E depends on $(a_M)_{MX_{1+\gamma}}$ and thus on the exact composition of the electrode. Sato calculated this dependence for the limiting cases of one phase in equilibrium with pure M, pure X or a second binary compound of closely defined composition. It is also important to note that providing M' does not react with $MX_{1+\gamma}$, it is unimportant what metal is used, since it is only involved in electron transfer. However, if it is the same metal M then the exact composition of $MX_{1+\gamma}$ may be defined by equilibration between them. For the case of mixed conductors the same comments apply. For the case of ternary and more complicated materials the same basic conclusions will still apply, but in this case the phase diagram will be more complicated and thus the extension of Sato's method for finding E for the case of limiting compositions is difficult.

In cases where the composition of $MX_{1+\gamma}$ is fixed by equilibration with a second phase, the possibility of both phases giving an electrode potential may arise. The result of such behaviour is discussed in more detail in chapter 4

2.7. Energy Levels of Ions in Solution

7.1. In a redox reaction electrons are transferred between the reduced form of the couple and the electrode, and transfer can occur only between levels of similar energy. For reduction there must be filled levels at the same level as the Ox orbitals in solution, whilst the Red orbitals must be at the same level as unfilled states on the electrode surface. In the case of metal electrodes these criteria are relatively easily met, but for semiconductors and insulators (i.e. for materials with a band gap) the orbital energies of Ox⇌Red may coincide with the gap and in the absence of surface states in the gap no electron transfer can occur. To describe a semiconductor - solution interface a common energy scale on which both the band structure of the semiconductor and the energy levels of the redox couple can be expressed, is needed. For a general redox reaction

$$ze^- + Ox^{(n+z)+} \rightleftharpoons Red^{n+}$$

it is possible to state

$$\tilde{\mu}_{Red} = \tilde{\mu}_{Ox} + z\tilde{\mu}_{e^-}$$

hence

$$\tilde{\mu}_e = \frac{1}{z}(\mu_{Red} - \mu_{Ox}) - F\phi_{SOLUTION}$$

$$\tilde{\mu}_e = \frac{1}{z}(\mu^0_{Red} - \mu^0_{Ox}) - \frac{RT}{z}\log_e \frac{a_{Ox}}{a_{Red}} - F\phi_{SOLN} \qquad \ldots 2.7.1$$

7.2. The electrochemical potential of the electrons in the electrode $\tilde{\mu}_e$ is related to the Fermi energy by

$$U_F = \frac{q\tilde{\mu}_e}{F} \qquad \ldots 2.7.2$$

q is the electronic charge. This equation simply expresses a change in units

from J mol^{-1} to eV, and hence,-

$$U_F/eV = q(\mu^O_{Red} - \mu^O_{Ox}) - \frac{qRT}{zF} \log_e \frac{a_{Ox}}{a_{Red}} - q\phi_{SOLN} \qquad ...2.7.3$$

$$= qU^O_F$$

The first term on the right hand side of equation 2.7.3 is related to the standard potential of the couple in eV, the third term depends on the reference system used. Equation 2.7.3 gives the Fermi energy (U_F) in a metal electrode contacting a mixture of Ox and Red with activities a_{Ox} and a_{Red}. In general Fermi energies (eV) are measured relative to the vacuum level of the electron, whereas redox potentials are measured relative to the NHE (V). To find U_F from potentiometric measurements of redox potentials the energy of the NHE relative to the vacuum level must be found. This is the energy required to remove an electron from H_2, under the conditions prevailing in the NHE, to infinity. It is very difficult to measure directly and it is normally calculated using a cycle such as[24,25]

1. $Ag^+(g) + e^- \leftrightharpoons Ag(g)$
2. $Ag(g) \leftrightharpoons Ag(s)$
3. $Ag^+(aq) \leftrightharpoons Ag^+(g)$
4. $H^+(aq) + Ag(s) \leftrightharpoons Ag^+(aq) + \frac{1}{2}H_2$

Energies for steps 1,2 and 4 can be measured experimentally, but 3 must be calculated. Various similar cycles have been proposed and must produce a value for the NHE energy of $\sim$ -4.5eV relative to the vacuum level. More recent estimates suggest a value of -4.7eV[26].

7.3. Once a value for the NHE energy has been accepted all tabulated electrode potentials can be expressed on the vacuum scale using

$$U/eV = \frac{qE^O}{F} - 4.5 \qquad ...2.7.4$$

It is obviously convenient to describe species in solution in terms of their energy levels when considering their interaction with semiconductors,

since the latter are best described using an energy level description.

7.4. Any given species may be associated with a number of energy levels since the precise value will be affected by variations in the geometry of the species itself and also by variations in the positions of surrounding solvent molecules and counter ions (for many complex ions these may be the same thing). The solvent is said to be polarized. In the Marcus[27,28] model variations in the polarization are accounted for by a quantity γ, which is defined such that the variation in polarization from the equilibrium value could occur if the ionic charge changed from qZ to $q(Z \pm \gamma)$. The energy of polarization ΔU_p is then given by

$$\Delta U_p = \frac{\gamma^2 q^2}{8\pi\epsilon_0 a}\left(\frac{1}{\epsilon_{op}} - \frac{1}{\epsilon_r}\right) = \gamma^2\lambda \qquad \ldots 2.7.5$$

where a is the ionic radius, ϵ_r is the static dielectric constant and ϵ_{op} is the high frequency (optical) dielectric constant. For a 1 electron reduction the Marcus model assumes that three basic steps occur.

(1) The solvent polarization alters from the equilibrium value so that the electronic energy level moves to an intermediate value U*. The change in thermal energy is then $(\gamma^2)\lambda$.

(2) Electron transfer occurs from the electrode at an energy U_{el} to the intermediate, the thermal energy change being $U^* - U_{el}$.

(3) The polarization relaxes to the new intermediate value. Since the ionic charge has changed to (z-1)q the energy change is $-(1-\gamma^*)^2\lambda$.

The total change in energy accompanying the reduction is thus

$$\Delta U = (\gamma^*)^2 - (1-\gamma^*)\lambda + U^* - U_{el} \qquad \ldots 2.7.6$$

If $\gamma^* = 0$, then equation 2.7.6 simplifies to

$$\Delta U = -\lambda + U^0 - U_{el} \qquad \ldots 2.7.7$$

where U^0 is the electronic energy for equilibrium polarization. Substituting

equation 2.7.7 into equation 2.7.6 gives

$$\gamma^* = \frac{(U^0 - U^*)}{2\lambda} \qquad \ldots 2.7.8$$

and

$$\Delta U_p = \frac{(U^0 - U^*)^2}{4\lambda} \qquad \ldots 2.7.9$$

Equation 2.7.9 expresses the change in electronic energy of an ion as a result of a change of ΔU_p in the thermal energy of the polarizing medium. In aqueous solutions, a hydrated ion has a radius of $\sim 3\text{Å}$ and the relative dielectric constant ϵ_r is ~80. In fact it must be realised that such a value for ϵ_r is obtained for the bulk solvent, which can be expected to have a different value to that for the orientated solvent in the vicinity of the ion. Thus calculations using the bulk value of ϵ_r will only be approximate. If λ is taken as ~1eV then for fluctuations in ΔE_p of the order of kT, the electronic energy level fluctuations that result $(U^0 - U^*)$ are about 0.3eV. The energy distribution of electronic levels can be found by applying the Boltzmann distribution

$$W(U) = \frac{\exp\left[-(U^0 - U^*)/4\lambda kT\right]}{\int_0^\infty \exp\left[-(U^0 - U^*)/4\lambda kT\right] dU}$$

$$= \frac{1}{(4\pi\lambda kT)^{1/2}} \exp\left[\frac{-(U^0 - U^*)}{4\lambda kT}\right] \qquad \ldots 2.7.10$$

The change in charge resulting from a redox process will have an effect on the polarization of the solvent and probably on the geometry of the ion as well, and hence the electronic energy of the reduced ion will be different to that of the oxidised ion. The difference in energy due to the change in solvent orientation is known as the Franck-Condon shift; it can be estimated using a cycle such as[29]:

(1) Electron transfer to the oxidised form in its equilibrium polarization. The change in electronic energy is $(U_F - U_{Ox})$, where U_{Ox} is the energy level of the oxidised ion in its equilibrium polarization and U_F is the Fermi level

24a/ CYCLE USED TO CALCULATE THE FRANCK-CONDON SHIFT

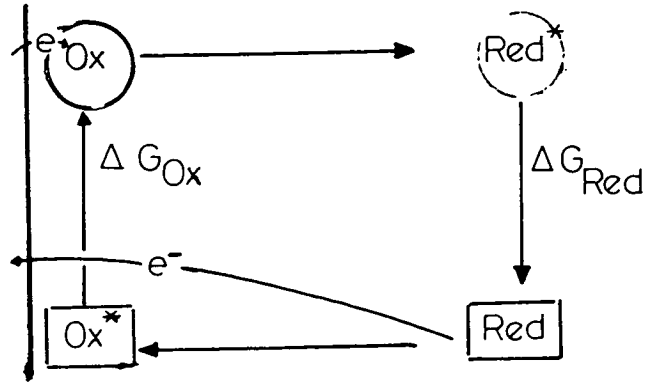

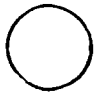

Equilibrium polarisation for Ox

" " " Red

b/ ENERGY LEVEL DIAGRAM FOR IONS IN SOLUTION

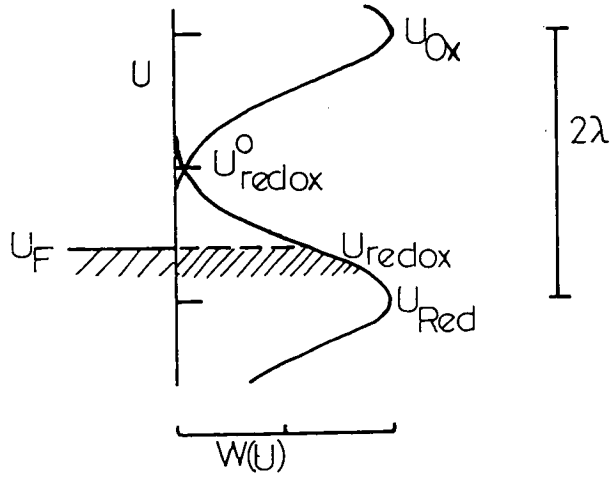

of the electrode.

(2) Reorganization of the ion and its surroundings, with a free energy change $-\Delta G_{Red}$.

(3) Reduction by electron transfer back to the conduction band with a change $-(U_F - U_{Red})$.

(4) Reorganization of the ion and its surroundings with a free energy change $-\Delta G_{Ox}$.

These steps are illustrated in figure 2.4a. Summing the changes and equating to zero gives,-

$$(U_F - U_{Ox}) - \Delta G_{Red} = (U_F - U_{Red}) + \Delta G_{Ox} \qquad ...2.7.11$$

or

$$U_{Ox} - U_{Red} = -(\Delta G_{Red} + \Delta G_{Ox}) \qquad ...2.7.12$$

Since ΔG_{Ox} and ΔG_{Red} represent transformations from excited to equilibrium states they must both be negative and thus,

$$(U_{Ox} - U_{Red}) > 0 \qquad \text{or} \qquad U_{Ox} > U_{Red}$$

The difference in energy due to changes in polarization can be calculated from equation 2.7.5 with $\gamma=1$ (for a change in oxidation state of 1).

$$U_{Pol} = \lambda = -\Delta G_{Ox} = -\Delta G_{Red} \qquad ...2.7.13$$

thus $$U_{Ox} - U_{Red} = 2\lambda \qquad ...2.7.14$$

Since in general $\lambda \sim 1eV$, the Franck-Condon splitting will be of the order of 2eV. The complete energy level diagram is shown in figure 2.4b.

Equation 2.7.4 relates a redox potential on the NHE electrode to an energy level on the vacuum zero scale.

Equation 2.7.11 shows that the energy levels for the reduced and oxidised forms differ. It is important therefore to relate U_{Redox}, the measured redox

energy to U_{Red} and U_{Ox} the energy levels of Ox and Red at their equilibrium polarizations.

$$E_{Redox} = E^{O}_{Redox} - \frac{RT}{F} \log_e \frac{a_{Red}}{a_{Ox}} \qquad ...2.7.15$$

$$\Rightarrow \quad U_{Redox} = U^{O}_{Redox} - kT \log_e \frac{a_{Red}}{a_{Ox}} \qquad ...2.7.16$$

where U^{O}_{Redox} is the redox energy when $a_{Red} = a_{Ox}$. If the change

$$Ox + e^- \xrightarrow{\Delta G_{Red}} Red$$

is considered, the overall energy change is

$$(U_F - U_{Ox} - \Delta G_{Red}) \qquad ...2.7.17a$$

The complementary process

$$Red \xrightarrow{\Delta G_{Ox}} Ox + e^-$$

involves a change

$$(U_F - U_{Red} + \Delta G_{Ox}) \qquad ...2.7.17b$$

since $U_F = U^{O}_{Redox}$, and since at equilibrium equations 2.7.17b and 2.7.17a must be the same, then-

$$U^{O}_{Redox} - U_{Red} + \Delta G_{Ox} = U^{O}_{Redox} - U_{Ox} - \Delta G_{Red}$$

$$\Rightarrow \quad U^{O}_{Redox} = \frac{1}{2}(U_{Ox} + U_{Red}) + \frac{1}{2}(\Delta G_{Red} - \Delta G_{Ox}) \qquad ...2.7.18$$

If it is true that $|\Delta G_{Red}| = |\Delta G_{Ox}|$, as was assumed in the derivation of 2.7.14, then

$$U^{O}_{Redox} = \frac{1}{2}(U_{Ox} + U_{Red})$$

The position of U^{0}_{Redox} on the energy level diagram is shown in figure 2.4b. The derivation above only takes account of changes in the polarization of solvent molecules that are assumed not to be chemically bonded to the ion. In practice most ions in solution have co-ordinating ligands which may be solvent molecules, counter ions or a different species. A change in oxidation state will lead to changes in the size and possibly the geometry of the complex and these will also affect the relative positions of U_{Red} and U_{Ox}. Furthermore fluctuations in size and geometry caused by bond vibration and bending modes will lead to a distribution of energy levels in the same way as caused by solvent polarization fluctuations. An extreme case of these 'chemical' fluctuations is where the redox couple consists of an ion and the metal

$$M \leftrightharpoons M^{z+}(aq) + ze^{-}$$

Often the Fermi level of the bulk level is well known, but if the metal is in the form of an amalgam or a plated monolayer it is unlikely that the bulk value will be appropriate.

2.8. Reactions at Semiconductor Electrodes

2.8.1. The presence of a space charge region at a semiconductor surface, extending perhaps as much as ~1000Å into the bulk of the semiconductor, leads to the qualitatively different behaviour of semiconductor electrodes as compared to metal electrodes. In general the surface of an electrode becomes charged either by

(a) Ionization of surface groups.

(b) Adsorption of ions.

(c) Trapping of charge carriers at surface states.

The analysis of the electron distribution within the electrode is similar to that used in section 5 to derive the distribution of ions in an ionically conducting solid state ISE. If N_A is the acceptor concentration, N_0 is the donor concentration, n_0 the bulk conduction electron concentration and p_0 is the hole concentration in the bulk, the charge density is given by

$$\rho(x) = [N_0 - N_A - n(x) + p(x)]e \qquad \ldots 2.8.1$$

It is assumed that all the acceptors and donors are ionized. If the electrostatic field derives entirely from the charge at the surfaces, n(x) and p(x) are given by the Boltzmann distribution law as

$$n(x) = n_0 \exp\frac{[e(\phi(x) - \phi_0)]}{kT} \qquad \ldots 2.8.2a$$

$$p(x) = p_0 \exp\frac{[-e(\phi(x) - \phi_0)]}{kT} \qquad \ldots 2.8.2b$$

Poisson's equation then gives

$$\frac{d^2\phi}{dx^2} = -\frac{1}{\epsilon}\left[N_0 - N_A - n_0 \exp\frac{[e(\phi(x) - \phi_0)]}{kT} + p_0 \exp\frac{[\phi(x) - \phi_0)]e}{kT}\right] \qquad \ldots 2.8.3$$

The solution of equation 2.8.3 can be found by producing the first

derivative using the identity

$$d\phi \frac{d^2\phi}{dx^2} = \frac{1}{2} d\left(\frac{d\phi}{dx}\right)^2$$

$$\frac{d\phi}{dx} = \pm \left[\frac{2kT}{\epsilon} -(N_D-N_A)y + p_0(\exp(-y)-1) + n_0(\exp(y)-1)\right]^{\frac{1}{2}} \quad ...2.8.4$$

where $y = \frac{e(\phi(x) - \phi_0)}{kT}$

Equation 2.8.4 gives the electric field distribution but not the potential. The potential can be calculated for cases where

$$\phi(x) - \phi_0 << \frac{kT}{e}$$

so that y is given by

$$y = 1 + \frac{e(\phi(x) - \phi_0)}{kT} \quad ...2.8.5$$

Otherwise numerical analysis must be employed. For n-type semiconductors N_A and p_0 are both zero, so that equation 2.8.3 simplifies to

$$\frac{d^2\phi}{dx^2} = -\frac{e}{\epsilon}\left[N_D - n_0\exp\left[\frac{e(\phi(x) - \phi_0)}{kT}\right]\right] \quad ...2.8.6$$

Applying the Taylor approximation and noting that when $n_0 = N_D$

$$\frac{d^2\phi}{dx^2} = -\frac{1}{\epsilon} n_0 \frac{e^2(\phi(x) - \phi_0)}{kT} \quad ...2.8.7$$

Equation 2.8.7 has a solution of the form

$$\phi(x) = \phi_0\exp\left(\frac{n_0e^2}{\epsilon kT}\right)x \quad ...2.8.8$$

The distance required for $\phi(x)$ to fall to a value of $e^{-1}\phi_0$ is called

the Debye length and can be used as a measure of the extent of the space charge region. For metals $n_0 \sim 10^{22} cm^{-3}$ but in semiconductors $n_0 \sim 10^{14} cm^{-3}$ thus for similar dielectric constants in the metal and semiconductor equation 2.8.8 predicts that the space charge region will be $\sim 10^4$ times wider than in a metal. For metals the Debye length is of the order of 1Å while for semiconductors it is typically 1000Å. The conduction and valence bands in the space charge region are bent away from their bulk values as shown in figure 2.5. If for an n-type semiconductor they are bent towards higher energies at the surface, a depletion region results in which there are relatively fewer conduction electrons. In extreme cases band bending may be so great that electrons are unable to occupy the high energy states of the valence band; in this case an inversion layer is said to have formed. For the n-type semiconductor considered, depletion and inversion layers will result from the formation of a negative surface charge (or by any or all of the mechanisms above). A positive surface charge bends the bands to lower energies, so that relatively more electrons appear at the surface and an accumulation layer results. For p-type semiconductors the opposite applies, i.e. a positive surface charge bends the bands downwards and depletes the surface of holes, whereas a negative surface charge bends the bands upwards and holes accumulate in the valence band at the surface.

The presence of uncompensated surface charge will repel ions of the same type of charge (co-ions) in solution and attract those of the opposite sign (counter-ions). Thus the distribution of ions in the vicinity of a charged surface is not uniform. Conventionally the region where the concentration of ions varies is divided into two parts; the inner or Helmholtz region, and the outer diffuse or Gouy region. The Helmholtz region comprises the charged surface itself, or in the case of adsorbed ions these, together with the first layer of counter-ions. The Helmholtz region thus behaves much like a parallel plate capacitor. The Gouy region comprises the remaining electrolyte in which the ions are not uniformly distributed. The extent of the Gouy region depends on the concentration of the ions and their valencies, but for high concentrations ($>10^{-1}$M) it is typically 10Å in width and is often simply merged with the Helmholtz region.

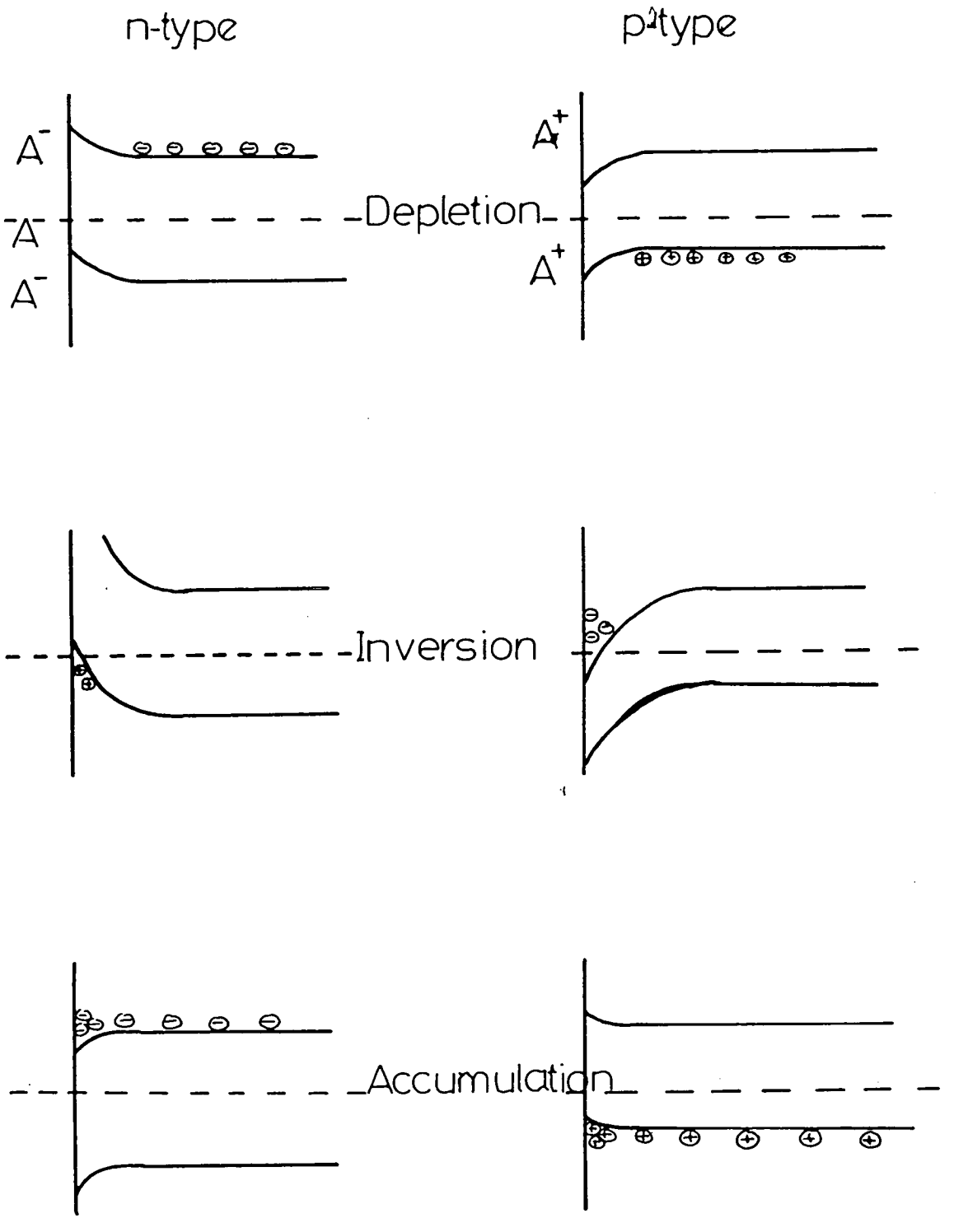

A adsorbed ion

⊖ electron

Fermi level

The half cell potential is the potential between the semiconductor bulk and the solution bulk and it is made up of the sum of the potentials dropped through the space charge, Helmholtz and Gouy layers. It should be noted that the same is true of metal electrodes, however in this case the space charge region is sufficiently small to allow tunnelling of electrons from the conduction band at its bulk level to ions in solution and vice versa. If an external EMF is applied between the solution and the electrode (i.e. between the reference electrode and the electrode of interest), then the bands in the bulk of the electrode will move relative to the energy levels of the species in solution (section 7). For a metal electrode, where the space charge region is sufficiently thin to allow tunnelling, this effectively means that the conduction electron energies can be altered until transfer occurs and that all the applied EMF appears as a potential difference in the Helmholtz region. However for a semiconductor electrode with a depletion region of 1000Å, tunnelling cannot occur and an applied EMF will move the bulk band levels relative to the solution energy levels but may not significantly affect the energies of the bands at the surface. The applied EMF in general appears as the sum of potentials dropped across the space charge and the Helmholtz layers (strictly speaking the Gouy layer should also be included). In the extreme case of the applied EMF appearing entirely as a potential difference in the space charge region then clearly the degree of band bending and thus the number of carriers at the surface is affected.

2.8.2. Semiconductor Electrode Kinetics

In section 2 it was noted that for a completely general analysis of electrode reactions the concentration of ions in solution together with the surface concentration of electrons, n_s (cathodic) or electron vacancies, p_s (anodic) must be considered. It was further noted that for a metal, n_s and p_s are independent of applied potential and were thus included in the rate constants. As shown above, for semiconductor electrodes n_s and/or p_s depend on an applied potential because of its effect on band bending. If a redox reaction

$$Ox + e^- \leftrightharpoons Red$$

is considered, the reduction (cathodic) process has a rate expression of the

form

$$\frac{-dN_{Ox}}{dt} = k^{c}_{an}\, C_{Ox}\, n_s \exp\left(\frac{\alpha F \phi_H}{RT}\right) \qquad \ldots 2.8.9a$$

where k^{c}_{an} is the anodic rate constant for the reduction involving conduction band electrons. The potential drop in the Helmholtz region is ϕ_H and the surface concentration of conduction electrons is n_s. If the valence band electrons are involved in the reduction

$$\frac{-dN_{Ox}}{dt} = k^{v}_{an}\, C_{Ox} \exp\left(\frac{\alpha F \phi_H}{RT}\right) \qquad \ldots 2.8.9b$$

For the reverse reaction involving injection of electrons from Red into the empty conduction band

$$\frac{-dN_{Red}}{dt} = k^{c}_{cat}\, C_{Red} \exp\left(-\frac{(1-\alpha)}{RT}\phi_H\right) \qquad \ldots 2.8.10a$$

where k^{c}_{cat} is the rate constant for the process involving the conduction band. For the rate where electrons are injected into the valence band, the corresponding relationship is

$$\frac{-dN_{Red}}{dt} = k^{v}_{cat}\, C_{Red}\, p_s \exp\left(-\frac{(1-\alpha)}{RT}\phi_H\right) \qquad \ldots 2.8.10b$$

Equations 2.8.9a and 2.8.10a can be combined to give the total electron current in the conduction band, i.e.-

$$\frac{I^{c}_{e}}{A} = k^{c}_{an} C_{Ox} n_s \exp\left(\frac{\alpha F \phi_H}{RT}\right) - k^{c}_{cat} C_{Red} \exp\left(-\frac{(1-\alpha)}{RT}\phi_H\right) \qquad \ldots 2.8.11$$

Similarly for the hole current in the valence band,-

$$\frac{I^{v}_{h}}{A} = k^{v}_{cat} C_{Red} p_s \exp\left(-\frac{(1-\alpha)}{RT}F\phi_H\right) - k^{v}_{an} C_{Ox} \exp\left(\frac{\alpha F \phi_H}{RT}\right) \qquad \ldots 2.8.12$$

At equilibrium, $I_e^{c,0}$ and/or $I_h^{v,0}$ are equal so that equation 2.8.11 becomes

$$\frac{I_e^{c,0}}{A} = k_{an}^{c,0} C_{Ox} n_s^0 \exp\left(\frac{\alpha F \phi_H^0}{RT}\right) = k_{cat}^{c,0} C_{Red} \exp\left(-\frac{(1-\alpha) F \phi_H^0}{RT}\right) \quad \ldots 2.8.13$$

where the superscript zero refers to equilibrium, a similar expression can be derived from equation 2.8.12. By defining

$$\Delta\phi_H = (\phi_H^0 - \phi_H) \quad \ldots 2.8.14$$

equation 2.8.11 can be rewritten to give the conduction electron current as a function of potential, i.e.-

$$\frac{I_e^c}{A} = \frac{I_e^{c,0}}{A} \left(\frac{n_s}{n_s^0} \exp\left(\frac{-\alpha F \Delta\phi_H}{RT}\right) - \exp\left(\frac{(1-\alpha) F \Delta\phi_H}{RT}\right)\right) \quad \ldots 2.8.15$$

If holes also contribute to the current the total is given by

$$I = I_e^c + I_h^v$$

and I_h^v can be found from equation 2.8.12, 2.8.14 and the valence band equivalent of equation 2.8.13. For the case of an n-type semiconductor only I_e^c contributes to I.

Equation 2.8.15 is the equivalent of equation 2.2.6 for a metal electrode since (n_s/n_s^0) depends on that part of the applied EMF which appears as a potential difference across the space charge region it is clearly not possible to proceed further without a knowledge of the relative sizes of $\Delta\phi_H$, $\Delta\phi_{sc}$ and, in cases where the Gouy layer cannot be incorporated into the Helmholtz layer, $\Delta\phi_G$.

2.8.3. Relation between $\Delta\phi_H$ and $\Delta\phi_{sc}$

Myamlin and Pleskov[30] have calculated the relationship between $\Delta\phi_H$ and $\Delta\phi_{sc}$. If the electrostatic field in the Helmholtz region, E_H is constant

(which will be the case if it behaves as a pure capacitance) then,

$$\Delta\phi_H = E_H d_H \qquad \ldots 2.8.16$$

where d_H is the thickness of the Helmholtz region. Now

$$\epsilon_H E_H = \epsilon_S E_S \qquad \ldots 2.8.17$$

where ϵ_H and ϵ_S are the permitivities of the Helmholtz region and the semiconductor surface respectively. The field at the surface, E_S, is given by equation 2.8.4 with $\phi(x)$ replaced by $\phi(0)$.

$$\left(\frac{d\phi_{sc}}{dx}\right)_{x=0} = E_S = \pm\left[\frac{2kT}{e}(-(N_D-N_A)Y_0 + p_0[\exp(-Y_0)-1] + n_0[\exp(Y_0)-1])\right]^{\frac{1}{2}} \qquad \ldots 2.8.18$$

where $$Y_0 = \frac{e(\phi_S-\phi_0)}{kT}$$

Equation 2.8.18 can be rewritten using $\lambda = (p_0/n_0)^{\frac{1}{2}}$ and $n_i=(n_0p_0)^{\frac{1}{2}}$ to give

$$E_S = \pm\left[\frac{2kTn_i}{e}(\lambda(\exp(-Y_0)-1) + \frac{1}{\lambda}(\exp(Y_0)-1) + (\lambda-\frac{1}{\lambda})Y_0)\right]^{\frac{1}{2}} \qquad \ldots 2.8.19$$

Using equation 2.8.17 the potential drop in the Helmholtz region is then given by

$$\Delta\phi_H = d_H E_H$$

$$= 2^{\frac{1}{2}}\frac{d_H}{\epsilon_H}\epsilon_S\left(\frac{kTn_i}{e}\right)^{\frac{1}{2}}(\lambda(\exp(-Y_0)-1) + \frac{1}{\lambda}(\exp(Y_0)-1) + (\lambda-\frac{1}{\lambda})Y_0)^{\frac{1}{2}} \qquad \ldots 2.8.20$$

The parameter Y_0 is a direct measure of the potential drop in the space charge region $\Delta\phi_{sc}$.

$$\Delta\phi_{sc} = \phi_S - \phi_0 = \frac{kT}{e}Y_0 \qquad \ldots 2.8.21$$

Equation 2.8.20 can be differentiated to determine the variation of $\Delta\phi_H$ by variations in $\Delta\phi_{sc}$ which are due to changes in applied EMF, E. Neglecting the potential drop in the Gouy layer and any ohmic drops in the remainder of the circuit

$$E = (\Delta\phi_{sc} + \Delta\phi_H) \qquad \ldots 2.8.22$$

$$\frac{d\Delta\phi_H}{d\Delta\phi_{sc}} = \left(\frac{2kTn_i}{e}\right)^{\frac{1}{2}} \frac{d_H\epsilon_s}{\epsilon_H} \frac{\left[-\lambda\exp(-Y_0) + \frac{1}{\lambda}\exp(Y_0) + \lambda - \frac{1}{\lambda}\right]}{\left[\lambda(\exp(-Y_0)-1) + \frac{1}{\lambda}(\exp(Y_0)-1) + (\lambda-\frac{1}{\lambda})Y_0\right]} \qquad \ldots 2.8.23$$

Equation 2.8.23 is a complete expression for the I-E characteristic. If $\Delta\phi_{sc}$ is found using 2.8.22 and 2.8.23 then n_s and/or p_s can be calculated using the Boltzmann distribution and thus the current can be found from 2.8.15. The Boltzmann distribution can be written:-

$$n_s = n_0\exp\frac{e(\phi_s - \phi_0)}{kT} = n_0\exp\frac{e\Delta\phi_{sc}}{kT} \qquad \ldots 2.8.24$$

Substitution of equation 2.8.24 into 2.8.15 gives

$$I_e^c = I_e^{c,0}\left(\frac{1}{n_s^0}\exp\frac{F(\Delta\phi_{sc} - \alpha\Delta\phi_H)}{RT} - \exp\frac{(1-\alpha)F\Delta\phi_H}{RT}\right) \qquad \ldots 2.8.25$$

From 2.8.24

$$n_s^0 = n_0\exp\frac{e(\phi_s^0 - \phi_0)}{kT} = n_0\exp\frac{e\Delta\phi_{sc}^0}{kT}$$

where $\Delta\phi_{sc}^0$ is the potential drop in the space charge region under equilibrium conditions. Thus equation 2.8.25 becomes:-

$$I_e^c = I_e^{c,0}\left(\exp\frac{F(\Delta\phi_{sc} - \Delta\phi_{sc}^0 - \alpha\Delta\phi_H)}{RT} - \exp\frac{(1-\alpha)F\Delta\phi_H}{RT}\right) \qquad \ldots 2.8.26$$

For the limiting case where $\Delta\phi_H$ is negligible equation 2.8.26 becomes

$$I_e^c = I_e^{c,0}[\exp(\frac{e(\Delta\phi_{sc} - \Delta\phi_{sc}^0)}{kT}) - 1] \qquad ...2.8.27$$

which is essentially the characteristic of a rectifier. By comparison with equation 2.2.6 it can be seen that the exchange constant α is unity.

2.8.4. Influence of Surface States

It has been assumed that the band structure of the semi-conductor bulk continues unchanged except for the energies of the band edges up to the surface. In practice the surface represents a severe perturbation to the lattice and additional energy levels form at the surface. Certain surface states will have energies in the band gap and in some circumstances the charge associated with them is the main source of the surface charge. If the surface states have an energy E_t and n_t is the concentration of electrons in the surface states,

$$n_t = \frac{N_t}{1 + g\exp(\frac{E_t - E_F}{RT})} \qquad ...2.8.28$$

where N_t is the concentration of surface states and g is a factor that can be ½, 1 or 2, depending on the nature of the state. The charge associated with the surface states is given by,

$$Q_t = \frac{eN_t}{1 + \exp(\frac{E_F - E_t^0 + e\Delta\phi_{sc}}{kT})} \qquad ...2.8.29$$

The effect of the surface states charge on the potential drop in the Helmholtz layer $\Delta\phi_H$ is found using the relationship

$$\epsilon_H E_H = (\epsilon_s E_s + Q_t) \qquad ...2.8.30$$

Hence, equation 2.8.20 becomes

$$\Delta\phi_{H,S} = \frac{eN_t d_H}{\epsilon_H(1 + \exp(\frac{E_F - E_t^0 + e\Delta\phi_{sc}}{kT}))} + \Delta\phi_H \qquad ...2.8.31$$

Similarly therate of change of $\Delta\phi_H$ with $\Delta\phi_{sc}$ is given by

$$\frac{d\Delta\phi_{H,s}}{d\Delta\phi_{sc}} = \frac{N_t d_H \exp\left(\frac{E_F - E_t^0 + \Delta\phi_{sc}}{kT}\right)}{kT\epsilon_H\left[1 + \exp\left(\frac{E_F - E_t^0 + \Delta\phi_{sc}}{kT}\right)\right]^2} \pm \frac{d\Delta\phi_H}{d\Delta\phi_{sc}} \qquad \ldots 2.8.32$$

When the surface state concentration is very high $d\Delta\phi_H/d\Delta\phi_{sc}$ may be neglected and equation 2.8.32 is simplified. Myamlin and Pleskov[30] have shown that if

$$N_t < \frac{\epsilon_H kT}{e^2 d_H}$$

the change in $\Delta\phi_H$ is always less than that in $\Delta\phi_{sc}$.

It should be noted that amorphous semiconductors are also characterised by the appearance of states in the gap and thus if the density of gap states is sufficiently high at the surface they may behave as metallic electrodes.

2.8.5. Other Experimental Techniques

In addition to the voltammetric techniques described in the next sections, in which the current through the cell is determined as a function of applied potential, measurements are also sometimes reported of surface conductivity and space charge capacitance as functions of electrode potential. Because the number of carriers n(x), p(x) in the space charge region of an electrode differs from the bulk concentrations n_0, p_0, it is reasonable to expect the conductivity of the space charge region to differ from that of the bulk. For semiconductors with wide space charge regions, the conductivity of thin samples should differ from that of thick samples because of the relative importance of the surface conductivity to the total. The variation of surface conductivity with $\Delta\phi_{sc}$ for an n-type semiconductor is given by

$$\sigma_s = eU_n n_0 \int_{\phi_s}^{\phi_0} \left[\exp\left(\frac{e\Delta\phi(x)}{kT}\right) - 1\right] / \frac{d\phi}{dx}\, d\phi \qquad \ldots 2.8.33$$

Comparison of equation 2.8.33 with $\Delta\phi_{sc}$ assumed to equal the total applied potential can give information on the relative importance of $\Delta\phi_{sc}$ and $\Delta\phi_{H}$. Krotova and Pleskov[31] have carried out this type of study on germanium in a KBr-methyl formamide electrolyte.

It was noted above that the Helmholtz region behaves as a parallel plate capacitor. The same is true of the space charge region. If a depletion region exists at the surface, the charge density is given by

$$\rho(x) = -N_{sc}e(\exp(-e\Delta\phi_{sc}(x))/kT - 1) \qquad \ldots 2.8.34$$

where N_{sc} is the concentration of donors and n is the conduction band electron concentration.

Poisson's equation gives

$$\frac{d^2\phi_{sc}}{dx^2} = \frac{-N_{sc}e}{\epsilon}[\exp\frac{e\phi}{kT} - 1] \qquad \ldots 2.8.35$$

Equation 2.8.35 can be differentiated to give

$$\left(\frac{d\phi}{dx}\right)^2 = \frac{2eN_{sc}}{\epsilon}[\phi + \frac{kT}{e}(\exp(-\frac{e\phi}{kT}) - 1)] \qquad \ldots 2.8.36$$

According to Gauss's law

$$E = \frac{\sigma}{\epsilon A} \qquad \ldots 2.8.37$$

where σ is the surface charge density which may be equated to the charge in the space charge region. Hence,

$$\left(\frac{d\phi}{dx}\right)_{x=0} = \frac{Q_{sc}}{\epsilon A} \qquad \ldots 2.8.38$$

Equating equation 2.8.38 with equation 2.8.36 gives Q_{sc} in terms of ϕ_{sc}.

The derivative $(dQ_{sc}/d\phi_{sc}) = C_{sc}$, gives the space charge capacity, i.e.

$$\frac{1}{C_{sc}^2} = \frac{2}{eN_{sc}\epsilon A^2}\left(\Delta\phi_{sc} - \frac{kT}{e}\right) \qquad \ldots 2.8.39$$

Equation 2.8.39 is known as the Schottky-Mott relation. If C_{sc}^{-2} is plotted against applied potential equation 2.8.39 allows a determination of the ionized donor concentration N_{sc} and the degree of band bending at the surface $\Delta\phi_{sc}$. It must be noted that the Helmholtz capacity has been ignored although any measurement will give the total capacitance. Providing the Helmholtz layer thickness is small compared to the depletion region thickness $C_H^{-2} << C_{sc}^{-2}$. Although this analysis deals with the case of a depletion region, equivalent formulae for inversion and accumulation layers have also been calculated.[30]

2.8.6. Effect of Illumination

In addition to the presence of a large space charge region ($\sim$1000Å) and the possibility of a forbidden band gap at the surface, semiconductor electrodes will also differ from metal electrodes in their response to light. There are two basic causes of photoeffects, the first is the generation of excess carriers in the space charge region and consequent change in ϕ_{sc}. The second is the generally different mobilities of electrons and holes when electron-hole pairs have formed in the semiconductor bulk, their different rates of diffusion leads to charge separation and the creation of an additional potential- often referred to as the Dember photo-EMF.

If the surface of a semiconductor is illuminated with radiation of frequency greater than that corresponding to the band gap energy, electron-hole pairs are created- these are sometimes termed non-equilibrium carriers.[30] The photo-generation of minority carriers will result in a high concentration gradient and consequently they move mainly under the influence of diffusion. On the other hand the photo-generated majority carriers do not significantly affect the local concentration of majority carriers and thus they move under the influence of the electrostatic field in the space charge region. On illumination, the concentration of carriers increases. If Q is the charge

in the space charge region then

$$Q = \epsilon E(0) \qquad \ldots 2.8.14$$

where E(0) is the field at the electrode surface.

$$E(0,\Delta p) = \frac{(2kTn_i)}{\epsilon}\left[\frac{-N_0+N_A}{n_i}\left[\frac{e(\phi+\Delta\phi)}{kT}-1\right]\frac{p_0+\Delta p}{n_i}\exp\left[\frac{-e(\phi_{sc}+\Delta\phi)}{kT}-1\right]\right.$$

$$\left.+\frac{(n_0+\Delta p)}{n_i}\left[\exp\left(\frac{e(\phi_{sc}+\Delta\phi)}{kT}-1\right)\right.\right. \qquad \ldots 2.8.15$$

where Δp is the concentration of photogenerated carriers (electrons or holes), n_0 is the bulk electron concentration, p_0 the bulk hole concentration and n_i is given by

$$n_i = (p_0 n_0)^{\frac{1}{2}}$$

$\Delta\phi$ is the photo EMF. In the dark $E_s(0)$ is found from equation 2.8.16 by setting $\Delta p=0$. Since the number of photo-generated holes equals the number of photo-generated electrons, the total charge in the space charge region Q does not vary on illumination. Thus

$$E(0,\Delta p) = E(0,0) \qquad \ldots 2.8.16$$

Finally, therefore-

$$\frac{\Delta p}{p_0} = \left\{\lambda\left[\exp\left[\frac{-e\phi_{sc}}{kT}\right]-1\right] + \lambda^{-1}\left[\exp\left[\frac{-e\phi_{sc}}{kT}\right]\right] + (\lambda-\lambda^{-1})\frac{\phi_{sc}e}{kT}\right.$$

$$-\lambda\left[\exp\frac{-e(\phi_{sc}+\Delta\phi)}{kT}-1\right] - \lambda^{-1}\left[\exp\frac{(e\phi_{sc}+\Delta\phi)}{kT}-1\right]$$

$$\left.-(\lambda-\lambda^{-1})\frac{e(\phi_{sc}+\Delta\phi)}{kT}\right\} G\left(\frac{e(\phi+\Delta\phi_{sc})}{kT}\right) \qquad \ldots 2.8.17$$

where λ is defined above and G is the function

2.6 THEORETICAL RELATIONSHIP BETWEEN PHOTO_POTENTIAL AND INJECTION LEVEL

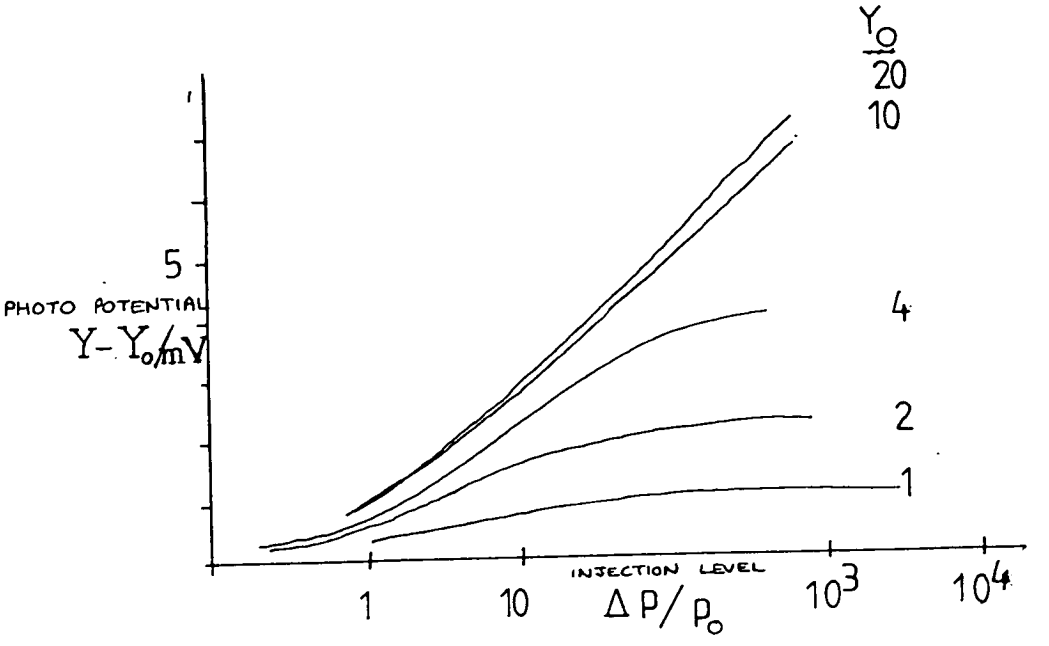

$$Y=(F/RT)\Delta\phi_{\text{SPACE CHARGE}}$$

$$G(Y,\lambda) = \lambda[\exp(Y) - \exp(-Y) - 2]$$

Plots of the photo-EMF $\Delta\phi$ as a function of injection level ($\Delta p/p_o$) are shown in figure 2.6. The injection level will depend on intensity and frequency of the radiation.

2.9 Current-Voltage Characteristics of Cells

2.9.1 Introduction

It has been noted in section 2.2 that the kinetics and mechanisms of cell reactions can be investigated by perturbing potential and measuring current. Such measurements are generally referred to as voltammetric techniques. Theoretical analyses have been made for a variety of mechanisms and types of perturbation so that a comparison of actual experimental results with theoretical results can often be made. In principle these allow the precise mechanism to be deduced and, by means of curve fitting procedures, kinetic parameters to be estimated.

The current is directly related to the flux (J) of the electro-active substance (i.e. the substance being reduced or oxidised).

$$I = zAJ \qquad 2.9.1$$

$$J = \frac{D\partial C}{\partial x} \qquad 2.9.2$$

Most models assume that the only mass transfer process occuring is diffusion and in practice most experiments are designed to suppress convection and electro-migration. Convection is reduced by avoiding stirring and electro-migration is reduced by carrying out the experiment in the presence of a large excess of an inert-base-electrolyte. The base-electrolyte then carries most of the current but takes no part in the electrode reaction. Two types of electrode reaction can be distinguished:

1. The reactants and products both remain in solution, so that the electrode acts simply as a source or a sink for electrons.

2. The reactants or products are intimately associated with the electrode surface.

The case of a redox system (case 1) will be considered first.

2.9.2 Analysis of the I-E Characteristics[32]

If diffusion is the only mass transfer process occuring, then the flux can be obtained by solving Ficks 2nd law:

$$\frac{\partial C(x,t)}{\partial t} = D \frac{\partial^2 C(x,t)}{\partial x^2} \qquad 2.9.3$$

This is best approached by transforming into the Laplacian domain to give a second order differential equation

$$D \frac{d}{dx^2} \bar{c}(x,s) - s\bar{c}(x,s) + c(x,T) = 0 \qquad 2.9.4$$

where

$$\bar{c}(x,s) = \int_0^\infty c(x,t)e^{-st}\, dt$$

Normally $c(x,t)$ is transformed to a second function $\mathcal{c}(x,t)$, in order that eqn. 2.9.4 is of a reduced form

$$D \frac{d\bar{\mathcal{c}}}{dx^2}(x,s) - s\bar{\mathcal{c}}(x,s) = 0 \qquad 2.9.5$$

for which a solution is

$$\bar{\mathcal{c}}(x,s) = A \exp \left(\frac{s}{D}\right)^{\frac{1}{2}} x + B \exp \left(\frac{s}{D}\right)^{\frac{1}{2}} x \qquad 2.9.6$$

It is not realistic for $\bar{\mathcal{c}}(x,s)$ to tend to infinity as x tends to infinity, so A = 0.

$$\bar{\mathcal{c}}(x,s) = B \exp \left[- \left(\frac{s}{D}\right)^{\frac{1}{2}} x \right] \qquad 2.9.7$$

The function C(x,t) is then found by transforming back into the time domain and by transforming from $\mathcal{L}(x,t)$ back to C(x,t). The current is found by substituting this into eqn. 2.9.2 and eqn. 2.9.1. In general the solution depends on the boundary conditions of the problem.

2.9.3 Derivation of the Polarographic Wave

The prototype system is a one stage rapid redox reaction

$$Ox + ze^- \leftrightharpoons Red$$

Since electron transfer is rapid the relative concentrations of "Ox" and "Red" at the surface are always given by the Nernst equation

$$\frac{C_{ox}(0,t)}{C_{Red}(0,t)} = \frac{\gamma_{Red}}{\gamma_{ox}} \exp \frac{zF}{RT}(E - E^\circ) = \theta \qquad B1 \qquad 2.9.8$$

This is the first boundary condition. The remaining boundary conditions are

$$C_{ox}(x,t) \to C^o_{ox} \quad \text{as } x \to \infty \qquad B2$$

$$C_{Red}(x,t) \to 0 \qquad B3$$

where it is assumed that the solution initially consists entirely of "Ox" distributed at a uniform concentration C^o_{ox}. A final boundary condition (B4) expresses the fact that the flux of "Red" from the surface must equal the flux of "Ox" to the surface.

$$D_{ox}\frac{\partial C_{ox}}{\partial x}(0,t) + D_{Red}\frac{\partial C_{Red}}{\partial x}(0,t) = 0 \qquad B4$$

The concentration function C(x,t) is transformed to the similar function c(x,t) in order to produce the reduced form of eqn. 2.9.5.

$$c_{ox}(x,t) = C^o_{ox} - C_{ox}(x,t) \qquad 2.9.9$$

The boundary conditions then become:

$$\frac{C^{o}_{ox} - c_{ox}(0,t)}{C_{Red}(0,t)} = \theta \qquad B'1$$

$$D_{ox} \frac{\partial}{\partial x} c_{ox}(0,t) = D_{Red} \frac{\partial C_{Red}}{\partial x}(0,t) \qquad B'4$$

These are transformed into Laplacian space to give

$$\frac{C^{o}_{ox}}{s} = \theta \bar{C}_{Red}(0,s) + \bar{c}_{ox}(0,s) \qquad B''1$$

$$D_{ox} \frac{d}{dx} \bar{c}_{ox}(0,s) = D_{Red} \frac{d}{dx} \bar{C}_{Red}(0,s) \qquad B''4$$

Since equation 2.9.9 was chosen to give a reduced 2nd order differential equation, the solution is eqn. 2.9.7, i.e.

$$\bar{c}_{ox}(x,s) = B_{ox} \exp\left[- \left(\frac{s}{D_{ox}}\right)^{\frac{1}{2}} x \right]$$

Similarly

$$\bar{C}_{Red}(x,s) = B_{Red} \exp\left[- \left(\frac{s}{D_{Red}}\right)^{\frac{1}{2}} x \right]$$

The boundary conditions then determine B_{ox} and B_{Red}. Using B''1

$$\frac{C^{o}_{ox}}{s} = \theta B_{Red} \exp\left[- \left(\frac{s}{D_{Red}}\right)^{\frac{1}{2}} x \right] + B_{ox} \exp\left[- \left(\frac{s}{D_{ox}}\right)^{\frac{1}{2}} x \right] \qquad 2.9.10$$

and thus

$$B_{ox} = B_{Red} \left(\frac{D_{Red}}{D_{ox}}\right)^{\frac{1}{2}} \exp\left[- s^{\frac{1}{2}} x \left(\frac{1}{D_{Red}^{\frac{1}{2}}} - \frac{1}{D_{ox}^{\frac{1}{2}}}\right) \right] \qquad 2.9.11$$

When $x = 0$

$$B_{ox} = B_{Red} \left(\frac{D_{Red}}{D_{ox}}\right)^{\frac{1}{2}} \qquad 2.9.12$$

Substitution of eqn. 2.9.12 back into 2.9.10 then gives expressions for B_{ox} and B_{Red} in terms of S, D and θ

$$\bar{c}_{ox}(x,s) = \frac{\frac{C^o}{s}_{ox} \exp\left[-\left(\frac{s}{D_{ox}}\right)^{\frac{1}{2}} x\right]}{1 + \left(\frac{D_{ox}}{D_{Red}}\right)^{\frac{1}{2}} \theta} \qquad 2.9.13a$$

$$\bar{C}_{Red}(x,s) = \frac{\frac{C^o}{s}_{ox} \left(\frac{D_{ox}}{D_{Red}}\right)^{\frac{1}{2}} \exp\left[-\left(\frac{s}{D_{ox}}\right)^{\frac{1}{2}} x\right]}{1 + \left(\frac{D_{ox}}{D_{Red}}\right)^{\frac{1}{2}} \theta} \qquad 2.9.13b$$

The inverse transformations into the time domain then yield

$$C_{ox}(x,t) = C^o_{ox} \left[\frac{\left(\frac{D_{ox}}{D_{Red}}\right)^{\frac{1}{2}} \theta + \operatorname{erf}\left(\frac{x}{2D_{ox}^{\frac{1}{2}} t^{\frac{1}{2}}}\right)}{1 + \left(\frac{D_{ox}}{D_{Red}}\right)^{\frac{1}{2}} \theta}\right] \qquad 2.9.14a$$

$$C_{Red}(x,t) = C^o_{ox} \left[\frac{\left(\frac{D_{ox}}{D_{Red}}\right)^{\frac{1}{2}} \operatorname{erfc}\left(\frac{x}{2D_{Red}^{\frac{1}{2}} t^{\frac{1}{2}}}\right)}{1 + \left(\frac{D_{ox}}{D_{Red}}\right)^{\frac{1}{2}} \theta}\right] \qquad 2.9.14b$$

The equations 2.9.14 contain all the information expressing the concentration profiles of ox and Red and also their time dependence. At the surface of the electrode x = 0, so that

$$C_{ox}(0,t) = C^{o}_{ox}\left[\frac{\delta\theta}{1+\delta\theta}\right] \qquad 2.9.15a$$

$$C_{Red}(0,t) = C^{o}_{ox}\left[\frac{\delta}{1+\delta\theta}\right] \qquad 2.9.15b$$

where $\delta = (D_{ox}/D_{Red})^{\frac{1}{2}}$. The current is found by substituting eqn. 2.9.15 into eqn. 2.9.1 and eqn. 2.9.2 to give

$$I(t) = ZAF\, D_{ox} \frac{\delta\, C_{ox}\,(0,t)}{\delta x}$$

$$= ZAF\, D_{ox}^{\frac{1}{2}}\, C^{o}_{ox}\, \frac{1}{\pi^{\frac{1}{2}}\, t^{\frac{1}{2}}\,(1+\delta\theta)} \qquad 2.9.16$$

The forms of the concentration profiles are shown in figure 2.7a. Since θ is a potential dependent factor it is possible to express $I(\tau)$ in terms of the applied potential E. The time τ is a constant time interval at which the current is sampled after the potential has been adjusted to E. The function $I(E)_{\tau}$ is known as the voltammetric wave.

If E is strongly reducing then $C_{ox}(0,t)$ will always be zero and thus θ will also equal zero. In this case I takes the form

$$I_d(\tau) = \frac{ZAF\, D_{ox}^{\frac{1}{2}}\, C_{ox}}{\pi^{\frac{1}{2}}\, \tau^{\frac{1}{2}}} \qquad 2.9.17$$

$$I(\tau) = \frac{I_d(\tau)}{1+\delta\theta} \qquad 2.9.18$$

2.7 ANALYSIS OF THE VOLTAMMETRIC WAVE

a./ concentration profiles as a function of time

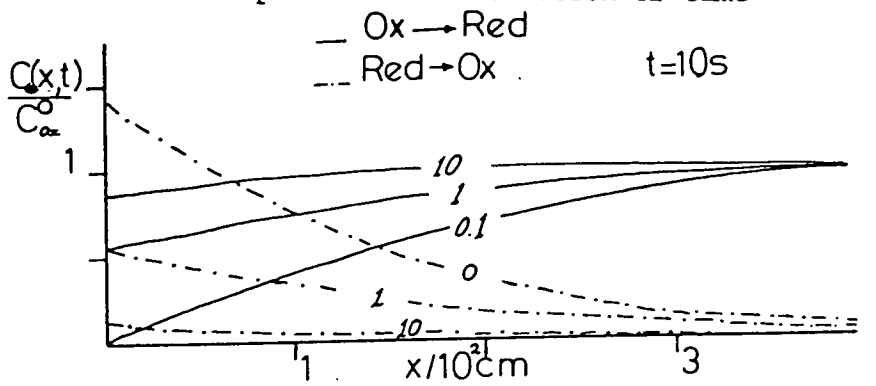

b./ The polarographic wave

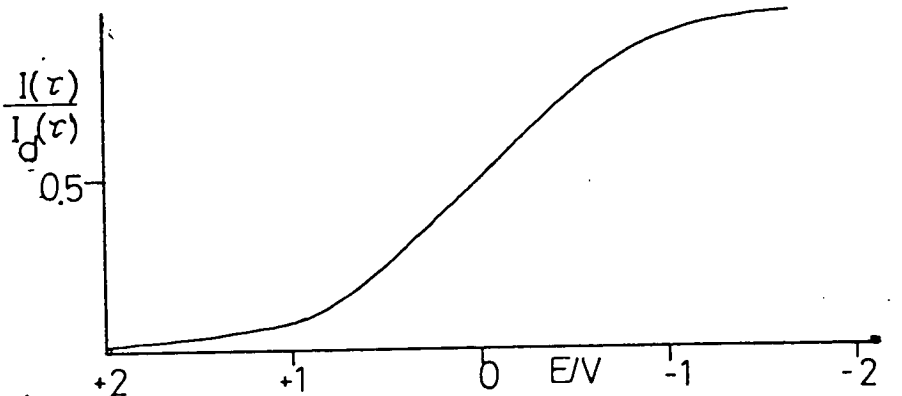

c./ The polarographic wave with time varying applied potential

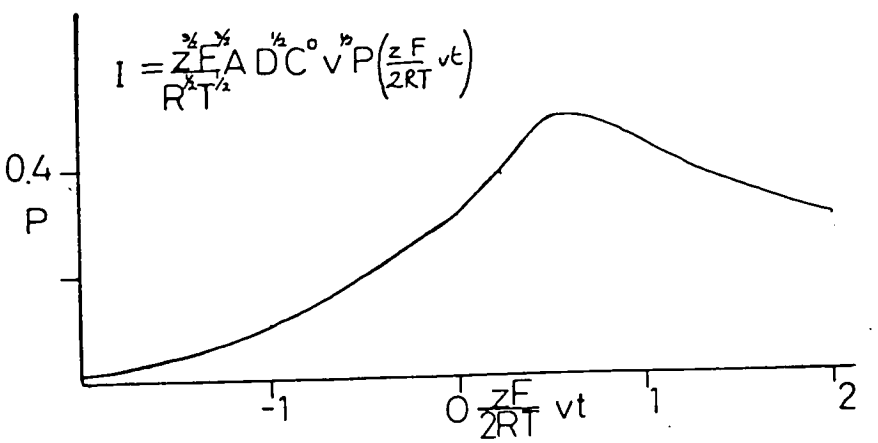

Substituting equation 2.9.8 (B1) for θ in eqn. 2.9.18 gives

$$E = E^{o} - \frac{RT}{ZF} \log_e \left(\frac{\gamma_{Red}}{\gamma_{ox}}\right) \left(\frac{D_{ox}}{D_{Red}}\right)^{\frac{1}{2}} + \frac{RT}{ZF} \log_e \frac{I_d - I}{I} \qquad 2.9.19$$

the equation of a polarographic wave for a single-step, rapid redox reaction. The form of equation 2.9.19 is shown in figure 2.7b. Experimentally such a curve is obtained by stepping the potential and measuring the current at a pre-determined time afterwards.

Qualitatively the curve can be considered to arise in the following way. At positive potentials very little "Ox" is reduced, however as the potential becomes more negative more "Ox" is reduced and a current flows. At large negative potentials all the "Ox" arriving at the surface is reduced and the current is limited by the rate at which fresh "Ox" can diffuse to the surface. The limiting current - I_d - is directly proportional to concentration and this fact is exploited in analytical methods based on voltammetry.

2.9.4 D.C. Sweep Voltammetry

In d.c. sweep voltammetry the potential is varied continuously as a ramp, of the form

$$E = E_{INIT} \pm vt \qquad 2.9.20$$

This means that the boundary condition giving the ratios of the concentrations of Ox and Red becomes time dependent

$$\frac{C_{ox}(0,t)}{C_{Red}(0,t)} = \theta \exp\left[\frac{-ZF}{RT} vt\right] \qquad 2.9.21$$

The remaining boundary conditions are the same as for the time independent case. The 2nd law equation has been solved graphically by Randles[33] and analytically by Sevcik.[34] Sevciks solution is of the form

$$J_{ox} = \frac{D_{ox}^{\frac{1}{2}}}{2} \quad 1 + \frac{1}{\theta}\left[\frac{D_{Red}}{D_{ox}}\right]^{\frac{1}{2}} \quad C^{o}_{ox} \int_{o}^{t} \frac{1}{\cosh^{2}(\delta/2)(-t_{\frac{1}{2}}} \quad \ldots$$

$$\ldots \frac{1}{\pi^{\frac{1}{2}}(t-\delta)^{\frac{1}{2}}} \quad \frac{\sigma}{2} \; d \qquad 2.9.22$$

where $\sigma = \frac{ZF}{RT} V$

and $t_{\frac{1}{2}}$ is the time where

$$E = E^{o} - \frac{RT}{ZF} \log_{e} \frac{\delta_{Red}}{\delta_{ox}} \left(\frac{D_{ox}}{D_{Red}}\right)^{\frac{1}{2}}$$

Sevcik evaluated the integral using a numerical method based on the trapezium rule. With the advent of computers, such calculations can be carried out quite easily. The form of eqn. 2.9.22 is shown in figure 2.7c; the current peak is often observed in practice. For the rapid redox reaction the peak potential is

$$E_{p} = E^{o} - \frac{RT}{ZF} \log_{e} \frac{\delta_{Red}}{\delta_{ox}} \left(\frac{D_{ox}}{D_{Red}}\right)^{\frac{1}{2}} - 1.10 \frac{RT}{ZF} \qquad 2.9.23$$

the peak current is given by

$$I_{p} = 0.452 \frac{Z \; F}{R^{\frac{1}{2}} \; T^{\frac{1}{2}}} \; A \; D_{ox}^{\frac{1}{2}} \; C^{o}_{ox} \; V^{\frac{1}{2}} \qquad 2.9.24$$

2.9.5 Cyclic Voltammetry

In cyclic voltammetry the potential sweep is reversed at a certain point. If the reaction being studied is reversible then any "Red" that formed during the forward sweep will be oxidised on the reverse sweep. The peaks for reduction and oxidation will be separated by

$$\Delta E_p = E_p^{ox} - E_p^{Red} \qquad 2.9.25$$

which from eqn. 2.9.23 and a similar expression for the reverse oxidation is

$$\Delta E_p = 2.20 \frac{RT}{ZF} = \frac{58}{Z} \text{ mV at 298 K.}$$

Thus cyclic voltammetry offers a simple way of testing whether a reaction is reversible and also whether electron transfer is rapid.

2.9.6 Reactions With Slow Electron Transfer

So far it has been assumed that electron transfer is rapid and that the only limit on the current is the diffusion rate of the electroactive substance. For cases where the rate of electron transfer is not negligible the flux expression is

$$D_{ox} \left(\frac{\partial C_{ox}}{\partial x}(0,t)\right)_{x=0} = k'_{f,h}\, C_{ox}(0,t) \exp \beta t \qquad 2.9.26$$

$$\text{where } k'_{f,h} = k^{o}_{f,h} \exp\left[\frac{-\alpha ZF\, E_{INIT}}{RT}\right] \qquad 2.9.27$$

$$\text{and } \beta = \frac{\alpha ZF}{RT} vt \qquad 2.9.28$$

The diffusion equation was solved by Delahay[35] who obtained a current-voltage characteristic of the form

$$I = \pi^{\frac{1}{2}} ZAF \beta^{\frac{1}{2}} D_{ox}^{\frac{1}{2}} C_{ox}^{o} \chi (\beta t) \qquad 2.9.29$$

The function $\chi (\beta t)$ is illustrated in figure 2.8b. A peak in the current is again observed, but is found to be a function of sweep rate.

2.9.7 Surface Processes

Surface processes are difficult to describe because in general a species at a surface is in a very different environment to a species existing in the bulk of the electrode or the bulk of the solution. In consequence it is difficult to assign a meaningful value of activity. This problem applies both to cases where a species is being dissolved from or deposited on an electrode of the same material and to cases where a species is being selectively dissolved from a compound electrode or is being deposited onto an electrode of a chemically different nature. In the latter cases however the problem of defining an activity is particularly acute. Another problem with surface electrode reactions is that in the case of deposition there must also occur nucleation and crystal growth which are activated processes and if they occur at a low rate they will effect the current.

The case of a metal depositing onto an electrode was considered by Berzins and Delahay[36] who assumed the activity of the deposited metal to be unity in which case the boundary condition B1 is replaced by

$$C_{ox} = \exp \frac{ZF}{RT} (E(t) - E^{o})$$

The current is given by

$$I = \frac{2 Z F}{\pi^{\frac{1}{2}} R^{\frac{1}{2}} T^{\frac{1}{2}}} A C_{ox}^{o} D_{ox}^{\frac{1}{2}} V^{\frac{1}{2}} \Phi [(\sigma t)^{\frac{1}{2}}] \qquad 2.9.30$$

GENERAL FORMS FOR VOLTAMMETRIC WAVES

a. Plating at an electrode

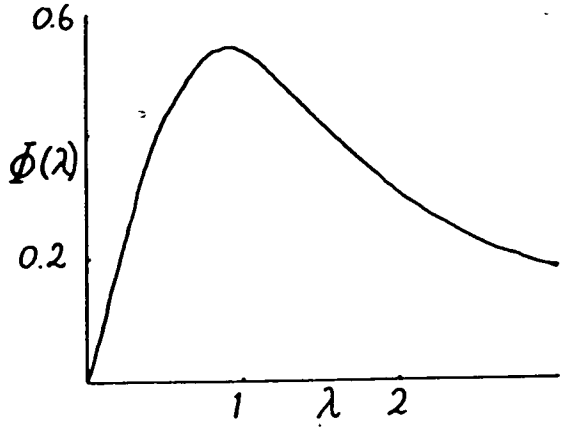

$$I = \frac{2z^{1/2}F^{1/2}}{\sqrt{\pi}R^{1/2}T^{1/2}} AC^{\circ} D^{1/2} v^{1/2} \Phi(\sigma t)$$

b. Reaction with slow electron transfer

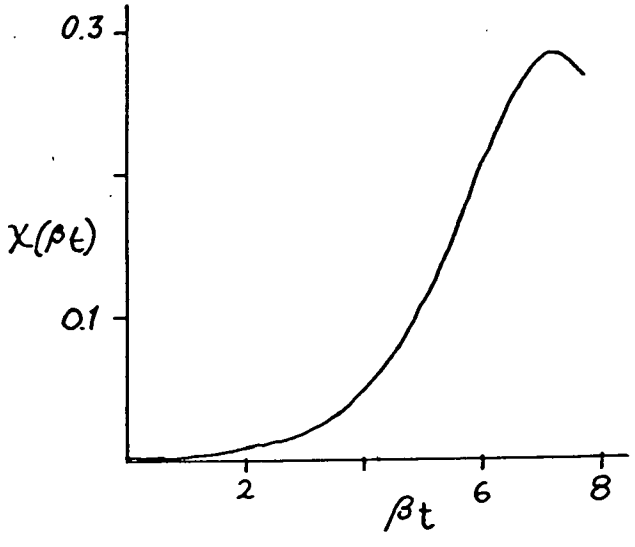

$$I_L = \pi^{1/2} z F A \beta^{1/2} D^{1/2} C^{\circ} \chi(\beta t)$$

$$\beta = \frac{\alpha z_a F}{RT} v$$

where

$$\Phi(\lambda) = \exp(-\lambda^2) \int_0^{\lambda} \exp(2^2)\, dz$$

which is illustrated in figure 2.8.a The peak current varies as $v^{\frac{1}{2}}$

$$I_p = 3.67 \times 10^5 \; Z \; A \; C_{ox}^o \; D^{\frac{1}{2}} \; v^{\frac{1}{2}} \qquad 2.9.31$$

and the peak potential depends on C_{ox}^o

$$E_p = E^o + \frac{0.0591}{Z} \log_e \gamma_{ox} \; C_{ox}^o - \frac{0.0218}{Z} \qquad 2.9.32$$

In fact experiments with cadmium[36] did not agree well with theory, the peak current generally occurred at potentials more positive than predicted although I_p was found to be proportional to $v^{\frac{1}{2}}$.

2.9.8 Capacity Currents

In section 2.8 it was noted that an electrode in contact with an electrolyte generally forms a double layer at the surface. The double layer behaves as a parallel plate capacitor and thus when potential varies some of the current is used to charge the double layer.

$$C_d = - \frac{dQ}{dE} \qquad 2.9.33$$

$$= V \frac{dQ}{dt} \qquad 2.9.34$$

For an electrode area A, the capacity current is thus

$$I_c = vA \; C_d \qquad 2.9.35$$

so that I_c is proportional to v. Some analytical methods remove I_c by using a sampling method in which the ramp is replaced by a series of pulses of linearly increasing magnitude. The capacity

current decays after the initial step. Hence, the current is sampled at the end of the pulse where it is predominately faradaic.

2.10 Controlled Current Methods

2.10.1 Introduction

Controlled current methods offer a simplification of both theoretical treatments and practical instrumentation. Theory is simpler because if current is controlled so also is the flux of the electroactive substance. In principle all the potential perturbations described in section 2.9 could be produced as analogous current perturbations, but only those methods relevant to the present work - the current step methods - will be reviewed.

2.10.2 Chronopotentiometry

Experiments in which a current step is applied to an electrode and the potential is followed as a function of time are referred to as chronopotentiometry.

For the case of a rapid reversible electron transfer

$$Ox + ze \rightleftharpoons Red$$

current is controlled entirely by the diffusive flux of Ox. The current is fixed however so that

$$I = zAF\, D_{ox} \frac{\partial C_{ox}}{\partial x} \qquad 2.10.1$$

The electrode potential depends on the ratio (C_{ox}/C_{Red}) which can be found as a function of time from Ficks 2nd law -

$$\frac{\partial C_{ox}}{\partial t} = D_{ox} \frac{\partial^2 C_{ox}}{\partial x^2} \qquad 2.10.2a$$

$$\frac{\partial C_{Red}}{\partial t} = D_{Red} \frac{\partial^2 C_{Red}}{\partial x^2} \qquad 2.10.2b$$

The boundary conditions are the same as those used to derive I(t) and I(E) together with 2.10.1.

Equation 2.10.1 can be transformed into the Laplacian

$$\frac{I}{s} = zAF\, D_{ox} \frac{\partial}{x} \overline{C}_{ox}\,(x,s) \qquad 2.10.3$$

and equations 2.10.2a and 2.10.2b are solved in the same way as in section 9 to give

$$\overline{C}_{ox}\,(x,s) = \frac{C^o}{s}ox + \left[\overline{C}_{ox}(0,s) - \frac{C^o}{s}ox\right] \exp\left(\frac{-s}{D_{ox}}\right)^{\frac{1}{2}} x \qquad 2.10.4a$$

and

$$\overline{C}_{Red}\,(x,s) = \frac{C^o}{s}Red + \left[\overline{C}_{Red}(0,s) - \frac{C^o}{s}Red\right] \exp\left(\frac{-s}{D_{Red}}\right)^{\frac{1}{2}} x \qquad 2.10.4b$$

where C^o_{Red} is the initial (bulk) concentration of C_{Red}. The boundary condition (B4 of section 9)

$$D_{ox} \frac{\partial \overline{C}_{ox}}{\partial x}\,(0,s) + D_{Red} \frac{\overline{C}_{Red}}{\partial x}\,(0,s) = 0 \qquad 2.10.5$$

yields

$$\bar{C}_{ox}(x,s) = \frac{C^{o}_{ox}}{s} + \frac{I}{zFA\, D_{ox}^{\frac{1}{2}}\, s} \qquad 2.10.6a$$

and

$$\bar{C}_{Red}(x,s) = \frac{C^{o}_{Red}}{s} + \frac{I}{zFA\, D_{Red}^{\frac{1}{2}}\, P} \qquad 2.10.6b$$

which transforms back to

$$C_{ox}(0,t) = C^{o}_{ox} - \frac{2It^{\frac{1}{2}}}{zAF\, D_{ox}^{\frac{1}{2}}\, \pi^{\frac{1}{2}}} \qquad 2.10.7a$$

and

$$C_{Red}(0,t) = C^{o}_{Red} - \frac{2It^{\frac{1}{2}}}{zAF\, D_{Red}^{\frac{1}{2}}\, \pi^{\frac{1}{2}}} \qquad 2.10.7b$$

The potential as a function of time is found by substituting $C_{ox}(0,t)$ and $C_{Red}(0,t)$ into the Nernst equation to give

$$E(t) = E^{o} - \frac{RT}{zF} \log_e \frac{\gamma_{Red}}{\gamma_{ox}} \left(\frac{D_{ox}}{D_{Red}}\right)^{\frac{1}{2}} + \frac{RT}{zF} \log_e \left[\left(\frac{\tau}{t}\right)^{\frac{1}{2}} - 1\right] \qquad 2.10.8$$

where τ is the transition time (i.e. the time where $C_{ox}(0,t) = 0$). The concentration profiles (equations 2.10.7a and 2.10.7b) and E(t) are shown in figure 2.9.

If the rate of electron transfer is significant the current can be written

a. Concentration profiles for Reactant OX undergoing Reduction

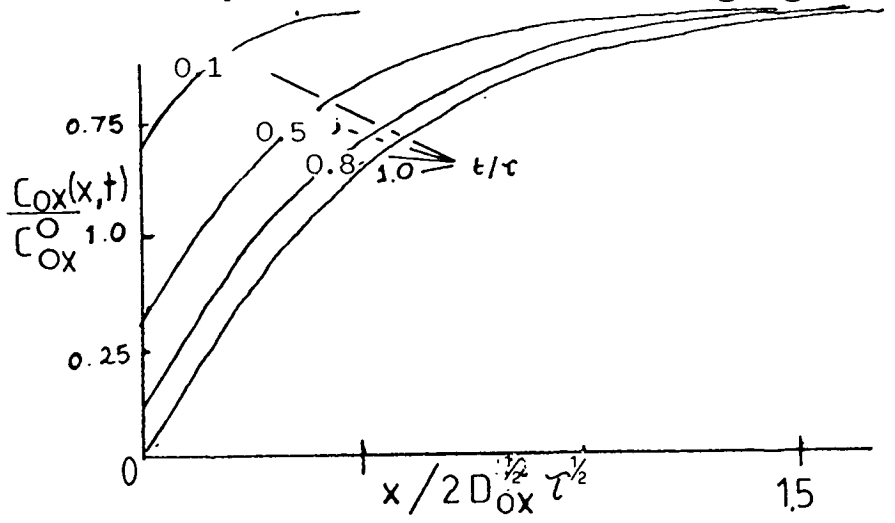

b/ Concentration profiles for Product RED of Reduction

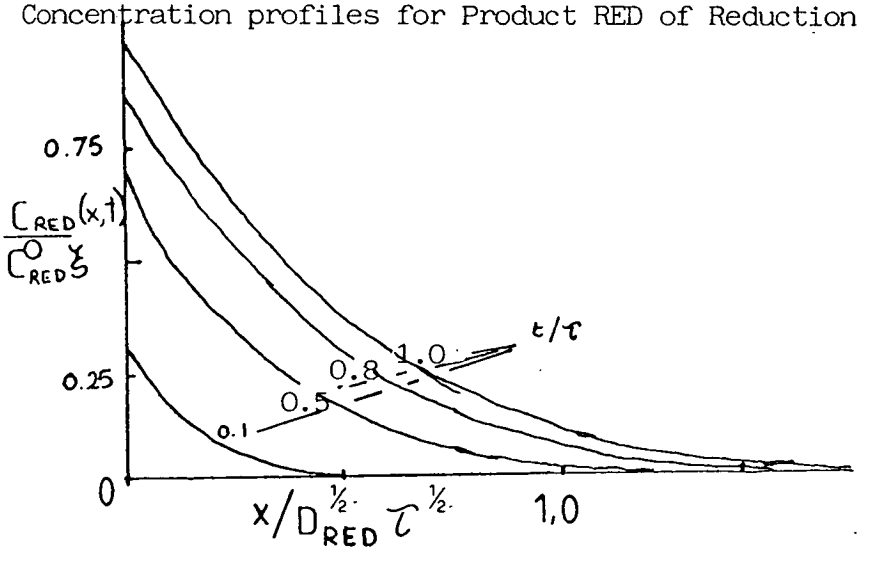

c/ Chronopotentiogram for $Ox + ze^- \leftrightharpoons Red$

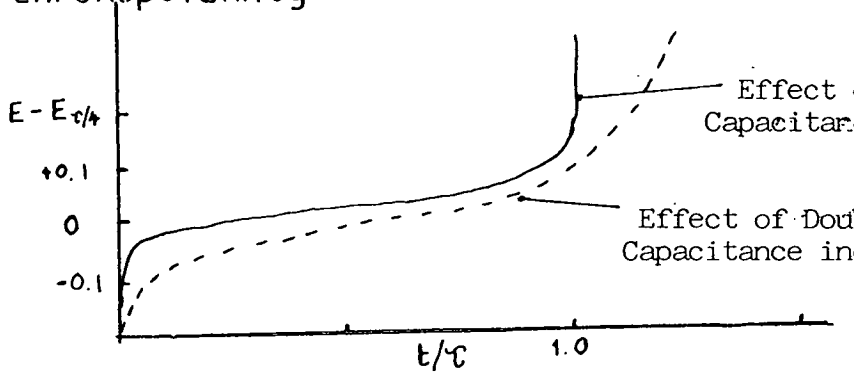

$$\frac{I}{zAF} = k_f \gamma_{ox} C_{ox}(0,t) - k_b \gamma_{Red} C_{Red}(0,t) \qquad 2.10.9$$

where $C_{ox}(0,t)$ and $C_{Red}(0,t)$ are given by 2.10.7a and 2.10.7b respectively. Thus

$$\frac{I}{zAF} = k_f \gamma_{ox} \left(C^o_{ox} - \frac{2It^{\frac{1}{2}}}{zAF\, D_{ox}^{\frac{1}{2}}\, \pi^{\frac{1}{2}}}\right) - k_b \gamma_{Red} \left(C^o_{Red} - \frac{2It^{\frac{1}{2}}}{zAF\, D_{ox}^{\frac{1}{2}}\, \pi^{\frac{1}{2}}}\right) \qquad 2.10.10$$

Depending on whether the current is anodic or cathodic k_f or k_b will be very small. Assuming k_b is small, -

$$\frac{I}{zAF} = k_f \gamma_{ox} \left(C^o_{ox} - \frac{2It^{\frac{1}{2}}}{zAF\, D_{ox}^{\frac{1}{2}}\, \pi^{\frac{1}{2}}}\right) \qquad 2.10.11$$

and from the definition of τ

$$k_f = \frac{\pi^{\frac{1}{2}} D_{ox}^{\frac{1}{2}}}{2\gamma_{ox} (\tau^{\frac{1}{2}} - t^{\frac{1}{2}})} \qquad 2.10.12$$

The same relation is obtained for irreversible reactions, since by definition k_b or k_f is zero.

2.10.3 Surface Reactions

As in the case of controlled potential experiments, surface reactions are more difficult to treat than the case of redox couples. A major problem is that the applied current is partitioned between capacitive and faradaic components, i.e. -

$$I = C_{dl} \frac{dE}{dt} + I_F \qquad 2.10.13$$

For a reaction of the type

$$M^{2+} + 2e^{-} \leftrightharpoons M$$

in which the current is controlled by the rate of electron transfer, a boundary condition is

$$I = C_{dl} \frac{dE}{dt} + I_o \left[\exp (1-\alpha) \frac{zFE}{RT} - \exp \frac{\alpha zFE}{RT} \right] \qquad 2.10.14$$

where the Faradaic contribution is given by equation 2.2.6

If $\frac{zFE}{RT} << 1$ then 2.10.14 can be approximated by

$$I = C_{dl} \frac{dE}{dt} + I_o \frac{\alpha zFE}{RT} \qquad 2.10.15$$

This equation can be solved to give[37]

$$E = E_\infty \left[1 - \exp \left(\frac{zFI_o}{RT} \frac{t}{C_{dl}} \right) \right]$$

in which E_∞ is the final steady potential.

The case of a two stage reduction has been analysed by Plonski.[37]

$$M \leftrightharpoons M^{z+} + ze^{-} \qquad A$$

$$M^{z+} \leftrightharpoons M^{y+} + (y - z)\, e^{-} \qquad B$$

Equation 2.10.13 becomes

$$I = C_{dl} \frac{dE}{dt} + I_A + I_B$$

the solution of which requires numerical methods. An interesting result of these methods is that for high currents, the potential passes through a maximum.

2.11 Voltammetry at Semiconductor Electrodes

In addition to measurements of surface conductivity and differential capacity as functions of electrode potential, the voltammetric and controlled current methods described in sections 2.9 and 2.10 have been applied to semiconductor electrodes. Voltammetric methods are useful for investigating surface reactions and also the behaviour of Redox couples at semiconductor electrodes. In section 2.8 it was noted that in the absence of surface states in the gap the cathodic reaction

$$Ox + ze^- \rightarrow Red$$

is only possible if the energy level of Ox coincides with filled electron states at the semiconductor surface. It was also noted that the application of an external EMF would not solely result in a change of the energies surface bands relative to the solution. For cyclic voltammetry a reversible Redox reaction will give a reduction and an oxidation peak at a metal electrode separated by 0.058/z V (eqn. 2.9.25). However the behaviour of the couple at a semiconductor electrode depends on its redox potential. The energy level of the redox couple can be found on the vacuum scale using the procedure outlined in section 2.7 and can thus be compared with energies of the bands of the electrode at the surface. If the energy level U^o_{Redox} is well above U_c - the conduction band edge and if n_s - the surface concentration of conduction band electrons - is high then the reduction can occur in precisely the same way as for a metal electrode. On reversal of the sweep oxidation will occur if the energy level U_{Red} remains above U_c. More precisely if a significant density of solution states overlap the conduction band at the surface, the oxidation will occur. The relative position of U^o_{Redox}, U_{Red} and U_{ox} depends on the factor λ as explained in section 2.7. By obtaining cyclic voltammograms for a range of redox couples with different redox energy levels, it is possible to infer the position of the

conduction band edge of a semiconductor electrode by noting for which couple reversible behaviour is first obtained. Bard[38,39] and co-workers have used this technique to investigate many binary semiconductors. In these studies acetonitrile was used as the solvent as this allows a much larger potential range to be swept, five volts compared to 1.5 V in aqueous solvents. Vanden-Berghe[40] et al. have employed the hexacyanoferrate couple in aqueous basic solutions to investigate the surface band edges of several semiconductors. This is the complementary technique to Bard in which one couple is used to investigate several semiconductors.

In practice the analysis of voltammograms recorded at semiconductor electrodes will be complicated by the presence of surface states and/or states in the gap due to other defects. These will allow exchange of electrons with species in solution even if U_{ox} and U_{Red} lie in the band gap. Analysis of the exact form of the voltammogram might help to distinguish between transfer with extended states and discrete states in the gap. Since in the former case the only rate determining step should be transfer to or from solution (i.e. electrons can be supplied or removed rapidly in the semiconductor bands). In the latter case it is quite possible that transfer of electrons within the semiconductor to the states in the gap is also a slow process. The quantitative analysis of voltammograms recorded at semiconductor electrodes is thus a potentially useful subject but so far it has never been attempted.

2.12 Reference Electrodes

It was noted in section 2.1 that the reference electrode defines the potential of the solution in contact with an electrode, in order that the potential difference between the electrode and the solution can be measured. In principal any half-cell can be used as a reference electrode but in practice certain systems will be more suitable than others. The reference electrode

must be stable and reproducible. In addition the electrode reaction responsible for the half-cell potential must be characterised by a high exchange current (I_o), i.e. the value of I_{CAT} or I_{AN} at equilibrium potential. This means the electrode potential does not vary significantly when small currents are drawn. For a cell such as that shown in figure 2.1 the reference electrode should also be chosen so that the liquid junction potential associated with the salt bridge can either be reduced to a minimum or be calculated and accounted for.

Reference electrodes in common usage can be classified as one of three basic types:

1. Anion reversible ("of the second kind").
2. Cation reversible.
3. Redox systems.

The most commonly used type in aqueous solution experiments are the anion reversible systems although the important Normal Hydrogen Electrode is a cation reversible electrode.

The importance of the Normal Hydrogen Electrode (NHE) is due to the fact that it is assigned a half-cell potential of 0.000 V at 25°C. Thus the equilibrium potential of any cell consisting of the NHE and another half-cell is defined as being equal to that of the other half-cell (plus any other potentials such as those associated with any junctions in the system). The construction of the NHE is shown schematically in figure 2.10a. Many different designs have been proposed and employed. The NHE of figure 2.10a consists basically of a platinum black sheet over which hydrogen gas is bubbled at a partial pressure of 1 atmosphere. The platinum is in contact with a 1 M solution of a strong acid, and catalyses the reaction

$$2H^+(aq) + 2e^-(Pt) \leftrightharpoons H_2(ads)$$

In spite of its fundamental importance the NHE is not generally used for measurements of equilibrium cell potentials, mainly because it is a very cumbersome device.

In an anion reversible electrode a metal contacts one of its own salts of low solubility. In some cases the metal may be present as an amalgam. The metal-salt combination is then immersed in a solution of fixed concentration of the anion (normally present as an alkali metal salt). The most important examples are the calomel and the silver-silver chloride electrodes. An example of the latter is shown in figure 2.10b. The silver-silver chloride electrode consists of silver metal covered with silver chloride and immersed in a solution of potassium or sodium chloride. The electrode reaction is

$$AgCl(s) + e^-(Ag) \leftrightharpoons Ag(s) + Cl^- (aq)$$

Thus the electrode potential depends on the concentration of chloride ion and furthermore AgCl can be used as the sensing material in a chloride ISE[42,18]. The Calomel electrode is based on similar principles to the Ag/AgCl electrode, the electrode reaction being

$$\tfrac{1}{2}\ Hg_2\ Cl_2(s) + e^-(l) \leftrightharpoons Hg(l) + Cl^-(aq.)$$

In addition to chloride ion reversible electrodes, sulphate[43] and carboxylate[44] reversible electrodes using the mercury (1) salts have also been proposed. These are useful where chloride ion must be excluded from the test cell. The thallous chloride-thallium amalgam (Thalamid)[45] reference electrode is claimed to be useable to higher temperatures than other reference electrodes.

For non-aqueous solutions cation reversible electrodes are more common. Bard[38] and co-workers use a silver-silver ion reference electrode for experiments in acetonitrile.

2.10 REFERENCE ELECTRODES

a/

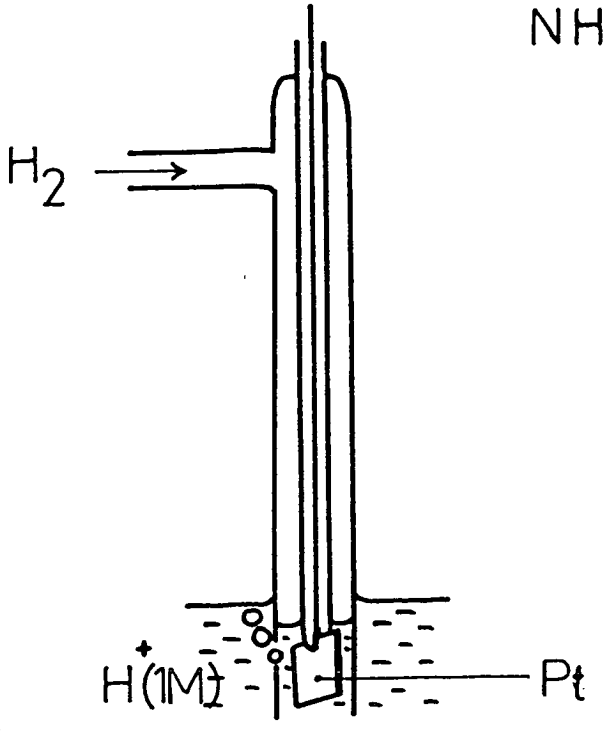

b/

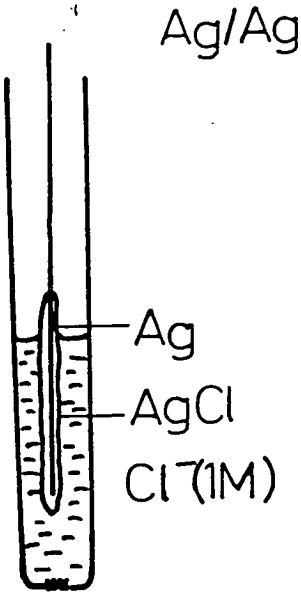

The use of a redox couple to provide a stable reference electrode in commercial pH sensors is becoming more common and it seems likely that these will replace the anion reversible electrodes employed in the past.[20]

Chapter 3

Chemical Sensors

3.1 Introduction

In Chapter 2 it was pointed out that certain structures give potentiometric responses to variations in ionic activities of the form:

$$E(a) = E_o + \frac{RT}{F} \log_e \frac{a_i}{a_i^o} \qquad 3.1.1$$

Furthermore in some cases the response was not affected by the presence of other ions. Such devices are known as Ion Selective Electrodes - ISEs. Providing they are truly selective and give stable, reproducible responses ISEs offer a convenient way of making quantitative chemical analysis. The minimal sample preparation required and the fact that the devices give a potentiometric output means they are particularly suitable for in-situ determinations of ionic concentrations. In this chapter ISEs that have been demonstrated in practice are discussed; many of these are of the membrane type introduced in section 2.4. Although this thesis is concerned primarily with the solid state devices described in sections 2.5 and 2.6 membrane devices are included in this chapter because of their practical importance - the majority of commercial ISEs are of this type - and because solid state devices that have been studied have normally been derived from them.

Although at first sight ISEs are potentially very useful devices all the electrodes described below have certain disadvantages:

(a) Their responses are never completely specific to one ion and are affected by temperature and ionic strength.

(b) The membrane devices are bulky and not very robust.

(c) They will only work in conductive solutions.

The ways in which these disadvantages can be overcome are discussed at the end of the chapter.

3.2 The Glass Electrode

Cremer[1], in 1906, first observed that a potential is developed across a glass membrane separating solutions of different pH. More detailed measurements on the relationship between membrane potential and the ratio of the hydrogen ion concentrations (or activity) on either side of the glass, followed in 1909[2] when the Nernstian relationship:

$$E_M = \frac{RT}{F} \log_e \frac{a^I_{H^+}}{a^{II}_{H^+}} \qquad 3.2.1$$

was established. In the 1930's commercially produced pH sensors, based on the glass electrode, began to appear. These were a result of detailed investigations into the effects of foreign ions and glass compositions.[3] The best glass composition was found to be Na_2O (22% by weight), CaO (6% by weight), SiO_2 (72% by weight) which was produced by Corning under the designation 015. In general the membrane potential was found to depend on Na^+, K^+, Ag^+, Zn^{2+} [3] in addition to H^+, although for many glass compositions the only significant interference came from high Na^+ concentrations together with high pHs. Early attempts to explain the functioning of the glass (pH) electrode assumed that the glass had a micro porous structure through which only the proton was small enough to pass. Tracer studies using tritium[4] showed that hydrogen ions do not pass through the membrane even when an external electric field is set up across it. Subsequently theories explaining membrane potentials[5] in terms of diffusion potentials and Donnan[6] equilibria allowed an explanation of the response of pH electrodes in terms of an ion exchange reaction at the glass solution interface between hydrogen ions and the mobile cations in the glass. In Corning 015 the exchange reaction is between hydrogen

ions and sodium ions:

$$H^+(aq) + Na^+(m) \rightleftharpoons H^+(m) + Na^+(aq) \qquad 3.2.2$$

where aq refers to the solution phase and m to the membrane and this explains why a Nernstian response is found only up to pH 11 or 12. Considering the Nickolsky equation for 2 ions (2.4.12):

$$\Delta\phi_m = \frac{RT}{F} \log_e \frac{a_{H^+}(1) + K_{H^+}^{pot}{}_{Na^+}\, a_{Na^+}(1)}{a_{H^+}(2)} \qquad 3.2.3$$

where 1 and 2 refer to the two solutions and it is assumed that $a_{Na^+}(2)$ - the activity of Na^+ in the test solution - is zero. If $a_{Na^+}(1)$ is sufficiently high, and $a_{H^+}(1)$ is low, as will occur in high pH solutions, the exchange equilibrium (3.2.2) will be well to the left and 3.2.3 takes the form:

$$\Delta\phi_m = \frac{RT}{F} \log_e \frac{K_{H^+}^{pot}{}_{Na^+}\, a_{Na^+}(1)}{a_{H^+}(2)} \qquad 3.2.4$$

characteristic of a sodium ion sensor. The idea of an exchange process was first proposed by Horovitz[6] to explain the dependence of membrane potential on the activities of certain other cations. In order to increase the pH range over which glass electrodes give a Nernstian response, compositions based on Li_2O have been used.[7]

The fact that monovalent cations interfere with the pH response of glass electrodes has lead to the development of sensors for other species. Eisenmann developed the so-called NAS 11-18 glass[8] for use in sodium Ion Selective Electrodes (ISE) and NAS 27-06 for use in potassium ISEs. These glasses are Na_2O: Al_2O_3: SiO_2 mixtures the coding NAS refers to the oxides used. The mobile species within the membrane is again Na^+ but the relevant exchange equilibria is this time between K^+ ions in the solution and Na^+. The potassium ISEs do not show high selectivity to K^+ being affected by pH and Na^+.

3.3 Crystalline Membrane Electrodes

Certain crystalline materials notably the sulphides such as Ag_2S and the rare earth fluorides are ionic conductors. Normally one type of ion is fixed at well defined lattice sites and the other ion then randomly fills the resulting network. Because only a certain proportion of the total number of sites are occupied, ions can readily move into adjacent vacant sites thus leading to ionic diffusion. The best known example of this behaviour is probably the low temperature β phase of silver sulphide, in which silver ion is the mobile species. The structure of β-Ag_2S is still not fully understood but it is known that the sulphide ions form a fixed lattice and silver ions fill about half the possible sites. If silver ion is the only species that has a high mobility within the silver sulphide membrane, the potentiometric selectivity cofficients $K^{pot}_{Ag,i}$ are

$$K^{pot}_{Ag,i} = K_{Ag,i} \frac{U_i}{U_{Ag}}$$

where U_i and U_{Ag} are the mobilities of i and Ag respectively. $U_i = \frac{D_i}{RT}$ will be small even if $K_{Ag,i}$ is large. Thus a silver sulphide membrane electrode represents a highly selective device. Furthermore, silver sulphide has a very low solubility and a high conductivity[9] ($K \sim 10^{-3}\ \Omega^{-1}$ cm) so that it is ideal for use in ISEs and it has been exploited in commercial devices since the 1960's. The only major interferents are the mercury (II) ion which reacts with the silver sulphide by a displacement reaction

$$Hg^{2+}(aq) + Ag_2S(s) \leftrightharpoons 2Ag^{+}(aq) + HgS(s)$$

and the cyanide ion[10] which tends to complex with Ag^+

$$6CN^{-}(aq) + AgS(s) \leftrightharpoons S^{2-}(aq) + 2Ag(CN)_3^{2-}(aq)$$

Silver sulphide membranes can be used to determine the concentration of either the Ag^+ or the S^{2-} ion. If the test

solution is equilibrated with silver sulphide, then the silver activity is fixed by the solubility product of the silver sulphide:

$$K_{SP}(Ag_2S) = a_{Ag}^2 \, a_S \qquad 3.3.1$$

hence

$$a_{Ag} = \left(\frac{K_{SP}}{a_S}(Ag_2S)\right)^{\frac{1}{2}} \qquad 3.3.2$$

Substituting 3.3.2 into the Nernst equation:

$$E = E^o + \frac{RT}{F} \log_e a_{Ag^+}$$

gives the result;

$$E = \{E^o + \frac{RT}{2F} \log_e K_{SP}(Ag_2S)\} - \frac{RT}{2F} \log_e a_S \qquad 3.3.3$$

The term in brackets is a constant so that a Nernstian response results. Various types of membrane have been proposed; single crystal[11], polycrystalline[12] and heterogeneous.[13] The latter involves dispersing silver sulphide in an inert matrix such as silicone rubber.

The high conductivity of silver sulphide has been exploited in membrane electrodes sensitive to other ions. In these devices, compacts of silver sulphide and a second binary sulphide MS, are used as the membrane.[14] The silver ion activity is controlled by two equilibria:

$$2Ag^+ + S^{2-} \rightleftharpoons Ag_2S \qquad K_{SP}(Ag_2S) = a_{Ag}^2 \, a_S \qquad 3.3.4$$

$$M^{2+} + S^{2-} \rightleftharpoons MS \qquad K_{SP}(MS) = a_m a_S \qquad 3.3.5$$

Combining 3.3.5 and 3.3.4 gives an expression for a_{Ag^+}

$$a_{Ag^+} = \left[\frac{K_{SP}(Ag_2S)}{K_{SP}(MS)} a_{m^{2+}} \right]^{\frac{1}{2}} \qquad 3.3.6$$

Substitution of 3.3.5 into the Nernst equation gives:

$$E = \text{const.} + \frac{RT}{2F} \log_e a_{m^{2+}} \qquad 3.3.7$$

The membrane responds to Ag^+ as well as M^{2+} of course and if this is initially present in the solution it will interfere. Furthermore, any other ion N^{2+} which is at a sufficiently high concentration can be expected to interfere by a displacement reaction:

$$N^{2+} + MS(aq) \rightleftharpoons NS(s) + M^{2+}(aq)$$

Mixed sulphide membrane ISEs have been demonstrated for Cu, Cd and Pb detection.[15] The interferents for each type of sensor can be predicted from a table of solubility products.

In addition to the mixed Ag_2S MS membranes, mixed Ag_2S-AgX membranes where X is a halide have also been described. Kolthoff demonstrated that silver halides could be used as sensing membranes for halide ions in the same way that silver sulphide is used as a sulphide ion detector. However the conductivity of silver halides is low and the membrane potential is also sensitive to light. Ross[12] showed that a mixed membrane avoided these undesirable characteristics, the mechanism is thus similar to that in Ag_2S-MS systems.

The rare earth fluorides represent the other main group of crystalline ionic conductors that have been used as membranes. The best known example is lanthanum fluoride,[14] but membranes comprising single crystals of NdF_3 and SmF_3 have also been demonstrated. The mobile species in these materials is the

flouride ion and the conductivity is about 10^{-7} Ω^{-1} cm^{-1}. The conductivity can be increased by doping with a second rare earth metal, usually Eu. The electrodes can be used for sensing F^- or La^{3+} by equilibrating the test solution with LaF_3. Detection limits under ideal conditions are $\sim 10^{-7}$ M. One of the main causes of interference is the complexation of the flouride ion in species such as HF_2^-, although OH^- ions also interfere. The hydroxyl interference is believed to be the result of these ions penetrating the membrane, thus setting up their own diffusion potential and altering the fluoride ion level at the membrane surface.[16]

3.4 Liquid Membrane Electrodes[14]

A large number of systems have been developed in which the membrane consists of a hydrophobic solvent and some means of confining it. The solvent contains a species that will complex with the ion of interest to give a lyophillic ion which can diffuse through the membrane. The complexing species is chosen to be highly selective in its reaction with ions and this reaction thus plays the role of the ion exchange described in section 2.4. Using this method ISEs have been developed for Ca^{2+}, NO_3^-, ClO_4^-, Cl^-, BF^- and CNS^-. In addition certain macrocyclic neutral molecules have been studied as possible complexing agents. Because of the well defined ring size such molecules could lead to exceptionally selective membranes.

A schematic diagram of an ISE employing a liquid ion exchanger is shown in fig. 3.1b. In this system the hydrophobic solvent is confined to a porous plug.

3.5 Solid State Ion Selective Electrodes Using Ionic Conductors

It is clear from the preceeding sections that membrane ISEs have been developed for a large number of ions. Nevertheless the application of ISEs, particularly as transducers in process

3.1 MEMBRANE I.S.E.

a

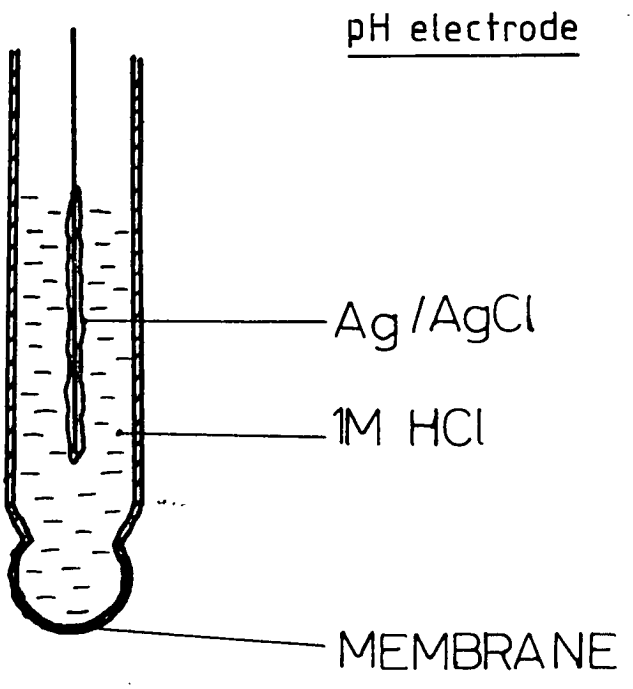

b

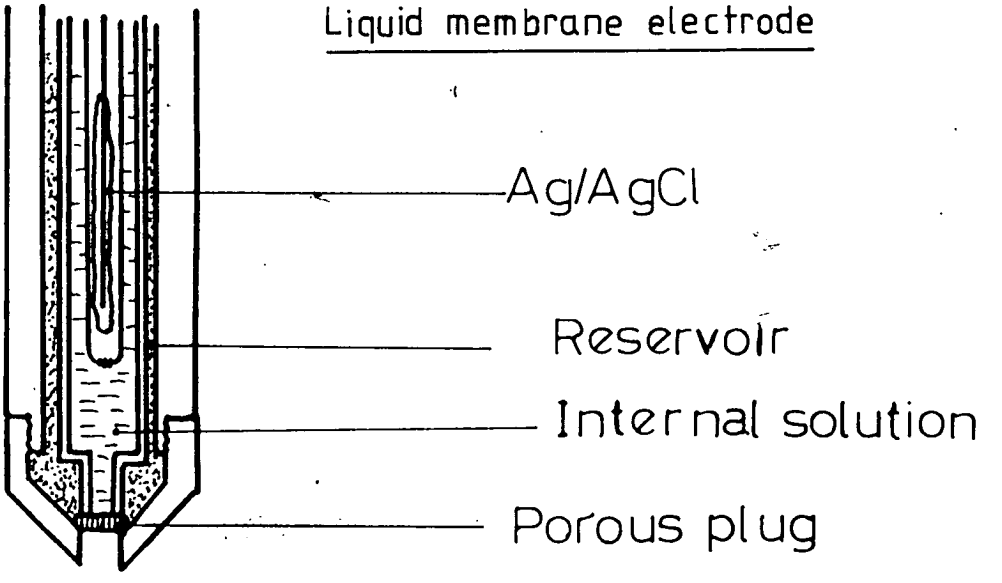

monitoring and control systems, has not been as widespread as might be expected. The reason for this is that the membrane structure is necessarily bulky and complicated. An extreme example is shown in fig. 3.1b where the liquid membrane electrode requires three concentric tubes in its construction. As a corrollary membrane electrodes are often delicate and expensive to produce. The cost remains high due to limited demand itself partly deriving from the high cost. Some of the undesirable properties of conventional membrane ISEs arise directly from the presence of the internal reference electrode and filling solution and, as discussed in sections 2.5 and 2.6, where it is possible to replace these with a direct electrical contact a much smaller, cheaper and more robust device can be produced. In this section solid state ISEs that have already been demonstrated will be reviewed. It should be noted again that many authors use the term "solid state" to refer to membranes that are based on solid materials, but are in fact membrane ISEs. In this thesis the term "solid state electrode" is used to mean those without a filling solution.

Solid state systems have been exploited for many years as reference electrodes. The silver-silver halide electrodes are good examples of systems that are usually employed as reference electrodes, but could equally well be used as halide ISEs. Solid state systems based on metal sulphides and oxides were also first investigated as reference electrodes, rather than as ISEs. For this reason many early studies considered half cells of the anion reversible type[16]

$$M \mid MS \mid S^{2-}(aq)$$

and

$$M \mid MO \mid H_2O + O^{2-} \quad OH^-$$

rather than the cation reversible systems related to the membrane electrodes described in section 2.4. Noddack[17] claimed that metal

sulphides could be considered as the metal diluted in an inert sulphide matrix, and that providing the differences in composition that can occur in sulphides are taken into account, their behaviour towards metal ions should be qualitatively the same as that of the metal itself. The investigation of sulphides and oxides as reference electrodes meant that attention was restricted to configurations in which the metal contact corresponded to the metal of the sulphide or oxide. Because the electrode reaction was of the type

$$me^- + M_m X_x(s) \leftrightharpoons mM(s) + x\, X^{m\overline{x}}(aq)$$

the presence of the metal M was seen as a thermodynamic necessity. Nevertheless in cases where different metals were used little or no difference was found in the electrode potential.[18] The electrode potential is often observed to be very sensitive to the way in which the half cell is prepared however and in particular to the exact composition of electrode and to the way in which the contact is made. Sato pointed out the important distinction between binary compounds showing mainly electronic conduction and those showing mixed or predominantly ionic conduction. Sato's discussion of electronic conductors has already been reviewed in section 2.6. The major conclusions were:

1. Providing the contact metal does not in any way react with the binary compound, its nature is immaterial to the half cell potential.

2. The half cell potential is strongly dependent on the exact composition of the phase.

Since most binary metal sulphides show negligible ionic conduction over the temperature range in which they could be used as ISEs (< 100°C) Sato's conclusions are expected to apply.

The case of ionic conduction was considered only briefly by Sato. For a half cell of the type:

$$M^{m+}(aq) \mid MX_{1+\gamma} \mid C$$

where C is a contacting metal that may or may not be M itself. At the interface between the solution and $MX_{1+\gamma}$ a small quantity "δ" of M^{m+} ions are exchanged. If $MX_{1+\gamma}$ is in equilibrium with pure M (as would be the case if the contact C is M) then electrons transferred to the binary simply discharge the M^{m+} ions, so that the composition is unaffected. This means that ions entering the MX phase do not affect the potential difference between this and the contact. On the other hand if $MX_{1+\gamma}$ is not equilibrated with M (i.e. the contact is a different metal) then the composition of the phase will change to $M_{1+\delta}\ X_{1+\gamma}$. The chemical potential of M in the phase $MX_{1+\delta}$ depends strongly on the exact composition and so the cell potential may also be expected to vary.

Koebel[19] considered the special case of a silver backed Ag_2S half cell and also of solid state MS-Ag_2S cells. Silver sulphide has an appreciable ionic conductivity and an electronic conductivity that depends strongly on the exact composition of the $Ag_{2+\delta}S$.[9] Specifically the cells

$$C \mid Ag \mid Ag^{+}(aq) \mid Ag_{2+}\ S \mid C$$

and

$$C \mid Me \mid Me^{2+}(aq) \left| \begin{array}{ll} Ag_{2+} & S \\ Me_x & S \end{array} \right| C$$

were considered. The total cell potential is given by the sum of the potential differences across each interface, it being tacitly assumed that each phase was a perfect conductor (see section 2.5). The potential differences themselves are given by:

$$\phi(II) - \phi(I) = \frac{-1}{F}\ (\mu_e(II) - \mu_e(I)) \qquad 3.5.1$$

where I and II refer to any two phases on either side of an interface. In the ionically conducting aqueous phase and $Ag_{2+\delta}S$ phase the total current at equilibrium is zero, so that

$$I_e + I_{Ag^+} = 0. \qquad 3.5.2$$

The Nernst Plank equation can be used to expand equation 3.5.2 into

$$\frac{-\kappa_e}{F}\frac{d\mu_e}{dx} - \kappa_e\frac{d\phi}{dx} \quad \frac{-\kappa_{Ag^+}}{F}\frac{d\mu_{Ag^+}}{dx} - \kappa_{Ag^+}\frac{d\phi}{dx} = 0 \qquad 3.5.3$$

where κ_i is the conductivity of i. If equation 3.5.3 is rearranged an expression for ϕ results

$$\frac{d\phi}{dx} = \frac{-1}{F}\left(\frac{\kappa_e}{\kappa_e + \kappa_{Ag^+}}\frac{d\mu_e}{dx} + \frac{\kappa_{Ag^+}}{\kappa_e + \kappa_{Ag^+}}\frac{d\mu_{Ag^+}}{dx}\right) \qquad 3.5.4$$

since $$d\mu_{Ag^+} + d\mu_{e^-} = d\mu_{Ag} \qquad 3.5.5$$

equation 3.5.4 can be rewritten,

$$\frac{d\phi}{dx} = \frac{-1}{F}\left(\frac{\kappa_{Ag^+}}{\kappa_e + \kappa_{Ag^+}}\frac{d\mu_{Ag}}{dx} - \frac{d\mu_e}{dx}\right) \qquad 3.5.6$$

The total potential difference is given by

$$\Delta\phi = \frac{-1}{F}\int_{x_1}^{x_2}\left[\frac{\kappa_{Ag^+}}{\kappa_e + \kappa_{Ag^+}}\,d\mu_{Ag} - d\mu_e\right] \qquad 3.5.7$$

This can be split into 2 integrals one for the aqueous phase and one for the Ag_2S. Koebel showed by summing all the potential drops that $\Delta\phi$ is the cell potential. The integral over $d\mu_e$ is accounted for at the Ag/Ag^+ and Ag_2S/C boundaries so that

$$\Delta\phi = \frac{-1}{F} \int_{(aq)} d\mu_{Ag} \frac{-1}{F} \int_{Ag_2S} \frac{\kappa_{Ag^+}}{\kappa_{Ag^+} + \kappa_{e^-}} d\mu_{Ag} \qquad 3.5.8$$

where it has been assumed that $\mu_e = 0$ in the aqueous (aq) phase. Koebel assumed that μ_{Ag} is uniform across the sulphide in which case

$$\Delta\phi = \frac{-1}{F} \int_{(aq)} d\mu_{Ag} = \frac{-1}{F} (\mu_{Ag}\ (Ag_{2+\delta}S) - \mu^o_{Ag}) \qquad 3.5.9$$

so that $\Delta\phi$ depends entirely on the chemical potential of silver in the silver sulphide, which itself depends strongly on composition. Because there are no data on the way in which μ_{Ag} varies with composition, Koebel was only able to calculate $\Delta\phi$ for the limiting compositions where Ag_2S is in equilibrium with sulphur and where it is in equilibrium with silver. The latter is interesting because this will be the case where the contacting metal is silver itself. In this case $\mu_{Ag}(Ag_{2+\delta}S)$ will be simply μ^o_{Ag} and $\Delta\phi$ will be zero. The electrode potential of a silver-silver sulphide electrode should be identical to that of a silver metal electrode. Koebel's experimental results agreed with this conclusion. The former case of Ag_2S in equilibrium with sulphur also gave a half cell potential that agreed closely with the theoretical value. This is interesting because Koebel used a graphite contact, thus proving that in general a silver contact is not necessary. The reason for this is that at the back contact the potential difference is due to the difference between the chemical potentials of electrons in the graphite and in the silver sulphide. At the solution contact a potential difference arises due to the difference in chemical potential of the silver in the silver sulphide and the silver in the solution. In this respect Koebel's description of the solution-ionic conductor system is different to that of Sato's in which the transfer of ions between the phases is assumed to alter the composition of the ionic conductor.

Koebel also considered the mixed sulphide systems Ag_2S-PbS, Ag_2S-CdS and Ag_2S-Cd_xS. The potentials were calculated for three

limiting cases in which the sulphide was equilibrated with (i) silver, (ii) sulphur and (iii) Cd, Pb or Cu. The copper system is complicated by the presence of several stable phases. In fact these results showed that Pb and Cd contacts would be unstable due to displacement of silver from silver sulphide. For electrodes contacted with silver the observed cell potentials were only within 50 mV of the calculated values. For electrodes using the sulphides equilibrated with sulphur and contacted with graphite agreement was better.

It is important to note that neither Sato nor Koebel assumed that the contacting metal must be that of the metal sulphide itself. Where this is the case, the metal contact fixes the chemical potential of the metal in the sulphide, which will not vary as a result of variations in the activity of the metal in the aqueous phase. The electrode potential is then given by the Nernstian relation alone. If the sulphide is equilibrated with excess metal, but contact is made with a different metal then a Nernstian response is still expected because $\mu_{Ag}\ (MS_{1+\delta})$ remains fixed. If the sulphide is equilibrated with excess sulphur $\mu_M\ (MS_{1+\delta})$ is again fixed but at a different value which can be found from the free energy of formation (ΔG_f) of the sulphide. For a general compound M_xX_m

$$m\mu_X + x\mu_M = \mu_{M_x\ X_m} \qquad 3.5.10$$

Since μ_X is fixed by the presence of excess X at the chemical potential of pure X i.e. zero, then

$$\mu_M = \frac{\Delta G_f}{x} \qquad 3.5.11$$

This value can be substituted into 3.5.9 to give the cell potential.

For all other compositions of $MX_{1+\delta}$ the composition will vary as the activity of M^{m+} in the solution varies. Thus $\mu_M(MX_{1+\delta})$ will vary with solution composition and the response will deviate

from Nernstian behaviour. In both the latter configurations M cannot be the contacting metal, but a reproducible response to M^{m+} is still expected.

From a practical point of view the important property is that there is a high exchange current of electrons and M^{m+} ions in order that equilibrium is rapidly established. The mixed sulphide solid state ISEs have been manufactured by Orion since the 1960s.[20]

The rare earth fluorides are an example of sensing materials where it is impractical to equilibrate with an excess of either component element; fluorine is a gas and lanthanum is prone to oxidation. Fjeldy and Nagy[21,22] have proposed a three layer structure in which a silver fluoride layer contacts the lanthanum fluoride. The AgF is itself contacted by Ag, i.e.:

$$Ag \mid AgF \mid LaF_3$$

It is assumed that fluoride ion transfer occurs at the AgF | LaF_3 interface whilst electron transfer occurs at the Ag | AgF interface. The reactions are,

$$\delta F^- (aq) \leftrightharpoons \delta F^- (LaF_3)$$

$$AgF + \delta F^- (LaF_3) \leftrightharpoons Ag\ F_{1+\delta} + \delta e^-$$

$$\delta e^- + \delta Ag^+ \leftrightharpoons \delta Ag$$

The overall process is therefore simply

$$AgF + e^- \leftrightharpoons Ag + F^- ;$$

the exchange reaction of a Ag/AgF fluoride ISE. Using this configuration rapid responses were obtained and a Nernstian response (60 mV decade) was found for flouride between 10^{-3} M and 5×10^{-6} M.

The preparation of the AgF/LaF_3 interface was difficult, requiring the fusion of two flourides at 450°C. Nernstian behaviour will only result if the exact stoichiometry of the LaF_3 and AgF remain fixed; in general this is not the case. Fluoride ion entering the LaF_3 will alter its composition at the LaF_3/AgF junction due to the following reaction:

$$\delta F^- + LaF_3 \leftrightharpoons LaF_{3+\delta} + \delta e^-$$

and similarly the AgF composition will be altered:

$$\delta e + \delta Ag^+ + AgF \leftrightharpoons Ag_{1+\delta} F$$

The latter composition change can be avoided if the AgF is first equilibrated with an excess of silver thereby fixing its composition (see section 4.2). The silver back contact in theory acts as the excess silver, but in practice the self diffusion of silver into AgF is probably too slow to fix the composition.

Even if it is assumed that LaF_3 is a purely ionic conductor it is still possible to discuss a device where LaF_3 is contacted by an inert electronically conducting back contact:

$$F^-(aq) \mid LaF_3 \mid C$$

Fluoride ions will enter the LaF_3 and diffuse to the LaF_3/C junction. There the fluoride ions must discharge their excess electrons:

$$\delta F^-(aq) \leftrightharpoons \delta F^- (AgF)$$

$$\delta F^-(AgF) + AgF \leftrightharpoons AgF_{1+\delta} + \delta e^-$$

$$\delta e^-(AgF) \leftrightharpoons \delta e^-(C)$$

This is nothing more than Sato's reaction scheme for an ionic conductor. Unless the variation of chemical potential with stoichiometry is known, no predictions can be made on the departure of the electrodes response from the ideal Nernstian. Such a device is considerably simpler than that proposed by Fjeldy et al.

3.6 Solid State ISEs Using Electronic Conductors

As was mentioned in the previous section, solid state sensors, using mixed sulphides, are manufactured by Orion Research. Such ISEs are available for Ag^+, Cd^{2+}, Pb^{2+}, Cu^{2+} and they exploit the high conductivity of Ag_2S. In the 1970s various workers experimented with the idea of replacing sulphur with one of the other chalcogenide elements, selenium or tellurium. The selenides are generally more conducting than the sulphides and their lower solubility in aqueous solution could mean that suitable ISEs may be prepared for ions other than those above. Hirata and Higashiyama[23] prepared solid state electrodes using Ag_2Se and Ag_2Te, and found that the Ag_2Se electrode could respond to Ag^+ concentrations between 10^{-1} and 10^{-10} M. This is a considerably lower detection limit than is generally accepted for Ag_2S (10^{-7} M). In addition to Ag sensors these workers also investigated the simple selenides of Cu, Pb, Cd, Zn, Mn, Cr(III), Cd(II) and Ni as possible replacements for mixed sulphide systems. Of these selenides the Cu, Pb, Cd and Zn electrodes were found to give Nernstian responses to 10^{-6} M, however the transition metal sensors were not particularly good. All the selenides and tellurides are predominantly electronic conductors and so the nature of the back contact is unimportant, providing it is un-reactive. Sekerka and Lechner[24] made a detailed study of mixed sulphides, selenides and tellurides using both silver and mercury (II) chalcogenides as the matrix materials. These workers also studied mixed chalcogenide-halide materials as possible halide ISEs. Ion selective electrodes for Ag^+, Hg^{2+}, Pb^{2+}, Cu^{2+} and Cd^{2+} were claimed to perform well and

$HgSe-Hg_2Cl_2$, $HgFe-Hg_2Cl_2$ chloride ISEs were said to have lower detection limits than the analogous silver systems (section 4.3). Neshkova and Sheytanov[25] describe a Cu^{2+} ISE in which a mixture of copper selenides is electrolytically deposited from a $CuSO_3/Na_2SeO_3$ solution. All the electrodes described so far are of the type discussed by Sato; that is they are based on a binary compound with a low solubility product. The surface stoichiometry is modified by the deposition reaction

$$M + X \leftrightharpoons MX$$

and this leads to the observed response. In general the electrode potential depends on the ratios of the activities of M (or X) in the solution and in the electronic conductor MX. The latter can be determined for special cases in which MX is in equilibrium with a neighbouring phase.

3.6.1 Semiconductor Electrodes - $Se_{60}Ge_{28}Sb_{12}$ Glasses

A different type of electrode was discovered in the 1970s by Jasinski and co workers.[26] These electrodes used semiconducting glasses either of stoichiometry $M_xSe_{60}Ge_{28}Sb_{12}$ ($x \cong 2$) or $Cu_x(As_2S_3)_{100-x}$ ($5 \leqq x \leqq 30$). Although these materials are normally termed glasses, as used by Jasinski they contained considerable amounts of crystalline material. The first materials to be studied were the metal doped $Se_{60}Ge_{28}Sb_{12}$ electrodes,[27] which were found to give Nernstian responses to ferric ions between 10^{-1} M and 10^{-5} M. The slope of the response (60 mV decade^{-1}) was indicative of a 1 electron process. It was found that the metal dopant could be either Fe, Co or Ni without affecting the response. Unfortunately the only detailed interference studies reported were those of Cu^{2+} which led to Nernstian responses with the 30 mV decade^{-1} slope characteristic of a 2 electron process in nitrate solution. In chloride solution the response was between 50 mV decade^{-1} and 60 mV decade^{-1}. Response to copper was only found if Fe^{3+} was absent. The presence

of Fe^{2+} was also investigated and was found to have no affect. It was noted that Cd^{2+}, Co^{2+}, Ni^{2+} and Pb^{2+} did not effect the electrodes response to Fe^{3+} whereas Cu^{2+}, Ag^{+}, Hg^{2+}, Mn^{3+} and Ce^{4+} did.

The authors proposed a mechanism in which the electrode potential depends on a redox reaction between Fe^{3+} and some form of reduced surface site - "SRed".

$$SRed + Fe^{3+} \leftrightharpoons SOx + Fe^{2+}$$

For Cu^{2+} in nitrate solution a 2 electron transfer is necessary. It should be noted that in all cases the concentration of the reduced form of the couple must somehow be kept constant, if the electrode is to respond only to changes in concentration of the oxidised form. The authors state without justification that, "the single electrode potential for the reducing agent is between -0.12 and +0.18 V".

Here it is suggested that it is important to divide the ions into those which form only one type of stable ion in solution (Ag^{+}, Hg^{2+}, Cd^{2+}, Ni^{+} and Pb^{2+}) and those forming more than one (Cu^{2+} [in Cl^{-}], Co^{2+}, Mn^{3+}, Ce^{4+}). This is because although metal/metal-ion processes have well-defined redox potentials, as explained in Chapter 2, the formation of the metal results in plating of the surface of the electrode and in any case may have a high activation energy due to the necessity for nucleation and growth. The ions Ag^{+} and Hg^{2+} are special cases that are found to interfere with all chalcogenide based electrodes and will be discussed later. Of the remaining ions the redox potentials are:

$$Co^{3+} \leftrightharpoons Co^{2+} + e^{-} \qquad +1.8\ V$$

$$Mn^{3+} \leftrightharpoons Mn^{3+} + e^{-} \qquad +1.6\ V$$

$$Ce^{4}+ \leftrightharpoons Ce^{3+} + 3e^{-} \qquad +1.44\ V$$

$$Fe^{3+} \leftrightharpoons Fe^{2+} + e^- \qquad +0.77\ V$$

$$Cu^{2+} \leftrightharpoons Cu^{+} + e^- \qquad +0.16\ V$$

These redox potentials can be converted to mean energy levels on the vacuum scale using the methods discussed in section 2.7. If 2 values can be calculated the actual positions of U_{Red} and U_{ox} can be estimated. Since the electrode's response to Fe^{3+} is the same regardless of whether the semiconductor is combined with low levels of Co, Fe or Ni, it appears that these metals are altering the electronic structure rather than creating sites which take part in a specific chemical reaction with Fe^{3+}. In other words they are behaving as dopants and the electrode's response derives from an electronic interaction between Fe^{3+} in solution and the energy levels in the doped semiconductor glass. Metal dopants are most likely to give n-type materials due to their ionization potentials. If positive ions are adsorbed at the electrode surface, as proposed by Jasinski,[28] then an accumulation region is likely to form at the surface. The maximum energy of the conduction electrons is then sufficient to reduce Fe^{3+}, Mn^{3+}, Ce^{4+} and Cu^{2+} but not Co^{3+}, which because of its high redox potential has a U_{ox} value that is well above the highest energy of the conduction electrons. This model could be tested using cyclic voltammetry, as discussed in section 2.11. Alternatively electron transfer may occur between surface states and the redox couples.

In a later paper, Jasinski and Trachtenberg[27] made more detailed studies of the behaviour of $Fe_xSe_{60}Ge_{28}Sb_{12}$ electrodes in Fe^{3+} solutions. They noted that Nernstian responses were only obtained after the electrode surface was properly "activated", a process which involved exposing the electrode surface to high Fe^{3+} concentrations for several hours. It was concluded that the Fe^{3+} in the activating solution oxidized the electrode surface and is then absorbed by some unspecified mechanism onto the oxidised sites (OxS) to create active sites (Act S). The response

is then supposed to result from an exchange between Fe^{3+} in solution and the active sites. In this study it was found that if an electrode originally exposed to high Fe^{3+} concentration is placed into a solution of much lower Fe^{3+} concentration, the concentration in solution actually rises, presumably as a result of Fe^{3+} desorbing from the active sites. The equilibrium

$$Fe^{3+} + \text{Act S} \leftrightharpoons \text{Act S } Fe^{II}$$

must be a 1 electron process to account for the 60 mV decade^{-1} dependence of electrode potential on Fe^{3+} concentration.

3.6.2 Semiconductor electrodes Based on As_2X_3 Glasses

Jasinski, Trachtenberg and Rice[28] discovered that alloys of Cu with As_2S_3 could be used to make a cupric ion ISE. In nitrate solutions a Nernstian behaviour with a slope of 30 mV decade^{-1} was found for concentrations between 10^{-1} M and 10^{-6} M. In chloride solutions a different response was obtained, the slope normally being steeper (50 mV decade^{-1}) and the individual electrode potentials being more negative than in nitrate solutions. The electrode potentials were sensitive to stirring and were more positive when stirring was in progress. The stirring dependence was greater in chloride solutions than in nitrate solutions and was greatest for high copper concentrations. Interference was not found from Cu^{2+}, Ni^{2+}, Pb^{2+}, Mn^{2+} or Zn^{2+} but was observed for Fe^{3+} and Ag^{+}.

In common with the $Se_{60}Ge_{28}Sb_{12}$ electrodes, the $Cu_2(As_2S_3)_{100-x}$ glasses require activation, in this case by immersion in a strong Cu^{2+} solution (10^{-1} M) for several hours. From these observations it was concluded that the response mechanism is similar to that proposed for the $Se_{60}Ge_{28}Sb_{12}$ electrodes. Active sites produced in the activation step react reversibly with Cu^{2+}

$$(\text{Act S}) + Cu^{2+} \leftrightharpoons (\text{Act S})\,Cu + 2e^{-}$$

A two electron process is necessary to explain the 30 mV decade^{-1} slope observed. The active sites Act S are themselves formed by oxidation of the electrode surface to give oxidised sites (OxS) which react with Cu^{2+} from solution to give the active sites. In the original work Jasinski stated that the OxS sites were the result of the oxidation of sinnerite, a crystalline compound that was found to be present in the glasses, but the only justification was that electrodes made entirely from sinnerite gave similar responses to the glass electrodes.

The quantitatively different behaviour of the electrode in chloride solutions was explained on the basis of the increased stability of the Cu^{+} ion in chloride solutions. Jasinski believes that in the presence of chloride Cu dissolves from the surface as cuprous chloride CuCl. Cuprous chloride then reacts with cupric chloride to give a soluble complex, thus reducing the level of free Cu^{2+} and in consequence the electrode potential drops below the expected value. A similar mechanism explains the different behaviour of $Se_{60}Ge_{28}Sb_{12}$ electrodes towards $Cu(NO_3)_2$ and $CuCl_2$ solutions.

In later studies Drennan[29] and Wheatley[30] investigated the possibility of using the analogous Se and Se/Te glasses. These studies, whilst not being as detailed as those of Jasinski, showed that the selenides and selenide-tellurides gave very similar responses to the sulphides, and had the advantages of being more resistant to chemical attack and more conductive (see Chapter 4).

3.7 Micro Ion Selective Electrodes

One of the principal disadvantages of membrane ISEs is their large size, particularly when they are to be used in small scale flow systems including those applications of medical interest. Nevertheless, membrane ISEs have been produced in a form suitable for *in vivo* measurements on living cells. Most ISEs that are selective to physiologically important ions (H^{+}, Na^{+}, K^{+}, Cl^{-}, Ca^{2+}) have been prepared in this form.[31]

The usual way of preparing a micro ISE is to draw the membrane material to a fine point which is then used to penetrate the cytoplasm. The remainder of the structure, the filling solution and internal reference electrode remain outside and can be of normal size. The external reference electrode is prepared in a similar manner from a system of normal size by drawing the stock into a fine capillary which also penetrates the cell. In some studies a second micro-ISE serves as the reference electrode, as this avoids contaminating the cyto-plasm. Such micro-electrodes obviously have extremely small active areas, but are nevertheless very delicate and would be expensive to produce.

Many industrial processes require rugged sensors but not necessarily the very small devices possible with micro-membrane structures. It is obviously possible to produce solid state ISEs by simply scaling down the devices described in sections 3.5, 3.6, 5.2 and in this way active sensing areas of c.a. 1 mm^2 should be easily attained.

It is useful in this context to consider briefly how cell potentials are measured. Although a potentiometer has been shown in fig. 2.1 it is more convenient to use a high impedance voltmeter to measure cell potentials. The first stage of such a device is usually a MOSFET which gives a very high input impedance (typically 10^{12} Ω). The way in which the MOSFET is employed to measure electrode potentials for a membrane and a solid state ISE is shown in fig. 3.3a and 3.3b. The current flowing from the source to drain is modulated by the potential difference between the gate and source and since the external reference electrode is always connected to source, current is modulated by cell potential. In practice, additional amplification, biasing and stabilisation circuitry must be present. The complete device can be produced in integrated form, either using only MOSFET technology or combining MOSFET and bi-polar devices on the same chip. In fig. 3.3c is shown the so-called

3.3 EVOLUTION OF THE "ISFET"

a/ MEMBRANE I.S.E.

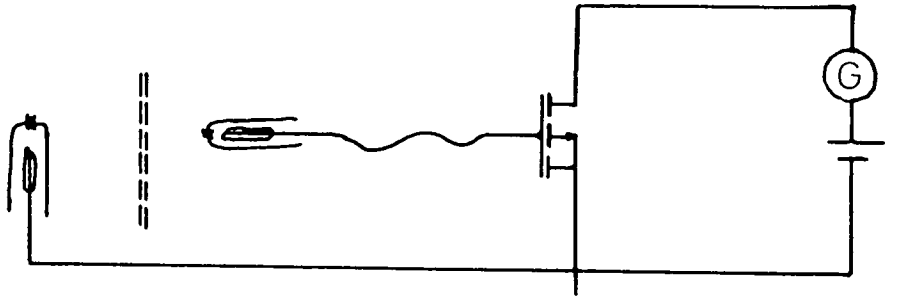

b/ SOLID STATE I.S.E.

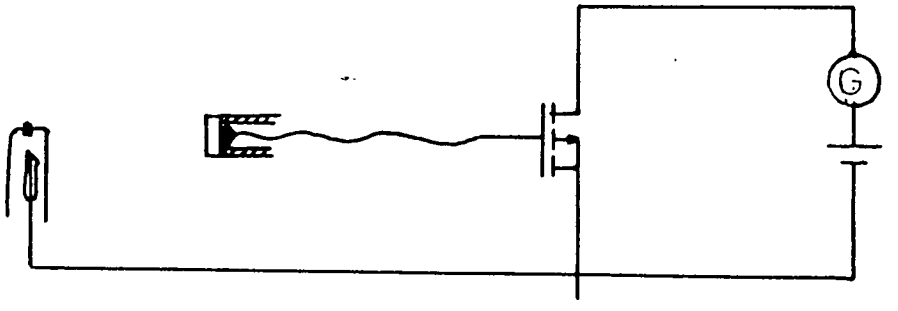

c/ I.S.F.E.T.

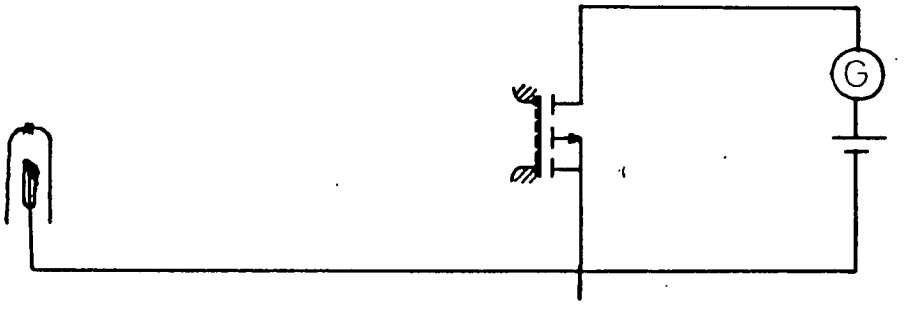

ISFET[35] (Ion Sensitive Field Effect Transistor). This can be thought of as being derived from the solid state ISE shown in fig. 3.3b by shortening the lead connecting the sensitive material to the gate to the point where it disappears altogether. The sensing material thus bonds directly to oxide of the MOSFET gate. In addition to the ISFET[32] other chemically sensitive semiconductor devices (CSSD)[33] have been described that are derived from MOS capacitors and gate controlled diodes.

From a practical point of view CSSDs are important because the sensor can be fabricated using the well-established techniques of silicon processing and thus, in principle, very small sensing areas (several μm square) are possible. Furthermore, it is quite possible to fabricate monolithic units containing the ISFET together with amplification, stabilisation and biasing circuitry.[33] Taking this one stage further it is possible to conceive of a monolithic unit incorporating ISFETs for several different ions, their ancillary data processing circuitry as well as temperature and conductivity measuring devices. Analogue to digital converters (ADC) could provide digital outputs from each sensor and a microprocessor would calculate the ionic activites taking into account mutual interference, temperature and conductivity effects.

Although a fully integrated sensor array appears very impressive at first sight it suffers several practical drawbacks. Firstly it must be remembered that silicon ICs are planar devices and whilst a single ISFET may have a sensing area of only a few microns, the entire array will be much larger. The more sophisticated the device the larger the area it occupies. Secondly with the exception of metallisation, silicon processing always involves silicon derived materials, so that unless an ion sensitive material can be found that is based on silicon, the ISFET can not be manufactured on a conventional integrated circuit production line. Whilst it is true that groups such as Janata's[35] have used impregnated polymers as sensing materials

the bonding of these materials requires steps outside the scope of normal silicon processing. Fortunately SiO_2 based materials can be used to sense H^+ and the alkali metal ions and individual ISFETs have been produced for these ions.[34] Thirdly, integrated circuits are sealed in hermetic packages to prevent damage; the ISFET must have its sensing material exposed, whilst the remaining circuitry is carefully protected. The encapsulation has proved to be a problem, which is worsened when it is considered that in industrial applications sensors may have to work in very hostile conditions.

The final problem is one of economics; an integrated circuit only becomes a viable proposition if it can be produced in very large numbers. This is a direct result of the high cost of development and setting up a silicon integrated circuit production line. Furthermore, these production lines once set up cannot be rapidly converted to a new circuit. In general the requirements of industry do not justify these costs.

Thus it appears that CSSDs are not a realistic answer to the requirement for cheap, robust and small chemical sensors. There is another approach to producing integrated circuits, which is increasingly popular for applications where a limited number of circuits are needed and the very small size of monolithic devices is not so important. These are the so-called hybrid circuits, where passive elements such as resistors, capacitors and interconnecting conductors are deposited on an inert insulating substrate. Two methods are possible: "thick-film" where these passive components are applied by screen printing and firing and "thin film" where they are sputtered on. Active components are bonded to the passive element network later (fig. 3.4a). Providing a suitable method of depositing the sensing material is available, any type of material can be used. Thus the copper sensing $Cu_x(As_2Se_3)_{100-x}$ electrodes have been prepared by sputtering (ref. 16 chap. 4). The only advantage of ISFETs over hybrid circuits is one of size, but where very small size is important

3.4 a./ THICK FILM INTEGRATED CHEMICAL SENSOR

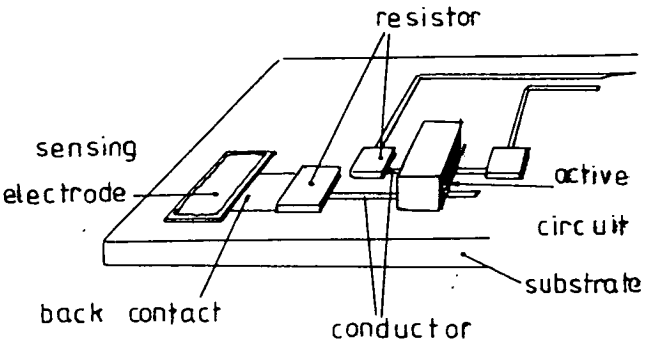

b./ ISFET IN "STAND-ALONE" MODE

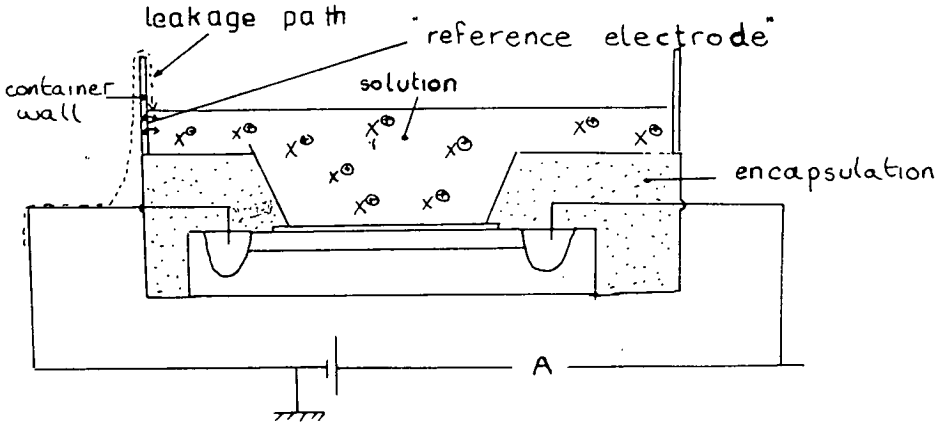

it is probably better to use solid state ISEs physically separated from their supporting electronics.

So far no mention has been made of the reference electrode, which in general suffers from the same problems as the membrane ISE. Almost all reference electrodes consist of a solid immersed in a solution of an ion of fixed concentration. The reference solution is normally confined to a separate container and this leads to a necessarily bulky structure. For certain cases, a particular species in the test solution may have an invariant activity, in which case it can fix the potential of a truly selective half cell. However, it is unlikely that (a) a species with constant activity can be found, and (b) a reversible electrode that is totally unaffected by variations in activity of all other species, can be found. In some cases micro reference electrodes of the type described earlier might be employed. It is also possible in some cases to place a conventional reference electrode at a point in the process where its large size is acceptable. The actual sensor is still placed at the point where the measurement is required.

Bergveld[34] originally believed that a reference electrode was unnecessary for use with ISFETs. This is now generally acknowledged to be incorrect, although reproducible gate-source currents as functions of ion activity have been obtained with single electrode devices. The problem is that although no specific electrical connection is made from the test solution to the ISFET source, leakage paths through the encapsulation (fig. 3.4b) nevertheless constitute such a connection. This is a high impedance path and will not give a stable reference potential. (The walls of the container effectively become the reference electrode.)

Thus the problem of providing a reference electrode compatible with the small size and low cost of solid state ISEs is probably the single biggest obstacle to their more wide-spread application. This problem will have to receive a lot of attention in the future.

3.8 Sensors for Species Other Than Simple Ions

The principle of the conventional ISE has been adapted to sense species other than simple ions, notably certain dissolved gases, enzymes[38] and other proteins. Most of these sensors employ a rapid, reversible reaction that produces a determinable ion in quantities that are simply related to the levels of the species of interest. The ion thus produced is detected by a conventional sensor. A schematic gas sensor is illustrated in fig. 3.5in which a membrane configuration is used to measure the ion level. There is no reason why a solid state system should not be used. A second membrane separates the test solution from the filling solution; this membrane must allow rapid diffusion of the gas that is to be sensed and several basic types have been suggested.[39] Some authors have proposed a homogeneous hydrophobic membrane such as silicone rubber[40] whilst others have suggested highly porous structures[41] so that the gas diffuses substantially in the gas phase. In an extreme case - the air gap electrode[42] - the membrane is simply a trapped air pocket. In all cases the gas dissolves in the solution on the sensor side of the membrane and alters the level of a particular ion. The majority of sensors use pH adjustment as the sensing mechanism so the solution contains the weak acid corresponding to the gas of interest,[43,44,45] (HCO_3^- for CO_2 detection, HSO_3^- for SO_2, $NaNO_2$ for NO_x). As a corollary to this most gas sensors have been developed for the acid gases CO_2, NO_x, SO_2, H_2S. The ammonia gas[46] sensor originally used pH changes in an NH_4CL solution to sense ammonia. Latterly however devices using changes in free Ag^+, Cu^{2+} or Hg^{2+} levels have been described.[47] Although these devices have been described for use in monitoring

3.5 GAS SENSORS

a/ **construction**

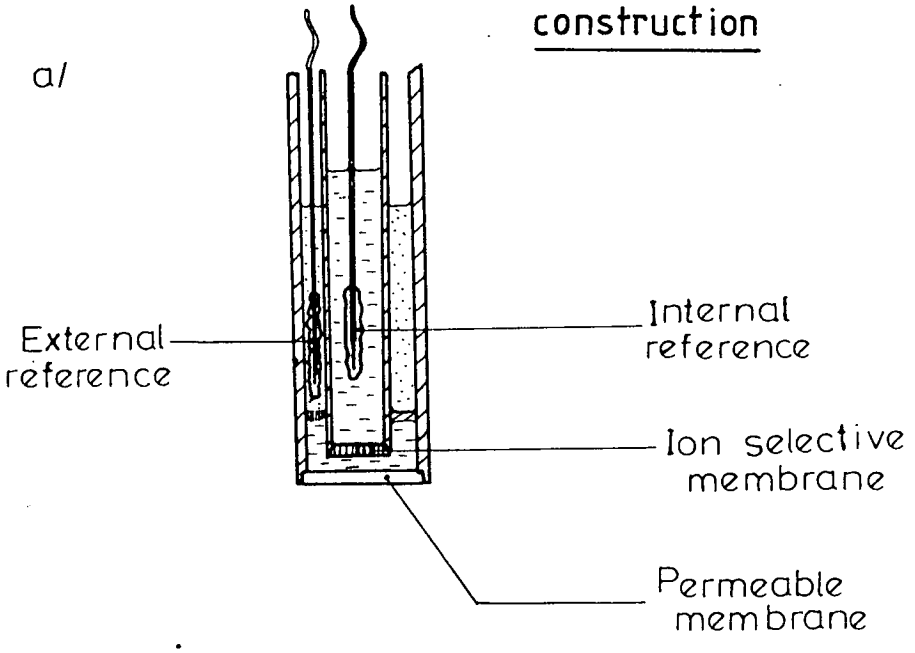

b/ **CO_2 sensor: schematic**

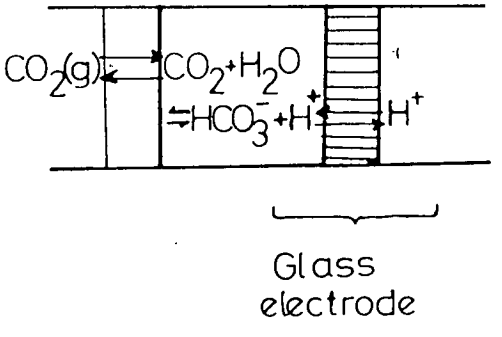

dissolved gases in aqueous solution, it is clear that they could equally well be used in non-aqueous or gaseous media thus considerably widening their range of application. The monitoring and control of gases such as CO_2, SO_2 and NO_x is particularly important in any combustion process involving hydro-carbon fuels so that potentially these sensors have far more use than simple ISEs.

The enzyme electrodes[38] employ either an enzyme or a particular substrate immobilized in a polymeric matrix. Enzyme reactions are characterised by extremely high selectivity for a particular substrate so providing a suitable ion is generated, enzyme electrodes offer the possibility of rapid determination of complex bio-molecules. The original electrode of this type was the urea electrode[48] in which urease confined in nylon was used to catalyse the reaction:

$$CO(NH_2)_2 + 2H_3O^+ \leftrightharpoons CO_2 + 2NH_4^+ + 2H_2O$$

The ammonium ion NH_4^+ was then determined using a glass electrode. Many other sensors have subsequently been described.

A few other special gas sensors are known which work on different principles. Jasinski et al have demonstrated that a solid state electrode based on $Fe_2Se_{60}Ge_{28}Sb_{12}$ (Fe 1173) could determine levels of NO_2 between 1 and 392 ppm.[49] The sensing material was contacted with a wick soaked in an electrolyte which also provides electrical contact with a conventional reference system. The mechanism proposed for the response involved adsorption of NO_2 at special activation sites, followed by a redox process to form the nitrite ion,

$$NO_2 + G \rightleftharpoons NO_2G \leftrightharpoons (NO_2^- + G^+)_{SOLID}$$

Lundstrom et al[50] have described a hydrogen gas sensor based on an MOS transistor with a Pd gate. Palladium can absorb large

amounts of hydrogen and this is believed to alter the difference in work function between the metal and the semiconductor. This in turn results in a change in the threshold voltage of the device.

Finally brief mention should be made of the oxygen sensors[51] based on solid electrolytes in which the oxide ion is the mobile species. A typical configuration is -

reference, Pt	solid oxide	Pt, test
gas $P^{o}_{O_2}$	electrolyte	gas P_{O_2}

where the electrolyte may be $CaO-ZrO_2$, $MgO-ZrO_2$, Al_2O_3, MgO or $ThO_2-Y_2O_3$. The oxide concentration in the test gas is given by the potential difference between the platinum electrodes as

$$E = \frac{RT}{4F} \log_e \frac{P_{O_2}}{P^{o}_{O_2}}$$

3.9 Strategies for Employing Chemical Sensors

Chemical sensors, and in particular ISEs, may be used in a direct mode where the species of interest itself affects the sensor, or in an indirect mode where the sensor detects an ion that is produced as the result of a side reaction indicating the presence of the relevant species. Strictly speaking, the gas sensors and enzyme sensors described in the previous section are examples of the latter, but the term is more likely to refer to cases such as potentiometric titration or reagent additions. Whilst the direct mode is considerably simpler to employ and will generally be quicker, the indirect mode allows a far wider range of substances - including non-ionic species - to be sensed. Furthermore the advent of cheap micro-computers and interfacing means that the complicated sampling methods that may be needed in indirect methods can be simply automated.

Sensors will always respond to some extent to species other than the one which they are intended to sense, and this interference will often be described by a Nikolski type equation, i.e.

$$E_i = E_i^o + \frac{RT}{F} \log_e a_i^{z_i} + \sum_{j \neq i} a_j^{z_j} k_{ij} \qquad 3.9.1$$

If there are n sensors there will generally be n mutually interfering species and 3.9.1 becomes,

$$\exp \frac{F}{RT} (E_i - E_i^o) = a_i^{z_i} + k_{i1} a_1^{z_1} + k_{i2} a_2^{z_2} \qquad 3.9.2$$

In general there will be n such equations which can be written more concisely as a matrix equation:

$$\begin{bmatrix} \exp F/RT\ (E_1 - E_1^o) \\ \exp F/RT\ (E_2 - E_2^o) \\ \vdots \\ \exp F/RT\ (E_n - E_n^o) \end{bmatrix} = \begin{bmatrix} 1 & K_{12} & K_{13} & \cdots \\ K_{21} & 1 & K_{23} & \cdots \\ \vdots & & & \\ K_{N1} & K_{N2} & K_{N3} & \cdots \end{bmatrix} \begin{bmatrix} a_1 \\ a_2 \\ \vdots \\ a_N \end{bmatrix}$$

or

$$\tilde{E} = K\tilde{A} \qquad 3.9.3$$

Since K is known, Cramer's rule can be used to solve the equations. The volume of calculation becomes fairly large for $n > 3$ so that careful thought must be given to the length of time available for computation. In many cases $n < 3$, in which case computation becomes very simple. Furthermore in practice many selectivity coefficients will be zero or at least insignificant. Problems arise for very high selectivity coefficients where the sensor may become completely insensitive to changes in the ion which it was designed to detect.

In addition to the effect of other ions the sensor is temperature

dependent; the temperature dependence appears explicitly in the Nernst equation and implicitly in the E^{o} term and the activity coeffiecient. Thus

$$E = E_i^o(T) + \frac{RT}{2F} \log_e \gamma_i(T)\ C_i \qquad 3.9.4$$

$$\frac{\partial E}{\partial T} = \frac{\partial E_i^o(T)}{\partial\ T} + \frac{R}{2F} \log_e \gamma_i(T)\ C_i + \ldots$$

$$\frac{RT}{2F} \frac{\partial \log_e}{\partial T}\ \gamma_i(T)\ C_i$$

Providing information is available on the temperature coefficients, their effect is easily dealt with. The explicit temperature dependence of the Nernst equation is often accountable for by using temperature compensation built into self-contained pH or ion selective meters. The latest units have automatic temperature compensation and the Orion 811 pH electrode measures temperature by the variation in the membrane resistance of the sensor, thereby eliminating with the necessity for a separate temperature sensor.

An increasing number of microprocessor controlled self-contained pH/ion analyzers are becoming available for use in analytical laboratories and it seems likely that these will be adapted for process control applications. Light[52] has reviewed the possible process applications for the various ISEs and these are summarized in table 3.2. So far very few of the possible applications have been exploited. This is probably due both to the undesirable characteristics of existing membrane ISEs and the fact that the processing industry is slow to introduce innovative technology.

Gas sensors would appear to be particularly attractive units since the type of gases to which they are sensitive are diagnostic of the state of a wide variety of systems, in particular those involving combustion. The gases CO_2 and NO_x are particularly

important from this point of view and seem ideal to make the basis of a complete monitoring and control system of the type illustrated in fig. 3.6.

36 POSSIBLE PROCESS CONTROL SYSTEM

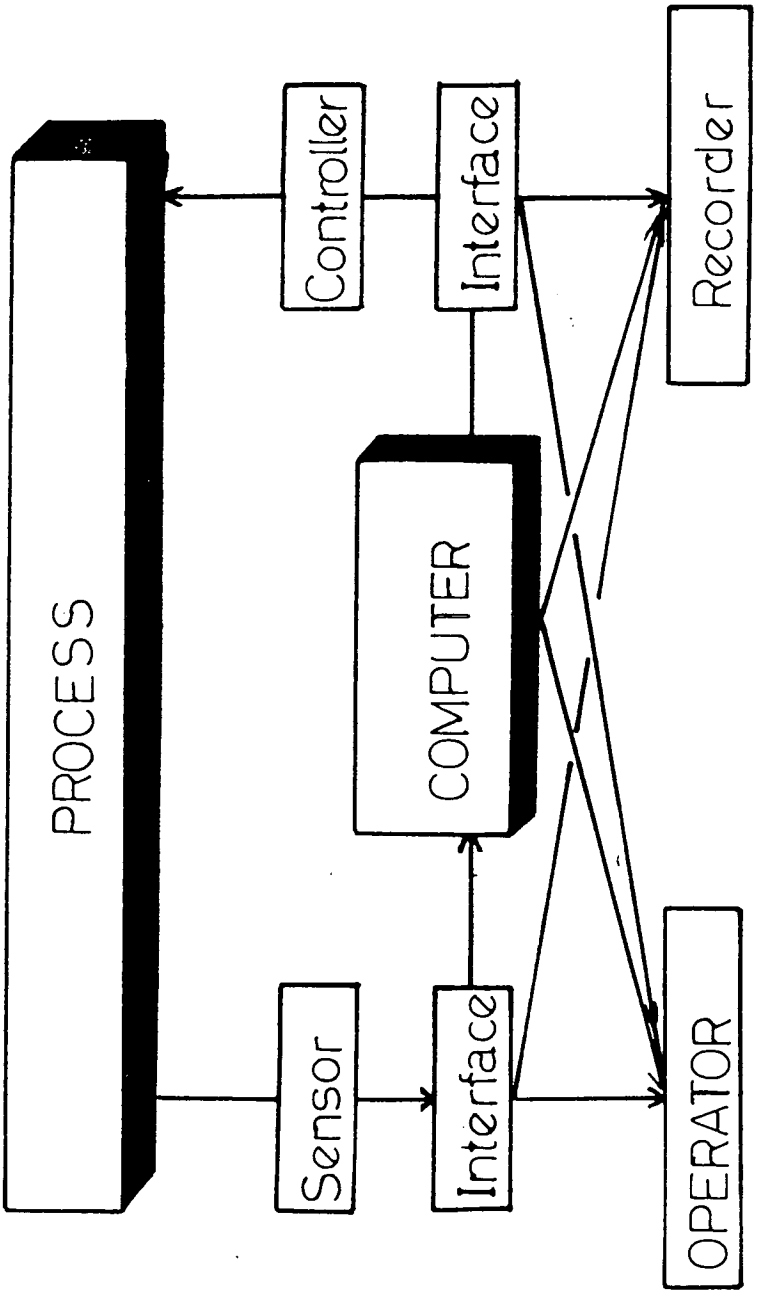

Application of Ion Selective Electrodes

Table 3.1

n	Electrode type	Selectivity and princpal interferents	Possible application
+	Glass membrane ISFETs	Now very high Na+, K+ are main interents	Bio-medical, water quality control, pH monitoring, pollution monitoring etc.
+	Glass membrane ISFET	OH^-	Bio-medical, water industry, break-through of ion exchangers
	Glass membrane ISFET	Na+, H+	"
+	Liquid membrane	None	Li analysis
$^{2+}$	Liquid membrane	"	Water industry Bio-medical
$2+$		None	Pollution monitoring, plating solutions.
+	Ag_2 S membranes or solid state	Hg^{2+}, S^{2-}	Photgraphic solutions plating solutions
$^{2+}$	HgS, Ag_2S/HgS compacts	Ag+ S^{2-}	Pollution monitoring
$^{2+}$	CuS/Ag_2S compacts $Cu_X(As_2\ Se_3)_{100-x}$ Solid state electrical	Ag+, Hg^{2+} Cl^-	Plating tanks, pollution monitoring, PCB manufacture, Ore extraction
$^{3+}$	Fe_X Se Sb Ge	Ag+, Hg^{2+}, Cu^{2+}	Corrosion monitoring
	La F_3	OH^-	Water quality control HF leaks, dental health Al/PO_3 industry
$-$	Ag_2S	Ag+, Hg^{2+}, Cu^{2+}	H_2S monitoring, metal refining, petroleum refining
$_3-$	Liquid membrane		Water quality control sewage. Food industry.

Chapter 4

Chalcogenide Glasses

4.1 Introduction

The chalcogenide elements O, S, Se and Te are known to form glasses quite readily when present in binary and more complicated systems. In general the electronic properties of amorphous semiconductors are less sensitive to the presence of impurities than those of their crystalline counterparts. This is explained by assuming that in an amorphous structure it is possible for impurities to completely satisfy their bonding requirements i.e. to become saturated. In crystalline semiconductors, where impurities occupy well defined lattice sites the number of bonds is determined by the parent semiconductor and in general is different to that preferred by the impurity. Structural studies on the glassy forms of the systems Ge_xTe_{1-x} [1] and As_xSe_{1-x} [2] suggest that Ge remains fourfold, As three fold and Se and Te two fold coordinate. On the other hand it has been observed that the electrical properties of alloys of metals with As_2S_3 and As_2Se_3 depends strongly on the amount of metal present. This observation prompted some detailed work on electronic, photoelectronic and structural properties of the Cu-As_2Se_3 system.[3,4,5] It has also been noted in Chapter 2, that materials of the form $Cu_x\ (As_2S_3)_{100-x}$, $Cu_x\ (As_2Se_3)_{100-x}$ and $Cu_x\ (As_2Se_{1.5}Te_{1.5})_{100-x}$ can form the basis of novel copper sensing Ion Selective Electrodes (ISEs).

It should be noted that various systems have been used to describe the stoichiometry of M - As_2X_3 systems (where M is a metal). These are summarized below:

System	Workers	Reference
$M_x\ As\ X_{1.5}$	Danilov et al.	3
$M_x\ (As_{0.4}Se_{0.6})_{100-x}$	Liang et al.	4
$M_x\ (As_2Se_3)_{100-x}$	Jasinski	
$M_x\ As_2Se_3$	Kolomiets	5

Thus particular care must be taken when comparing results from different research groups. In this study the $M_x (As_2Se_3)_{100-x}$ system will be used.

4.2 Multi-Component Mixtures in Condensed Phases

The study of multi-component systems is particularly important in the metal and petroleum refining industries and has thus received considerable attention. The problem is essentially one of determining whether a mixture of well defined composition will exist as a single homogeneous phase or as two or more chemically distinct phases. At equilibrium this information is contained in a diagram showing free energy of formation as a function of composition. Three examples of this are shown in fig. 4.1 for the simple case of a two component system MX. The heavy line refers to the formation of a homogeneous phase. In cases where a two-phase mixture is more stable it is strictly not meaningful to write a free energy of formation for a single phase.

If A and B refer to two different phases in the MX system then at equilibrium

$$\mu_X^A = \mu_X^B \qquad 4.2.1a$$

$$\mu_M^A = \mu_M^B \qquad 4.2.1b$$

The chemical potentials can be written

$$\mu_X^A = g^A - x_M^A \left(\frac{\partial g}{\partial x_M}\right)^A_{P,T} \qquad 4.2.2a$$

$$\mu_X^B = g^B - x_M^B \left(\frac{\partial g}{\partial x_M}\right)^B_{P,T} \qquad 4.2.2b$$

$$\mu_M^A = g^A + x_X^A \left(\frac{\partial g}{\partial x_X}\right)^A_{P,T} \qquad 4.2.2c$$

$$\mu_M^B = g^B + x_X^B \left(\frac{\partial g}{\partial x_X}\right)^B_{P,T} \qquad 4.2.2d$$

where x_i^A is the mole fraction of A in phase i and g^i is the free energy of i. From equations 4.2.1a and 4.2.1b it follows that

$$\left(\frac{\partial g}{\partial x_M}\right)^A = \left(\frac{\partial g}{\partial x_M}\right)^B = \frac{\partial g}{\partial x_M} \quad \text{say.} \qquad 4.2.3$$

Substituting into eqn. 4.2.2a and 4.2.2b gives, -

$$\frac{\partial g}{\partial x_M} = \frac{g^A - g^B}{x_M^A - x_M^B} \qquad 4.2.4$$

Graphically, this is a straight line that is tangential to the g(x) curves of two neighbouring phases. Any composition with a value x such that

$$x_M^A < x < x_M^B$$

will always form two phases at equilibrium, corresponding to $M_x^A X_{1-x}^A$ and $M_X^B X_{1-x}^B$. It should be noted that x^A can equal 1 or 0 corresponding to pure M or pure X respectively.

In chapters 2 and 3 it was noted that electrode potentials are strongly dependent on the exact composition of the sensing material. If x is such that a heterogeneous mixture results, the two phases will have their compositions precisely defined. As an example in fig. 4.2c an equilibrium mixture with $x_c^M < x < 1$ will consist of the two phases M and $M_{x_c^M} X_{1-x_c^M}$ regardless of the exact value of x. Similarly for $x_A^M < x < x_B^M$, the two phases will be $M_{x_c^M} X_{1-x_A^M}$ and $M_{x_B^M} X_{1-x_B^M}$, and only their relative amounts will vary with x. In general such a system is preferable to that shown in fig. 4.2b in which all compositions form a single phase. Any electrode process which alters x will alter the cell potential. The potential of electrodes composed of a heterogeneous mixture will be discussed later (section 4.5).

4.1 FREE ENERGY VS. COMPOSITION FOR A TWO COMPONENT MIXTURE

a/

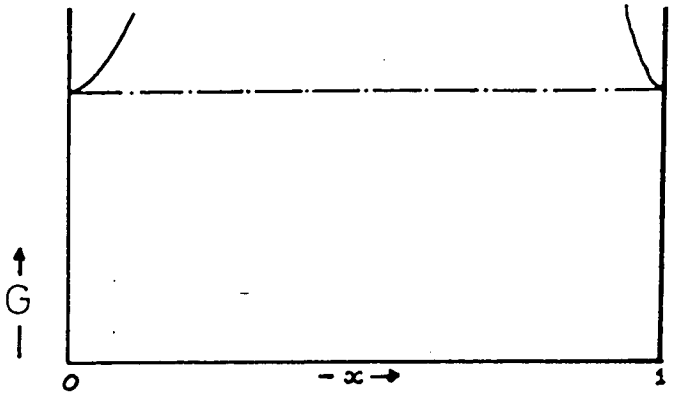

b/

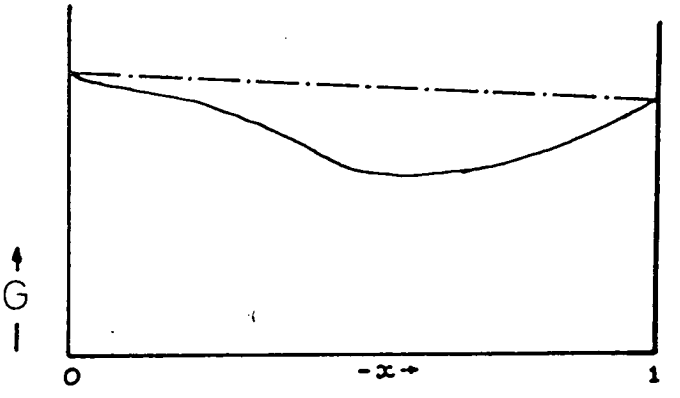

c/

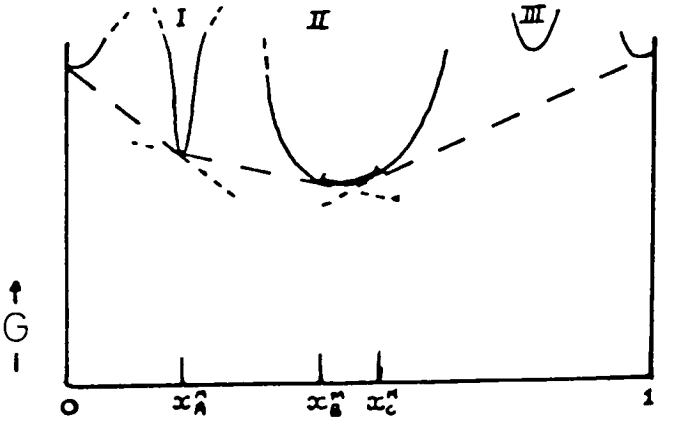

It must be remembered that these arguments refer to equilibrium conditions. It is quite possible to produce a thermodynamically unstable system which for practical purposes is nevertheless stable because of the slowness of kinetic factors. If a liquid is cooled sufficiently rapidly a homogeneous glass may result despite the fact that at equilibrium a two-phase system is the thermodynamically stable state. Furthermore in some cases it may be very difficult to produce the equilibrium system (e.g. if nucleation or crystal growth is a slow process).

When three or more components are considered the discussion, whilst following exactly the same lines as for MX, becomes considerably more complicated. For a ternary mixture there are two degrees of freedom so that a particular composition requires two values of mole fraction to characterise it. Generally there will be more than two neighbouring phases.

4.3 The Copper Arsenic Selenium System

The phase diagram of the copper-arsenic-selenium system is shown in fig. 4.2. The glass forming region was established by Asahara and Izumitani[7] using the criterion that air-quenched materials showed no lines on an X-ray powder photograph. No information on the cooling rate was given by these authors, so that the glass forming region has been deliberately shown as poorly defined. In other studies[8] it has been found that it is difficult to prepare homogeneous glasses of the type $Cu_x (As_2Se_3)_{100-x}$, for $x > 68$ ($Cu_x (As_{0.4}Se_{0.6})_{100-x}$, $x > 30$)). The binary and ternary compounds that have been identified to date are also shown on the diagram.[9,10,15] Liang, Bienenstock and Bates[4] darried out detailed structural investigations on glasses $Cu_x (As_{0.4}Se_{0.6})_{100-x}$ for $0 \leqq x \leqq 30$ ($Cu_x (As_2Se_3)_{100-x}$, $0 \leqq x \leqq 68$ and compared their results with those obtained for $CuAsSe_2$. As can be seen from the phase diagram $CuAsSe_2$ can be prepared as an amorphous material. The experimental methods used were differential thermal analysis (DTA), electron spectroscopy for chemical analysis (ESCA) and the computation of radial distribution

4,2 Cu-As-Se SYSTEM

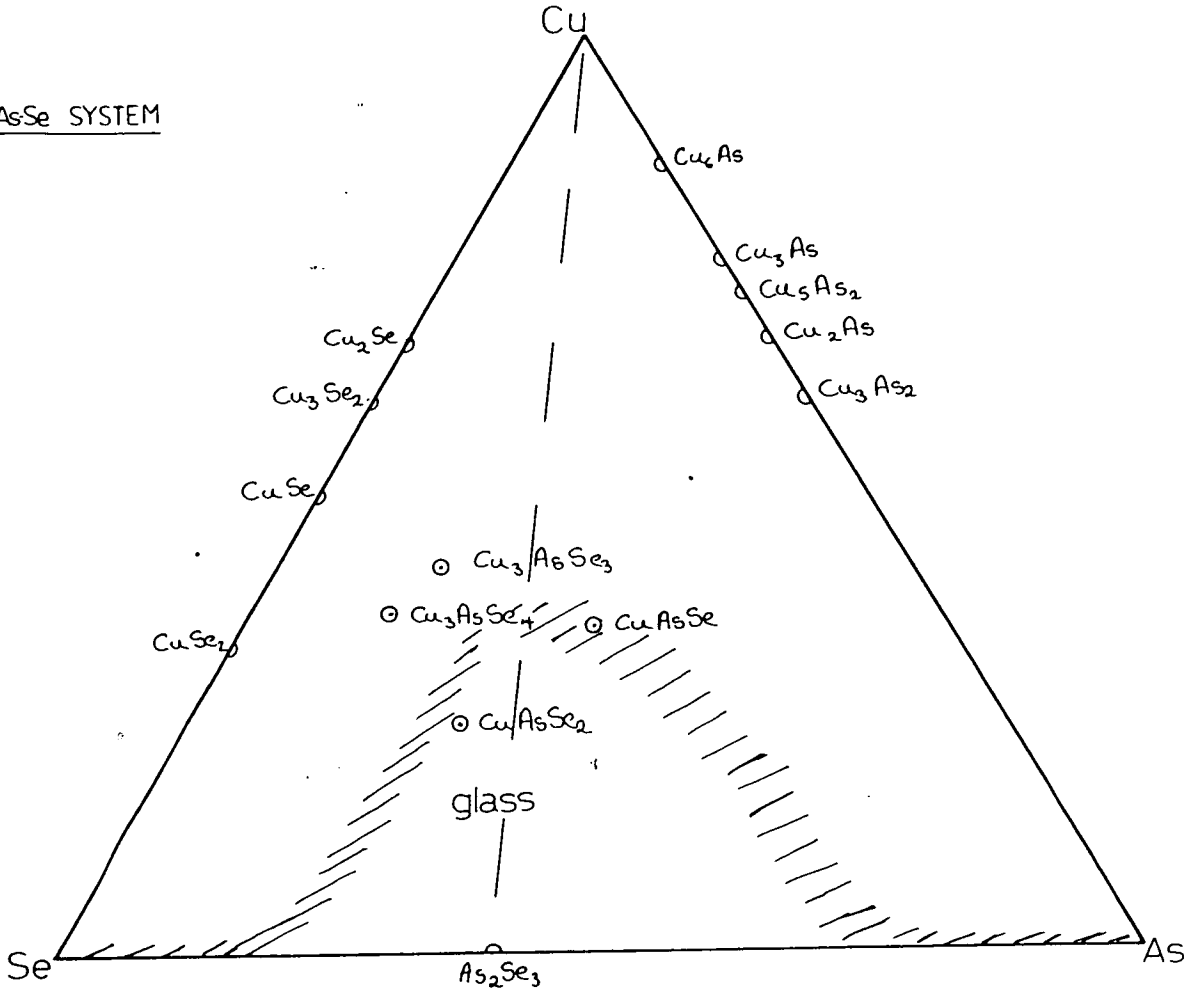

functions from X-ray diffraction data. A later study by Hunter and Bienenstock[10] used extended X-ray absorption fine structure (EXAFS) to probe the structure. The DTA work showed amorphous As_2Se_3 changes continuously to the liquid state as the temperature rises above the glass transition temperature. In contrast the $Cu-As_2Se_3$ glasses devitrify prior to melting. An X-ray examination of the materials after devitrification showed the crystalline phase was either $CuAsSe_2$ or Cu_3AsSe_4; the diffraction patterns of these two components are very similar. The melting points for devitrification products in the $Cu_x(As_{0.4}Se_{0.6})_{100-x}$ system were 415°C or less; the melting point of $CuAsSe_2$ is 415°C and that of Cu_3AsSe_4 is 460°C. Borisova[15] states that the cyrstalline phase is the high melting point compound Cu_3AsSe_4 formed by the decomposition of $CuAsSe_2$.

$$3CuAsSe_2 \rightarrow Cu_3AsSe_4 + 2AsSe$$

$$3AsSe \rightarrow As_2Se_3 + As$$

The X-ray and ESCA studies of Liang et al. indicated that as the Cu content of the $Cu_x(As_2Se_3)_{100-x}$ glasses increases, the mean co-ordination number also increases from 2.4 in $a-As_2Se_3$ towards the value 4 characteristic of $c-CuAsSe_2$. It is assumed that large parts of the structure take on the short range order characteristic of $CuAsSe_2$. According to Danilov[3] the similar effective radii of Cu (1.28 Å), As (1.25 Å) and Se (1.16 Å) allow the formation of single phases with "anomolously" large amounts of copper (as compared to other elements). The high capacity of copper to form co-ordinate (co-valent) bonds impedes crystallization. In addition to structural units of the $CuAsSe_2$ type, Borosova[15] claims $CuAs_2Se_2$ units are also present in the glass.

A crystalline compound CuAsSe[12] has recently been characterised and as can be seen from fig. 4.1 this lies on the edge of the glass forming region.

4.4 Electrical Properties of the Copper-Arsenic-Selenium System

The conductivities of the $Cu_x(As_2Se_3)_{100-x}$ glasses show a

4.3 a/ VARIATION OF CONDUCTIVITY WITH TEMPERATURE FOR Cu-As_2Se_3 GLASSES

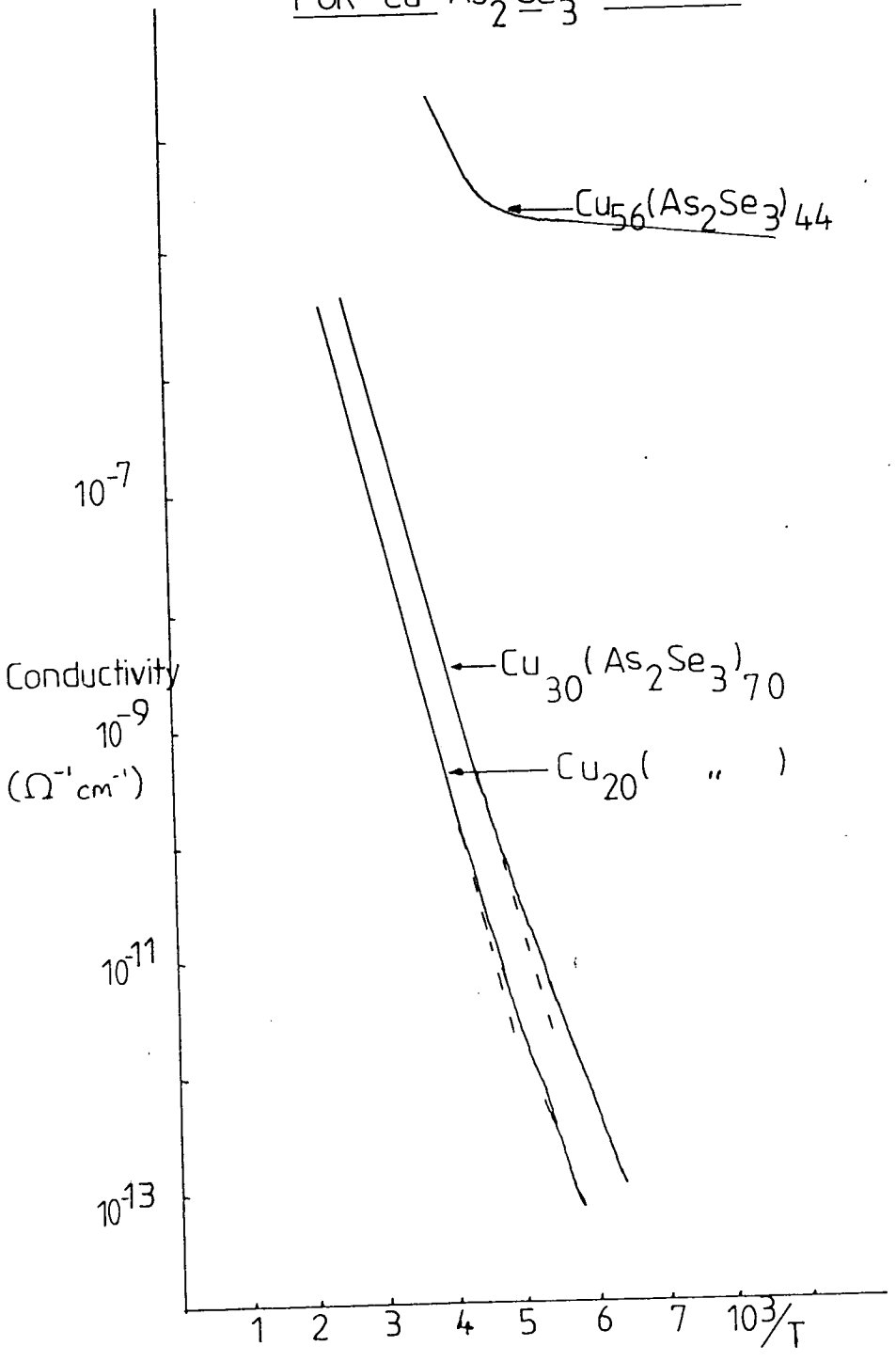

4,3 VARIATION OF CONDUCTIVITY PARAMETERS WITH COPPER CONTENT FOR THE Cu-As_2Se_3 GLASSES

b./conductivty at 20°c

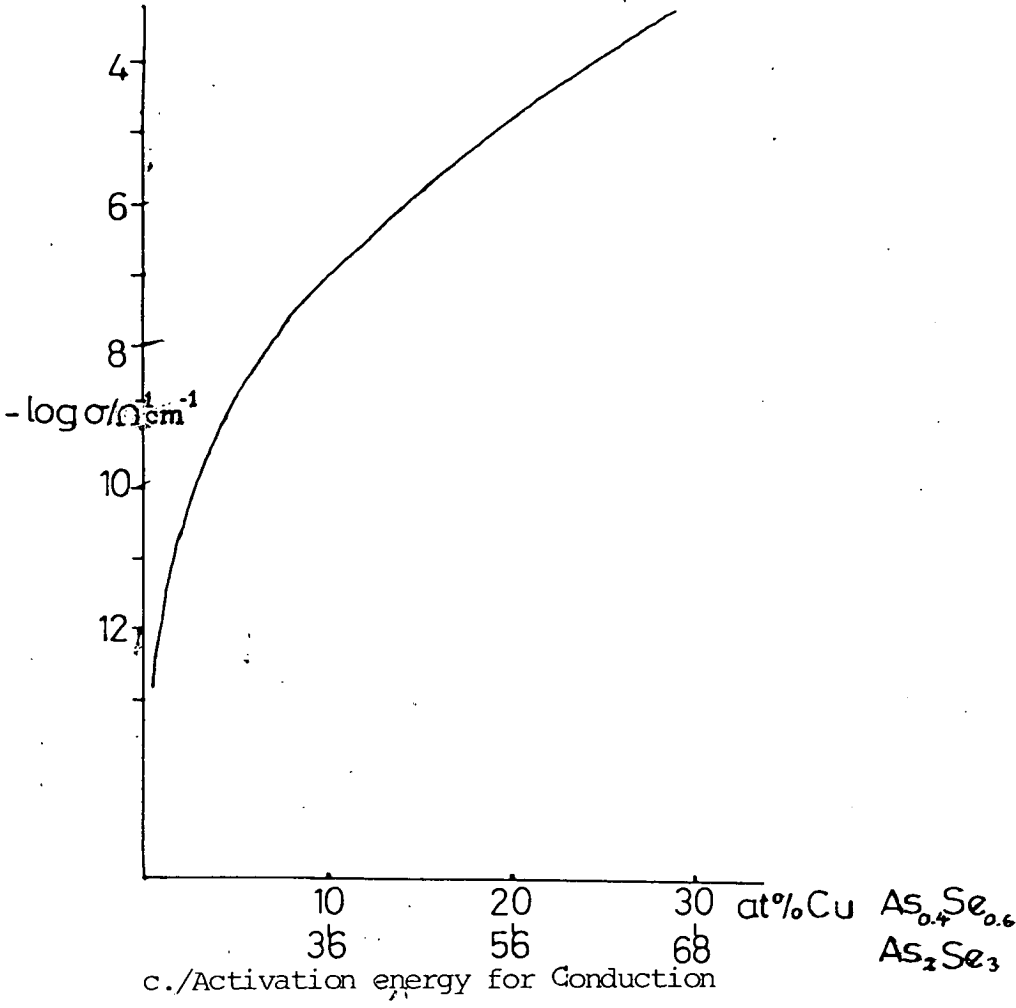

c./Activation energy for Conduction

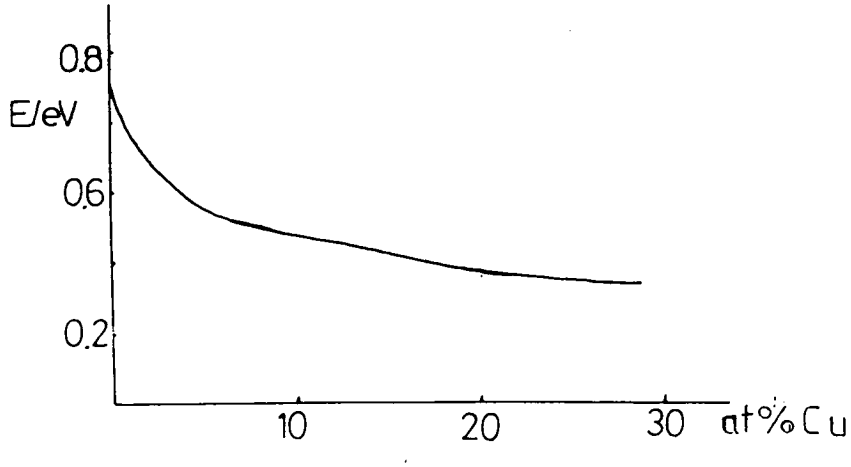

temperature dependence typical for semiconductors. The conductivity increases with increasing temperature according to the following law

$$\sigma(T) = \sigma_o e^{-E\sigma/kT} \qquad 4.4.1$$

where T is the absolute temperature, σ is the conductivity and $E\sigma$ is an activation energy for conduction which is related to the width of the band gap. The values of conductivity at 20°C, activation energy and also bulk density for some glasses in the $Cu_x(As_2Se_3)_{100-x}$ system are given in table 4.1. In addition data for a-$CuAsSe_2$ and c-Cu_3AsSe_4 are included. It is immediately clear that at a particular temperature the conductivity rises with the level of copper, at the same time the activation energy decreases. Some actual examples of conductivity-temperature curves are shown in fig. 4.3[8], where it can be seen that at high copper concentrations ($x \cong 60$) the temperature dependence departs from the simple law of equation 4.4.1.

It is also interesting to note that the crystalline compound Cu_3AsSe_4 has a conductivity at room temperatures which is 4 orders of magnitude higher than any of the glasses. Thus if any crystallisation occurs the conductivity of the material will be considerably higher than that of the homogeneous glass.

The conductivities of heterogeneous systems has been studied theoretically by Maxwell[13]. For a mixture in which spherical particles of a material A, with conductivity σ_A and volume fraction v_a, are embedded in a matrix B, with corresponding parameters σ_B and v_B, and the distance between particles of A is large compared with their radius, the conductivity of the mixture is given by:

$$\sigma_{mix} = \frac{2\sigma_A+\sigma_B - \frac{2v_B}{v_{MIX}}(\sigma_A-\sigma_B)}{2\sigma_A+\sigma_B + \frac{2v_B}{v_{MIX}}(\sigma_A-\sigma_B)}\ \sigma_A \qquad 4.4.2$$

where $v_{MIX} = v_A + v_B$ - the total volume. A is taken to be Cu_3AsSe_4 then $\sigma_A > 10^4 \cdot \sigma_B$ so that 4.4.1 can be approximated by

cpd	cpd	Ref	$-\log_{10}(\sigma/\Omega^{-1}cm^{-1})$ (20°C)	$E\sigma$/eV	ρ_b/gam^{-3}
As_2Se_3	$AsSe_{1.5}$	5	12.2	0.9	4.6
$Cu_2(As_2Se_3)_{98}$	$Se_{1.5}Cu_{0.01}$	5	11.8	0.85	4.6
$Cu_{7.5}(As_2Se_3)_{92.5}$	$AsSe_{1.5}Cu_{0.04}$	5	10.8	0.7	4.7
$Cu_{16.7}(As_2Se_3)_{83.3}$	$AsSe_{1.5}Cu_{0.1}$	8	9.0	0.55	4.7
$Cu_{24.2}(As_2Se_3)_{75.8}$	$AsSe_{1.5}Cu_{0.16}$	8	7.8	0.4	4.8
$Cu_{39}(As_2Se_3)_{61}$	$AsSe_{1.5}Cu_{0.32}$	8	5.9	1.1	5.0
$Cu_{45.5}(As_2Se_3)_{54.5}$	$AsSe_{2.5}Cu_{0.40}$	8	5.6	1.15	5.1
$Cu_{50}(As_2Se_3)_{50}$	$AsSe_{1.5}Cu_{0.50}$	8	4.9	1.3	5.1
$Cu_{54.5}(As_2Se_3)_{45.5}$	$AsSe_{1.5}Cu_{0.10}$	8	4.3	0.3	5.2
$CuAsSe_2$		5	3.4	0.275	5.4
c-Cu_3AsSe_4		5	0.3 - 0.0	0.15 - 0.05	5.6

TABLE 4.1

$$\sigma_{MIX} = \frac{2\left(\frac{1 - v_B}{v_A}\right)}{2\left(\frac{1 + v_B}{v_A}\right)} \sigma_A \qquad 4.4.3$$

$$\text{or} \quad \sigma_{MIX} = \frac{2(V_A/V_{MIX})}{3 - (V_A/V_{MIX}} \sigma_A \qquad 4.4.4$$

This function is shown in fig. 4.4 where it is clear that even if the matrix is composed of the most conductive glass - $Cu_{55}(As_2Se_3)_{45}$ - a volume fraction of only 0.1% Cu_3AsSe_4 is capable of increasing the conductivity 10-fold! The analysis takes no account of the possibility of a continuous network of the more conductive phase. Neither does it give a satisfactory answer at low frequencies or d.c. (consider the case of conductive spheres embedded in a perfect insulator). Nevertheless the problem is sufficiently important in practice that it has received a lot of attention. For the determination of formation water resistivites (R_w) in porous media the following empirically established formulae are used:

$$R_t = \frac{1}{\phi^x} R_w \qquad 4.4.5$$

where R_t is the resistivity of the complete mixture, ϕ is the "porosity" of the media i.e. the fraction occupied by fluid, x is a constant close to 2 but varies with lithology. Re-writing this using the same symbols as before gives:

$$\frac{1}{\sigma_{MIX}} = \frac{1}{\sigma_A} \frac{1}{(V_A/V_{MIX})^2} \qquad 4.4.6$$

$$\sigma_{MIX} = \sigma_A \left(\frac{V_A}{V_{MIX}}\right)^2 \qquad 4.4.7$$

These formulae were found for volume fractions in the range 1%-35% and assume a matrix of zero conductivity. A volume fraction of 10% will give a 100 fold increase in conductivity assuming $\sigma_A = 10^4 \sigma_B$ and that the equation is applicable for a matrix with some conductivity. A volume fraction of 1% has no effect on the conductivity. The

4.4 VARIATION OF CONDUCTIVITY WITH COMPOSITION FOR A HETEROGENEOUS MIXTURE

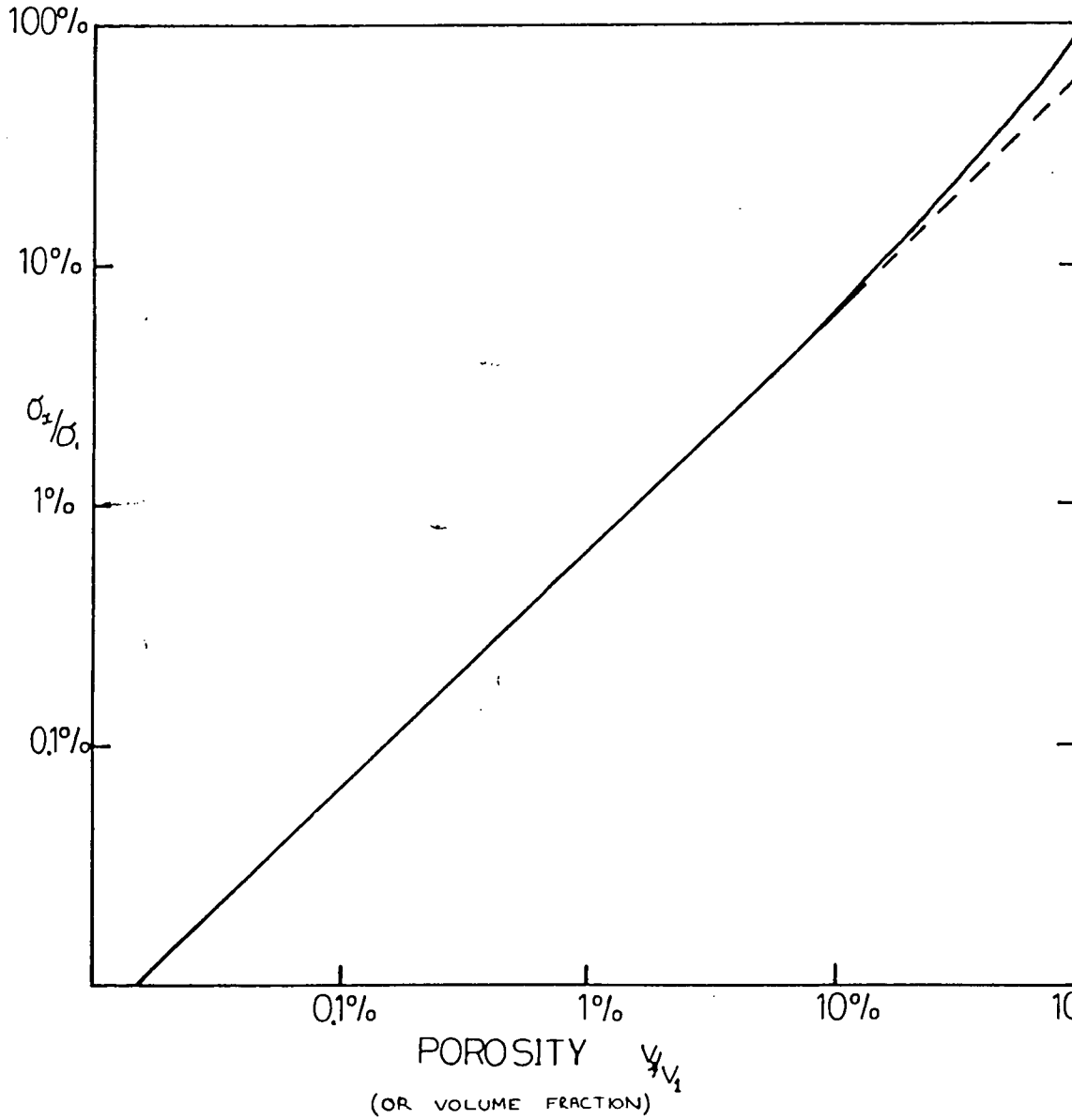

situation becomes more complex when additional phases are considered, particularly if these show metallic conduction as could occur for glasses with high copper contents when some pure copper or alloys such as Cu_3As may form.

4.5 Electrode Potentials for Materials in the Cu-As-Se System

The electrode potentials for electronically conducting binary compounds has been discussed in chapter 2. The major conclusion was that the electrode potential is determined by the exact composition of the electrode and that in general the composition varied at the surface with ionic activity. In special cases however the composition is fixed, i.e. when the electrode material is in equilibrium with an excess of one or other of the neighbouring phases (in some cases these may simply be the component elements). For a three-phase system the situation is much more complicated because of the presence of more than two neighbouring phases.

In the $Cu_x(As_2Se_3)_{100-x}$ system-shown in fig. 4.1 - it might be expected that any glass on the Cu-As_2Se_3 tie-line would separate into Cu and As_2Se_3 but this is contrary to the observation that devitrification leads to $CuAsSe_2$ and/or Cu_3AsSe_4. Any $Cu_x(As_2Se_3)_{100-x}$ glass can form a ternary crystalline compound and another glassy phase which may itself separate further. It might be expected that the slower the cooling the greater will be the proportion of thermodynamically stable compounds. Furthermore the slower the cooling rate the more thermodynamically stable will the products formed be. It is not necessarily true that only stable compounds will result. Thus the exact composition depends strongly on the cooling rate and also on the presence of impurities which may act as nucleation centres for crystal growth.

In general therefore the electrode surface will consist of many separate phases each of which will give rise to its own particular electrode potential when it contacts a solution. A similar problem may exist at the back contact where each phase

will lead to its own junction potential. Such a compound electrode can be modelled by the cell shown in fig. 4.5a, where each phase is represented by a different electrode and all the electrodes are connected to the same terminal of the potentiometer. The equivalent circuit of 4.5a is shown in fig. 4.5b, where the cells E_i represent the electrode potentials and the resistances R_i represent the resistance of the phase. The overall potential E can be found in terms of E_i and R_i from Kirchoff's laws which, for the circuit shown, give:

$$E(t) = \frac{1}{n-1} \sum_{i=1}^{n} \frac{R_{i-1} E_i(t) + R_i(E_{i-1}(t) + E_{i+1}(t))}{R_{i-1} - 2R_{i+2}} \qquad 4.5.1$$

where R_o^{-1}, E_o, R_{n+1}^{-1}, E_{n+1} are all zero. When the cell is initially formed currents flow between the various phases and the solution, so that generally the surface composition of each phase will alter. This in turn means that E_i is a function of time and thus E is also a function of time. When all the E_is equal the same value, current will no longer flow and the system then behaves as a simple electrode. If the individual electrode potentials vary with ionic activity in the same manner, Nernstian behaviour is to be expected.

Complications will occur if the different phases respond to the ion of interest by different mechanisms. For example if one phase exchanges two electrons with Cu^{2+} while another only exchanges one electron so the individual electrode potentials will vary by different amounts (30 mV decade^{-1} in one case and 60 mV decade^{-1} in the other). Once again current will flow until the individual electrode potentials are equal. This will lead to a response that is not Nernstian and may also lead to a slow approach to the steady state potential. Even in cases where all the phases respond by essentially the same mechanism (1 or 2 electron exchange) complications will arise when one phase exchanges electrons faster than another and when certain phases respond to a foreign ion and others do not.

4.5 MODEL OF A COMPOUND ELECTRODE

a/

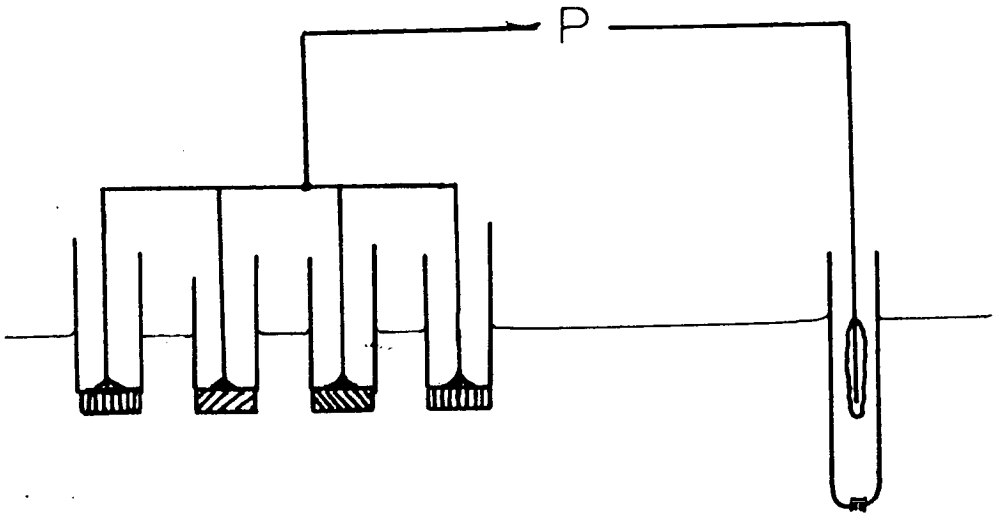

b/

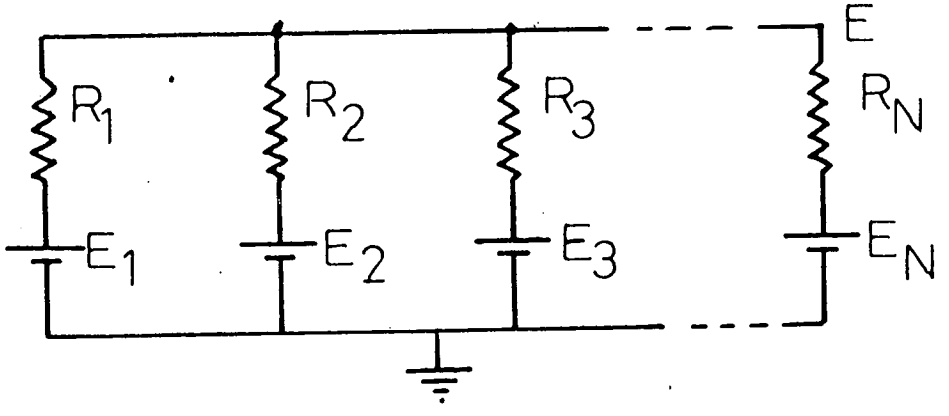

Some authors[16] have noted that a single homogeneous phase is preferable to a heterogeneous mixture. The reason generally given is that this allows a reproducible back contact but a far more important reason for preferring a single phase is that it avoids the complications outlined above.

In the work of Jasinski et al. and Drennan on the $Cu_x(As_2S_3)_{100-x}$ glasses discussed in chapter 3, crystalline compounds of the $Cu_6As_4S_9$ type were found. Subsequently Cu_6AsS_9 was found to be capable of acting as a Cu^{2+} electrode in isolation. The mechanism proposed involved the oxidation of $Cu_6As_4S_9$ to an oxidized surface OxS.

$$Cu_6As_4S_9 + Cu^{2+} \rightarrow OxS + Cu^{+}$$

The surface was subsequently activated by Cu^{2+}

$$OxS + Cu^{2+} \rightarrow Act\ S$$

and the activated surface then responded to Cu^{2+} in a reversible redox process involving a two electron transfer

$$(Act\ S) + Cu^{2+} \rightleftharpoons (Act\ S)\ Cu^{o}(ads) + 2e^{-}$$

4.6 The Copper-Arsenic-Selenium-Tellurium System

Materials of composition $Cu_x(As_2Se_{1.5}Te_{1.5})_{100-x}$ have similar ion-selective properties to the selenides and sulphides.[8,14] A study of their electrical properties has been made by M.I. Fraser[7] and in general the conductivities are higher than the corresponding selenides. Typical conductivities at 20°C are shown in Table 4.2 together with those of the corresponding selenides. No studies have been reported of the extent of the glass forming region in the Cu-As-Se-Te system or of the presence of any crystalline compounds. It is interesting to note that the conductivity in the tellurium containing glasses is less affected by changes in the copper level than that in the $Cu_x(As_2Se_3)_{100-x}$ glasses.

Composition	$\sigma_{10°C}/\Omega^{-1}cm^{-1}$	$\log_{10} \sigma_{20°}$
$Cu_{21}(As_2Se_{1.5}Te_{1.5})_{79}$	4.4×10^{-7}	-7.64
$Cu_{25}(As_2Se_{1.5}Te_{1.5})_{75}$	9.1×10^{-7}	-7.94
$Cu_{30}(As_2Se_{1.5}Te_{1.5})_{70}$	10.0×10^{-7}	-6.00
$Cu_{20}(As_2Se_3)_{80}$	2.5×10^{-9}	
$Cu_{25}(As_2Se_3)_{75}$	6.3×10^{-9}	
$Cu_{30}(As_2Se_3)_{70}$	25.0×10^{-9}	

TABLE 4.2

CHAPTER 5

PREPARATION AND CHARACTERISATION OF ION SELECTIVE GLASSES

5.1 Preparation of Glasses

The term "glass" here refers to compositions which lie in the glass forming region of the Cu-As-Se system. Some of the compositions actually contained considerable amounts of crystalline compounds presumably as a result of the cooling rates used.

Glasses were prepared by the usual method[1] of melting together the elements in sealed evacuated quartz tubes. The quantities of materials were calculated to give a 10 g melt. After evacuation to a pressure of 10^{-6} torr, the tubes were sealed by a torch and placed in a rocking furnace at 500°C. The temperature was held constant for 24 hours, then raised to 850°C and held at that point for a further 24 hours. At this time rocking stopped and the melt was allowed to cool to 500°C - at this temperature the Cu-As_2Se_3 glasses are still molten. They were then transferred rapidly to a heated metal block that allowed controlled cooling to room temperature.

The temperature of the block was reduced to the glass transition temperature Tg where it was held constant for several hours (2-16). The glass transition temperature for various compositions was found from DTA analysis by Fraser[1] and Liang et al[2]. After annealing the glass was cooled to room temperature at a rate of 1°C min^{-1}.

The resulting ingots were sliced up in their tubes with a diamond saw. The blade was lubricated with a water glycerol mixture. Slices were normally 2 mm to 4 mm thick so that for

tubes of i.d. 10 mm a 10 g melt would yield between 7 and 10 slices. A complete list of the compositions prepared is given in table 5.1.

The surfaces of the slices were polished with a slurry of grinding compound in deionized water and in some cases a highly polished surface was produced using a sheet of photographic paper.

Electrical contacts to the discs were made by the vacuum evaporation of a metal from a heated tungsten filament, or by painting on a colloidal suspension of the contact material. Metal evaporations were made using either a Nanotech 300A automatic evaporator or a similar manual system constructed in the Department. The pressure at which evaporation was carried out was between 10^{-5} and 10^{-6} torr.

For the majority of electrochemical studies gold contacts were used, but in some cases copper, zinc and graphite were also used. The latter contact was prepared by painting Aqua DAG - colloidal graphite - directly onto a freshly prepared surface.

5.2 Electrode Construction

The basic construction of the electrode is shown in figure 5.1. A lead was cemented to the back contact using "silver DAG" high conductivity paint. The disc and lead assembly were then glued into a perspex tube of 8 mm i.d., using a silicone rubber sealant (Dow Corning 732 RTV). Normally the sealant filled the bottom 1 cm of the tube in order to lock the lead rigidly in place and also to prevent any solution from seeping into the electrode body.

For certain optical measurements a special configuration was used so that the electrode surface could be placed in the path of a horizontal light beam from a spectrometer. This consisted of a short 15 mm section of perspex that could clip

Table 5.1 List of Melts Prepared for Electrochemical Studies

$Cu_{20}(As_2Se_3)_{80}$	air quenched
$Cu_{20}(As_2Se_3)_{80}$	cooled at 1°C min^{-1}
$Cu_{25}(As_2Se_3)_{75}$	
$Cu_{56}(As_2Se_3)_{44}$	
$CuAsSe_2$	
$Cu_{20}(As_2Se_{1.5}Te_{1.5})_{80}$	
$Cu_{25}(As_2Se_{1.5}Te_{1.5})_{75}$	

ELECTRODE CONSTRUCTION

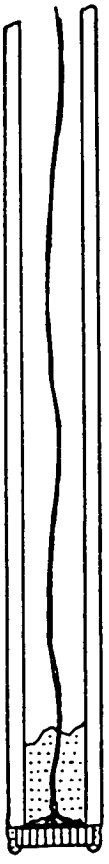

Perspex
Metal contact
Silicone sealant
Sensing material

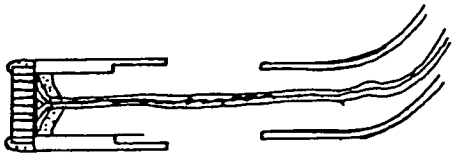

b/configuration for use with spectrophotometer

into a length of polythene pipe bent through 90°, this is also shown in figure 5.1.

Before electrochemical measurements were made the electrode surface was normally etched in 5M KOH, washed in de-ionized water and immersed in a 10^{-1} M solution of copper (II) nitrate. The electrode was left until a stable electrode potential, measured against a Ag/AgCl reference, was obtained.

5.3 X-Ray Powder Photographs

Powder Diffraction Photographs were taken using a Debye Scherrer rotation camera. A small sample of the melt was ground to a fine powder using an agate pestle and mortar. The powder was packed into a 0.5 mm diameter capilliary tube and normally about 7 mm of hard packed material was present. The ends of the tube were sealed and it was mounted in the camera on a block of sealing wax.

In all cases the Cu($K\alpha_1$) line was used and generally exposures were made for 20 minutes although in some cases additional 60 min. exposures were made. The positions of any lines were measured by hand.

The following compositions were investigated:

Cu_2Se
$CuAsSe_2$
$Cu_{20}(As_2Se_3)_{80}$
α-$Cu_{20}(As_2Se_3)_{80}$
$Cu_{56}(As_2Se_3)_{44}$
$Cu_{20}(As_2Se_{1.5}Te_{1.5})_{80}$

The positions of any lines observed are given in table 5.2. As can be seen no lines were obtained for the tellurium containing composition. In fact in more detailed studies with Fraser[1] it was found that all the tellurium containing compositions studied

Table 5.2 X-Ray Lines for Cu-As-Se Compounds

Material	θ°	$\frac{1.54}{2 \sin \theta}$/Å
$CuAsSe_2$	28.2	1.63
	46.7	1.06
	55.3	0.94
	68.1	0.83
	75.1	0.80
	86.6	0.77
	104.1	0.79
$Cu_{20}(As_2Se_3)_{80}$	20.9	2.16
	21.8	2.07
	24.3	1.87
	28.2	1.63
	46.7	1.06
	55.3	0.94
	68.1	0.83
	75.1	0.80
	86.6	0.77
$Cu_{56}(As_2Se_3)_{44}$	25.4	1.80
	28.2	1.63
	41.9	1.15
	46.7	1.06
	49.6	1.01
	55.3	0.94
	60.8	0.88
	66.8	0.84
	68.1	0.83
$Cu_{56}(As_2Se_3)_{44}$	68.1	0.83
	75.1	0.80
	76.7	0.79
	86.6	0.77

continued/...

Table 5.2 continued

Material	θ°	$\frac{1.54}{2 \sin \theta}$/Å
Cu_2Se	26.5	1.72
	40.0	1.20
	44.2	1.10
	52.0	0.98
	36 (w)	1.31
	47 (w)	1.05

gave no evidence of crystalline phases. No lines were obtained for one of the $Cu_{20}(As_2Se_3)_{80}$ compositions, this was designated a-$Cu_{20}(As_2Se_3)_{80}$. The compositions Cu_2 Se and $CuAsSe_2$ gave sharp well defined lines. All the lines from $CuAsSe_2$ were also found in the copper-arsenic selenide melts, but additional lines were also found in these compositions. The lines from Cu_2Se did not correspond to any of the lines of the ternary compositions.

5.4 Resistivity Measurements

Resistivity measurements were made at 20°C for all compositions that would be used in electrochemical studies. The sample was placed in series with a known standard resistance, the value of which was selected to be comparable with the resistance of the sample. A small potential difference was applied across the sample-resistor using a stabilized power supply. The potential difference across the known resistor was measured with a high impedance voltmeter. This gives the current flowing in the sample, by measuring the potential drop across the complete sample-resistor combination the sample resistance is then simply given by

$$R_{SAMPLE} = R_{ST} \frac{(\Delta V_{TOT} - \Delta V_{ST})}{\Delta V_{ST}}$$

ΔV_{TOT} = P.D. across sample and resistor
ΔV_{ST} = P.D. across standard
R_{ST} = Resistance of standard.

For some samples the temperature dependence of resistivity was measured using the apparatus shown in figure 5.2.

Temperature was measured with a copper-constantan thermocouple.

Results are shown in table 5.3 and the temperature dependence

Table 5.3 Electrical Properties of Cu-As-Se Compositions

Composition	$R_{20°}/\Omega$ cm
a-$Cu_{20}(As_2Se_3)_{80}$	2×10^{-8}
c-$Cu_{20}(As_2Se_3)_{80}$	5.2×10^{-2}
c-$Cu_{25}(As_2Se_3)_{75}$	~ 1
c-$Cu_{56}(As\ Se)_{44}$	~ 10
c-$CuAsSe_2$	4.0×10^{-4}
a-$Cu_{20}(As_2Se_{1.5}Te_{1.5})_{80}$	2.9×10^{-7}

5.2 COLD FINGER APPARATUS FOR CONDUCTIVITY MEASUREMENT

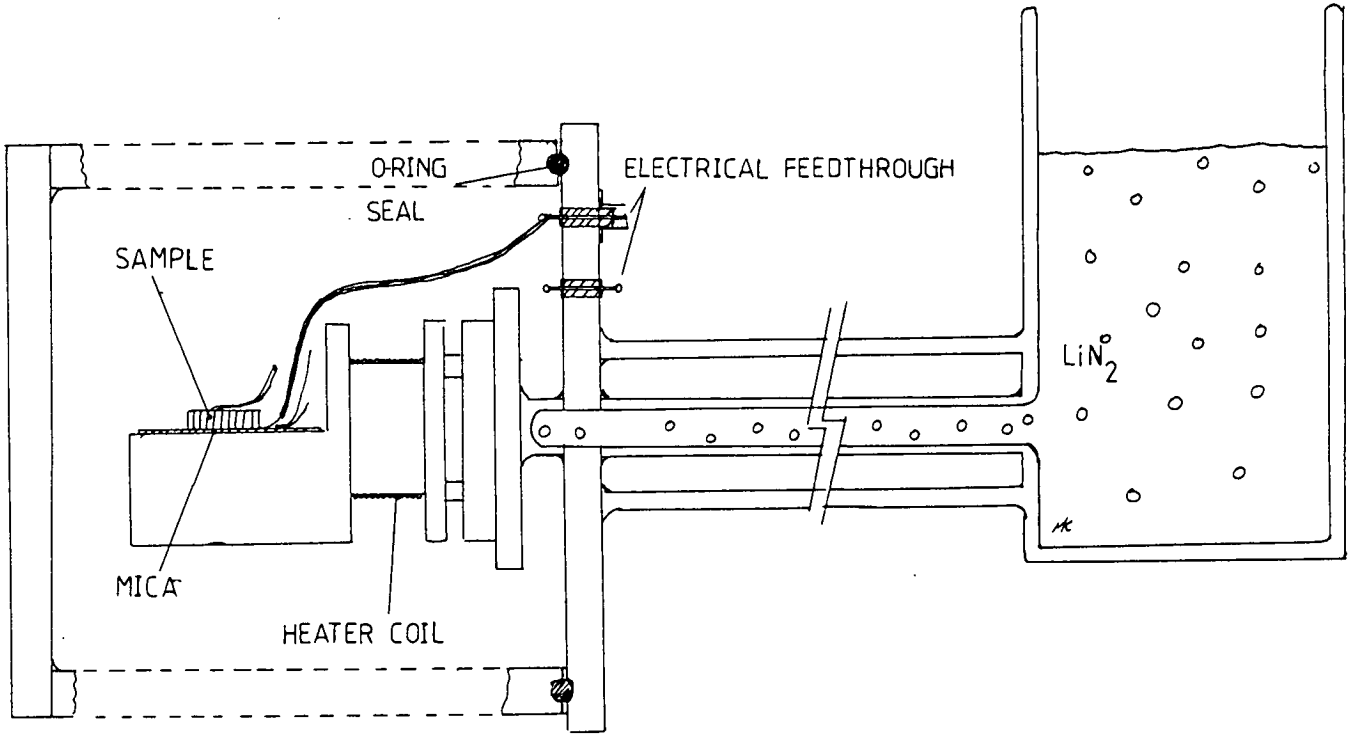

of $CuAsSe_2$ is plotted in figure 5.3. It should be noted that when high currents ($\sim$ 0.5 A) were passed through the samples considerable ohmic heating occurred. The resistance of the high copper containing $Cu_{56}(As_2Se_3)_{44}$ actually increased where as materials with lower copper contents showed a decrease of resistance with heating. Since the resistivity of $Cu_{56}(As_2Se_3)_{44}$ is lower at 20°C than that of $CuAsSe_2$ it may be concluded that in addition to $CuAsSe_2$ there is a high conductivity phase which may lead to the additional X-ray lines. The temperature dependence of the bulk $Cu_{56}(As_2Se_3)_{44}$ suggests this phase is a metallic conductor.

5.3 CONDUCTIVITY OF $CuAsSe_2$ 0°c-80°c

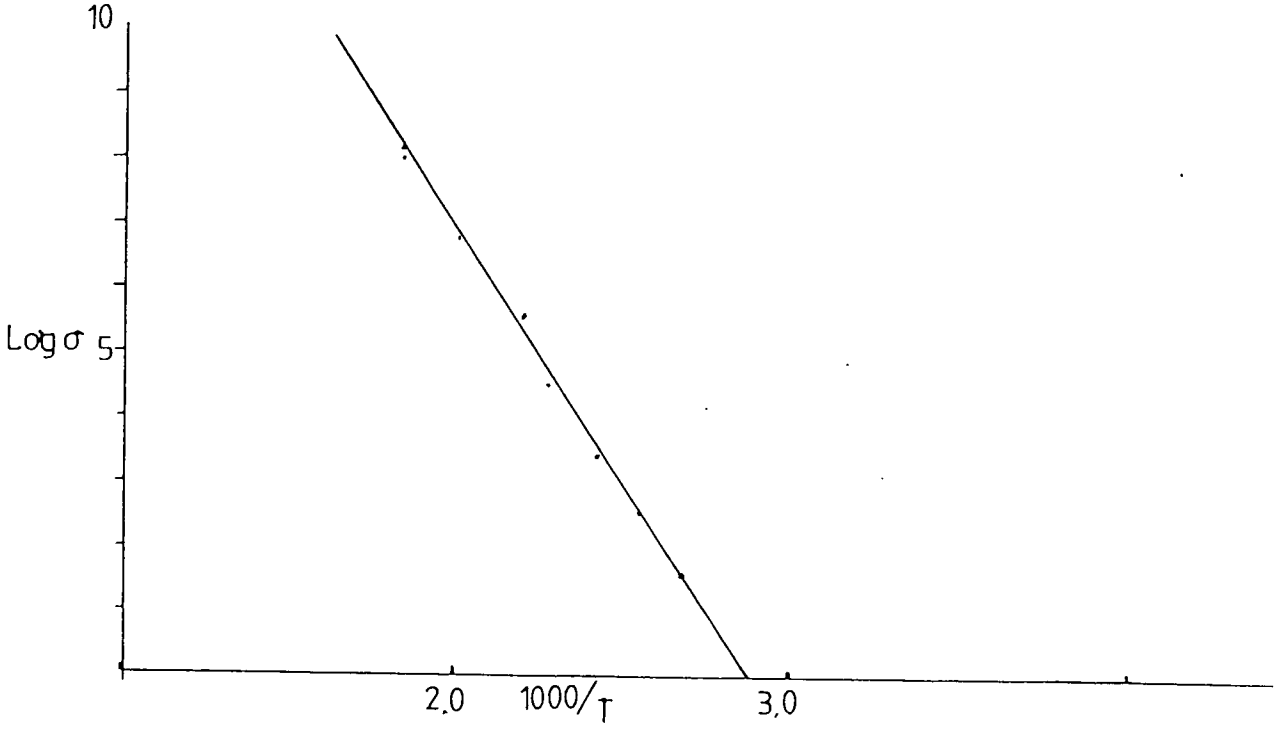

Chapter 6

Experimental

6.1 Introduction

The experimental methods used in this project to study electrode/solution interfaces are described below. For convenience the experimental results will be presented in the following chapter in the same order and under the same headings.

6.2 Potentiometry in Copper Solutions

Solutions of copper (II) chloride, copper (II) nitrate, copper (II) sulphate and copper (II) acetate were prepared by dissolving Analar grade salts in deionized water. In some cases 'super Q' (triply distilled and deionized) water was used but this was found to make no difference to the results. Normally a stock solution of concentration 10^{-1}M was prepared and successively diluted to give a range of solutions with concentrations down to 10^{-5}M or 10^{-6}M. For most experiments an inert base electrolyte was also present, this consisted of a 10^{-1}M solution of the potassium salt of the relevant anion.

The EMFs of cells made up of the experimental chalcogenide electrode and a calomel or silver/silver chloride reference electrode were measured with a Keithley 610B or 610C electrometer. The input impedance of both of these electrometers is $\sim 10^{+14}\Omega$. The chloride concentration in the reference electrodes was usually 10^{-1}M so that the reference potentials were 0.336 V and 0.282V[2] for the calomel and silver/silver chloride electrodes respectively.

In section 5.1 it was noted that Au was normally used as the metal for back contacts to the chalcogenide electrodes. A few experiments were carried out to determine the effect, if any, of different back contacts on the electrodes' response to copper (II) ion. The chalcogenide compositions and the contacts used are repeated below:

$Cu_{20}(As_2Se_3)_{80}$	Au, Cu, Zn, C
$CuAsSe_2$	Au, Cu, C

The effect of stirring on the response to copper (II) nitrate and copper (II) chloride was investigated for $CuAsSe_2$, $Cu_{20}(As_2Se_3)_{80}$ and $Cu_{56}(As_2Se_3)_{44}$ electrodes. The stirring was carried out by means of a magnetic stirrer.

6.3 The Effect of Foreign Cations

The effects of the following ions on the response of the copper chalcogenide electrodes were investigated:

H^+
Li^+, Na^+, K^+
Mg^{2+}, Ca^{2+}
Ag^+
Zn^{2+}, Cd^{2+}, Hg^{2+}
Mn^{2+}, Fe^{3+}

In most cases solutions of the nitrates were prepared from AnalaR grade reagents dissolved in deionized water mixed with copper (II) solutions. Any change in the cell potential from that expected from copper (II) alone was noted. In general the foreign ion was arranged to have a much higher concentration than the copper (II). If strong interference effects were observed more detailed studies were carried out in which both the foreign ion concentration and the copper concentration were varied. Of the ions listed above only Fe^{3+}, Hg^{2+} and Ag^+ were found to cause pronounced interference. Iron (III) was investigated as the chloride because nitrate solutions were observed to darken gradually, probably because of the precipitation of $Fe(OH)_3$ via the reaction

$$Fe(NO_3)_3\ (aq) + 3H_2O \rightleftharpoons Fe(OH)_3\ (s) + 3HNO_3\ (aq)$$

Silver (I) and mercury (II) interference was investigated using a

silver/silver chloride double junction reference electrode with 10^{-1}M KNO_3 in the outer container. The purpose of the double junction electrode is to avoid problems due to precipitation of the chloride at the junction between the test solution and the reference electrode.

6.4 Instrumentation

In Chapter 2 it was noted that kinetic experiments on electrode reactions involve applying either a potential perturbation and measuring current or a current perturbation and measuring potential. In section 2.9 it was shown that the I-V characteristics of cells are non-linear and often show current peaks. It is essential therefore to control the potential at the working electrode, otherwise the varying ohmic drop in the cell will lead to uncertainty in the value of the electrode potential at any one time. Circuits which control potential are known as potentiostats and a prototype circuit based on an operational amplifier is shown in figure 6.1b. The inverting input is grounded and because a virtual short exists between the two inputs the non-inverting input is also grounded. This forces point A in the resistor chain (Z_1,Z_2) to -E, the potential of the source V. The point A will remain at a potential of -E even if Z_1 and Z_2 change. This is precisely what is required in controlled potential electrochemical experiments where it is necessary to hold the working electrode at a well-defined potential relative to the reference electrode despite widely varying currents in the cell. If the battery is replaced by a signal generator, the potential at A can be varied in a pre-determined manner.

Figure 6.1a is the block diagram of a basic electrochemical potentiostatic instrument. The operational amplifier of the potentiostat has been configured as a summing amplifier - the Control Amplifier (CA); the summing network allows the synthesis of complex waveforms from simpler functions. The network shown in Figure 6.1b is entirely resistive so that all the input signals are D.C. coupled, although in practice A.C. coupling may also be employed. The reference electrode is connected to a device known as a voltage follower (V.F.) which simply acts as a buffer so that no current is drawn

1 a/ Basic Voltammetry Circuit

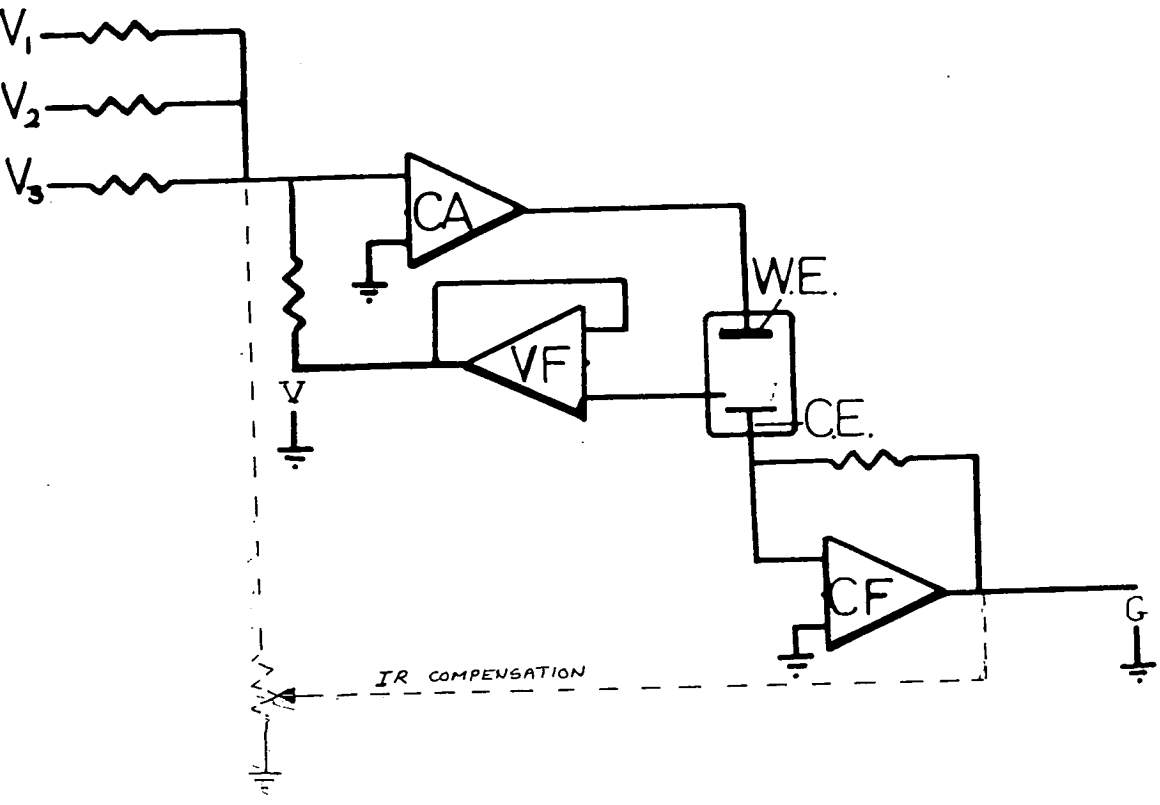

b/ Basic Potentiostat

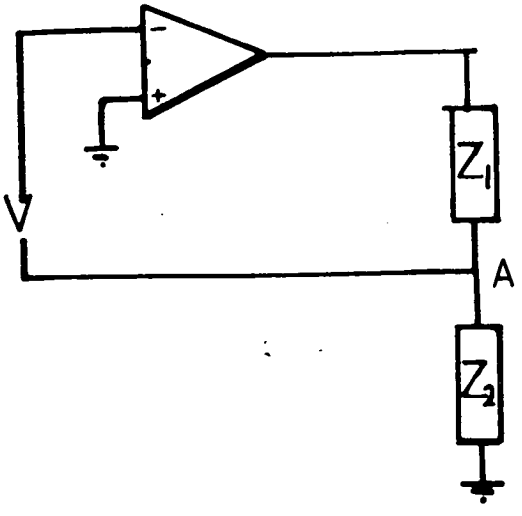

from the reference electrode but sufficient current is delivered to the potentiostat. The output from the voltage follower feeds into the summing amplifier and completes the potentiostat circuit. The remaining unit is a current follower (CF) which is basically a current to voltage converter and allows for the measurement of current flowing between the working and counter electrodes. The counter electrode is connected directly to the non-inverting input and as the inverting input is earthed, the current effectively flows to earth. Clearly the solution between the working electrode and the reference electrode replaces Z_1 in Figure 6.1a and the solution between the reference and counter electrodes replaces Z_2.

In addition to the basic summing amplifier, voltage follower and current follower stages discussed above, additional amplification stages, known as boosters (B), may be necessary to produce the necessary currents in the cell and the input to the summing amplifier.

In a controlled potential experiment it is necessary to hold the working electrode at a well-defined potential with respect to the reference electrode and thus also to the solution. This is achieved by passing the necessary current between the working and counter electrodes using the potentiostat. The presence of a current results in an ohmic drop through the solution which shifts the potential of the working electrode from its required value. For non-aqueous systems the IR drop can be quite considerable and must be accounted for. The usual way of avoiding the IR drop is to feed back a potential, that is directly proportional to the current, into the summing amplifier. This can be achieved by connecting the current follower to the summing amplifier as shown by the dashed line in Figure 6.1a.

In this study the instrument used for most experiments was the Bruker E310 modular polarograph. This instrument consists of a variety of modules which, depending on the way in which they are interconnected, allow various experiments to be performed. The basic Control Amplifier module is based on a TP 1426 02 integrated instrumentation amplifier configured as a summing amplifier, together with a second TP 1426 02 which acts as the voltage

follower. There are seven inputs to the summing network, three are via 1M resistors for D.C. coupling, two have a 4.7pF capacitance in parallel with the 1MΩ resistor for A.C. coupling, one has a 2MΩ resistor and one is gated to allow synchronised switching between potentials. Of the seven inputs, one is externally connected to the output of the voltage follower to allow potentiostatic operation. A second input provides the starting potential for any experiment. This can be between -5V and +5V and is controlled by a potentiostat within the module. A booster consisting of a class B push-pull amplifier is placed between the output of the summing amplifier and the cell. A basic circuit diagram of the control amplifier is given in Ref 1 .

The current follower is housed in a separate I-E converter module and again is based on a TP 1426. The output is buffered by a booster which allows current to be measured directly with low impedance instruments; the maximum output voltage is 5V into 1kΩ. The current range depends on the resistor value between the non-inverting input and the output, and is variable between 50nA maximum for a 5MΩ resistor and 50mA maximum for a 20Ω resistor. The I-E converter also houses the circuitry for sample and hold, differentiation and synchronisation functions necessary for some of the sampling techniques.

IR compensation is provided by a separate module which inserts a voltage divider between the output of the current follower and the summing network of the control amplifier. Since the feedback is from a passive network the maximum IR compensation is limited by the output of the I-E converter to ±5V. For highly resistive glasses this was insufficient to overcome the IR drop in the electrode.

The other modules provided the potential waveforms and timing sequences. The D.C. sweep module comprises a simple analogue integrator with a variable time constant and voltage range. Sweep rates from 0.1mV s^{-1} to 500mV s^{-1} and an amplitude of up to 5V are available. The cyclic module also uses an analogue integrator. As supplied the sweep rates are very high, (ca 10V s^{-1})

6.3 CHRONO POTENTIOMETRY

a.

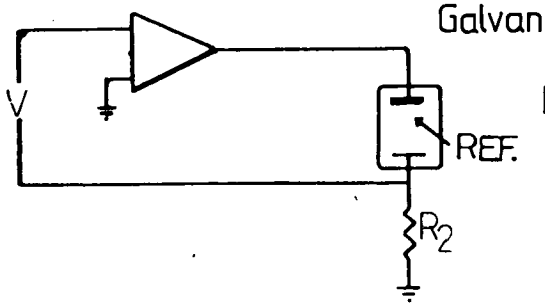

Galvanostat derived from a potentiostat

b.

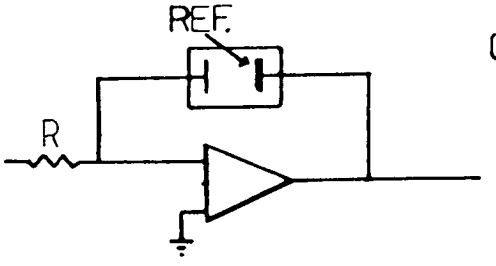

Galvanostat based on a feed back loop

c.

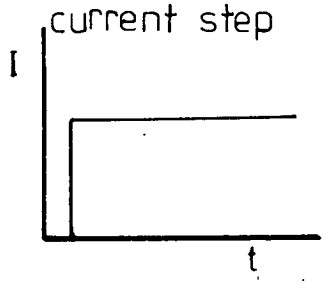

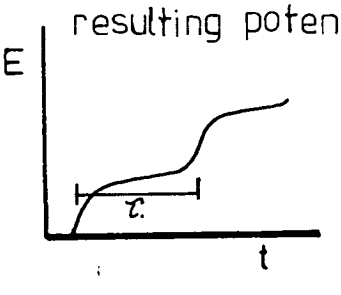

however the time constants of the integrator circuit were altered to give sweep rates of the same order as those of the D.C. sweep module.

An additional module allowed the instrument to be used for controlled current experiments. In general it is easier to control current than potential. Two possible circuits are shown in Figure 6.3. The circuit in Figure 6.3a is derived directly from the potentiostat; R_2 is fixed so the current is automatically set at E/R_2. In Figure 6.3b the cell is made the feed-back loop of an operational amplifier. The junction between the resistor, the inverting input and the cell is at ground, and since the operational amplifier has virtually infinite impedance any current flowing across the resistor must also flow through the cell. The current is given by V/R where V is the input voltage.

In the E310 system the circuit of Figure 6.3a is used and the current is continuously variable from 0 to 10mA. The operational amplifier used as the Galvanostat is the summing amplifier in the Control Amplifier module. The potential of the working electrode is measured by a voltage follower in the Galvanostat module; the potential of the reference electrode is measured using the voltage follower in the Control Amplifier. The potential of the working electrode with respect to the reference is obtained by applying the outputs of the voltage followers to a 741 operational amplifier used in the differential mode. By using the signal generators various controlled current waveforms can be obtained but in this study only steps were used.

As mentioned above the E310 can only be used with cells that have a low resistance because the maximum output voltage for IR compensation is 10 Volts. For the tellurium-containing glasses this was not sufficient to overcome the large IR drops in the electrodes. For these materials cyclic voltammetry was carried out in the 2-electrode mode using a high voltage (-100V to +100V stabilized ramp generator. Current was measured with a current follower circuit based on a 709 operational amplifier. In some preliminary experiments voltammetry was carried out using a summing amplifier constructed for the purpose and a class B booster based on complementary high-power transistors. The results from this system were the same as from the E310.

6.5 Chronopotentiometry

All chronopotentiometry experiments were carried out using the E310 configured as a galvanostat, as described in the previous section. Normally the working current output of the Galvanostat module was connected to the gated input of the summing amplifier. The gate was operated by a signal from the timer unit (which could give TTL compatible pulses of 0.1s to 99.9s duration in 0.1s intervals) and this was generally arranged to give a 90s current pulse. In some cases however the timer was set up to give a series of 90s pulses separated by intervals of 0.1s in which the current was switched off. The intervals provided useful timing markers and did not appear to affect the general shape of the chronopotentiograms.

Chronopotentiograms were measured for various electrode materials in various concentrations of copper (II) nitrate. A base electrolyte of 10^{-1}M KNO_3 was always present . In some cases chronopotentiograms were also obtained for chloride solutions, as a comparison.

6.6 Cyclic Voltammetry

As mentioned in section 6.4 most experiments were performed with the E310 configured as a cyclic voltammeter. The cyclic voltammetry module was modified to allow sweep rates as low as 1mV s^{-1}. The cyclic voltammograms were recorded on an X-Y plotter, either a Bryans 26000 or a Hewlett- Packard 7035A A4 model. As mentioned earlier some preliminary studies were also made using a purpose-built summing amplifier and current follower; the triangular waveform was provided by a Chemical Electronics Co. linear sweep generator.

Cyclic voltammograms were obtained for electrodes in various copper concentrations, acid solutions, basic solutions, hexacyanoferrate solutions, and solutions of NNNN′-tetramethyl p-phenylene-diamine dihydrochloride (TMPD) and hydroquinone solution. The sweep range was either from -0.75V to +0.50V or from 0.00V to +1.25V. The reference

electrode was always a silver/silver chloride electrode in a 10^{-1}M KCl solution. The counter electrode was a platinum wire or platinum foil electrode. In most cases the cell, reference electrode and counter electrode were supplied by Methrohm AG. In some preliminary studies however other apparatus was used. The base electrolyte for all experiments was either 10^{-1}M KNO_3, 10^{-1}M $KClO_4$ or 10^{-1}M KCl. The sweep rate was normally 1.25V in 10s, so that a complete cycle took 20s. Usually the potential was varied over several cycles.

As a comparison, cyclic voltammograms were also obtained at a platinum foil electrode used as the working electrode. In a typical measurement the cell would be allowed to come to equilibrium and the equilibrium potential was measured by a Keithly 610B. The electrometer was then switched out of circuit and the E310 switched in; a potential was applied to the cell and the sweep immediately started. After several cycles the electrode was held at the initial potential for 60s and then cycling was resumed. In some cases the electrode was also held at the final potential for 60s before resuming sweeps.

As mentioned above the behaviour of three redox couples was also investigated. The hexacyanoferrate couple

$$[Fe(CN)_6]^{3-} + e^- \rightleftharpoons [Fe(CN)_6]^{4-}$$

was made up as a $5x10^{-4}$M : $5x10^{-4}$M mixture in 10^{-1}M KNO_3. Other ratios were also made up to investigate the potentiometric response of the electrodes to the couple. The quinone/hydroquinone couple was made up as a $5x10^{-3}$M solution of quinone in 10^{-1}M $KClO_4$ or KNO_3. The NNNN' tetramethyl p-phenylene-diamine dihydrochloride (TMPD) was made up as a 10^{-3}M solution in 10^{-1}M $KClO_4$.

6.7 Photo-effect Measurements

Two types of cell were used for optical measurements and they are illustrated in figures 6.4a and 6.4b. The type A cell used an LED for the

light source. Three colours were available; red centred on 700nm, yellow (580 nm) and green (563nm). The spectral distributions were measured using a Carl Zeiss MQ2 monochromator and a photo-electric cell. The spectral responses are shown in figure 6.5. The radiated power from the top of the optical guide was measured using an Optronix 730 A radiometer. The sensitivity was taken as the value at the centre frequency although a more accurate power could be obtained using the relationship

$$\text{power} = \int_{\lambda_1}^{\lambda_2} \text{sens.}(\lambda) \times \text{intensity}(\lambda)\, d\lambda$$

The LED was driven by the circuit shown in figure 6.4c so that intensity could be varied. In some cases a 1Hz square wave signal was applied.

The type B cell is shown in figure 6.4b and was used in conjunction with the special electrode configuration described in section 5.2. The cell was designed to fit into the sample compartment of a Pye Unicam SP 500 UV-visible spectrophotometer. The power emitted at each frequency was determined with the Optronix radiometer. The power was also determined as a function of slit width in order that photo-effects could be measured as a function of frequency at constant power. The spectral distribution is shown in figure 6.5 and it is clear that the slit width must be made much wider at 500nm and 700nm than 600nm to get the same level of power. The variation of $\Delta\lambda$ with slit width is also shown in figure 6.5, so the 'purity' of the incident light can be judged. In actual experiments attempts were made to make power density constant by spreading the beam to a constant area with a curved glass placed between the beam and the cell. It was difficult to position the glass accurately however and in general it was not found to affect the results.

All electrodes were tested in the type A cell and normally the transient response of the cell potential on the application of 700nm illumination was measured. The potential was measured against a calomel electrode with a black plastic coating on the electrode body to shield

CELLS FOR PHOTO-ELECTRO CHEMICAL EXPERIMENTS

6.4 a./

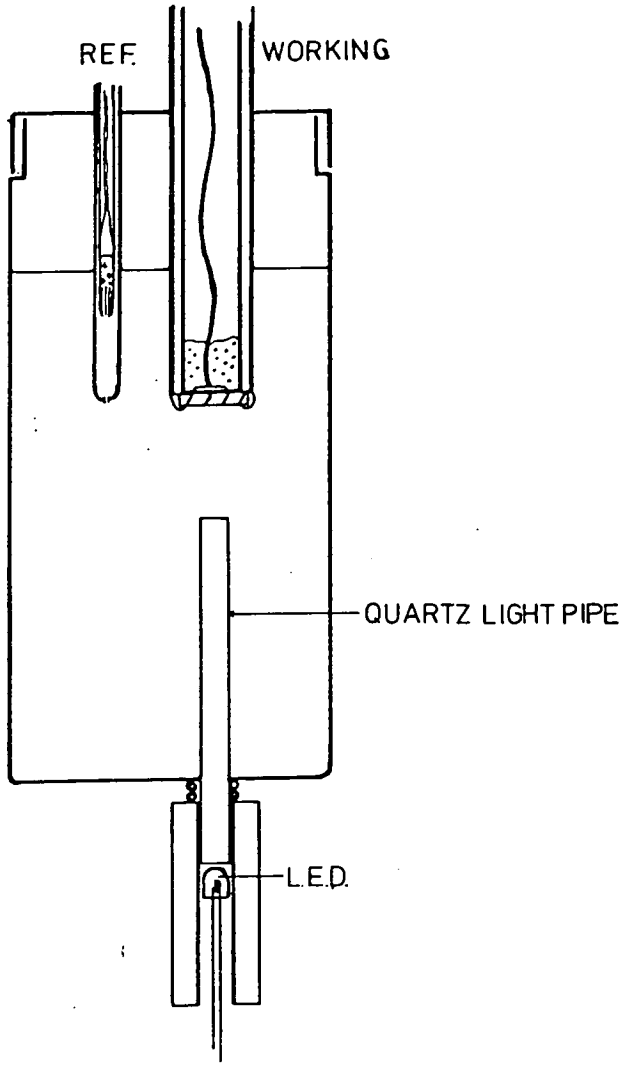

b./

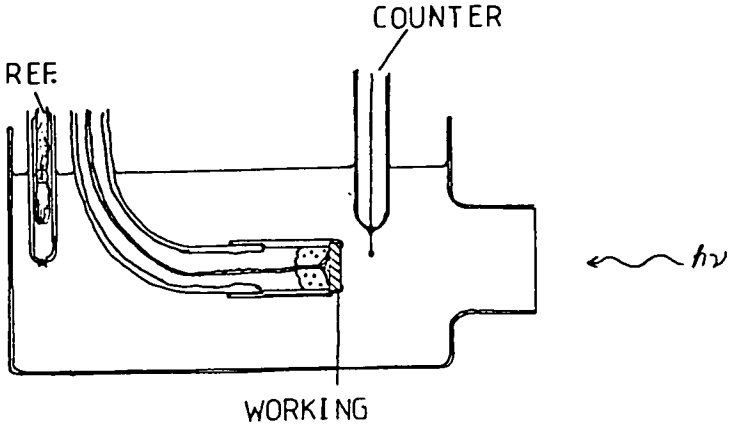

5 a/ Outputs from LEDs used in photoeffect experiments

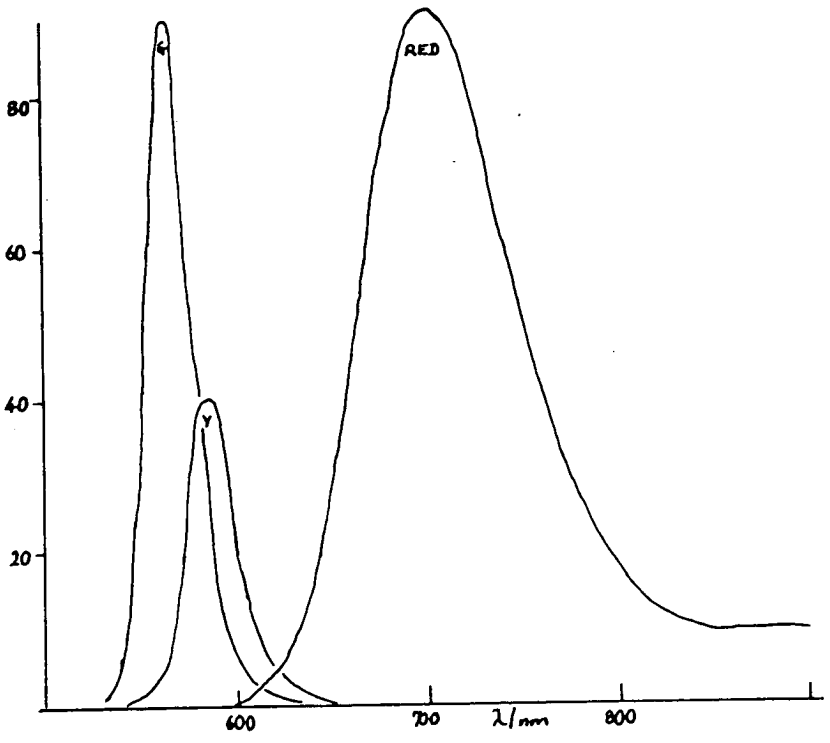

b/ i Output from modified SP 500

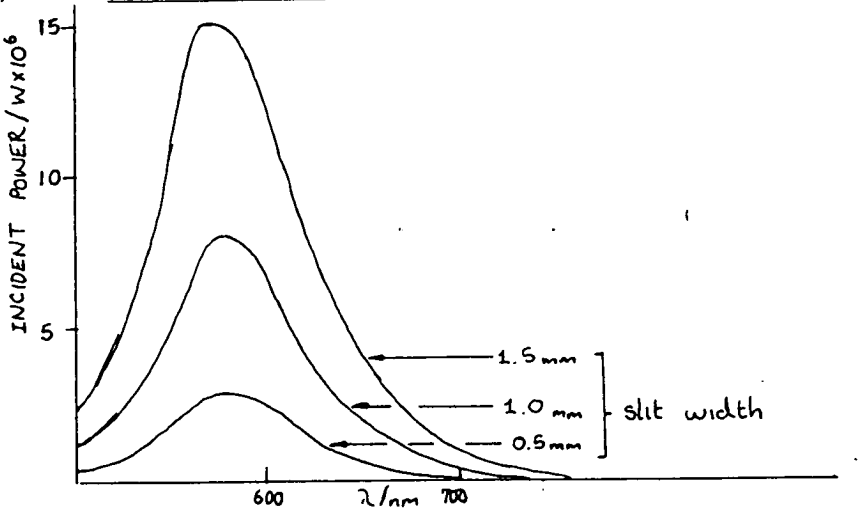

ii variation of band width with slit width

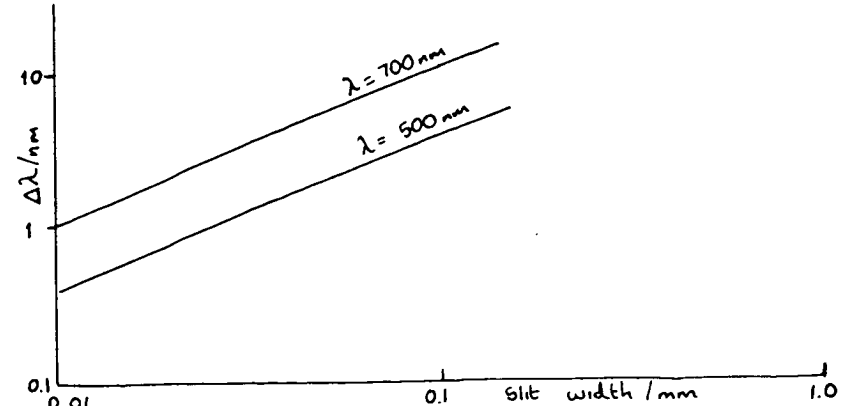

it from the light. A Keithley 610C was used to measure potential. The output from the 610C was applied to an offset amplifier so that only changes in potential were measured. An attempt was made to measure the potential against a similar electrode so that very low equilibrium cell potentials would in principle result, however shielding of the 'reference' electrode against stray light was found to be a problem and furthermore the cell potential was not very reproducible in base electrolyte alone. Where a photo-effect was observed it was measured as a function of copper concentration and of light intensity. In some cases the 563nm LED was substituted for the 700nm. Electrodes showing photo-effects were rebuilt in the special configuration of section 5.2 in order that their spectral response could be measured using the type B cell.

Both cells were designed to accommodate a third electrode in order that voltammetry in the presence of light could be carried out. However the results from these experiments were not very interesting; the enhancement of the current generally being too small to measure.

CHAPTER 7

Results of Electrochemical Studies

7.1 Introduction

The results obtained from the experiments described in chapter 6 are presented below. They are set out in the same order and under the same section headings as the experimental sections of chapter 6.

7.2 Potentiometry in Copper (II) solutions

All the compositions investigated show a linear relationship between electrode potential and the logarithm of copper (II) nitrate concentration over the range 10^{-5}M to 10^{-2}M. Typical results are shown in figure 7.1 and figure 7.2. The exact slopes and E^{o} values are summarized in table 7.1. The value E^{o} is here defined as the potential that would be obtained at a copper (II) ion concentration of 1.0M if the linear relationship observed at lower concentrations continued to this value. The slopes are all within 3mV (decade)$^{-1}$ of the Nernstian value - 29 mV (decade)$^{-1}$ - for a 2 electron process (at t = 20°C). Also shown in table 7.1 are the deviations from the potential expected at 10^{-1}M Cu^{2+}, if a linear relationship continued over the complete range of concentrations. All such deviations are negative and in the case of one batch of Cu_{20} $(As_2\ Se_3)_{80}$ were as high as 25mV.

The data displayed in figure 7.1 includes results obtained for the same electrode composition with a variety of different metal back contacts. It is clear that, initially at least, the back contact has no effect on the electrode response. After several weeks however, the Zn backed electrode no longer gave a linear relationship between electrode potential and log (concentration); the potentials being higher than expected for low concentrations ($[Cu^{2+}] < 10^{-2}$M). This effect was not found with any other back contact even after several months of use.

The response of electrodes of the same composition varied, depending on the original melt from which the electrode was made. In table 7.1, 3 different Cu_{20} $(As_2\ Se_3)_{80}$ and 2 different Cu_{25} $(As_2\ Se_3)_{75}$ electrodes are shown, in each case E^{o} and the deviation at 10^{-1}M Cu^{2+} vary. This is probably a result of differences in the types and relative quantities of the various phases present. The two different amorphous electrodes gave similar results, inspite of being prepared quite independently.

7,1 RESPONSES OF Cu-As-Se ELECTRODES TO $Cu(NO_3)_2$ SOLUTIONS

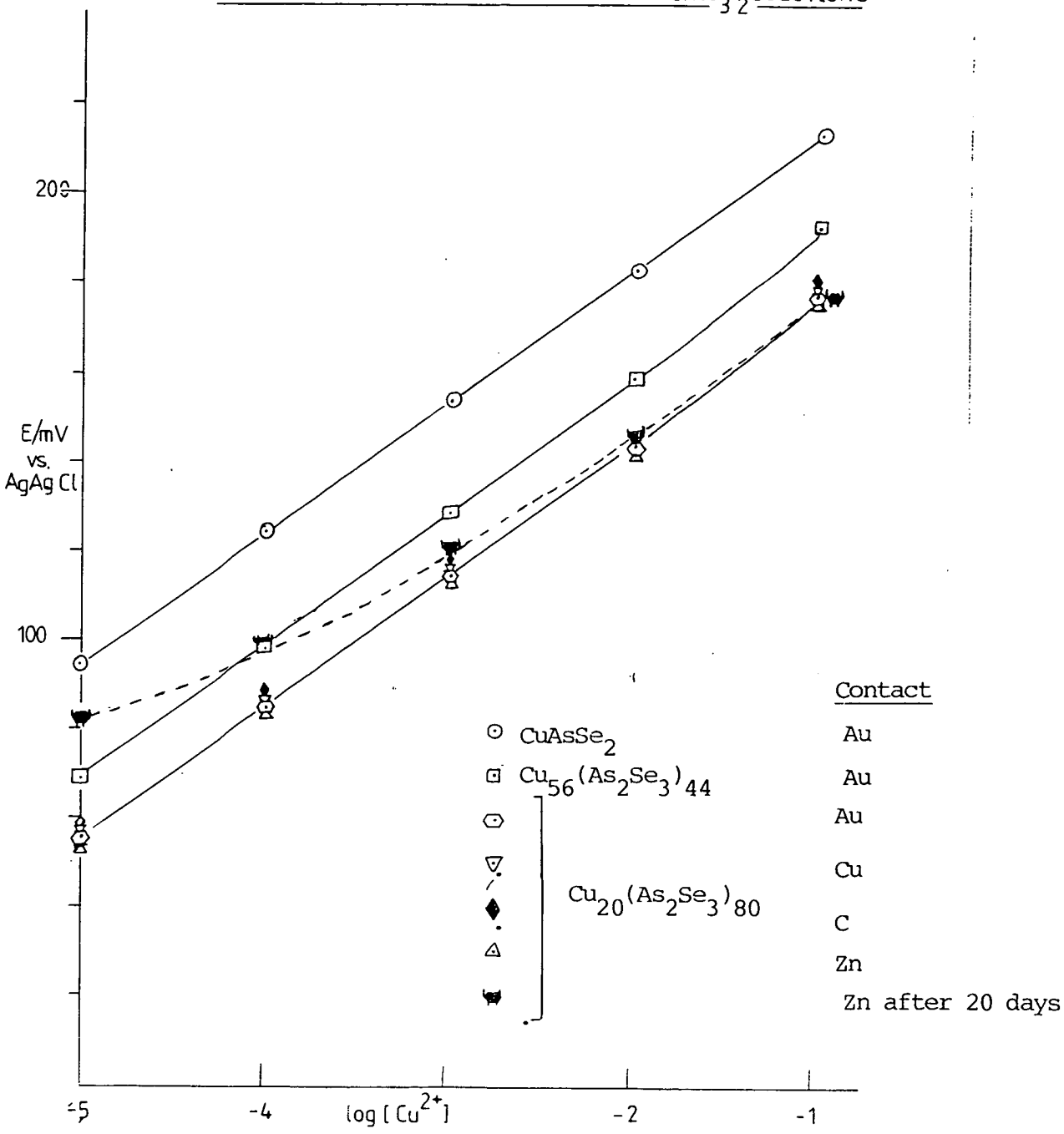

7.2 RESPONSES OF Cu-As-Se ELECTRODES TO $Cu(NO_3)_2$

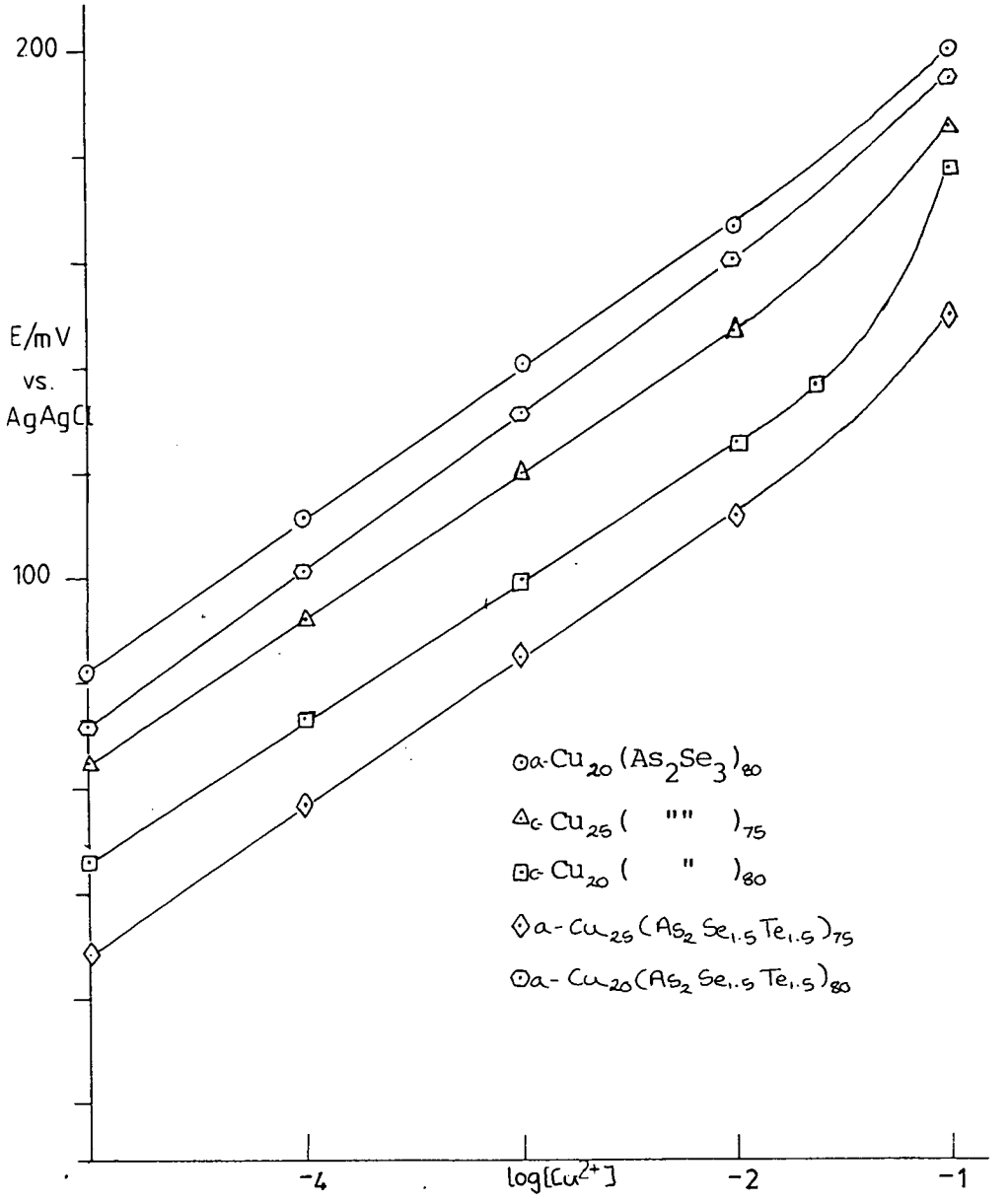

They are however sensitive to illumination (see below).

7.2.2 The response of the electrodes in sulphate solutions is identical to that in nitrate (i.e. slope, E^{o} value and, where applicable, deviation in potential from the expected value at $10^{-1}M$ are the same). In acetate solutions the slope is reduced to 16mV $(decade)^{-1}$ although the linear relationship persists. On returning the electrode to nitrate solutions the original response is immediately recovered.

7.2.3 In chloride solutions the behaviour is qualitatively different to that in nitrate or sulphate solutions. The electrode potential is not linearly related to log ($[Cu^{2+}]$) and the slopes are greater than the Nernstian values. The electrode potentials are always more positive in chloride than in nitrate solution. A typical result is shown in figure 7.3 for the $CuAsSe_2$ electrode.

In nitrate solutions, electrode potentials were not affected by stirring where as in chloride solutions stirring caused the electrode potentials to become more positive. The magnitude of the stirring effect depends on the copper (II) concentration, being greatest at the highest concentrations. When stirring is stopped the electrode potential decreases but it was never observed to return to the original value.

If the electrode is returned to nitrate solution, the response remains the same as found in the chloride solution.

7.2.4 The time required for the electrode potential to reach a steady value was generally less than 2 minutes. However, if the concentration was changed by more than an order of magnitude the time required was longer. Generally, the electrodes giving Nernstian slopes responded fastest. The response times appear to be correlated with the complexity of the x-ray powder photographs; those compositions showing the least number of phases giving the fastest response times.

Table 7.1

ELECTRODE	E^0/mV (vs.Ag/AgCl)	slope/mV(dec)$^{-1}$	ΔE/mV	Fig.
$CuAsSe_2$	243	29	0	7.1
$Cu_{20}(As_2Se_3)_{80}$	206	29	0	7.1
$Cu_{20}(As_2Se_3)_{80}$	181	27.5	21	7.2
a-$Cu_{20}(As_2Se_3)_{80}$	222	26.7	3	7.2
$Cu_{25}(As_2Se_3)_{75}$	170	28.9	11	—
a-$Cu_{25}(As_2Se_3)_{75}$	185	27.2	15	7.2
$Cu_{56}(As_2Se_3)_{44}$	219	28.8	4	7.1
$Cu_{20}(As_2Se_{1.5}Te_{1.5})_{80}$	219	28.5	5	7.2
$Cu_{28}(As_2Se_{1.5}Te_{1.5})_{75}$	205	28.6	5	7.2

notes: ΔE is the difference between electrode potential measured at $[Cu^{2+}]=10^{-1}$M and the expected potential if a Nernst type equation continued to apply at this concentration.

7.3 RESPONSES OF Cu/As_2Se_3 ELECTRODES TO CHLORIDE ION

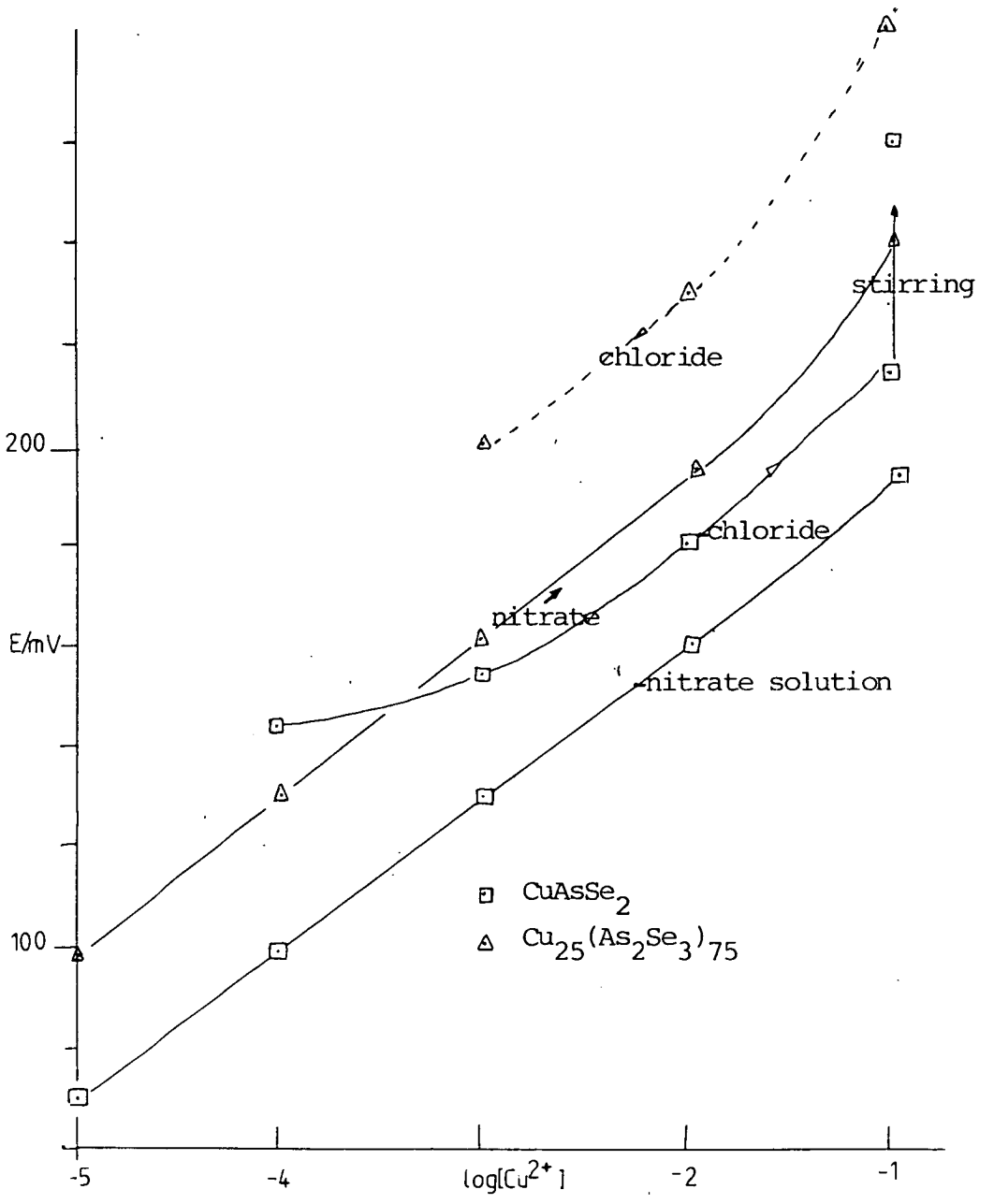

7.3 Potentiometry in the presence of foreign cations

The majority of cations investigated had no effect on the electrode response to copper (II) ions, except when they were at high concentrations ($>10^{-1}$M), where all caused a slight decrease -c.a. 5mV (decade)$^{-1}$ in electrode potential from the value in copper nitrate alone. It was concluded that this is an ionic strength effect. Major interference is found for Ag^{+}, Hg^{2+} and Fe^{3+} however. Detailed studies were made of the Ag^{+} and Hg^{2+} interference on the electrodes of composition Cu_{20} $(As_2\ Se_3)_{80}$ and $Cu_{20}(Se_{1.5}\ Te_{1.5})_{80}$, and of Ag^{+} interference on crystalline $CuAsSe_2$ electrode. Graphs of potential versus the concentration of interfering ion are shown in figure 7.4, 7.5 and 7.6. Reproducible measurements were difficult to obtain but the following general observations were made:

1. For Ag^{+} concentrations above 10^{-4}M the electrode could no longer distinguish between different copper levels. Instead it becomes a silver ion sensor with a slope of 58mV (decade)$^{-1}$. This is the Nernstian slope characteristic of a univalent ion.

2. The response to Ag^{+} at concentrations below 10^{-4}M depends on the past history of the electrode. If it has not previously been exposed to high silver levels its response to copper is unaffected by silver levels below 10^{-5}M. On the other hand, reducing the silver level in stages from 5×10^{-2}M causes a varying response to silver ions down to concentrations of at least 10^{-8}M. If copper ions are also present the electrode potential for silver concentrations less than 10^{-5}M depends both on silver and copper concentration.

3. The electrode recovers very slowly after removal from silver ion solutions - c.a. 24 hours is required if the copper concentration is 10^{-4}M. If the electrode is returned to a concentrated (10^{-1}M) Cu^{2+} solution, the potential recovers much more quickly c.a. 2 hours.

4. When an electrode is immersed in a 10^{-4}M Ag^{+} solution, after previously standing in a copper solution, the potential initially drops before slowly rising to the high values characteristic of silver ions. This feature was always observed, but the time to reach the potential minimum and the value of the minimum are variable. A typical example of this behaviour is shown in figure 7.7.

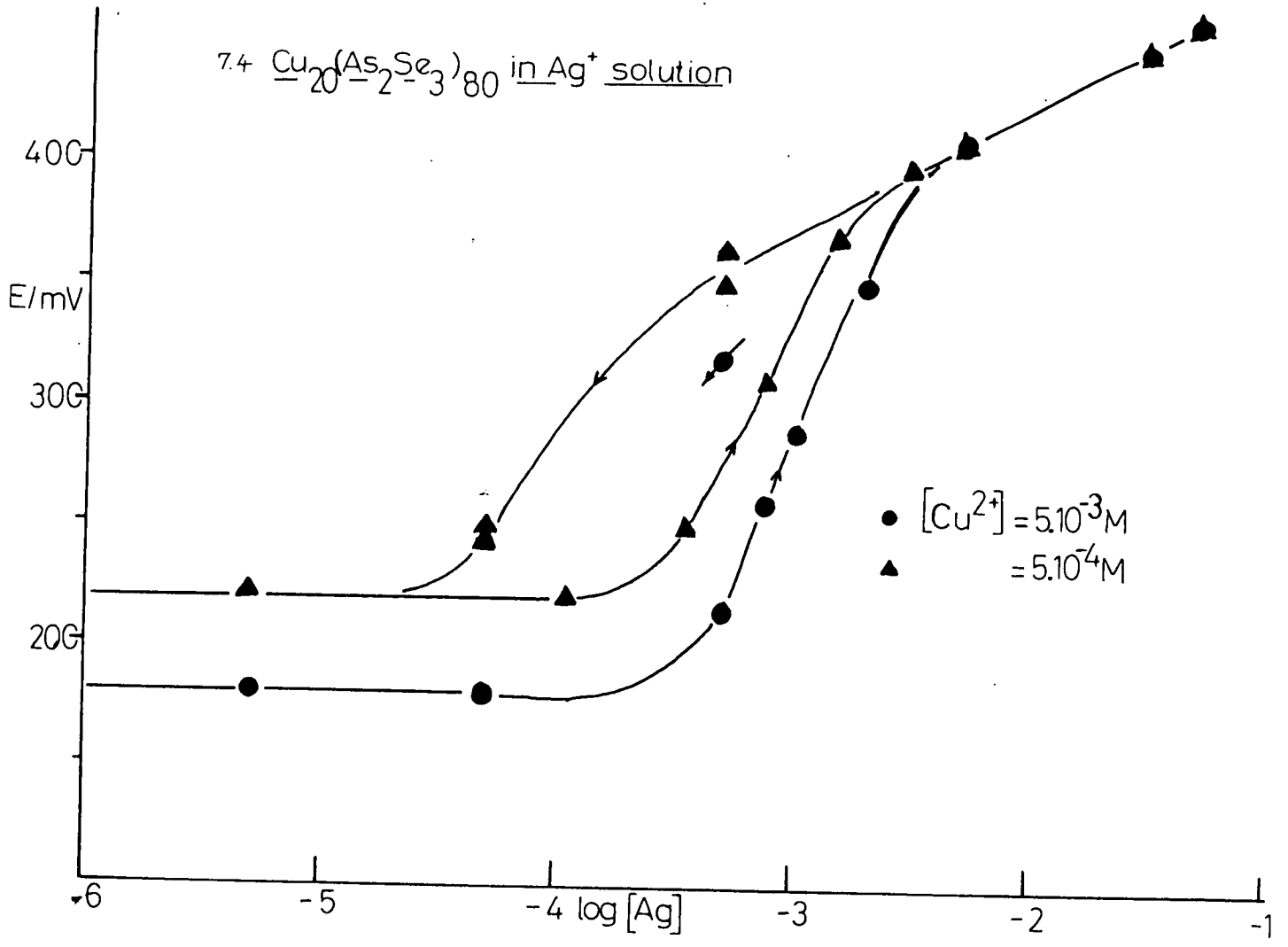
7.4 Cu20(As2Se3)80 in Ag+ solution
400
E/mV
300
200
[Cu2+] = 5.10-3M
= 5.10-4M
-6
-5
-4 log [Ag]
-3
-2
-1

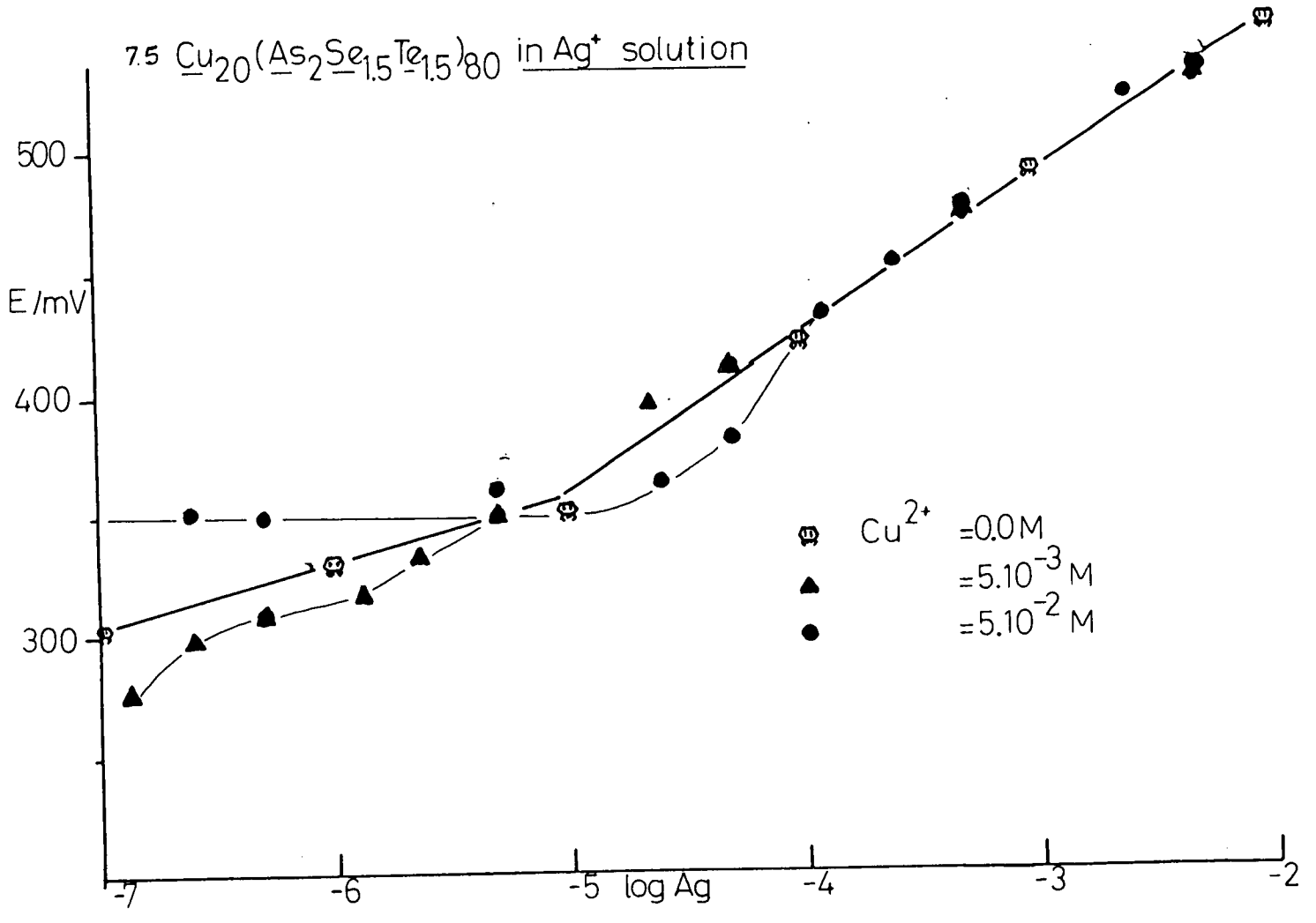
7.5 Cu20(As2Se1.5Te1.5)80 in Ag+ solution
500
400
300
E/mV
-7
-6
-5
-4
-3
-2
log Ag
Cu2+ =0.0 M
=5.10-3 M
=5.10-2 M

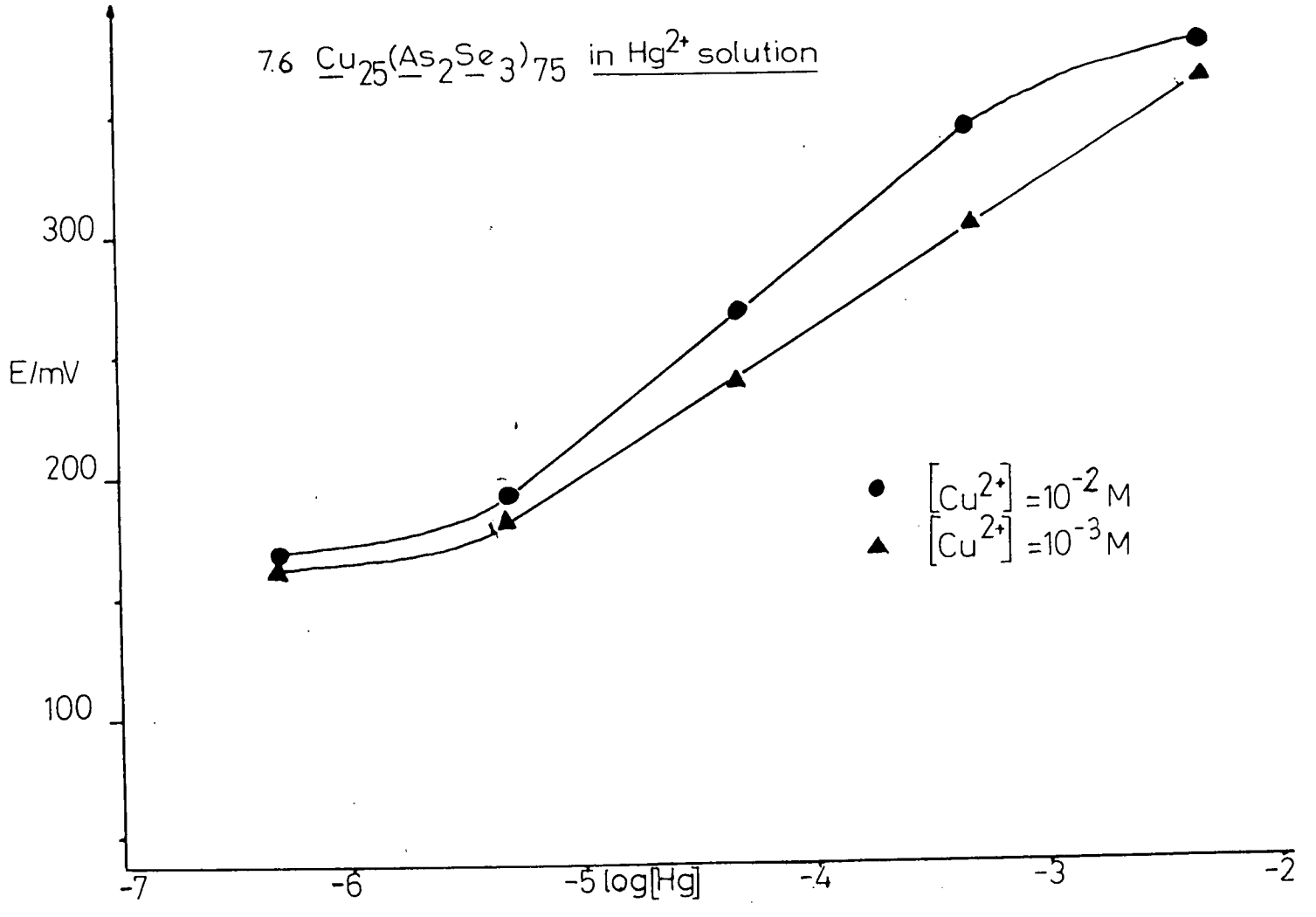
7.6 Cu25(As2Se3)75 in Hg2+ solution
300
200
100
E/mV
-7
-6
-5 log[Hg]
-4
-3
-2
[Cu2+] =10-2 M
[Cu2+] =10-3 M

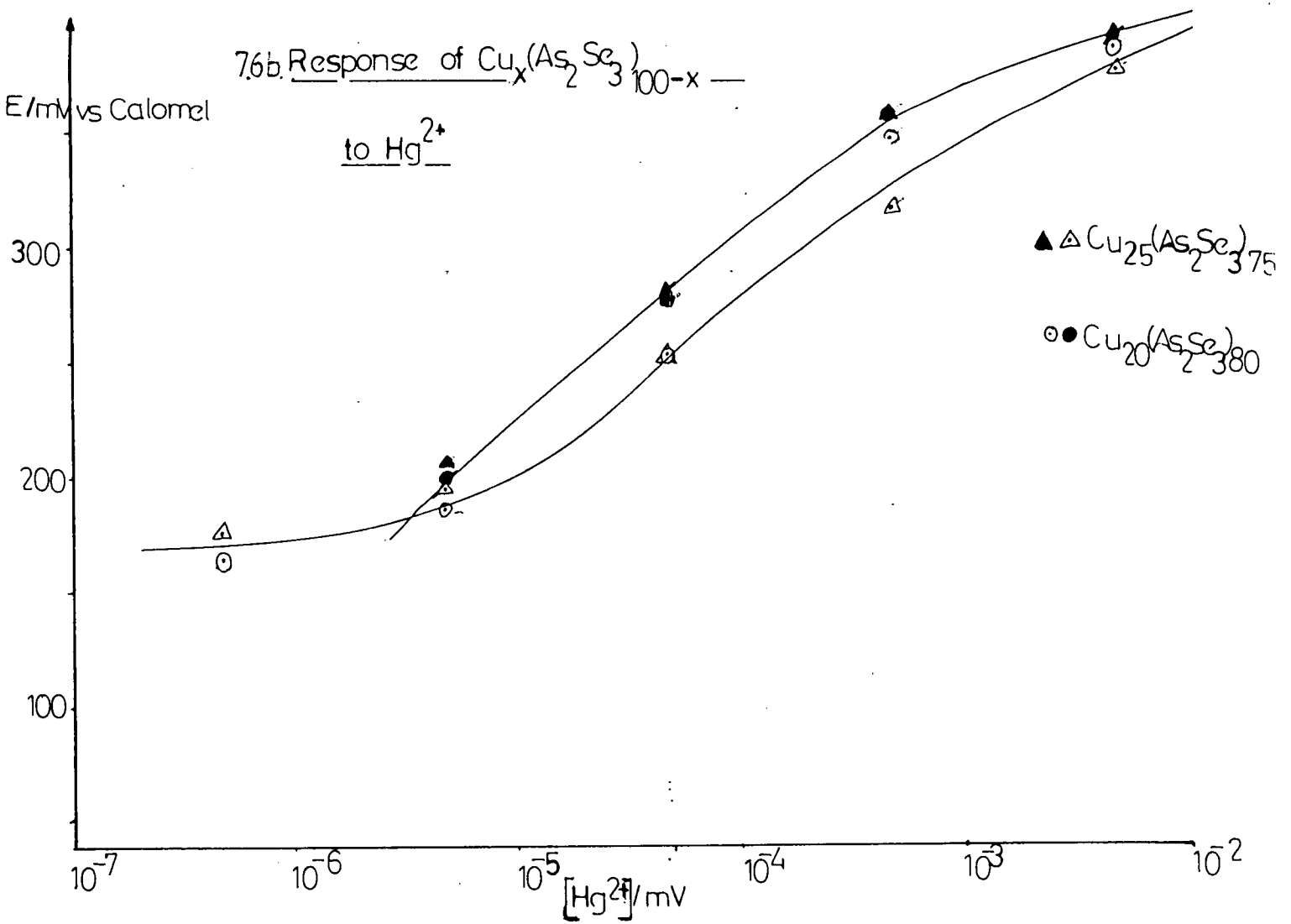
7.6b. Response of $Cu_x(As_2Se_3)_{100-x}$ — to Hg^{2+}
E/mV vs Calomel
300
200
100
10^{-7}
10^{-6}
10^{-5}
10^{-4}
10^{-3}
10^{-2}
$[Hg^{2+}]$/mV
▲△ $Cu_{25}(As_2Se_3)_{75}$
⊙● $Cu_{20}(As_2Se_3)_{80}$

7.7 Time dependence of Electrode Potential after exposure to $Ag^{\oplus}$

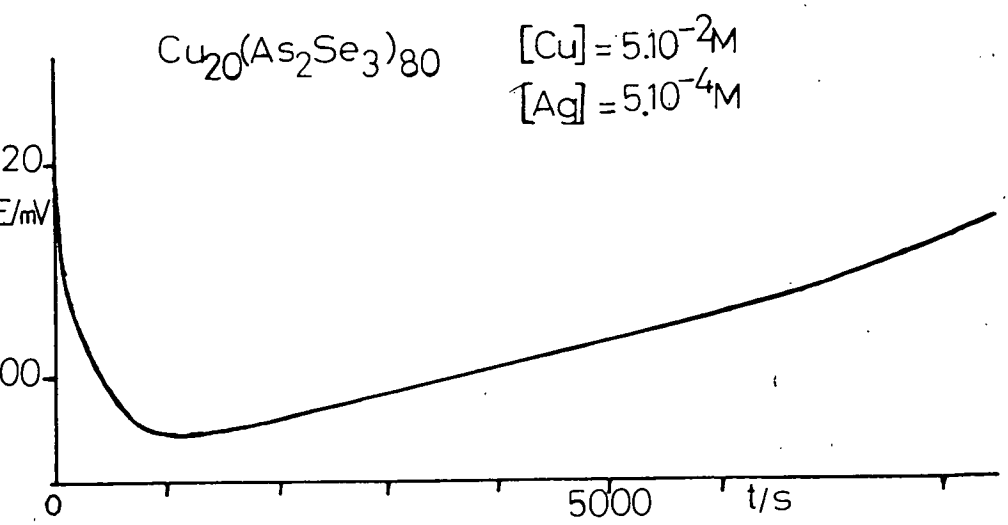

7.8 Response of Ag_2S Electrode to Ag^{2+} Ion

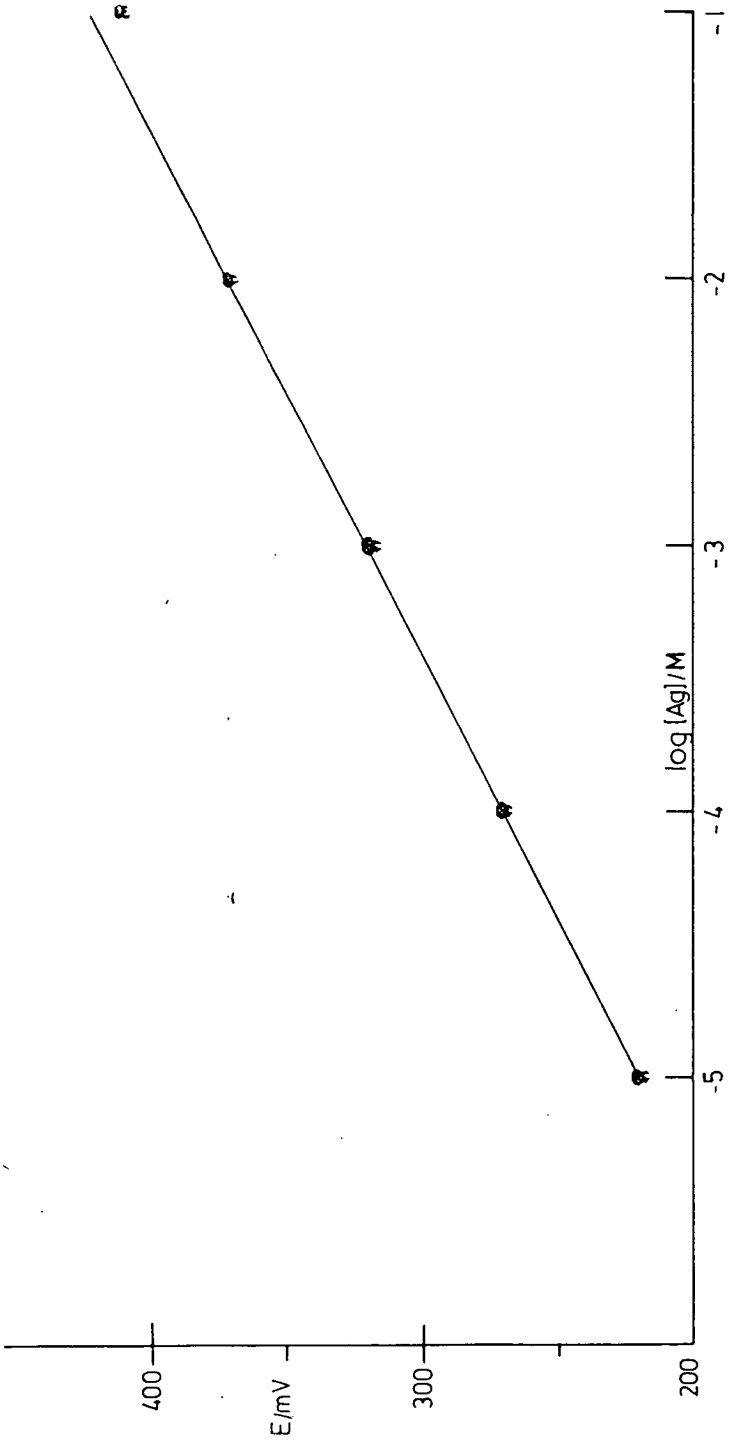

. Values of E^{O} for silver are very high (c.a. 500mV). As a omparison a gold backed, polycrystalline silver sulphide sensor was repared in the same way as the copper sensors. The response to ilver ion is shown in figure 7.8, it is clear that the E^{O} values of he copper electrodes in silver ion solutions are similar to those of he Ag_2S.

In Hg^{2+} solutions, electrodes could still distinguish between ifferent copper levels even at high mercury levels (10^{-2}M). The lectrodes recovered much more quickly from exposure to mercury than as the case for silver (c.a. 2 hours compared to 24 hours for silver). lectrode potentials were not shifted to the high positive values found or Ag^{+} interference. No detailed investigation was carried out for ercury, but the silver ion interference was broadly similar to that escribed above. Ferric nitrate was found to interfere strongly with lectrodes of composition Cu_{20} $(As_2\ Se_3)_{80}$. The solutions were observed o darken over a period of a few hours and it seems likely that the erric nitrate was hydrolysed [1] i.e. $Fe(NO_3)_3(aq) + 3H_2O(1) = Fe(OH)_3(S) + 3HNO_3(aq)$. Thus the effect on the copper sensor is complicated. erric chloride solutions are stable and interference studies were carried ut with the results shown in figure 7.9. The electrode potential enerally required 20 minutes to reach a stable value when either the Fe^{3+} or Cu^{2+} concentration was reduced.

7.9 $Cu_{25}(As_2Se_3)_{75}$ in $CuCl_2/FeCl_3$ solution

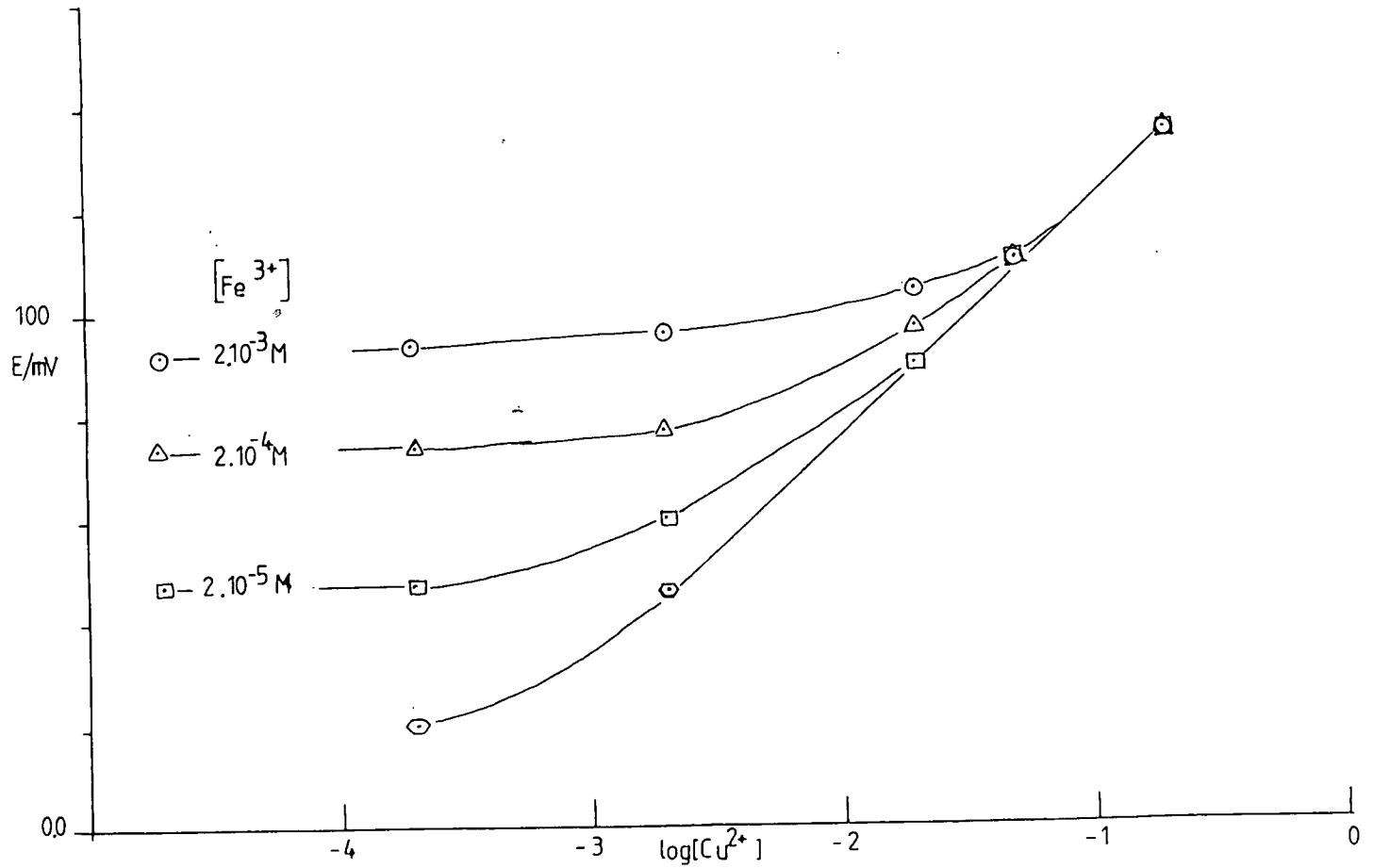

7.4 Chrono-Potentiograms

Typical examples of chrono-potentiograms are shown in figure 7.10, 7.11, 7.12 and 7.13. It will be noticed that the only instances of a chrono-potentiogram showing the behaviour described in chapter 2, i.e. an initial rapid change in electrode potential followed by a period of almost constant potential which is terminated by another rapid change of potential, are for the composite materials c-Cu As_2 Se_2 and c-Cu_{56} $(As_2$ $Se_3)_{44}$. Even then, this behaviour is only found for negative - cathodic - currents.

Chrono-potentiograms recorded at a sputtered film Cu_{20} $(As_2$ $Se_3)_{80}$ electrode are shown in figure 7.10 a and 7.10 b. The chrono-potentiograms are virtually unaffected by the presence of copper (ii) ion in solution, any differences between the two sets of curves are of the same order as differences found between different runs in the same solution.

In figure 7.11 a and b chrono-potentiograms recorded at a conventional Cu As_2 Se_2 electrode are shown. The inflexions in the cathodic waves are clearly visible, although the chrono-potentiograms do not show the form predicted by the Sand equation. This is almost certainly because the Sand equation was derived for a redox couple which rapidly exchanges electrons and for which both halves of the couple remain in solution. The c-Cu_{56} $(As_2$ $Se_3)_{44}$ elecrode, the chrono-potentiograms of which are shown in figure 7.12 a, behaves in a similar manner to the Cu As_2 Se_2 electrode except that the changes in potential for a particular current are smaller, this probably results from the lower resistivity of the Cu_{56} $(As_2$ $Se_3)_{44}$ material used. The Cu_{56} $(As_2$ $Se_3)_{44}$ electrode also shows considerably smaller changes in potential for anodic currents than for cathodic currents of the same magnitude. If the counter-ion is changed from nitrate to chloride the form of the chrono-potentiogram for cathodic currents is effected quite drastically. This is shown in figure 7.12 b and it is clear that the inflexions are no longer present and the potential varies almost linearly with time. The anodic currents are not affected.

7.10 CHRONO-POTENTIOMETRY of $Cu_{20}(As_2Se_3)_{80}$ ELECTRODE

a) a-$Cu_{20}(As_2Se_3)_{80}$

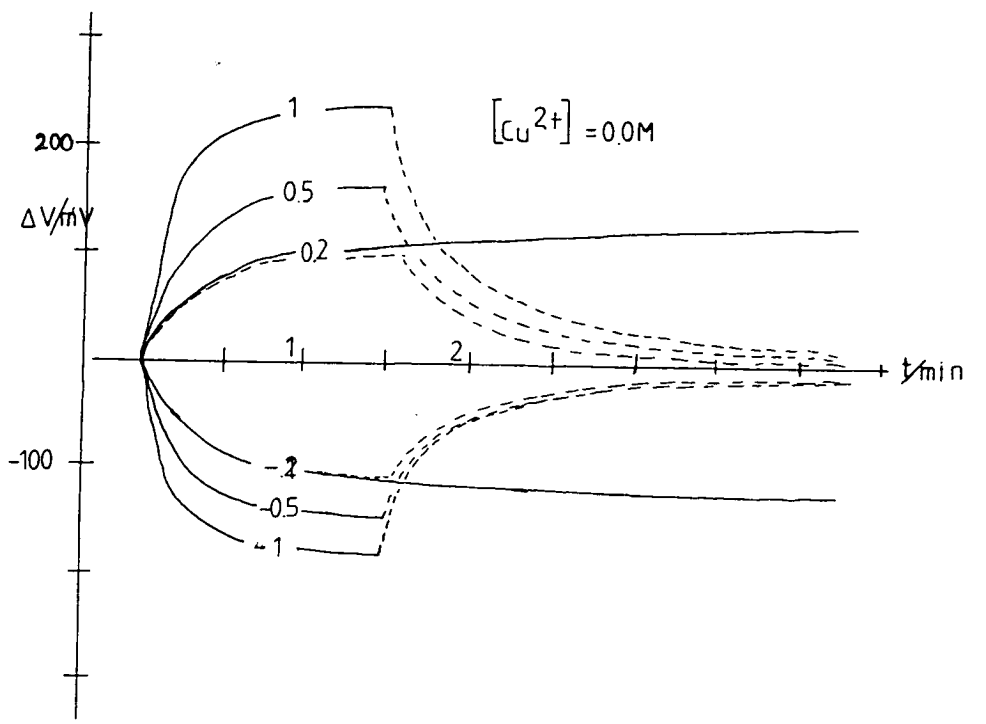

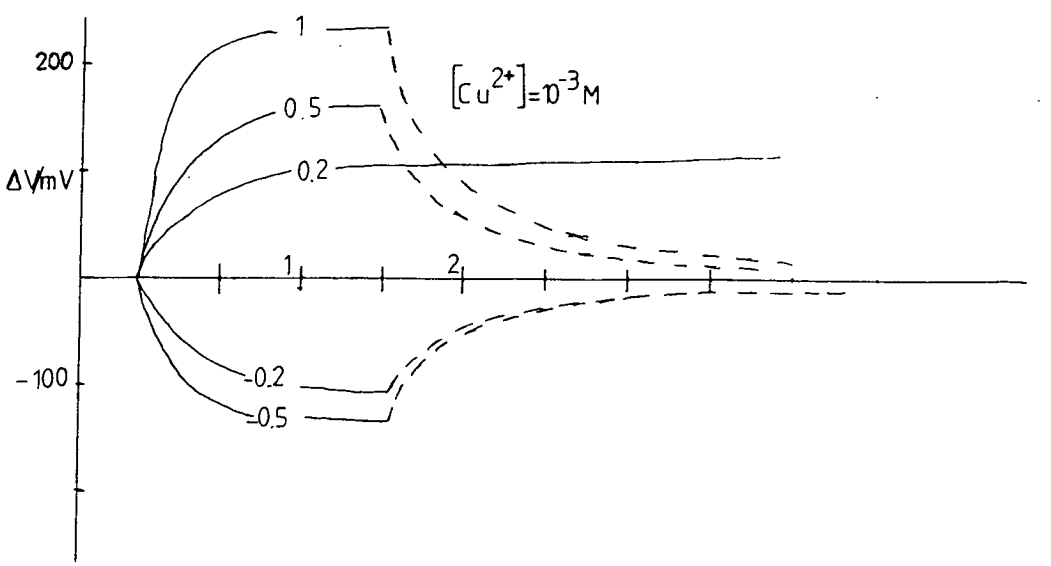

7.11 CHRONO-POTENTIOMETRY of $CuAsSe_2$ ELECTRODE

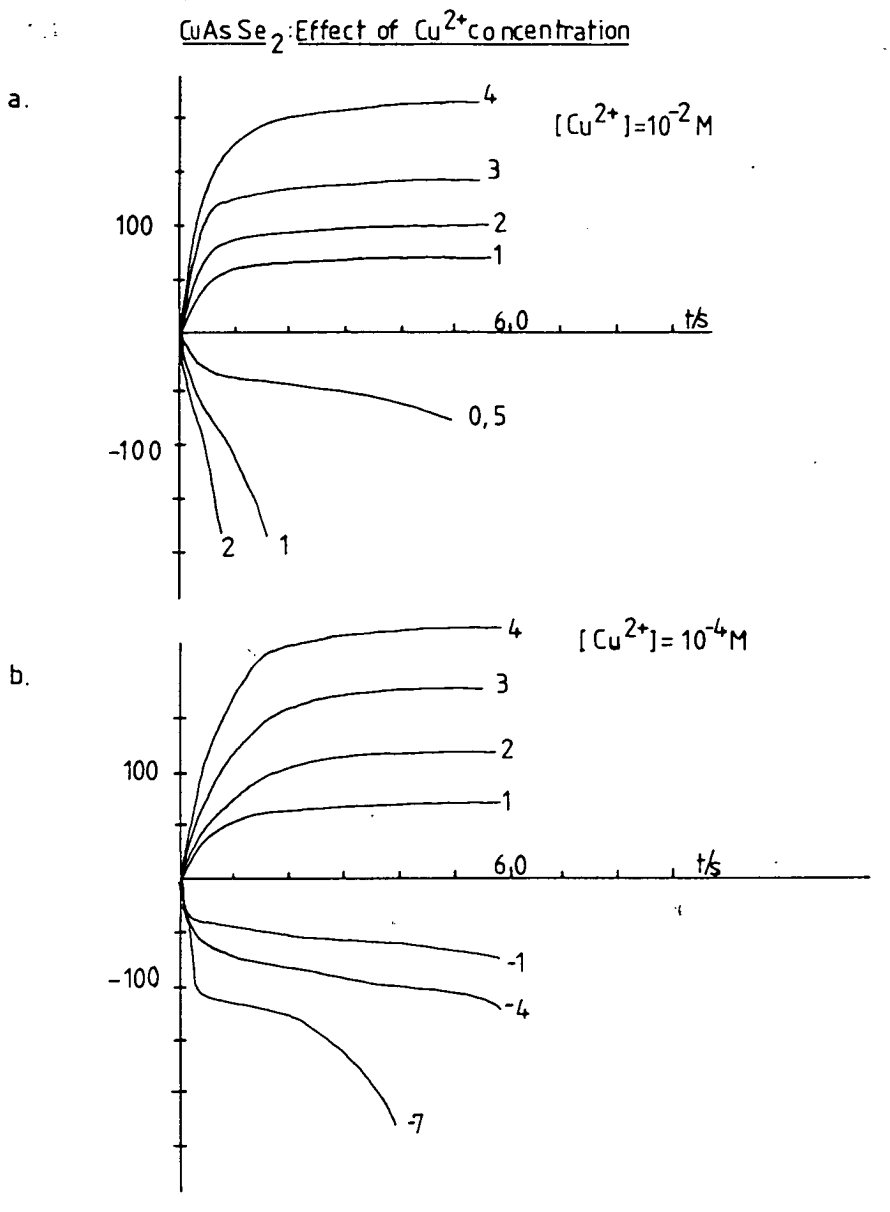

7,12 EFFECT OF ANION ON CHRONOPOTENTIOGRAM

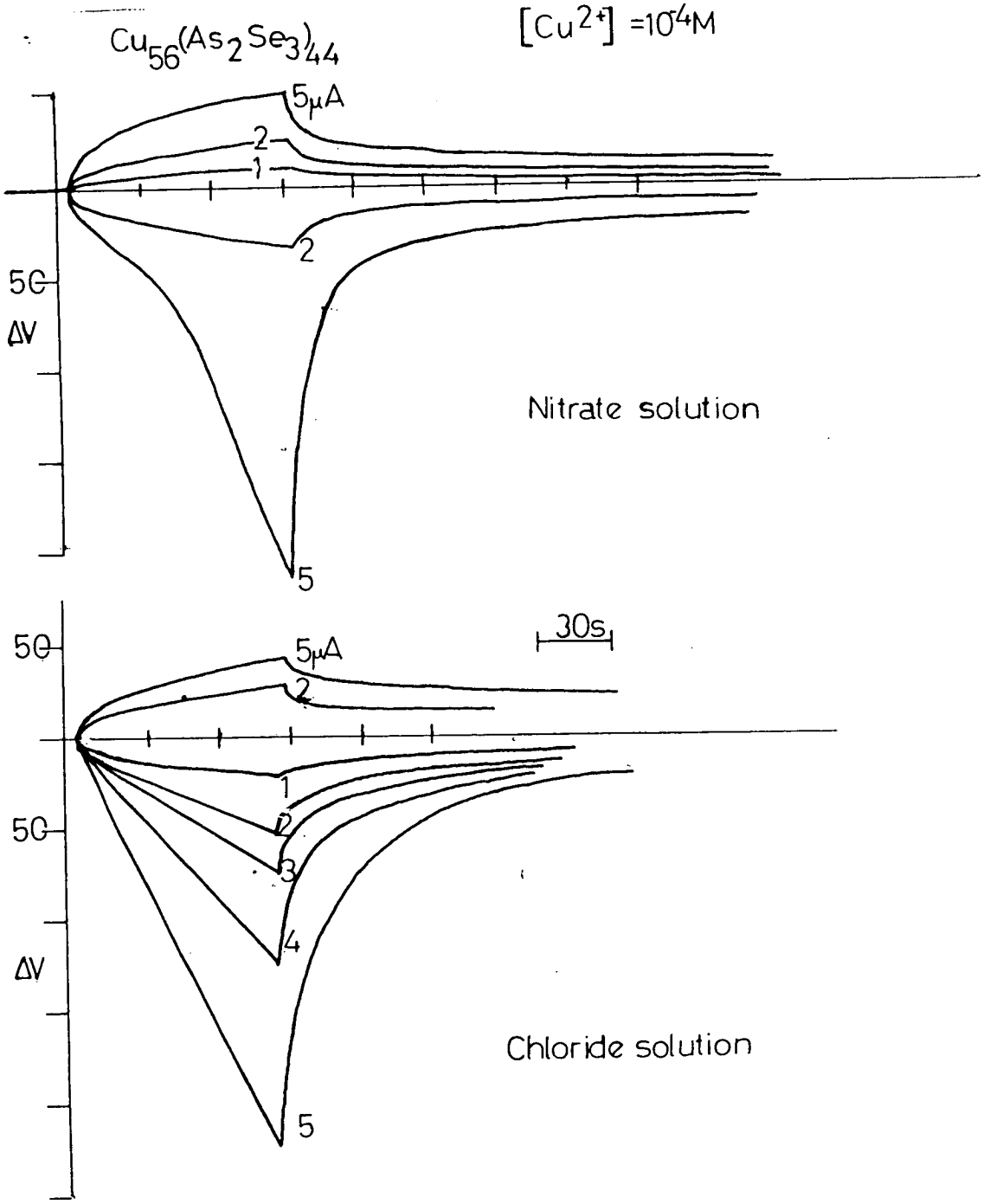

7,13 CHRONOPOTENTIOGRAMS RECORDED AT THE

$Cu_{20}(As_2Se_{1.5}Te_{1.5})_{80}$ ELECTRODE

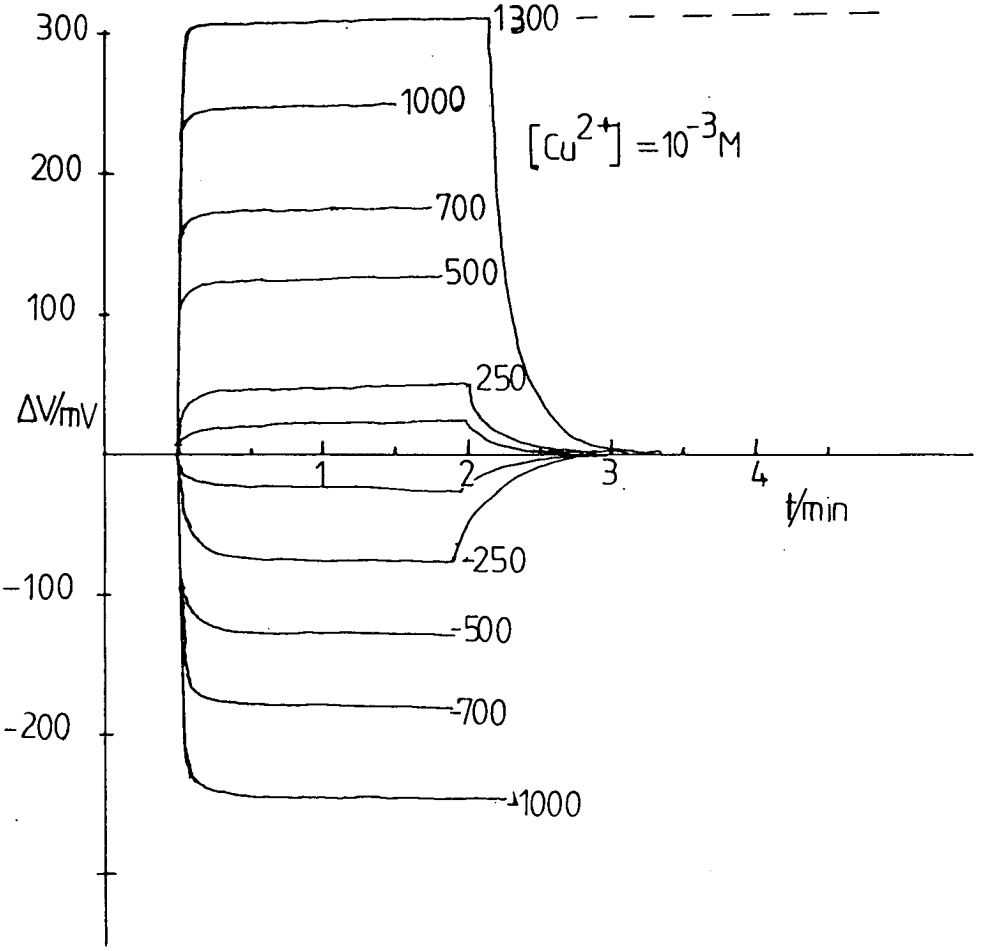

Chrono-potentiograms recorded at the Cu_{20} $(As_2\ Se_{1.5}\ Te_{1.5})_{80}$ electrodes are shown in figure 7.13. A conventional electrode was used so the resistance of the electrode is high ($\sim$100 kΩ) and consequently much of the potential change observed is due to the ohmic drop through the electrode. After the initial potential change due to the ohmic drop the potential behaved in a similar manner to the a-C_{20} $(As_2\ Se_3)_{80}$ electrode.

7.5 Cyclic Voltammetry in Copper Solutions

Cyclic voltammograms recorded at Pt, c-Cu As Se_2, c-Cu_{20} $(As_2\ Se_3)_{80}$ and a-Cu_{20} $(As_2\ Se_3)_{80}$ electrodes are shown in figure 7.16 and 7.15 for copper ion concentrations of 0.0M(base electrolyte) and 10^{-4}M respectively. The reduction in the current scale for the voltammogram recorded at the Pt electrode should be noted.

The copper containing electrodes show an increase in current as the applied potential rises above 0.6v (relative to Ag/AgCl; 0.82v relative to NHE). This is not observed for the Pt electrode and must therefore be due to the electrode materials rather than the electrolyte. In particular, it is likely to be caused by the oxidation of some surface species. The current gradient -(dI/dE) depends on the rate of potential change. It is interesting that the small reduction wave at 0.0v disappears with stirring for the Cu As Se_2 electrode but not for the a-Cu_{20} $(As_2\ Se_3)_{80}$ electrode. This suggests that the reducible substance is not bound to the surface for Cu As Se_2 whereas for the glass it is. This result was reproduced with two different batches of glass in 4 out of 4 trials. The voltammograms are not affected by the presence of copper (ii) ion.

Figure 7.14 shows the same electrodes but with voltammograms recorded with a more negative range of potentials (-0.65v to +0.5v wrt Ag/AgCl). In this case the oxidation and reduction peaks at +0.05v and -0.05v respectively increase when copper (ii) ion is present. The oxidation and reduction peaks are separated by 0.1v which is considerably higher than the 14mV predicted for 2-electron reactions that are diffusion limited. The effect of varying potential sweep rate is shown in figure 7.17 where peak currents are plotted against sweep rate for each of the electrodes.

7,14 Cyclic Voltammetry of $Cu(NO_3)_2$ Solutions

$[Cu^{2+}] = 0.0$ M

a/

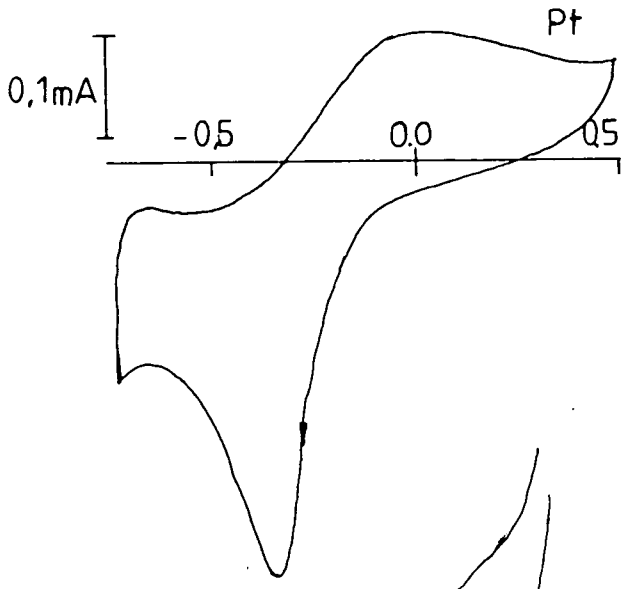

b/

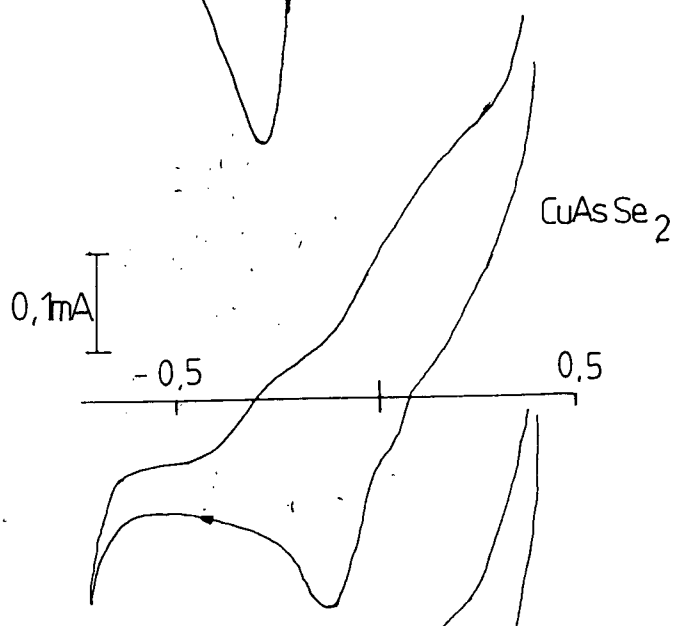

c/

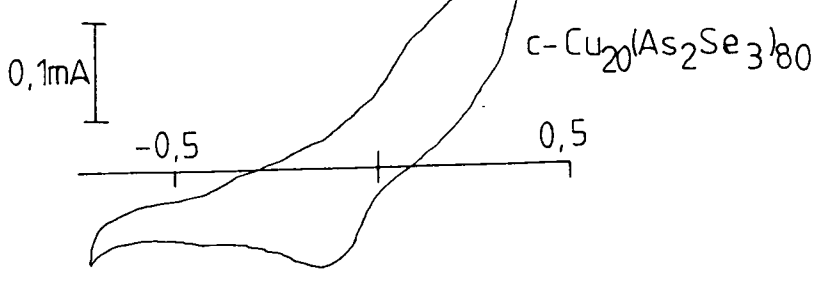

d/

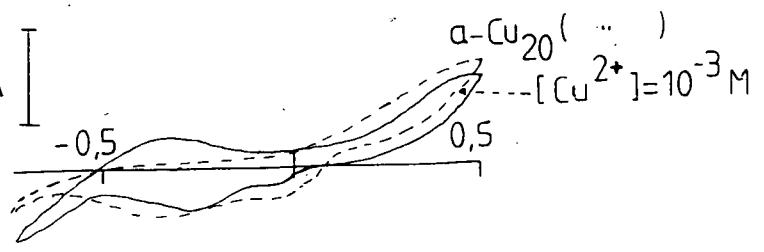

7.15 Cyclic Voltammetry of $Cu(NO_3)_2$ solutions: 10^{-4}M Cu^{2+} ion solution

a/.

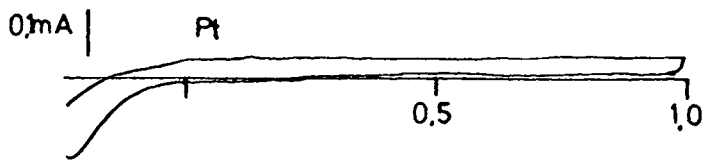

——— unstirred

------ stirred

b/.

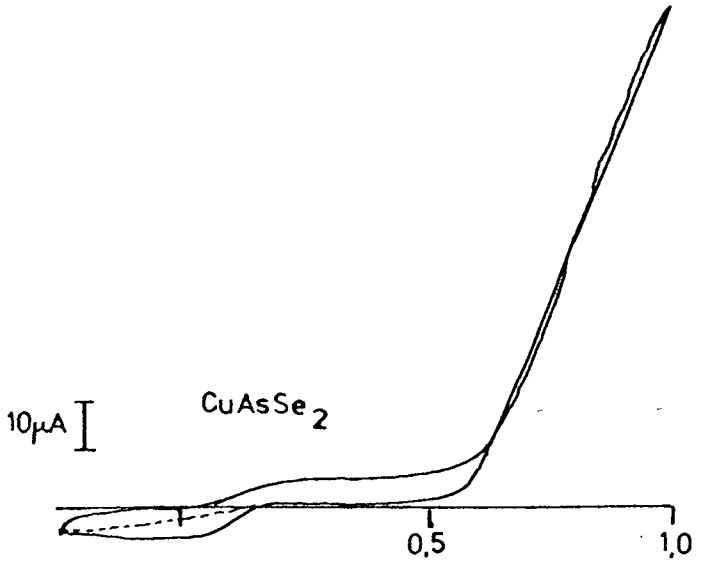

c/.

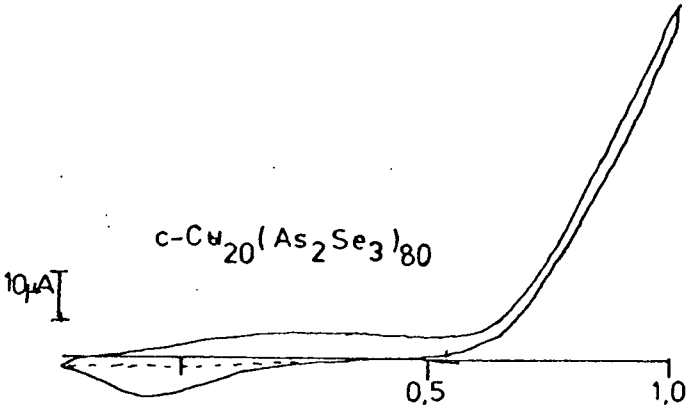

d/.

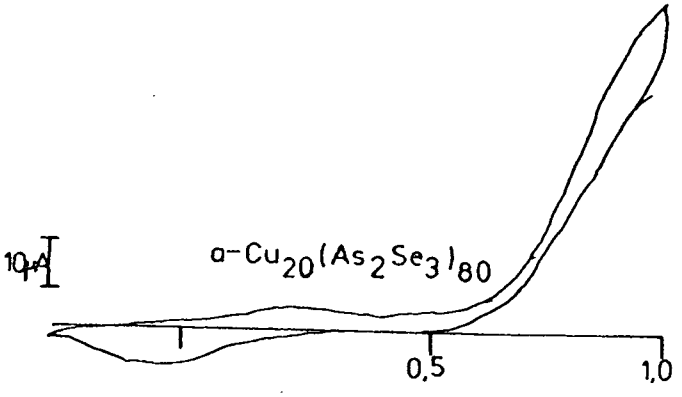

7.16 Cyclic Voltammetry of $Cu(NO_3)_2$ Solutions : base electrolyte

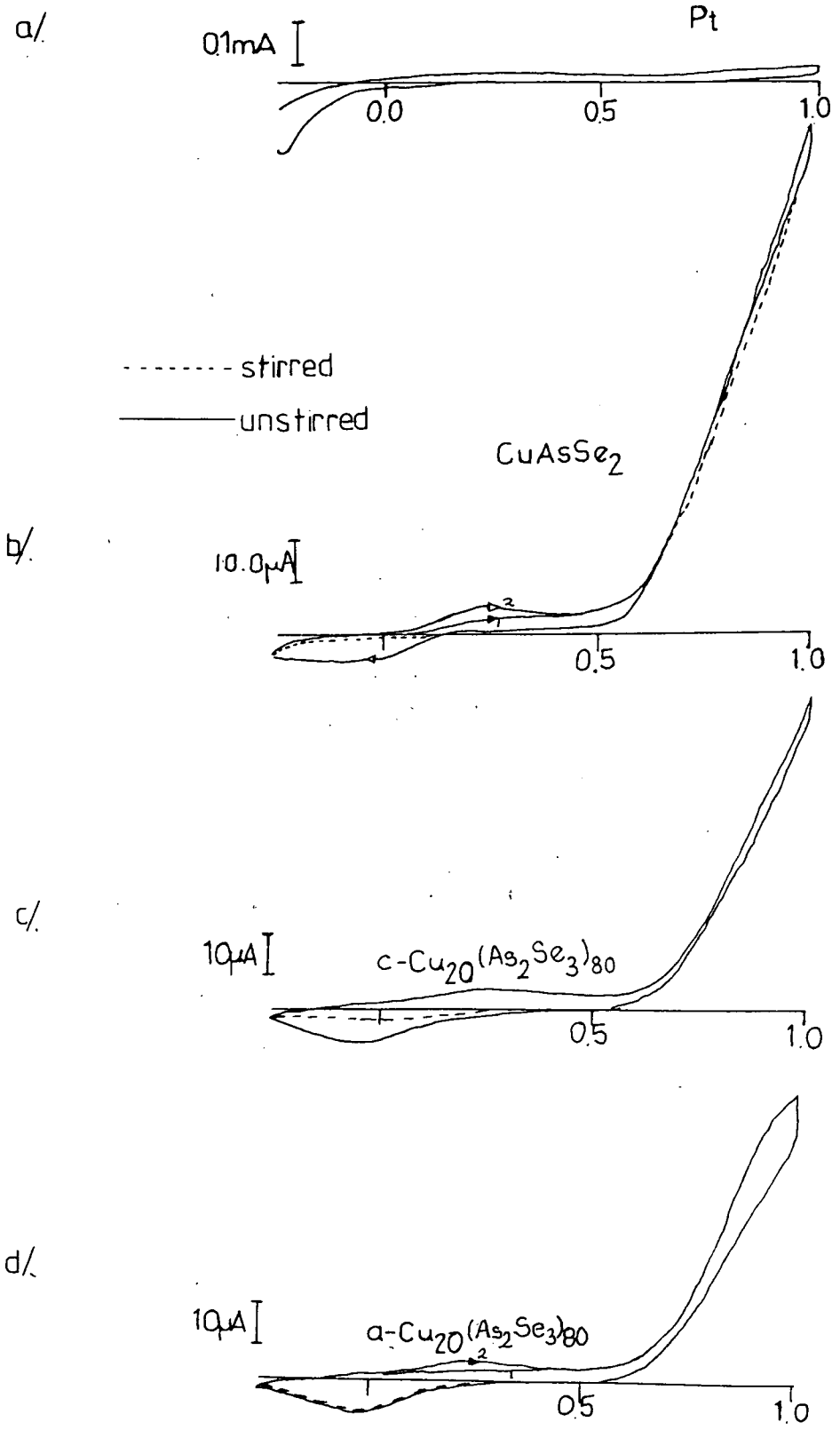

7,17 EFFECT OF SWEEP RATE(v) ON PEAK CURRENT AT -0,1V

a. $CuAsSe_2$

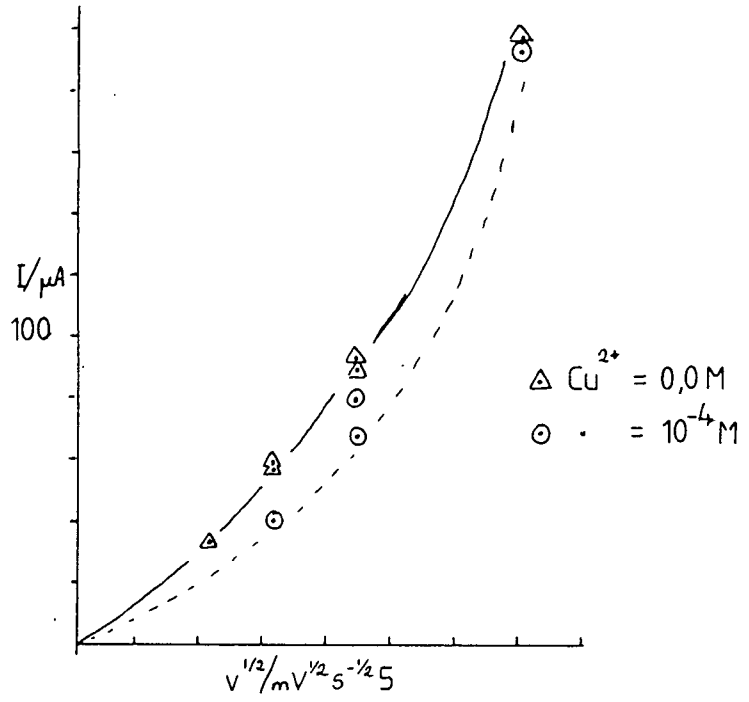

b $a-Cu_{20}(As_2Se_3)_{80}$

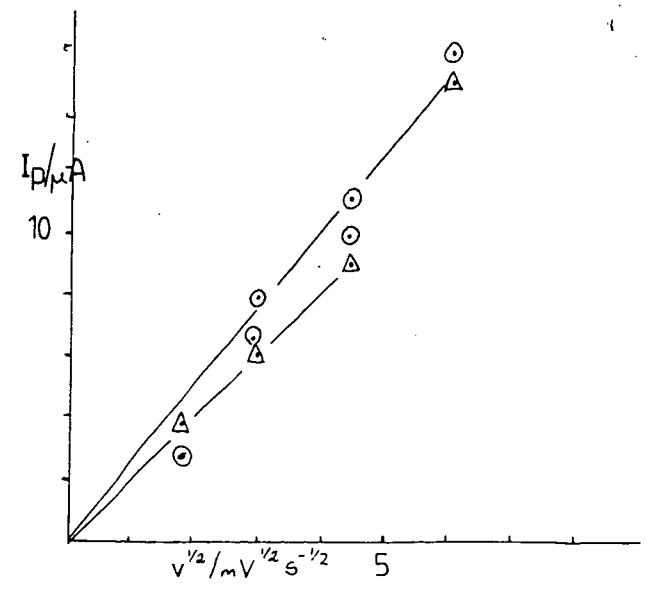

7.6 Cyclic Voltammetry in the presence of Redox couples

Of the three couples tested; ferrocyanide, benzoquinone and TPMD, only the latter two gave directly useful results. In the presence of the ferricyanide/ferrocyanide couple, copper metal was found to plate irreversibly onto the electrode surfaces. This is probably due to the reduction of a soluble copper species by ferrocyanide ion.

$$2[Fe^{III}(CN)_6]^{3-} + Cu^{2+} \leftrightharpoons 2\ [Fe^{II}\ (CN)_6]^{4-} + Cu(S)$$

The soluble copper species itself must derive from the electrode surface since care was taken to exclude copper ion from the solutions prior to the experiments. The voltammograms produced with the other couples are considered separately.

7.6.1 Benzoquinone

Benzo-quinone produces an oxidation and a reduction wave at the platinum electrode, the current peaks are separated by 0.06v which is the separation predicted for a reversible 1 electron process (chapter 2). The measured half wave potential -0.2v allows the potentials to be converted to the NHE scale.

The voltammograms obtained at the chalcogenide electrodes and the platinum electrode are shown in figure 7.18. For Cu As Se_2 the cyclic voltammogram is not substantially different to that obtained in the base electrolyte. Close inspection reveals the presence of broad oxidation and reduction peaks at the same potentials as those found at the Pt electrode. This broadening may be due either to the oxidation and reduction reactions being slower at the Cu As Se_2 electrode or simply to the fact that it is impossible to separate them from the electrode reactions in the base electrolyte.

The composite c-Cu_{20} $(As_2\ Se_3)_{80}$ electrode shows the oxidation and reduction waves quite clearly although the peaks are considerably broadened. The amorphous Cu_{20} $(As_2\ Se_3)_{80}$ electrode however shows only the oxidation wave. There is no corresponding reduction wave, the current actually becomes less negative at the potential where the reduction wave is expected. This implies that the energy levels of the reduced form of the couple overlap with filled states of the semiconductor but that energy levels of the oxidised form do not.

7.18 CYCLIC VOLTAMMETRY IN BENZOQUINONE SOLUTIONS
[Cu_{20}-" =$Cu_{20}(As_2Se_3)_{80}$]

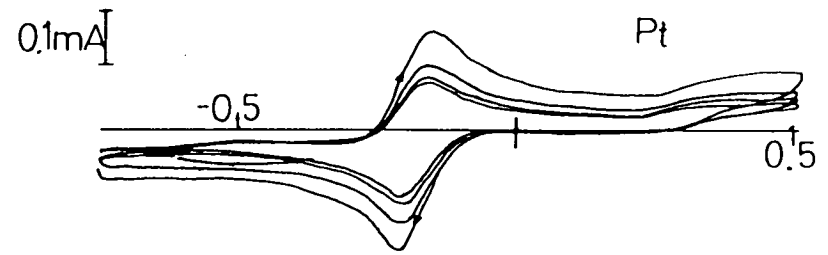

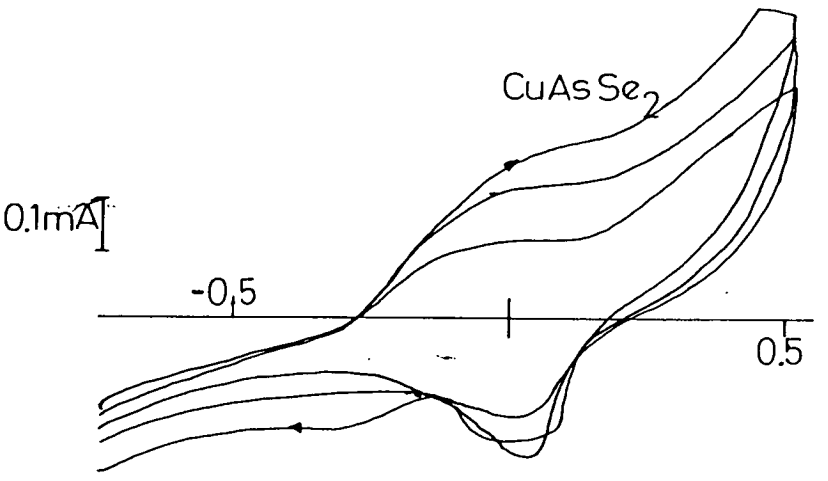

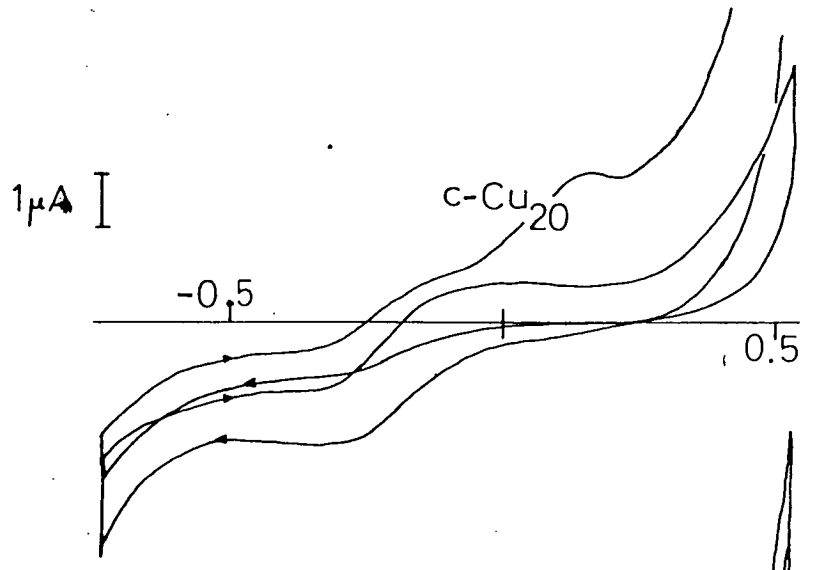

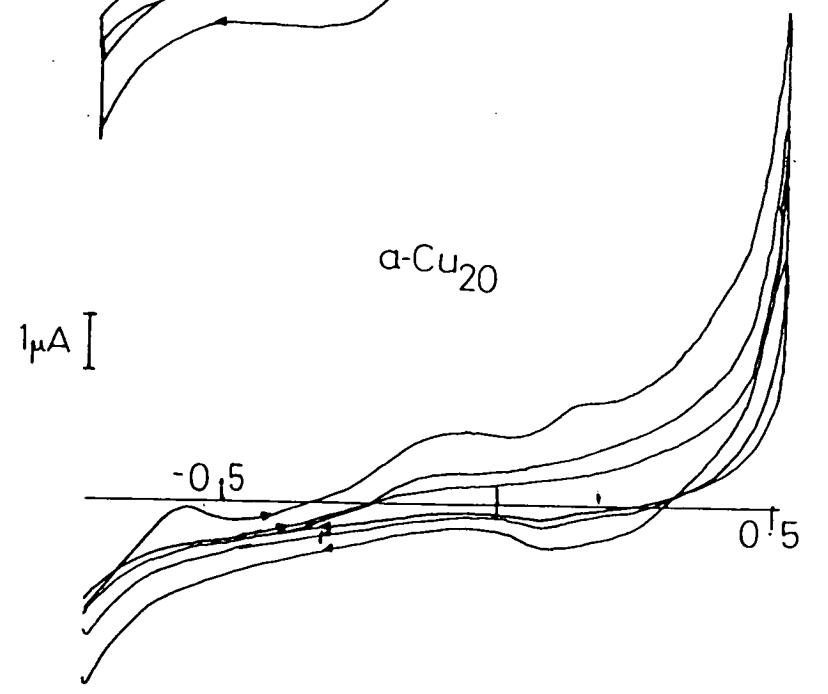

7.6.2 TPMD

The corresponding voltammograms for TPMD (NNNN' Tetra methyl p-phenylene diamme dihydrochloride) are shown in figure 7.19. Four oxidation and four reduction peaks are clearly visible, for simplicity in comparing voltammograms from different electrodes these have been labeled A,B,C and D. The measured half wave potentials for each set of peaks are summarized below.

Peak	$E_{\frac{1}{2}}$ (vs. Ag/AgCl)	
A	-0.6	-0.38
B	-0.5	-0.28
C	+0.15	0.37
D	+0.45	0.67

At the c-$CuAsSe_2$ electrode all these processes can be identified although those corresponding to the more positive potentials - C and D - are obscured by background reactions. For both Cu_{20} $(As_2\ Se_3)_{80}$ electrodes the two most positive processes - C and D - show both oxidation and reduction peaks. For process A on the other hand only the oxidation wave is clearly visible, the reduction wave is possibly present at the crystalline electrode but is not present at the corresponding glassy electrode. In the case of process B neither oxidation nor reduction waves are present for either composite or amorphous electrodes. As discussed in chapter 2, these simple qualitative observations can yield a lot of information on the surface band structure of these electrodes.

7.7 Photo-electrochemical studies

Before detailing the specific results the following general observations can be made.

1. The only electrodes showing permanent photo-effects were the amorphous a-$Cu/As_2\ Se_3$ electrodes.

2. The composite materials occasionally showed photo-effects, but they were never permanent and the change in potential on illumination took several minutes to reach a steady value.

3. The $Cu/As_2\ Se_{1.5}\ Te_{1.5}$ electrodes never showed photo-effects.

7.19 CYCLIC VOLTAMMETRY IN TMPD SOLUTIONS

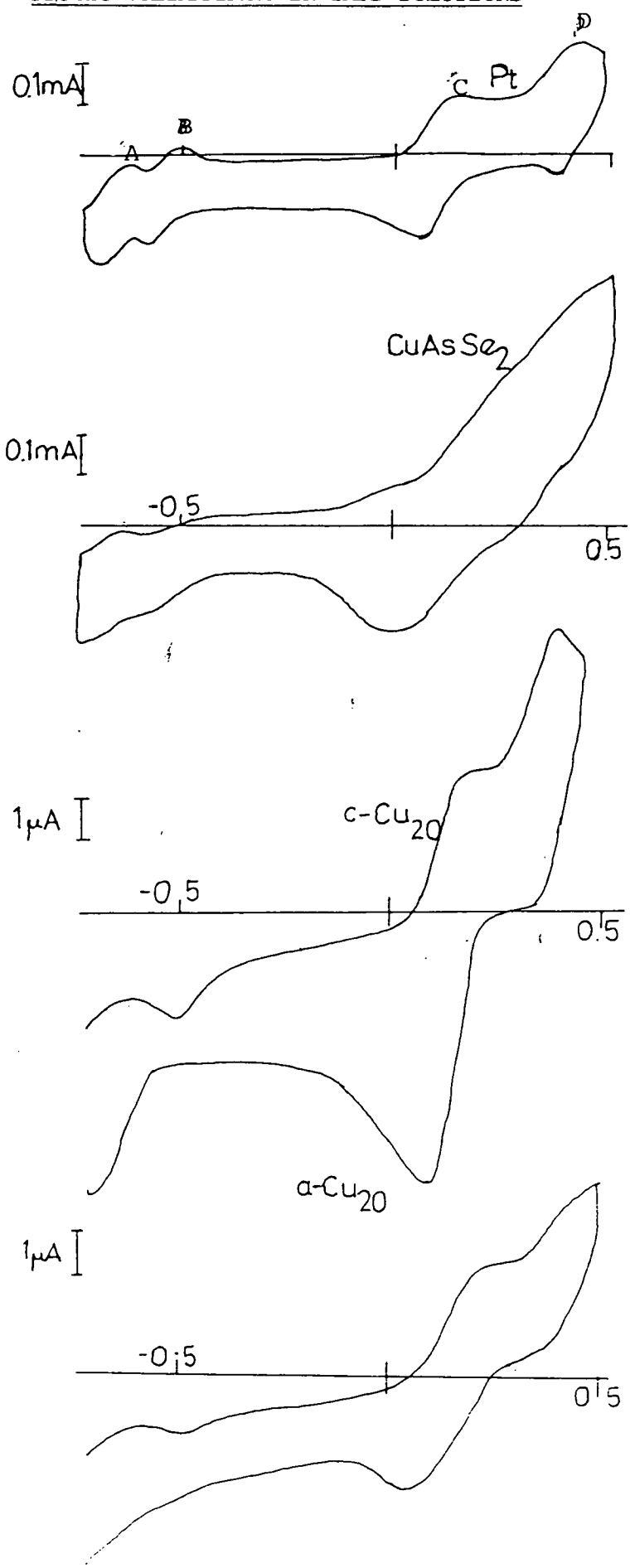

7.19 cont.

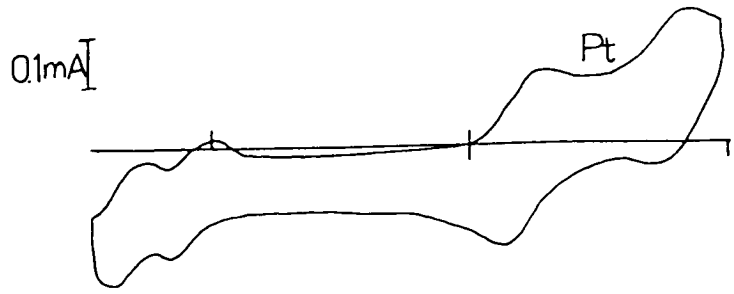

e/ sputtered film- $CuAs_2Se_{1.5}Te_{1.5}$

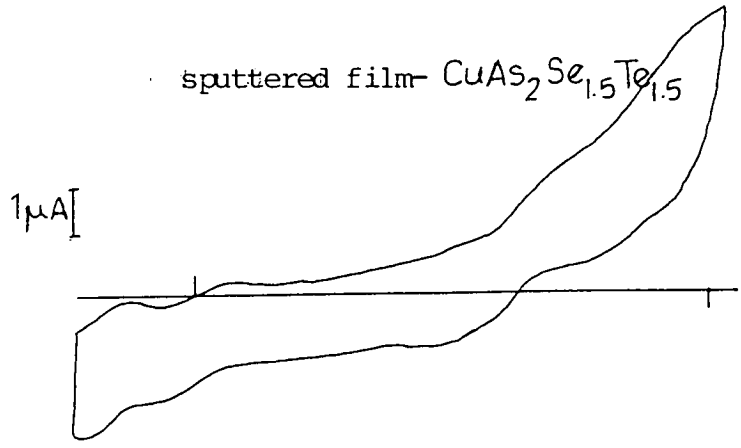

4. Illumination had no measurable effect on the voltammograms.

The change in potential when the a-Cu_{20} $(As_2\ Se_3)_{80}$ electrode was illuminated is shown in figure 7.20. The change produced by three different wave lengths of the same intensity (10^{-6} Wcm^{-2}) is shown, the copper ion concentration is constant at $10^{-3}M$. The response to changes in illumination is very rapid, any delay visible is due to the slow response of the recorder (this was confirmed by applying a step change in voltage to the recorder input). By contrast the response of a composite electrode of the same composition is shown in figure 7.21. The electrode potential is still changing after 5 minutes. When the experiment was repeated two weeks later the photo-effect was undetectable for the composite material whereas the glassy electrode gave the same result as before.

The effect of the copper (ii) ion concentration on the photo-effect is shown in figure7.22, as the copper concentration increases the photo-effect for a particular frequency and intensity drops. This trend can not be due to the increased absorption of the solution as it is observed at frequencies where the solution does not absorb. Furthermore, the absorption by solutions of concentrations weaker than $10^{-3}M$ is too low to account for the observed changes. A crude photo-effect spectrum for the a-Cu_{20} $(As_2\ Se_3)_{80}$ electrode is shown in figure 7.23, the absorption spectrum of a $Cu\ (NO_3)_2$ solution is also shown. Note that at high Cu^{2+} concentrations ($10^{-1}M$) the absorption of the solution does affect (reduce) the photo-effect at the red end of the spectrum.

7.20 EFFECT OF ILLUMINATION ON ELECTRODE POTENTIAL

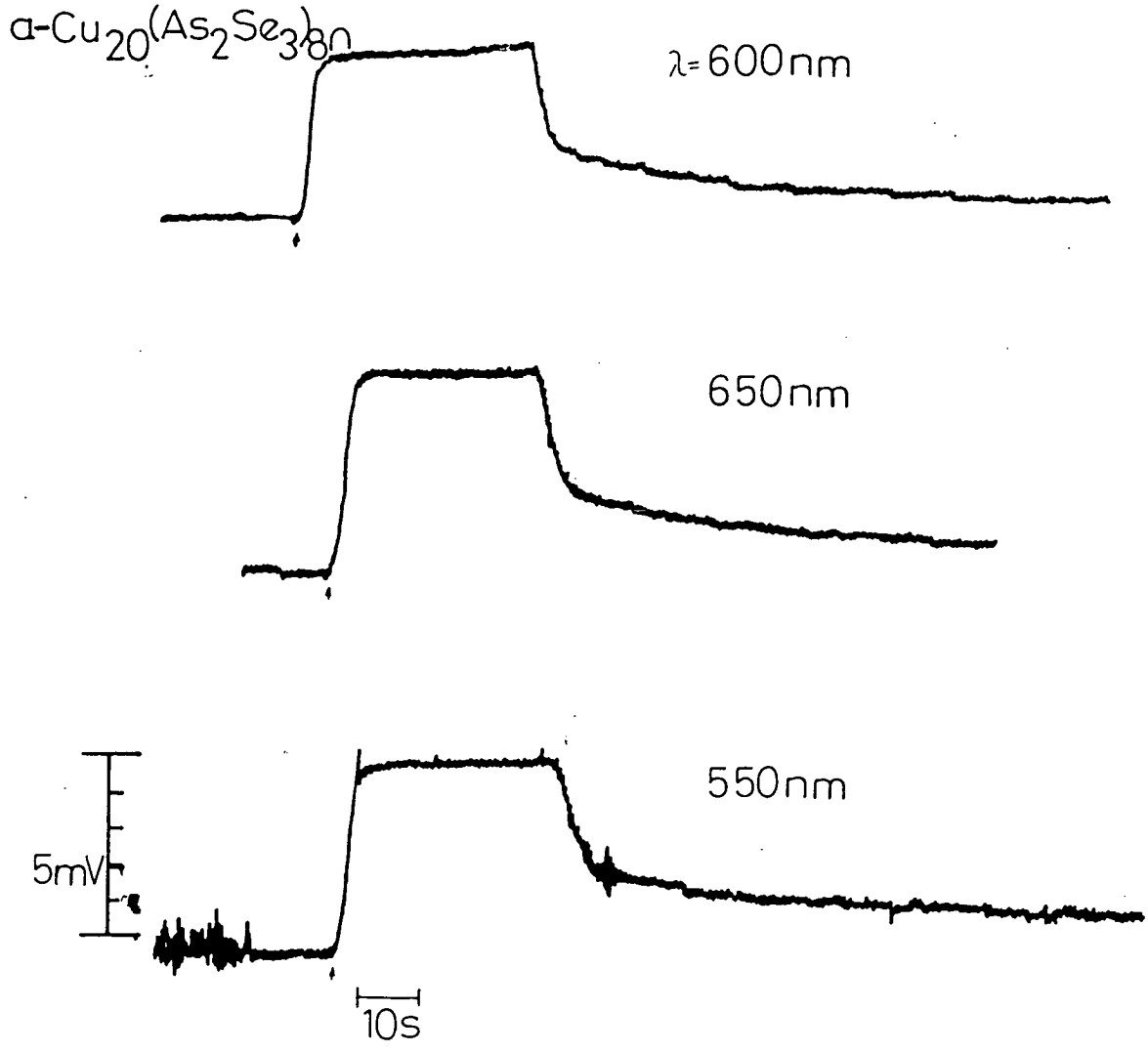

$[Cu^{2+}]=10^{-3}M$

$I = 10^{-6}Wcm^{-2}$

7.21 EFFECT OF ILLUMINATION, FROM RED L.E.D, ON ELECTRODE RESPONSE c- $Cu_{20}(As_2Se_3)_{80}$

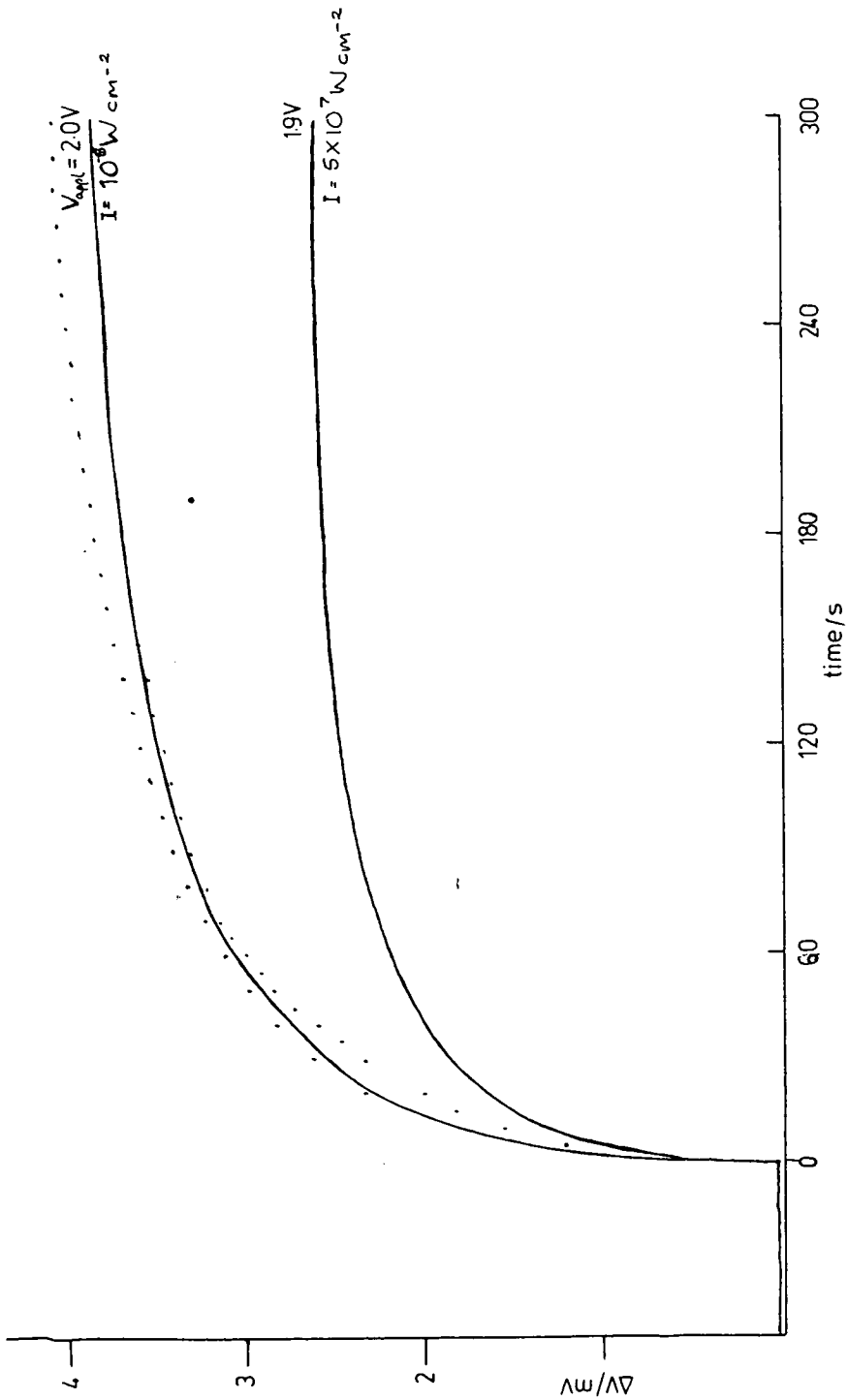

7.22 EFFCT OF COPPER CONCENTRATION ON ΔV

λ 563 nm

$a\text{-}Cu_{20}(As_2Se_3)_{80}$

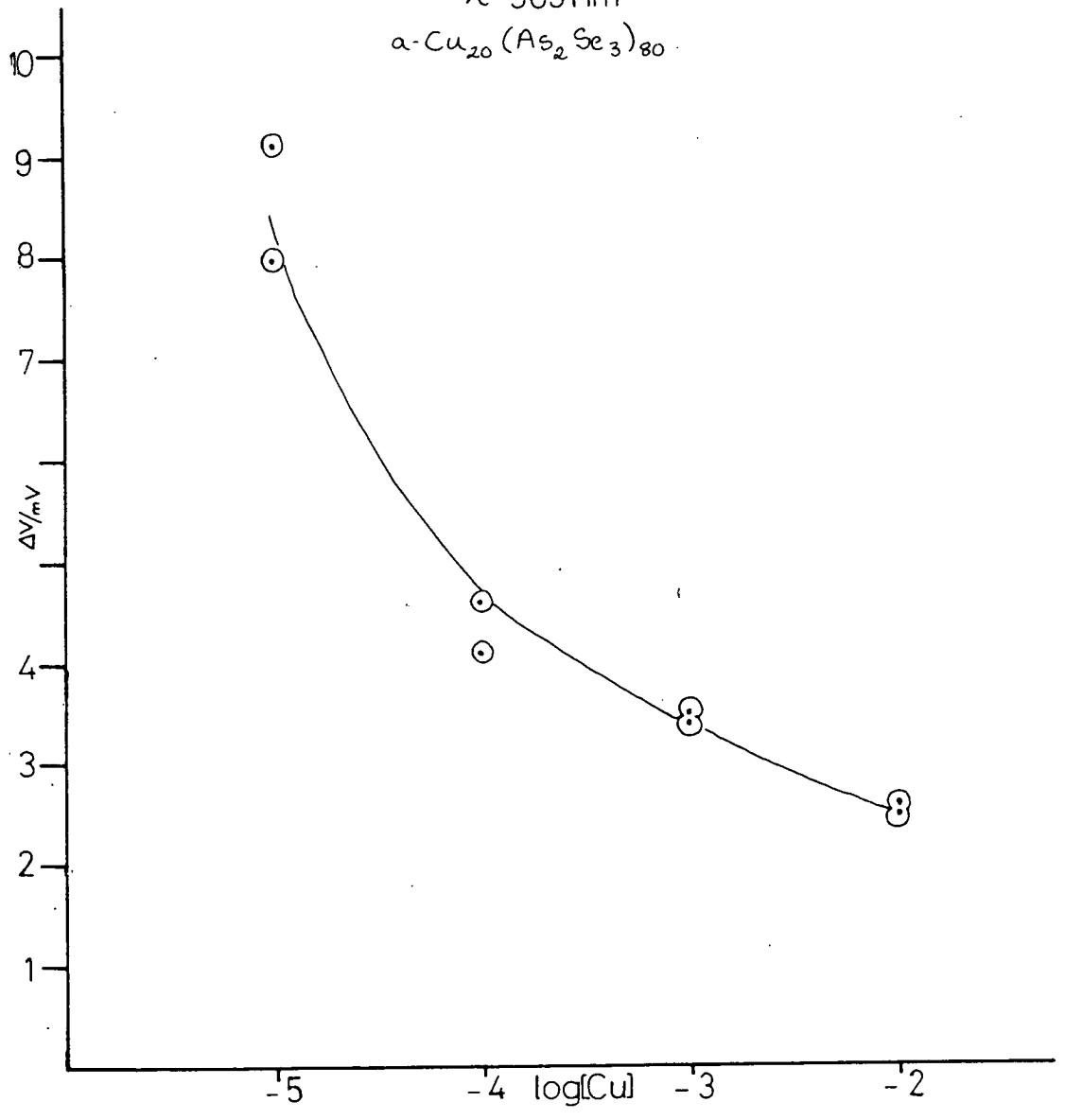

7.23 PHOTO EFFECT SPECTRUM

a-$Cu_{20}(As_2Se_3)_{80}$

3.6×10^{-6} W cm^{-2}

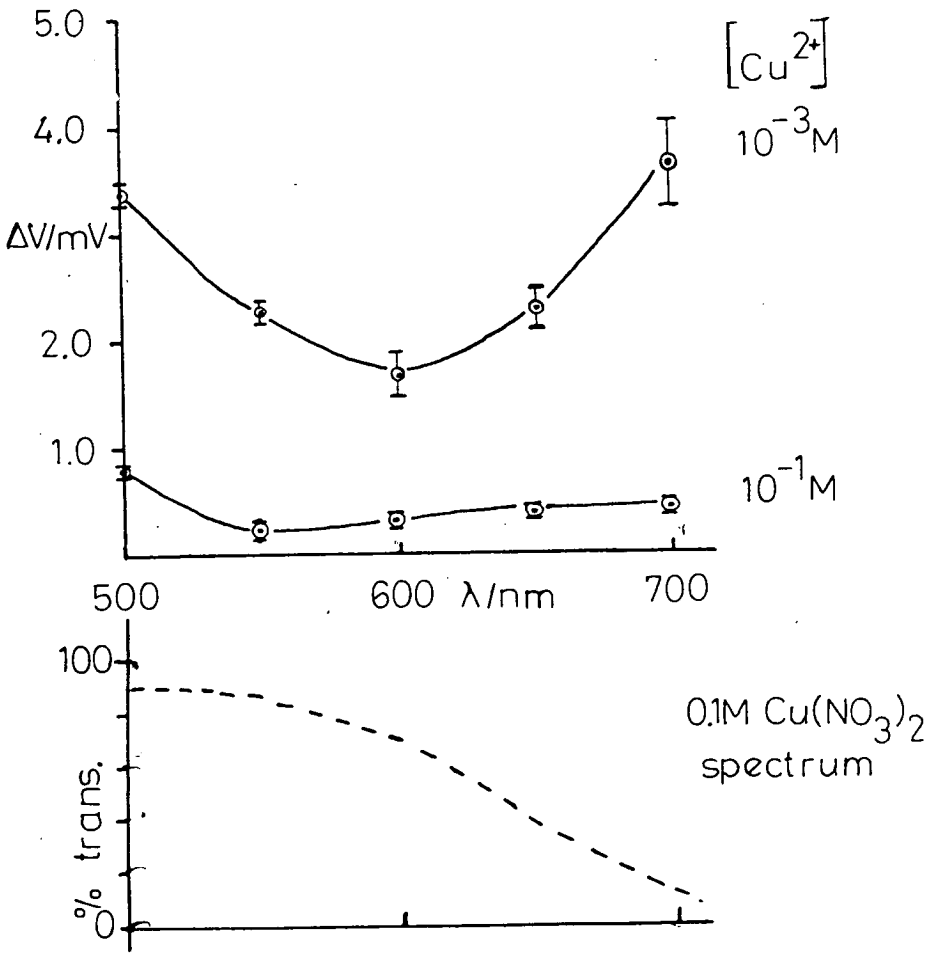

7,24 EFFECT OF INTENSITY ON ΔV

$\lambda = 563\,nm$ c - $Cu_{20}(As_2Se_3)_{80}$

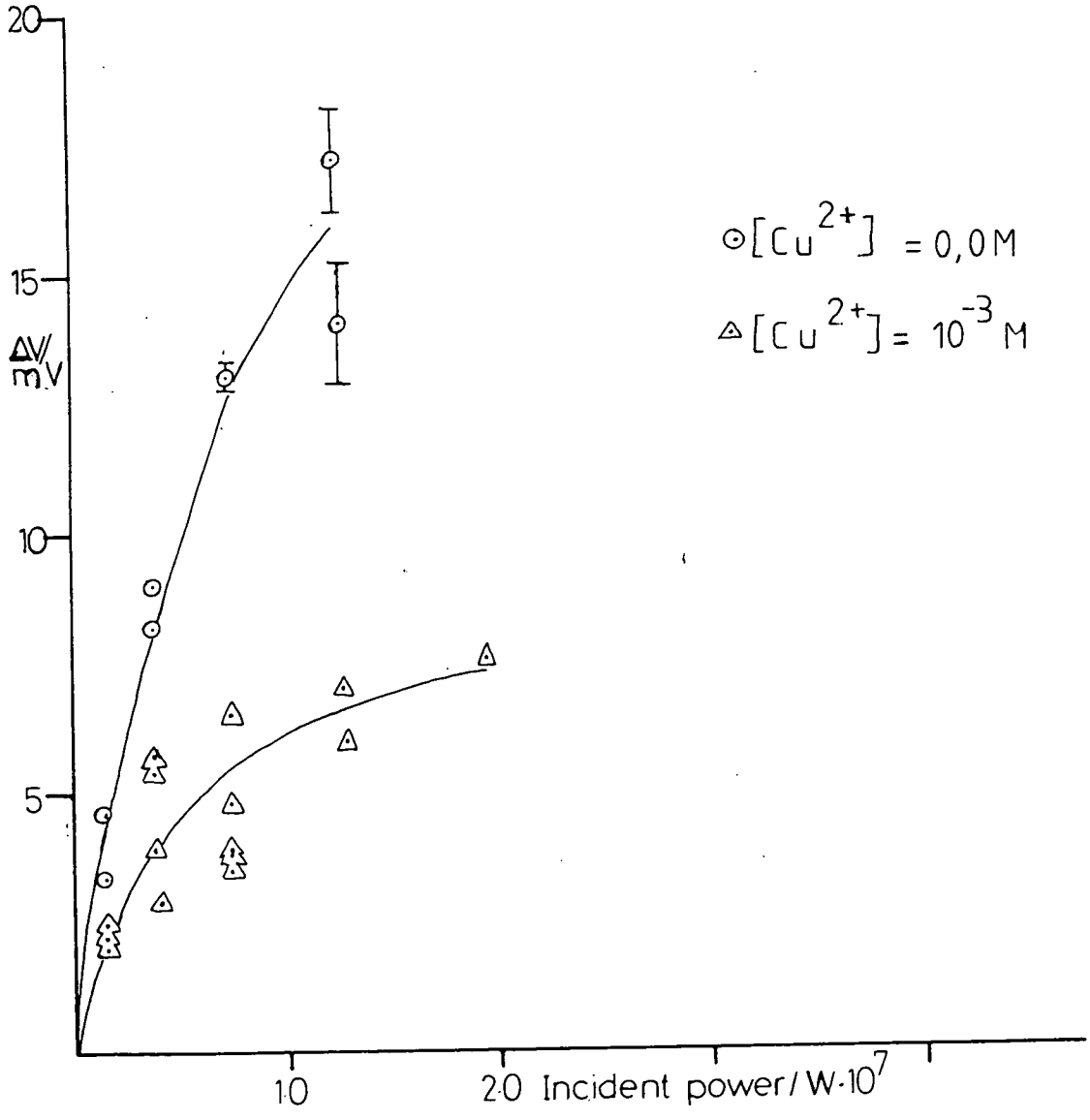

CHAPTER 8

CONCLUSIONS AND DISCUSSIONS

8.1 Introduction

The results will be discussed in the same order as they were presented. Reference will also be made to introductory sections except where relevant results of another worker were not mentioned in these chapters. Conclusions that arise from a number of different experiments will generally be given at the end of this chapter although their relevence may also be shown earlier.

8.2 Electrode Potentials in Copper (ii) Nitrate Solutions

Inspection of figure 7.1, 7.2 and 7.3 shows that a linear relationship normally exists between electrode potential and logarithm of concentration for concentrations between 10^{-5} M. and 10^{-2}. In some cases the response is linear up to 10^{-1} M. The slopes lie between 26.0 mv (decade)$^{-1}$ and the Nernstian value for a 2 electrode process of 29.1 mv (decade)$^{-1}$. None of the materials studied showed a slope greater than the Nernstian value. Since the electrodes included both amorphous and composite materials it is clear that the presence of a crystalline phase is not a necessary condition for a linear response. There seems no reason why the analogous sulphides studied by Jasinski et al. [1] should require the presence of crystalline material when the selenides do not.

From table 7.1 it can be seen that the electrodes which show Nernstian behaviour also show the smallest deviations from the expected electrode potential in 10^{-1} M Copper (ii) solutions. These deviations are always positive, i.e. the measured potential is more positive than expected. In the introductory chapters 2, 3 and 4, the possibility of deviations from Nernstian behaviour were discussed. For electronic conductors, it was noted that the electrode potential depends on the activity of the ion in solution and also on its activity in the surface region of the sensing material. To obtain a Nernstian response the latter must be constant. Thus in the cases of materials exhibiting sub-Nernstian responses it is possible to conclude that the copper activity in the surface region depends on the copper (ii) ion concentration in solution. According to Sato[2] the electrode potential is given by an expression of the form

$$E = E^* + \frac{RT}{zF} \log_e \frac{C_{M^{2+}}}{a^{s,sm}_m} \qquad (8.1.1)$$

where E^* is a constant, $a^{s,sm}_m$ is the activity of m at the surface of the sensing material and $C_m 2+$ is the concentration of M^{2+} in the solution. To obtain a sub-Nernstian response $a^{s,sm}$ must therefore increase with increasing M^{2+} concentration. It is not un-reasonable to expect the surface concentration, and hence activity, will rise with increasing copper (ii) ion concentration. Sub-Nernstian responses are therefore to be expected.

For the electrodes showing Nernstian responses, the surface activity of copper must remain constant. This is possible if the surface consists of two or more stable components. A change in copper activity will then result in changes in the proportions of the different phases but will not alter their individual compositions and thus electrode potentials will also remain constant. In chapter 5 it was noted that melts which are cooled at a rate of $1^oc\ min^{-1}$ give crystalline material. Electrodes based on these materials will have several phases and the surface activity of copper in each phase can be kept constant. On the other hand the electrodes based on a-Cu_{20} $(As_2\ Se_3)_{80}$ consist of only one phase and thus the copper activity is expected to vary with solution copper concentration. This explains the sub-Nernstian slopes (26.7 mv per decade) found for these electrodes.

The tellurium containing compositions give single phase glasses even when cooled slowly. The responses are only just sub-Nernstian (28.5 mv per decade), but the error in the gradient ($\pm$ 0.1 mv per decade) is too small to account for the difference between this and the Nernstian value (29.1 mv per decade). This implies that the activity (or chemical potential) of the copper in the Cu_x $(As_2Se_{1.8}Te_{1.8})_{100-x}$ system varies very little with x.

The deviation of the slopes from the Nernstian value allows the change in the surface activity of the copper to be calculated as a function of the change in copper (ii) ion concentration. From equation 8.1.1

$$E_1 - E_2 = \frac{RT}{zF}\left\{ \log_e \frac{C^1_m z+}{a^{s,sm}_{m,1}} - \log_e \frac{C^2_m 2+}{a^{s,sm}_{m,2}} \right\}$$

$$= \frac{RT}{zF} \ln \left(\frac{C^1_{m^{2+}}}{C^2_{m^{2+}}} \quad \frac{a^{s,sm}_{m,2}}{a^{s,sm}_{m,1}} \right) \qquad (8.1.2)$$

if the concentration is varied by a factor of 10, equation 8.1.2 gives

$$10 \exp \left(\frac{zF\Delta E}{RT}\right) = \frac{a^{s,sm}_{m,2}}{a^{s,sm}_{m,1}}$$

For a-Cu_{20} $(As_2Se_3)_{80}$ ΔE = 26.7mV and for the tellurium containing glass it is 28.7mV, giving activity ratios of 1.22 and 1.01 respectively.

In the case of certain electrodes which showed sub-Nernstian responses, x-ray photographs indicated the presence of several phases. These electrodes also showed positive deviations from the expected electrode potential at 10^{-1}M copper (ii) ion. This behaviour can be rationalised by assuming that although several phases are present, they are not present in sufficient quantity to fix the copper activity. Under certain conditions a particular phase may disappear altogether and the surface activity of copper will then inevitably vary. At high concentrations of copper, new phases may form on the surface, these could have widely varying values of copper activity. Since these deviations are positive, the surface activity of copper must be lower in the presence of high copper (ii) ion concentrations in solution. This is consistent with the formation of a more thermo-dynamically stable phase. Nucleation of such a phase may not occur until the copper concentration in solution is above a certain value. It is however, surprising that for electrodes exhibiting such positive deviations, the relationship between concentration and electrode potential repeated over several cycles. If a more stable phase is formed at high concentrations it should continue to affect the overall electrode potential when returning to low concentrations. A possible explanation for this anomaly is that this new phase is only stable at high concentrations in solution.

It was also found that electrodes showing deviations from expected behaviour at high concentrations tended to take a long time-several minutes- to reach a steady potential. This can be explained by assuming that as new phases form, currents will flow between them because of their differing electrode potentials (chapter 4). These currents will continue to flow until equilibrium is reached, where the electrode potential is the same over the entire surface, such non-equilibrium currents may flow for a considerable time.

It is interesting that electrodes made from $CuAsSe_2$ exhibit Nernstian behaviour from 10^{-5}M to 10^{-1}M. This implies either that it consists of two or more phases that continually adjust their relative proportions in order that the copper activity in the surface is kept constant, or that the surface activity of the copper varies very little with changes in concentration of copper. For the latter to be the case the surface must be even less sensitive to changes in copper concentration than was found for the tellurium containing glasses. If $CuAsSe_2$ is a stable crystalline compound it might be expected that small changes in copper level lead to large changes in the copper activity and hence to deviations from Nernstian behaviour.

The above discussion treats the ternary Cu-As-Se compunds and quaternary tellurium containing glasses in the same way as Sato[2] discussed binary compounds. By contrast Jasinski[1] specifically excluded "solubility product type mechanisms" and instead proposed the presence of one type of sensing site. The fact that glassy as well as crystalline materials respond in a similar manner suggest that each phase, including thermodynamically unstable phases, must be involved in establishing the electrode potential. As has already been stated it is certainly not necessary to have a particular type of material present. It may be true that only certain sites will interact with copper ions in solution, but these sites are probably found at the surface of all phases.

8.3 Electrode Potentials in Chloride Solutions

A major difference between chloride solutions and those of other ions is that the copper [1] state is considerably more stable. Jasinski[1] made detailed studies of the behaviour of $Cu_x (As_2S_3)_{100-x}$ electrodes in chloride solutions and obtained similar results to those obtained here for selenide electrodes. He concluded that in chloride solution copper [1] ion dissolves from the surface and forms a complex with the copper (ii) ions in solution, thus reducing free copper (ii) ion levels in inverse proportion to the amount initially present. Unfortunately, whilst this explains the super-Nernstian slopes, it does not explain why the electrode potentials should always be higher in chloride solutions. Either the activity of the copper (ii) ion in chloride solutions must be much higher than in nitrate solution, or the activity of the copper in the surface must decrease in the presence of chloride ion. The former possibility is unlikely as other copper sensing electrodes, in particular copper metal, are unaffected by the presence of chloride ion. Thus it is concluded that chloride ions actually reduce the surface activity of copper. From figure 7.3 it is apparent that

the reduction in activity is dependent on the copper (ii) ion concentration, being greatest at the highest concentrations. Therefore, the activity is reduced by complex formation between the copper (ii) ions and copper atoms or ions in the surface. The complex formed may be the soluble complex invoked by Jasinski[1] or it may be a surface species. The latter is consistent with the fact that the super-Nernstian behaviour continues after the chloride has been replaced by nitrate.

It is suggested that chloride reacts with the surface copper to give a species which will complex reversibly with copper (ii) ion. The complexation reduces the surface activity and thus increases the electrode potential

$$\text{Act-Cu} + \text{Cl} \leftrightharpoons \text{Act-Cu-Cl}$$

$$\text{Act-Cu-Cl} + \text{Cu}^{2+} \leftrightharpoons \text{Act-Cu-Cu[11]-Cl}$$

If, as Jasinski suggested, the chloride ion complexation gives rise to a soluble species, the copper activity is reduced by virtue of a reduction in the surface concentration of copper. This would also explain the dependence of the potential on stirring; when the solution is stirred the soluble complex is more rapidly removed and chloride is more efficiently brought to the surface for further reaction. On the other hand it does not explain why the behaviour remains super-Nernstian when the chloride is replaced by nitrate. A simple reduction in surface copper activity should simply result in a constant shift of the electrode potentials to more positive values. By analogy with section 8.1 the change in surface activity resulting from a change in copper concentration can be calculated. Taking a value for the slope of 50mV gives a reduction in activities of 5 when the concentration is reduced by a factor of 10. The chloride ion must have a drastic effect on the electrode surface.

8.4 Potentiometry in the Presence of Foreign Cations

As noted in chapter 7, the majority of the cations investigated had no effect on the electrodes response to copper (ii) ion except when the foreign ion was present at high concentrations ($>10^{-1}$M). At high concentrations the ionic strength, given by

$$\mu = \tfrac{1}{2} \sum_i z_i^2 \, C_i \qquad 8.4.1$$

reduces the activity coefficients of all ions in solution. In the Debye-Huckel

theory activity coefficients are related to ionic strength by

$$\log \gamma = -0.509 \; z^2 \mu^{\frac{1}{2}} \qquad 8.4.2$$

The activity coefficient for a di-valent ion that is dissolved in a 0.1M solution of a uni -uni-valent salt is given by

$$\log_{10} \gamma = -0.6$$

assuming complete dissociation of the salt. The deviation from ideal behaviour is given by

$$\Delta E = \frac{RT}{zF} \log_e \gamma \qquad 8.4.3$$

which on substitution gives a deviation of -18mV. The observed deviations from the expected electrode potential in the presence of 0.1M of the foreign salt were typically -5mV. The lower value is probably due to the fact that the salts, particularly those of heavy metals, do not dissociate completely in solution. In any case the assumptions made in the Debye-Huckel theory strictly apply only at low concentrations.

Silver and mercury ions probably interfere in a manner that is similar to their interference towards binary chalcogenide and mixed chalcogenide electrodes, that is they displace the metal from the surface of the sensor. The sulphides of Cu, Hg and Ag have very low solubility products (compared to other metals) and of these three Ag_2S and HgS have the lowest products (table 8.1).

Table 8.1 Solubility products of Sulphides

HgS	4×10^{-53} - 2×10^{-49}
AgS	1.6×10^{-49}
CuS	8.5×10^{-45}
PbS	3.4×10^{-28}
CoS	3×10^{-26}
CdS	3.6×10^{-29}
ZnS	1.2×10^{-23}
NiS	1.4×10^{-24}
MnS	1.4×10^{-15}

It is reasonable to expect similar trends for the other chalcogenides.

The Ag-As-Se and Ag-As-S systems have been studied[4,5,6], Kawomoto et. al. have shown that Ag-As-S glasses are silver ion conductors; the same may be true for the structurally similar Ag-As-Se glasses. Thus in the presence of high silver ion concentrations ($>10^{-4}$M) copper is displaced by silver.

$Cu\text{-}(As\text{-}Se) + 2Ag^{+} \leftrightharpoons \frac{1}{2} Cu^{2+} + Ag_2\text{-}(As\text{-}Se)$. The compound(s) $Ag_2(As\text{-}Se)$ willthen behave as a silver ion sensor and give the slope characteristic of a univalent ion (58mV per decade at 20°C). If the silver compounds are ionic conductors then the sensing mechanism will be similar to that of the Ag_2S sensors discussed in chapter 3. The copper containing material in the bulk of the electrode simply acts as a contact.

At lower silver ion concentrations ($>10^{-4}$M) and in the presence of copper ion, copper may displace silver. The highest rate of silver displacement will occur at the highest copper concentrations; this explains why electrodes recover from exposure to silver ion more quickly in the strongest copper solutions. Furthermore, an electrode that has been exposed to high silver levels and is subsequently exposed to lower levels of silver together with copper (ii) ion will have regions of Ag-As-Se and Cu-As-Se. These will develop their own characteristic potentials and surface currents will flow in the way already discussed for composite electrodes. The situation is even more complicated if Ag-As-Se is an ionic or mixed conductor. The approach to equilibrium takes a long time and this explains the difficulty in obtaining stable reproducible electrode potentials for silver ion concentrations below 10^{-4}M.

The occurence of minima in the potential-time curves when electrodes are first exposed to silver ion occurs as silver displaces copper from the surface region thus causing the electrode to lose its sensitivity to copper ion. The electrode may not become fully sensitive to silver until the silver has occupied all the possible sites in the surface layers. The electrode will then respond to changes in silver concentration by a mechanism similar to that proposed by Koebel[7] for Ag_2S electrodes.

Mercury will probably displace copper in the same way that silver does. The mercury chalcogenides are however believed to be electronic conductors[8]; this has two consequences:

1. Displacement of copper will only occur from the surface.

2. The Hg-As-Se compounds will be susceptible to interference from redox couples.

If any Cu is left in the electrode surface it will continue to give an electrode potential when Cu^{2+} ion is in solution. Furthermore, Cu^{2+} may still be able to exchange electrons with a mercury containing phase. This explains why sensors can still distinguish between different copper levels in the presence of high concentrations of mercury on (10^{-1}M). It also shows that glasses containing metals other than copper may be suitable for use in copper ISEs. Wheatley[9] described lead ion sensors based on a glass of composition, -

$$Cu_5\ Pb_{20}\ (As_2Se_3)_{75}$$

These are also sensitive to copper (ii) ion.[10]

8.5 Chrono-potentiometry

In chrono-potentiometry a constant current is passed across the electrode solution interface, this can result in two possible types of reaction

1. The oxidation or reduction of one or more constituents of the solution.

2. The dissolution of the electrode material.

It has already been shown in chapter 2 that chrono-potentiograms are difficult to analyse except in cases where the electrode remains unaltered during the experiment, this condition is unlikely to be met here. For the currents and durations used in these experiments the electrode potential varied a maximum of $\pm$ 0.3v so that electrolysis of the solvent is unlikely to have occured. This means that the possible reactions that occurred were cathodic discharge of copper ion or cathodic dissolution of the electrode when negative currents were passed and anodic dissolution of the electrode when positive currents are passed. In addition tothese Faradaic processes, some current will also be used to charge double layer capacitances that exist in the solution (Helmholtz and Gouy layers) and the space charge region of the semiconductor.

It is instructive to calculate the amount of copper that could be plated out of the solution with the currents and durations used. A 1μA current flowing for 100s is equivalent to 10^{-9} Mol of electrons or 5×10^{-10} Mol of copper ions. The volume occupied by this number of copper atoms is $\sim 6 \times 10^{-9} cm^3$, if the electrode area is taken as $1cm^2$ and it is assumed that the copper discharges uniformly over the surface this is equivalent to a layer 10^{-11}m thick. In fact the atomic diameter of copper atoms can be taken as $\sim 10^{-10}$m so that a complete monolayer will not form. Nevertheless, even a 1μA current is seen to be capable of producing a monolayer that could extend over 10% of the electrode area and is thus likely to alter the surface composition of the electrode considerably. In some cases currents of 10μA flowed for 600s. Even when it is considered that the electrode surface will not be perfectly flat and will therefore have a larger area than used in the calculation above, this amount of charge represents the equivalent of at least a monolayer of copper plated onto the surface.

When the current is removed, the surface composition of the glass should have been so drastically altered that the electrode potential would not be expected to return to its original value. Nevertheless, in all cases the electrode potential had returned to within ±5mV of the original electrode potential 5 minutes after the current was switched off. Moreover chrono-potentiograms recorded in copper free solutions were often similar to those recorded in copper containing solutions. These observations suggest that the cathodic discharge of copper ions is not the only process that occurs when a negative current is passed and it is possible that it does not occur at all. The cathodic chrono-potentiogram must be due in part to the dissolution of the electrode as well as the charging of double layers. The electrolytic dissolution of semiconductors has been studied as it is important in understanding how etching solutions work. Gerischer[11] has reviewed these phenomena and has drawn up possible reaction schemes for both anodic and cathodic dissolution. These are illustrated in figure 8.1, it should be noted that for the electrode potential to return to its original value the activity of copper in the electrode should not vary between the start of the current and it being switched off. For this condition to be met the glass must dissolve uniformly and not with one element being selectively removed.

Gerischer's theory on the dissolution of semiconductors uses the fact that a hole in the valence band can be considered as being localised in a single chemical bond. Similarly, an electron in the conduction band is considered as occupying a particular anti-bonding orbital. When these situations occur at the surface of a semiconductor the bond is vulnerable to attack by agents in solution. Although localising a hole or an electron in this way is not permitted in a purely quantum mechanical description of a crystalline semiconductor, it must be remembered that a solid surface represents a severe imperfection in the crystal structure so that the usual Bloch function description will not apply, in particular surface states should not be delocalised in the way bulk ones are. Gerischer's theory really only applies to tetrahedral semiconductors such as Si or GaAs. In the case of the chalcogenides the non-bonding lone pair electrons might be expected to complicate the situation.[3] If a hole or an extra electron is associated with a non-bonding orbital it will not affect the reactivity of the surface. It was shown in chapter 4 however, that when high concentrations of copper are introduced to the As_2 Se_3 glass it starts to take on a tetrahedral structure.

8.1 Dissolution schemes for Semiconductor (after Gerischer)

a/Anodic dissolution of Cu-As-Se type semiconductor

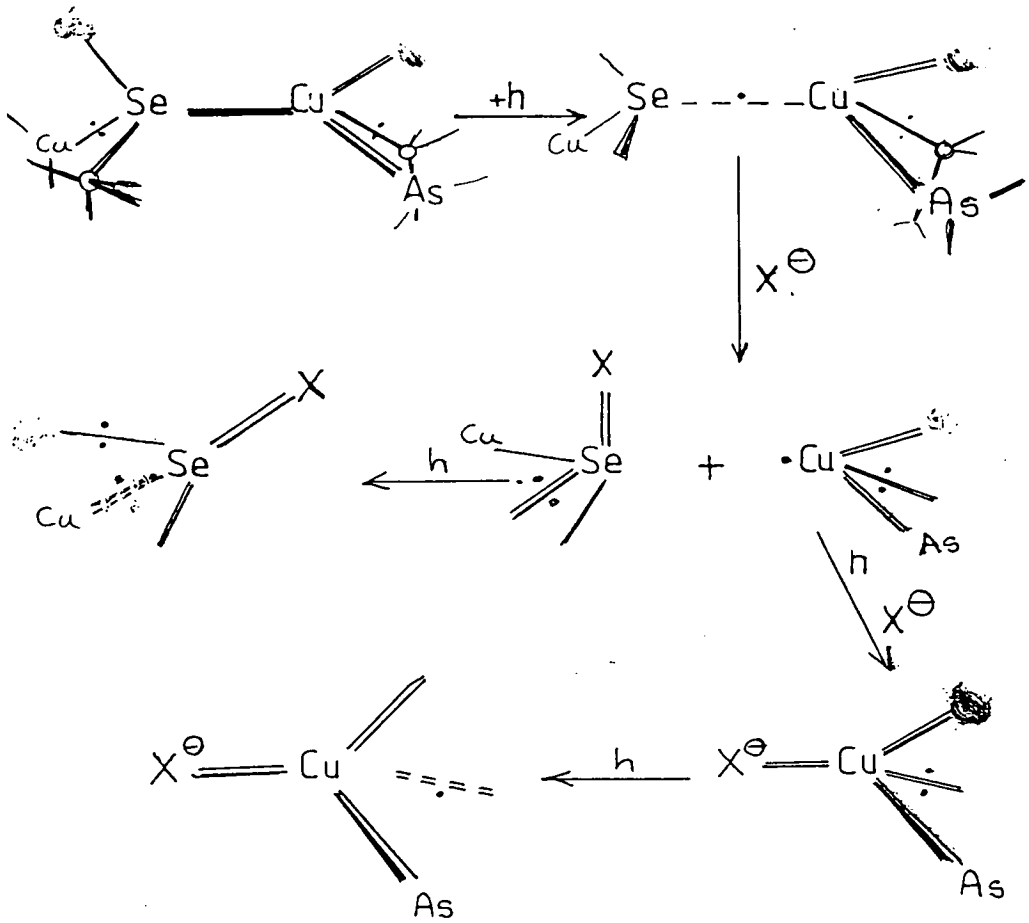

b/Cathodic dissolution of Cu-As-Se type semiconductor

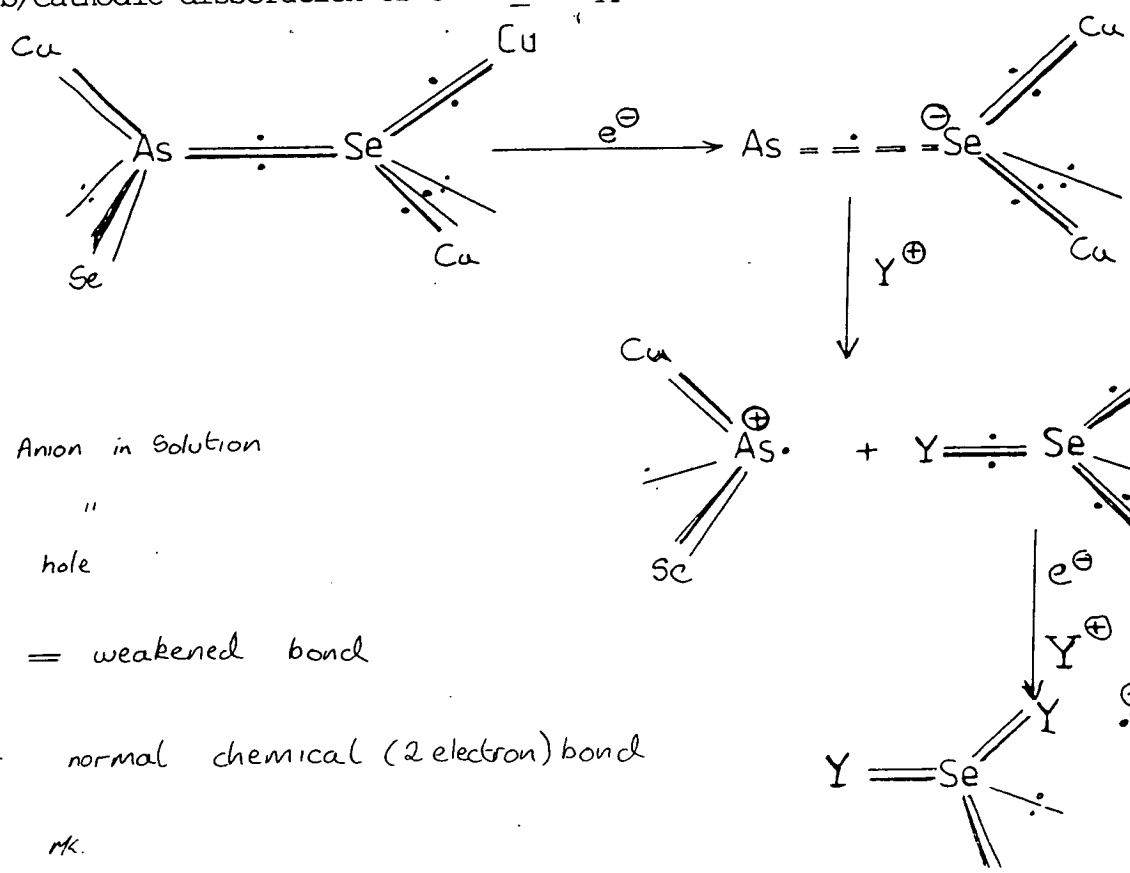

$X^{\ominus}$ Anion in Solution

$Y^{\oplus}$ "

h hole

= = = = weakened bond

—·— normal chemical (2 electron) bond

MK.

In any case during a chrono-potentiometric survey a significant amount of charge is moved to the electrode (either positive or negative). If this is simply taken up in non-bonding states the electrode is storing charge and should behave like a simple capacitor, where the potential drop increases continuously with time. This type of behaviour was never seen in nitrate solutions; after an initial rise the potential versus time curves all tended to flatten off. It appears then that the chrono-potentiograms recorded are those of the dissolving electrode. In the case of some electrodes, cathodic currents may also cause copper deposition from solution. Thus in figure 7.11 the chrono-potentiograms of an Cu As Se_2 electrode in two different copper ion solutions are shown. For the cathodic process the potentiogram shows a clear inflexion; the length of time that the potential varies slowly is reduced when the copper ion concentration in solution is increased. This may be due to the deposition of copper at a particular type of site, this will obviously be accomplished in a shorter time at higher copper ion concentrations. In the discussion of potentiometric results it was pointed out that Cu As Se_2 must consist of more than one pure compound so that limited plating at one type of site is quite possible and may not affect the final electrode potential. Similar results were obtained for the Cu_{56} $(As_2\ Se_3)_{44}$ electrode, which was shown by x-ray analysis to comprise several crystalline phases (chapter 5) and to have the resistivity-temperature relationship of a metal. It is quite possible that some metallic copper is present in this electrode, in which case the deposition of additional copper from solution will have no effect on the electrode potential.

The glassy Cu_{20} $(As_2\ Se_3)_{80}$ and Cu_{20} $(As_2\ Se_{1.5}\ Te_{1.5})_{80}$ electrodes never show inflexions in the chrono-potentiograms, this may be due to the absence of any discharge of copper.

It is interesting (figure 7.12) that inflexions are not found in chloride solutions, even when they are observed with the electrodes in nitrate solution. It has already been shown that electrode potentials measured in chloride solutions are different to those in nitrate, sulphate or perchlorate solution and that the behaviour characteristic of a chloride solution continues after the electrode has been replaced in the nitrate solution. It appears that the chloride affects the surface activity of copper in some way. Close inspection of figure 7.12 shows that in the presence of chloride the electrode potential varies linearly with time which is the way in which the voltage across a capacitor

would vary when a constant current is applied. It may be that the electrode is not undergoing cathodic dissolution in the presence of chloride ion; presumably the chloride must chemically bond to the surface, preventing any other species from attacking. The anodic chronopotentiograms in chloride and nitrate are similar, suggesting that anodic dissolution is not affected by the nature of the anion in solution. This is consistent with Gerischer's scheme for anodic dissolution where an anion initially attacks the weakened bond in the surface (figure 8.1a). This further implies that the anion is common to both chloride and nitrate solutions and is thus likely to be the hydroxyl ion.

Notice that for both anodic and cathodic dissolution, three bonds must be broken to free an atom from the surface (assuming all atoms are tetrahedrally bonded and at the surface each atom has three nearest neighbours). Thus three electrons or holes must be transported to the surface to liberate one atom. The dissolution rate is 2/3 as slow as the theoretical deposition rate of copper calculated above.

8.6 Cyclic voltammetry in copper (ii) solutions

In chapter 7.5 it was shown that the Cu-As-Se electrodes all show an oxidation wave starting at +0.6v (relative to the Ag/Ag Cl electrode) and this is not found with Pt electrodes. This wave was found even in base electrolyte and because there is no evidence for gas formation, which might indicate electrolysis of the solvent, the wave is probably associated with a surface species of the chalcogenide glass. One possibility is that Cu atoms are being converted to a higher oxidation state. The corresponding reduction wave almost overlaps the oxidation wave (figure 7.15 or 7.16). In chapter 2 it was shown that waves should only be coincident if diffusion and reaction can proceed to completion. This in turn requires an infinitely slow sweep rate (section 2.9), which was not used in these experiments. This probably means that the "wave" is not the result of single oxidation/reduction, but is the result of a sum of processes each occurring at slightly different electrode potentials. Each process is due to a slightly different type of site, and because the surface concentration of each type of site is low the magnitude of each individual wave is low. The end result is that the waves tend to smear into one giving the

8.2 ORIGIN OF SUPERIMPOSED OXIDATION AND REDUCTION WAVES

a,

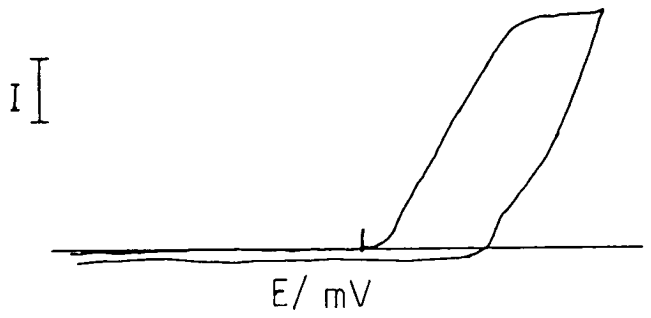

Single Oxidation-Reduction process

b.

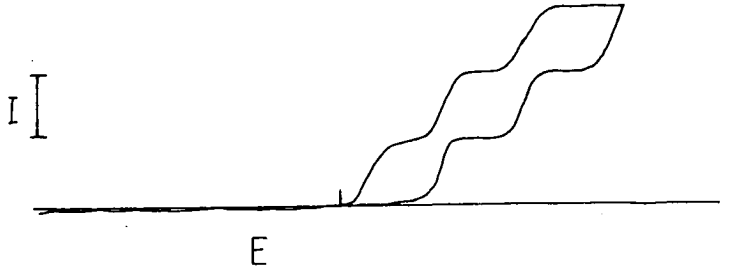

3 Similar Oxidation-Reduction processes.

c.

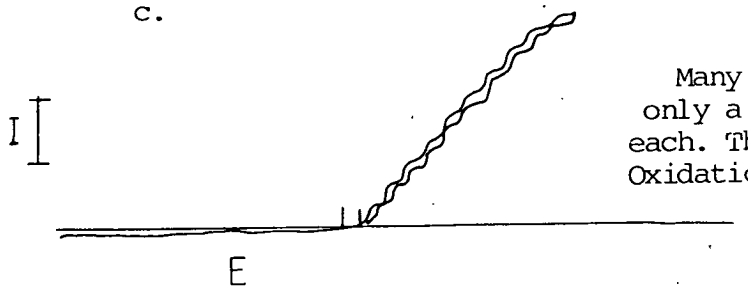

Many similar processes, with only a few sites available for each. This leads to superimposed Oxidation and Reduction waves.

observed result. Significantly the glassy a-Cu_{20} $(As_2\ Se_3)_{80}$ electrode does show a clear separation between the oxidation and reduction waves; since there is only one phase in this electrode there may be a more limited number of sites than for the composite electrode. The way in which a large number of similar site types can lead to apparantly coincident oxidation and reduction waves is shown in figure 8.2.

The smaller oxidation wave observed at 0.25v (relative to Ag/Ag Cl) is also not found with the Pt electrode. The oxidation product formed from the composite electrodes and also Cu As Se_2 electrodes, appears to be soluble, because when the solution is stirred, the corresponding wave is not observed. On the other hand a reduction wave is always found for a-Cu_{20} $(As_2\ Se_3)_{80}$ electrodes, even when the solution is vigourously stirred, this suggests the product is tightly bound to the surface of the glassy electrode. The glassy electrode also differs from the composite electrode in its behaviour towards light (section 8.8). The fact that a blue colouration was often observed in the solution adjacent to the composite electrode surface after oxidation is further evidence that copper is the oxidised species.

An alternative explanation of the voltammograms uses Gerischers'[11] model of the dissolution of a semiconductor discussed in the previous section. The cyclic voltammograms are then simply the current-voltage characteristics of a metal-solution-semiconductor cell. No current will flow until the holes, or electrons, necessary to weaken the bonds are present in the surface, the concentration of these is modulated by the surface potential (see section 2.6). In this case when the applied potential is +0.6v (w.r.t. the Ag/Ag Cl electrode) the number of holes at the surface is high enough to start weakening bonding states and thus promoting the anodic dissolution of the glass.

8.7 Cyclic Voltammetry of Redox Couples

In chapter 2 (section 2.7) the way in which redox potentials could be related to the energy levels of electrons associated with ions in solution was shown. The NHE has an energy on the vacuum scale of -4.7 ($\pm$0.2)eV and therefore if the electrode potential of a particular process is known it can be related to the vacuum scale by

$$U/eV = zE - 4.7$$

For benzo-quinone the standard electrode potential is 0.7V and so the energy levels of the oxidised and reduced forms lie at -4eV on the vacuum scale. It is not possible to measure the separation of the energy levels and calculations of this are, so far, only approximate. Nevertheless, converting standard potentials to energies on the vacuum zero scale is a useful way of analysing the voltammograms. Inspection of figure 7.18 shows that the crystalline electrodes show both oxidation and reduction waves, although there is no clear peak for the reduction at c-Cu_{20} $(As_2 Se_3)_{80}$. On the other hand the a-Cu_{20} $(As_2 Se_3)_{80}$ electrode shows no trace of the reduction wave, so although the oxidation occurs the corresponding reduction does not. This could mean the energy levels of the oxidised form of benzo-quinone coincide with the gap of the semiconductor. For reduction to occur the energy levels of the oxidised form of the couple must coincide with filled levels in the semiconductor. Similarly for oxidation to occur the energy levels of the reduced form, which are lower in energy than those of the oxidised form, must overlap vacant levels in the semiconductor. These facts allow the approximate position of the benzo-quinone couple on the energy level diagram of Cu_{20} $(As_2 Se_3)_{80}$ to be deduced. The voltammograms of TMPD show 4 oxidation/reduction processes at the Pt electrode, thus together with benzo-quinone there are a total of 5 processes with measured half wave potentials of:

D	+0.43	TMPD
C	+0.18	TMPD
BQ	-0.1	Benzo-quinone
B	-0.50	TMPD
A	-0.82	TMPD

At a-Cu_{20} $(As_2\ Se_3)_{80}$ only processes corresponding to A, BQ, C and D occur at all and of these A and BQ only show the oxidation wave. Thus species giving rise to processes C and D seem to be able to exchange electrons readily with the semiconductor and thus their energy levels must be outside the gap. On the other hand species giving rise to B, whose energy levels must be lower than those of C or D, cannot exchange electrons and therefore lie within the gap. Benzo-quinone and species A can only donate electrons to the semiconductor. Using these facts the redox couples may be positioned on the energy level diagram for the glass as shown in figure 8.3. It is interesting that the states in the gap proposed by Fraser[12] to explain the electrical properties of the Cu_X $(As_2\ Se_3)_{100-X}$ glasses are also required to explain the behaviour of the cyclic voltammograms.

For the tellurium containing glass reduction and oxidation waves were observed for each of the five species. This suggests that states extend all the way across the gap in these glasses. Since $As_2\ Te_3$ has a very different structure to $As_2\ Se_3$ it is not unreasonable that adding tellurium to the glass will alter its electronic structure considerably. It should be noted however, that if there are pin pricks in the electrode surface that allow the solution to touch the back contact, all reductions and oxidations will be able to take place as the back contact is metallic.

It should also be noted that the absence of a particular wave may indicate that the corresponding electron transfer is forbidden by selection rules, themselves deriving from symmetry considerations. This explanation is unlikely because: a) For two of the processes, only transfer in one direction-reduction-does not occur. (Since the structure of the two forms of the couple is unlikely to change greatly, it is unlikely that the symmetry will change. Hence electron transfer will either be forbidden for oxidation and reduction or not at all.) b) In amorphous solids there is no long range order and thus no symmetry. Selection rules deriving from symmetry restrictions will consequently not apply to these types of electron transfer.

Finally, it is tempting to try to relate the electrochemical processes discussed in chapter 8.6 to the vacuum zero energy scale. This is very difficult because the relevant electrochemical couple is of the form

$$Cu^{2+}\ (aq) \leftrightharpoons Cu(s) - As\ Se$$

8.3 ENERGY LEVELS OF REDOX COUPLES IN SOLUTION COMPARED TO SURFACE BAND STRUCTURE

a. $Cu_{20}(As_2Se_3)_{80}$

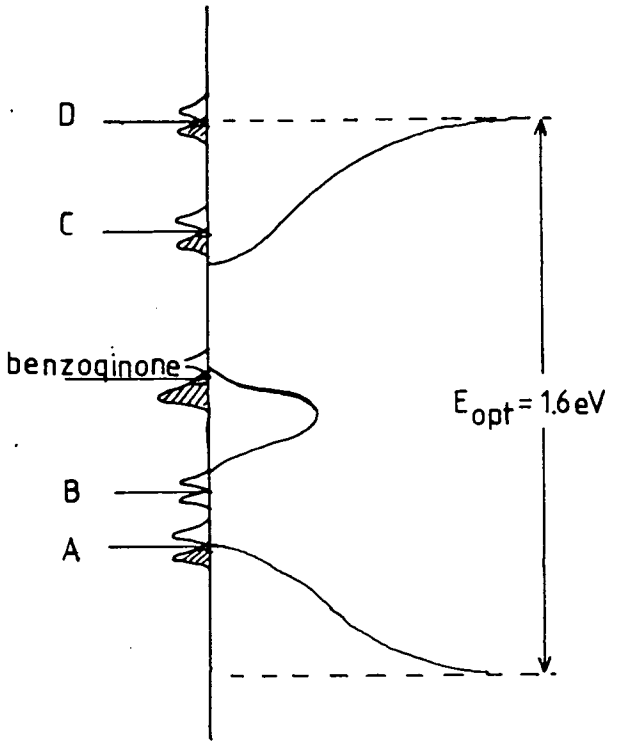

b. $Cu_{20}(As_2Se_{1.5}Te_{1.5})_{80}$

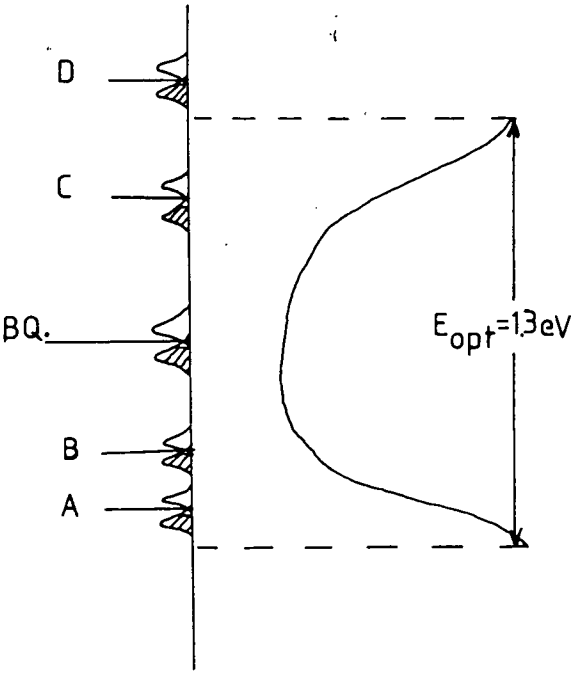

with only one species in solution. It is very difficult to assign energy levels to the copper in solid form.

8.8 Photo-electrochemical effects

Photo-effects were only found consistently with the single phase a-Cu_x $(As_2\ Se_3)_{100-x}$ compositions. They were never observed in either of the tellurium containing glasses and were only found in one of the crystalline c-Cu_x $(As_2\ Se_3)_{100-x}$ electrodes (for x = 20), even then the effect became smaller with time and eventually disappeared. It appears therefore, that it is the thermodynamically unstable glassy phase that gives rise to the photo-effects and the presence of crystalline material actually suppresses the effect. Furthermore, the c-Cu_{20} $(As_2\ Se_3)_{80}$ electrode required several minutes for the potential to reach a steady value whereas the glassy electrodes reacted almost instantaneously.

The origin of photo-effects in semiconductor electrodes was discussed in section 2.8. It was pointed out that there are two components to the photo-potential. One is due to the separation of electrons and holes under the influence of the electrostatic field and diffusion gradient which result from the space charge at the semiconductor or surface. The other, the Dember EMF, results from the different mobilities of the electrons and holes. In practice it is not possible to separate the two components, although it might be possible to estimate the magnitude of these effects from a knowledge of the electronic properties.

Any theory explaining the origin of the photo-effect must also explain why it is observed only in the Cu_x $(As_2\ Se_3)_{100-x}$ glasses and not the tellurium containing compositions. It must also explain why the effect increases with decreasing copper ion concentration. As the copper ion concentration increases the solution will become more strongly absorbing but as shown in figure 7.21 the strongest absorption is at the red end of the spectrum, whereas a decrease in photo-effect with increasing concentration is still observed at short wave lengths (500-550mm). Furthermore, the relationship between photo-effect and concentration is clearly established at low concentrations 0.0M-10^{-4}M where absorption is not very strong.

Fraser[12] was able to measure the absorption spectra of thin films the glasses and showed that the absorption coefficients for both es of glasses -Cu_x $(As_2\ Se_3)_{100-x}$ and Cu_x $(As_2\ Se_{1.5}\ Te_{1.5})_{100-x}$ e of similar magnitude. It is consequently not possible for the sence of photo-effects in tellurium containing glasses to be due the fact that optical absorption does not occur. The optical gaps tained by Fraser - 1.62eV and 1.28eV for Cu_{20} $(As_2\ Se_3)_{80}$ and $_{20}$ $(As_2\ Se_{1.5}\ Te_{1.5})_{80}$ respectively - are smaller than the photon ergies used in these experiments - 2.5-1.8eV (for wave lengths 0-700nm) so that all the wave lengths used should be sufficient boost electrons from the valence to the conduction band. The sence of a photo-potential in the tellurium containing glass must us either be due to rapid recombination of the photo-generated ectrons or due to all incident radiation being reflected from the lass surface. Although reflectance spectra were never measured, the $_{20}$ $(As_2\ Se_{1.5}\ Te_{1.5})_{80}$ electrode surface did not appear to reflect ay more strongly than the Cu_{20} $(As_2\ Se_3)_{80}$ electrode. In section 8.7 was pointed out that the cyclic voltammograms of redox couples xchanging electrons with the Cu_{20} $(As_2\ Se_{1.5}\ Te_{1.5})_{80}$ electrode could e explained by assuming that electronic states exist all the way across ne gap of the semiconductor. If this is the case electrons and holes ould easily be trapped and then lose energy in small increments before e-combining (see figure 8.3). On the other hand for the Cu_{20} $(As_2\ Se_3)_{80}$ lass there appears to be a true gap, albeit with some states in the entre. Electrons and holes would not recombine so readily under these onditions; this would allow time for the charge separation which creates he additional potential drop measured as a photo-potential.

As the copper concentration in solution increases the photo-effect decreases, this implies that recombination becomes a more efficient process. Copper ions presumably form the Helmholtz plane and thus create a sheet of positive charge at the electrode surface, this could have two possible effects on the electronic structure of the glass.

1. Additional surface states will be created, possibly in the gap.

2. Electrons will be attracted to the surface and these will occupy some of the gap states.

The creation of additional states in the gap will make re-combination more efficient and thus reduce the photo-effect, as observed. Increasing the number of electrons in the space charge region will mean that when a hole is created, it is more likely to recombine with an electron in the gap state. This will leave a vacant gap state which could trap the photo-generated electron created initially. In this way the gap state behaves rather like a catalyst in that it increases the rate of re-combination but is itself unaffected at the end of the re-combination. The energy lost by the electrons is gained by the glass as a whole as vibrational energy phonons.

8.9 Practical Devices

A large number of materials and electrode configurations have been investigated in this and other studies. It is clear that almost any combination of arsenic, copper and the chalcogenide elements will give a material with ion selective properties. It has been shown that the structure and properties of the materials depend on the way they are prepared as well as their bulk compositions, in particular the Cu-As-Se compositions are prone to the formation of crystalline phases if cooled slowly. The presence of some crystalline material has the advantage that it reduces the resistivity of the material and also makes electrodes less sensitive to light. Single phase glasses in the Cu-As-Se system are affected by the light and the high resistivities of the glasses makes instrumentation more complicated and shielding more important. It is however, more difficult to prepare batches of crystalline materials with similar electrochemical properties. More over the responses of some electrodes based on crystalline material were too slow to be of use in a practical device. The tellurium containing materials do not suffer from photo-effects, have lower resistivities and are more easily prepared in glassy form than their selenium analogues. Thus Cu_x $(As_2$ $Se_{1.5}$ $Te_{1.5})_{100-x}$ seem the best materials to form the basis of practical devices. Fraser[12] has prepared these glasses with up to 35% copper, it would be interesting to see how far the glass forming region extends. It is also worth reiterating that the electrode responses of these glasses were very close to the Nernstian value for 2 electron processes. This would be an advantage when using existing instrumentation in conjunction with these electrodes.

Electrodes have been prepared by sputtering these glasses onto a metal-normally gold-surface[12] . These electrodes give responses that are close to Nernstian, although they were not studied in detail. The composition of sputtered electrodes differs slightly from the source but this is not likely to effect their suitability as electrode materials. The ability to sputter the electrodes has two consequences of practical importance.

1. They can be used in devices employing thin film manufacturing techniques.

2. Thin film electrodes imply the resistance of the devices can be considerably reduced compared to most of the devices described in the experimental chapter (chapter 5,6) which were 2-5mm thick. This may simplify instrumentation. The only problem with sputtering is that so-called pin holes may form, this would allow the solution to contact the back contact directly, which would then be subject to interference from redox couples.

The glasses suffer interference from a similar range of ions to those that affect existing commercial devices. Silver and mercury ions interfere with all available devices[1] because of the very low solubility products of their sulphides and other chalcogenides. Nevertheless, at low silver concentrations ($<10^{-4}$M) and at any mercury concentration the electrodes can distinguish between different copper concentrations. In principle if the response to silver and mercury can be found their effects can be accounted for. In practice the response to changes in silver or copper concentration may be too slow to do this.

The glasses also suffer from chloride ion interference and this has been observed with other copper sensing electrodes. Chloride ion is found in many naturally occuring systems (sea water, biological fluids) and so this is a serious drawback. Although responses are not Nernstian in chloride ion, they are reproducible so that electrodes based on these glasses could be used, providing they are carefully calibrated and chloride is the only co-ion present in the system being analysed.

Wheatly and Fraser investigated lead ion sensors based on $Cu\ As_2\ Se_3$ and $Pb/Cu\ As_2\ Se_{1.5}\ Te_{1.5}$ glasses. Whilst these show ernstian response to lead (ii) ion they are sensitive to copper as l.[10] They were not studied in detail here but could be useful, ticularly if they respond to changes in lead ion concentration n in the presence of high concentrations of copper.

Although the ferric ion sensing Fe-Se-Ge-Sb glasses were not idied in detail it is worth mentioning that a reliable ferric ion nsor would have many applications because of the importance of rrous metals in construction and heavy engineering.

10 Further Work

Although a variety of electrochemical techniques have been applied cells of the form

$$M \mid Ref \vdots Cu^{2+}_{(aq)} \mid Cu_x\ (As_2\ Se_3)_{100-x} \mid M$$

is clear from proceeding sections that more work must be done to gain a ll understanding of the response mechanism. In particular, it would be seful to extend the techniques to a greater range of compositions. It is oteworthy that the simple potentiometric studies revealed a lot of nformation on the thermodynamics of the response and it would now be nteresting to measure the effect of altering the copper content of the lass on the slopes and deviations (as defined in section 8.2) of the esponses to copper ion. These studies should also include the stable ompounds in the Cu-As-Se system such as $Cu_3\ As\ Se_4$ and Cu As Se. It ight also be useful to use cells of the type

$$Cu \mid Cu^{2+}(aq) \mid Cu_x\ (As_2\ Se_3)_{100-x} \mid Cu$$

n these studies as these avoid complications due to liquid and other unctions.

The effect of composition on photo-potential could reveal more about the basic causes of this effect, particularly when Frasers optical absorption work is taken into account.

Cyclic Voltammetry of redox couples is a very powerful technique for probing the surface electronic structure of all semiconductors and should thus also be used to study the whole range of Cu_x $(As_2$ $Se_3)_{100-x}$ glasses. Obviously, the more redox couples that can be used the greater the detail that can be gained. If a non-polar solvent such as aceto-nitrile is used the electrochemical range can be extended to 5V.[13]

In addition to the techniques that have been already used and are described above, the A.C.impedance techniques could reveal more information on the actual charge transfer processes. As shown in chapter 2 the A.C. methods encompass many perturbation schemes, in which either a constant frequency signal is superimposed on one of the D.C. signals (a ramp, step or constant potential) or frequency is varied. The former techniques are useful for investigating how A.C. properties such as surface capacitance vary with applied potential. The latter techniques can provide quantitative information on the capacitances associated with the double layers in the cell and the charge transfer processes. The construction of Schottky-Mott plots would be the ultimate aim of A.C. impedence techniques as these allow the densities of donors and/or acceptors to be calculated.

In addition to the electrochemical techniques described above certain other experiments could help to discover the mechanism of response, e.g to measure the so-called zeta potentials of small particles of the glass in copper ion solutions. The glass would have to be finely ground so as to have a high surface area to volume ratio, linear dimensions of 1μm would be adequate. The zeta potential is related to the surface charge carried by colloidal particles and thus in turn depends on the ionic strength of the solution. Since a highly specific surface reaction with Cu^{2+} ions is believed to occur, the surface charge of particles might depend strongly on the copper ion concentration in the solution.

Further experiments on the electronic and optical properties of the Cu/As_2 Se_3 and Cu/As_2 $Se_{1.5}$ $Te_{1.5}$ glasses have been proposed by Fraser.[12] The most important of these are probably Hall effect measurements to measure the density of the charge carriers. The electronic structure could also be probed with electron beam techniques and electron emission methods; a review of the applications of such methods to semiconductors has been given by Mark[14]. As already stated such information complements the qualitative band structures that can be derived from cyclic voltammetry.

REFERENCES

Chapter 1

1. T.S.Light in "Ion Selective Electrodes" p.354 NBS special 314 R.Durst(ed.) Nov. 1969
2. T.Baker,I.Trachtenberg J.Electrochem.Soc. 118 571 (1971)
3. R.Jasinski,I.Trachtenberg,G.Rice J.Electrochem.Soc. 121 363 (1974)
4. D.Adler Sci.Am May 1977 p.36

Chapter 2

1. G.Laidler "Chemical Kinetics" McGraw Hill 1977
2. G.E.Kimball J.Chem.Phys. 8 200 (1940)
3. T.Berzins and P.Delahay J.Am.Chem.Soc 75 2486 (1953)
4. J.E.Carroll "Physical Models for Semiconductor Devices" Arnold 1974
5. M.Planck Ann.Phys.Chem.N.F. 40 561 (1890)
6. Z.Schlogl Z.Physik.Chim.N.F. 1 305 (1954)
7. P.Henderson Z.Physik.Chim.N.F. 59 118 (1907)
8. D.J.G.Ives and G.J.Janz "Reference Electrodes" Academic Press NY1961
9. T.R.Bonnam "The Donnan Potential" Bell London 1932
10. D.H.Everett "Introduction to the Study of Chemical Thermodynamics" Longmanns 1955
11. F.Conti,G.Eisenmann Biophys.J. 5 247 & 511 (1965)
12. M.Koebel,Anal.Chem. 46 1559 (1974)
13. R.P.Buck Anal.Chem. 40 1432 (1968)
14. T.B.Grimley,N.F.Mott Trans.Far.Soc. 43 3 (1947)
15. J.Koryta "Ion Selective Electrodes" Cambridge 1975
16. M.Koebel,N.Ibl,A.M.Frei Electrochimica Acta 19 287 (1974)
17. J.B.Wagner,C.Wagner J.Chem.Phys. 26 1602 (1957)
18. I.M.Kolthoff,H.L.Sanders J.Am.Chem.Soc 59 416 (1937)
19. T.S,Light in "Ion Selective Electrodes" p.354 NBS spec.314 1969
20. T.Baker,I.Trachtenberg J.Electrochem.Soc. 118 571 (1971)
21. R.Jasinski,I.Trachtenberg,G.Rice J.Electrochem.Soc 121 363 (1974)
22. M.Sato Electrochimica Acta 11 361 (1966)
23. F.Lohmann Z.Naturforsch. 22A 843 (1967)
24. S.Trasatti J.Electroanal.Chem. 52 313 (1974)
25. W.Hansen,D.Kolb J.Electroanal.Chem. 100 493 (1979)
26. S.Roy Morrison "Electrochemistry at Semiconductor and Oxidised Metal Electrodes" Plenum New York 1980
27. R.A.Marcus J.Chem.Phys. 24 966 (1956)
28. R.A.marcus J.Chem.Phys. 43 679 (1965)
29. G.E.Kimball J.Chem.Phys. 8 199 (1940)
30. V.A.Myamlin,Y.V.Pleskov "Electrochemistry of Semiconductors" Plenum 1967
31. M.D.Krotova,Y.V.Pleskov Solid State Phys. 2 411 (1962)
32. D.D.McDonald "Transient Techniques in Electrochemistry"
33. J.E.B.Randles Trans.Far.Soc. 44 327 (1948)
34. M.M.Nciholson J.Am.Chem.Soc. 76 2539 (1954)
35. P.Delahay J.Am.Chem.Soc. 75 1190 (1953)
36. T.Berzins,P.Delahay J.Am.Chem.soc. 75 555 (1953)
37. M.Plonski J.Electrochem.Soc. 116 1688 (1969)
38. S.N.Frank,A.J.Bard J.Am.Chem.Soc. 97 7427 (1975)
39. R.A.Fredlein,A.J.Bard J.Electrochem Soc. 126 1892 (1979)
40. R.A.L.Vanden-Berghe,F.Carden,W.P.Gomes Z.Phys.Chem. 86 330(1973)
41. A.K.Covington in ref.19 p.107

REFERENCES(cont)

42. G.J.Janz,H.Taniguchi Chem.Rev. 53 397 (1953)
43. G.A.Hullett Phys.Rev. 32 257 1911
44. W.D.Larsen,F.H.McDougall J.Phys.Chem. 41 493 (1937)
45. H.K.Fricke Zuker 14 (no.7) 1961

Chapter 3

1.M.Cremer Z.Biol. 47 562 1906
2. F.Haber,Z.Klemensiewicz Z.Physik.Chim. 67 385 (1909)
3. M.Dole "The Glass Electrode" Wiley 1941
4. K.Scwabe,H.Dahms Z.Electrochemie 65 518 (1961)
5. F.Conti,G.Eisenmann Biophys.J. 5 247 (1965)
6. Horovitz Z.Physik. 15 369 (1923)
7. S.I.Solokov,A.H.Passynsky Z.Physik.Chem. A160 366 (1932)
8. G.Eisenmann "Glass Electrodes for Hydrogen and other Cations, Priciples and Practice" Decker 1967
9. M.Koebel,N.Ibl,A.M.Frei Electrochim.Acta 19 287(1974)
10. J.Vasely,O.Jensen,B.Nicholaisen Anal.Chim.Acta. 62 1 (1972)
11. L.Suchha,M.Suchanek,Z.Urner Proc.2nd.Conf.Appl.Phys.Chem.Vezprem Budapest 1971
12. J.W.Ross in "Ion Selective Electrodes" chpt.2 NBS spec 314 1969
13. E.Schmidt,E.Pungor Anal.Lett. 4 641 (1971)
14. J.Koryta "Ion Selective Electrodes" chpt.5 Cambridge 1975
15. J.N.Butler chpt.5 of ref.12
16. D.J.G.Ives,DG.Janz "Reference Electrodes" NY 1961
17. W.Noddack,K.Wrabetz,W.Herbst Z.Electrochem. 59 752 (1955)
18. M.Sato Electrochimica Acta 11 361 (1966)
19. M.Koebel Anal.Chem. 46 1559 (1974)
20. See Orion Newsletters or Advertising literature
21. T.A.Fjeldy,K.Nagl J.Electrochem.Soc. 127 1299 (1980)
22. T.A.Fjeldy,K.Nagl J.Electrochem.Soc. 129 660 (1982)
23. H.Hirata,K.Higashiyama Anal.Chim.Acta 54 415(1971)
24. J.F.Lechner,I.Sekerka Anal.Chim.Acta 93 129 (1977)
25. M.Neshkova,H.Sheytanov "Ion Selective Electrodes Conference" pp.503-510 Elsevier Amdam. 1978
26. C.Baker,I.Trachtenberg J.Electrochem.Soc. 118 571 (1971)
27. R.Jasinski,I.Trachtenberg J.Electrochem.Soc. 120 1169 (1973)
28. R.Jasinski,I.Trachtenberg,G.Rice J.Electrochem.Soc. 121 363(1974)
29. G.Drennan B.Sc.project Edinburgh University 1976
30. C.J.Wheatley Research Report Edin.Univ. 1977
31. R.N.Khuri chpt.8 of ref.12
32. J.Janata,R.F.Huber in "Ion Selective Electrodes in Analytical Chemistry" Plenum NY 1980 (H.Freiser ed.)
33. J.N.Zemel Anal.Chem. 47 255a (1975)
34. P.Bergveld IEEE Trans. (BME-19) 342 (1972)
35. J.Janata et.al. Anal.Chim.Acta. 101 239 (1978)
36. Chpt.8 of ref.14
37. —
38. P.Vadgama in "Ion Selective Electrode Methodology. vol.2" p.23 (A.K.Covington ed.) CRC 1980
39 M.Riley p.1 of ref.38
40. Orion Research Analytical Methods Guide (May 1975)
41. N.T.Crosby J.Appl.Chem. 92 100 (1969)
42. E.Belack Am.Water Works Assoc. 64 62 (1972)
43. J.W.Ross,J.H.Riseman,J.H.Krueger Pure Appl.Chem. 36 473 (1973)
44. Electronic Instruments Ltd. Leaflet Dec.1974
45. U.Fiedler,E.H.Hansen,J.Ruzicka Anal Chim.Acta 74 423 (1975)
46. J.Ruzicka,E.H.Hansen,P.Bisgaard,E.Reymann Anal.Chim.Acta 72 215(1974)
47. T.Anfahlt,A.Granelli,D.Jagner Anal.Chim.Acta 76 253 (1975)
48. G.G.Guilbault,J.G.Montalvo J.AM.Chem.Soc. 92 2533 (1970)

REFERENCES(cont)
48. G.G.Guilbault,J.G.Montalvo J.Am.Chem.Soc. 92 2533 (1970)
49. R.Jasinski,G.Barna,I.Trachtenberg J.Electrochem.Soc 121 1575 (1974)
50.I.Lundstrom et.al. Appl.Phys.Lett 26 55 (1975)
51. K.P.Jagannathan et.al. in "Solid Electrolytes" Plenum NY 1980 p.201 (E.C.Subarao ed.)
52. T.S.Light in chpt.9 ref.12

Chapter 4.

1. A.Bienenstock J.Non-cryst.sol. 11 447 (1973)
2. A.A.Mostovsky Fiz.Tverd.Tela 6 493 (1964)
3. Danilov,Mosli Zh. Prikl.Khim. 35 2012 (1962)
4. Liang,Bienenstock,Bates Phys.Rev.B 10 1528 (1974)
5. Kolomiets,Rukhlyadev,Shilo J.Non.Cryst.Sol. 5 389 (1971)
6. S.R.Rowlinson "Liquids and Liquid Mixtures" Oxford
7. Asahara,Izumitani J.Non.Cryst.Sol. 11 97 (1972)
8. M.I.Fraser Ph.D. Thesis Edinburgh 1983
9. G.Busch,F.Holliger Helv.Phys.Acta. 33 657 (1960)
10. Wernick,Benson J.Phys.Chem.Sol 3 157 (1957)
11. S.H.Hunter&Bienenstock Proc.VI Int.Conf.on Amorphous and Liquid Semiconductors 151 Leningrad (1975)
12. J.Whitfield Sol.State Chem. 39 209 (1981)
13. James Clerk Maxwell "A Feature on Electricity and Magnetics" Clarendon Oxford 1892
14. C.J.Wheatley Research Report Edinburgh 1977
15. Z.U.Borosova "Glassy Semiconductors" Plenum NY
16. R.G.Kelly Ph.D. Thesis Edinburgh 1975

Chapter 5

1. M.I.Fraser Ph.D. Thesis Edinburgh 1983
2. Liang&Bienenstock,Bates Phys.Rev.B 10 1528 (1974)

Chapter 6

1. Bruker Research E310 Maintenance Manual
2. CRC Handbook 1974-5 (55th edn.)

Chapter 8

1. R.Jasinski,I.Trachtenberg,G.Rice J.Electrochem Soc. 121 363 (1974)
2. M.Sato Electochimica Acta 11 361 (1966)
3. —D.Adler in Scientific American May 1977 (an elementary introduction)
4. A.P.Firth Ph.D. thesis Edinburgh 1985
5. B.T.Kolomiets,V.P.Shilo J.Non.Cryst.Sol 5 389 (1971)
6. K.Kawomoto,Nagura,S.Tsuchashi J.Am.Ceramic Soc. 57, 489 (1974)
7.M.Koebl Anal.Chem. 46 1559 (1974)
8. G.Lorenz,C.Wagner J.Chem.Phys. 26 1607 (1957)
9. C.J.Wheatley Research Report Edinburgh 1977
10. Recent measurements by the author suggest that all sesitivity to Pb^{2+} is lost when the Cu^{2+} concentration is greater than 10^{-5}M. See Appendix A
11. H.Gerischer in "Electrode Processes in Solid State Ionics" p.227 (M.Kleitz,J.Dupuy eds.) Reidel 1976
12 M.I.Fraser Ph.D. thesis Edinburgh 1983
13. S.N.Frank,A.J.Bard J.Am.Chem.Soc. 97 7427 (1975)
14. R.Mark in ref.11 p.19

APPENDIX 1

IN fig. A1 are shown the response of a $Pb_5Cu_{20}(As_2Se_3)_{75}$ electrode to lead nitrate solutions in the presence of copper nitrate. It is clear that copper inteferes strongly, and that at concentrations above $5*10^{-5}$M the electrode can no longer detect changes in lead ion concentration. The inteference from copper is to be expected because of the similarity of the glass composition to those used in copper ion sensors.

A1

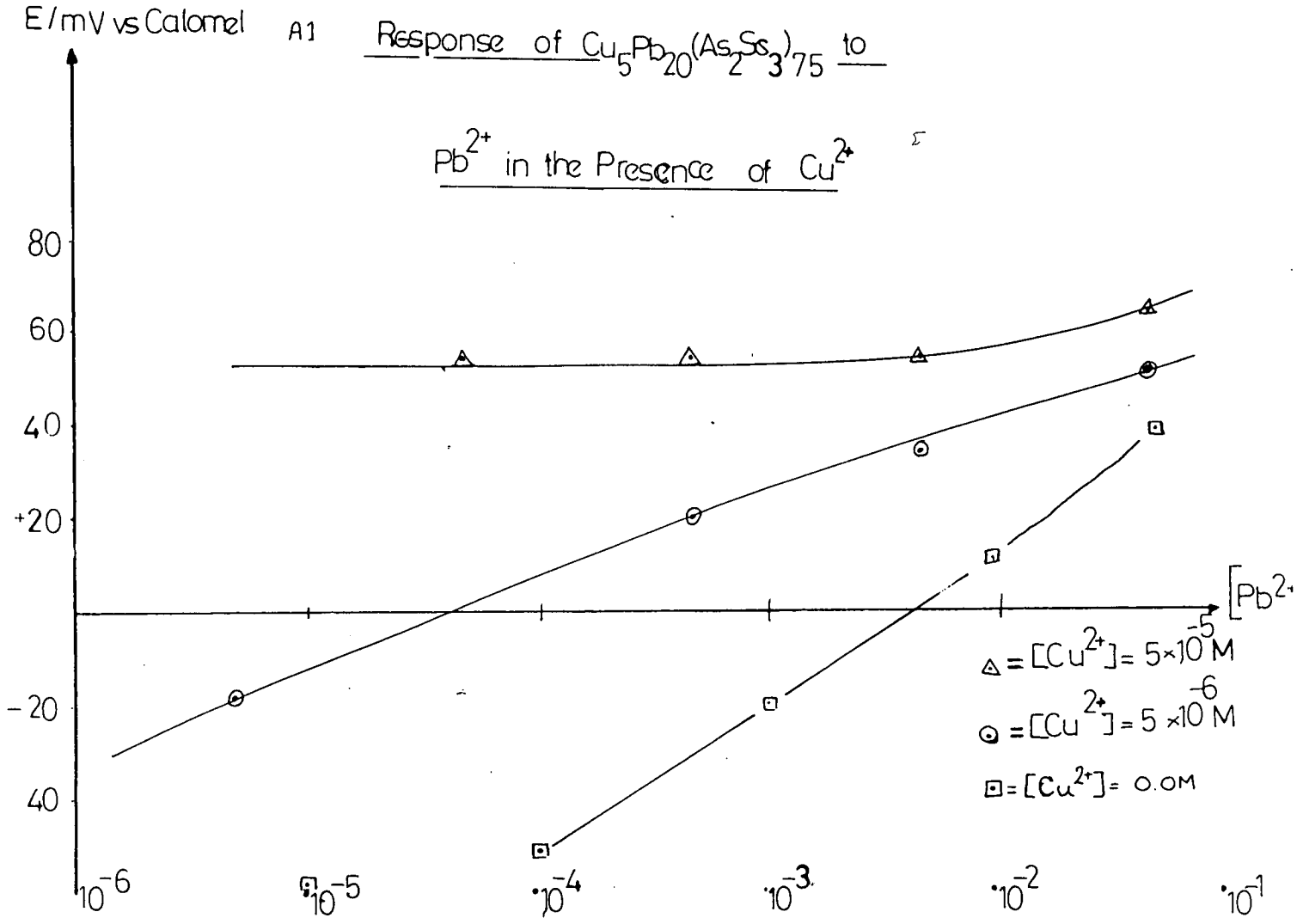
E/mV vs Calomel
Response of $Cu_5Pb_{20}(As_2Se_3)_{75}$ to
Pb^{2+} in the Presence of Cu^{2+}
80
60
40
+20
-20
40
10^{-6}
10^{-5}
10^{-4}
10^{-3}
10^{-2}
10^{-1}
$[Pb^{2+}$
$\triangle = [Cu^{2+}] = 5\times10^{-5}$ M
$\odot = [Cu^{2+}] = 5\times10^{-6}$ M
$\boxdot = [Cu^{2+}] = 0.0$M